Tim-3-galectin-9 immunosuppressive pathway in human acute myeloid leukaemia and solid tumour cells and biochemical functions of its crucial components

Thesis by

Svetlana Sakhnevych

A thesis submitted in partial fulfilment of the requirements of the University of Kent and the University of Greenwich for the Degree of Doctor of Philosophy

September 2019

DECLARATION

"I certify that this work has not been accepted in substance for any degree, and is not concurrently being submitted for any degree other that of Doctor of Philosophy being studied at the Universities of Greenwich and Kent. I also declare that this work is the result of my own investigations except where otherwise identified by references and that I have not plagiarised the work of others."

The Candidate

_____ Date_____

The Supervisor

_____ Date_____

ACKOWLEDGEMENTS

I would like to thank all the collaborators that made this project possible.

Many thanks to Dr Inna Yasinska, Dr Isabel Bernardo Gonçalves Oliveira Silva and Anette Teo Hansen Selnø for permission to include some of their results in my thesis.

I would like to give a special thanks to Prof Yuri Ushkaryov for the help and guidance during my PhD.

Finally, I would like to express my deepest gratitude to Dr Vadim Sumbayev for the guidance and support in completing this PhD project. It is with his supervision that this work came into existence.

ABSTRACT

Cancer is one of the primary causes of human death worldwide. Acute myeloid leukaemia (AML), one of the most severe types of blood/bone marrow cancers, is derived from transformed human myeloid precursor cells which developed mechanisms allowing them to escape host immune surveillance by inactivating cytotoxic lymphoid cells. Further studies suggested that solid tumours operate similar immune escape strategies. Molecular mechanisms of the immune evasion by malignant cells are poorly understood, however a better comprehension of the biochemistry underlying these processes are vital for development of anti-cancer immunotherapy – a cure of new generation.

Recent evidence suggested the crucial involvement of Tim-3 and galectin-9 proteins in the immunosuppression operated by malignant cells. Therefore, the aim of our work was to investigate the activity of Tim-3-galectin-9 immunosuppressive pathway in human malignant cells and biochemical functions of its crucial components.

We discovered that triggering of the receptor called latrophilin (LPHN) 1, expressed in AML cells but absent in healthy leukocytes, induces biosynthesis and exocytosis of T-cell immunoglobulin and mucin domain 3 (Tim-3) and galectin-9. Galectin-9 suppresses anti-cancer immunity by impairing anti-cancer activities of cytotoxic lymphoid cells. Tim-3 is trafficking galectin-9 but also can act on its own and prevent generation of interleukin-2 (IL-2) required for activation of cytotoxic lymphoid cells. Furthermore, AML cells recruit crucial components of normal human metabolism to escape surveillance and progress the disease. In particular, human adrenal cortex hormone cortisol upregulates LPHN1 expression in AML cells; blood-available fibronectin leucine rich transmembrane protein 3 (FLRT3) interacts with LPHN1 leading to galetin-9/Tim-3 synthesis and exocytosis in AML cells. Crucial components of FLRT3/LPHN/Tim-3/galectin-9 pathway are expressed in the majority of cancer cell lines

and thus may be common for a variety of malignant tumours. Tim-3-galectin-9 pathway is active in breast cancer and variety of other solid tumour cells and is used to protect malignant cells from host immune attack. However, unlike some other members of galectin family of proteins (for example, galectin-3), galectin-9 doesn't protect cancer cells against apoptosis *via* mitochondrial defunctionalisation. On the other hand, mitochondrial defunctionalisation reduces galectin-9 surface expression and leads to its accumulation in mitochondria in malignant cells but not in healthy ones. Therefore, targeted mitochondrial defunctionalisation may be a novel strategy for anti-cancer immunotherapy, since it would reduce galectin-9 surface expression allowing better elimination of cancer cells by immune system cells. Taken together our work demonstrates for the first time that Tim-3-galectin-9 immunosuppressive pathway plays a pivotal role in protection of AML and various solid tumour cells towards host immune surveillance – the machinery operated by cytotoxic lymphoid cells.

CONTENTS

DECLARATION i

ACKOWLEDGEMENTS ii

ABSTRACT iii

FIGURES x

TABLES xxx

ABBREVIATIONS xxxi

1. INTRODUCTION 1

1.1 Cancer development and metastasis (stages of cancer development) 3

1.1.1 Types of cancer – “solid” and “liquid” tumours 10

1.2 Normal physiological barriers preventing cancer development 13

1.2.1 Cell-cycle checkpoints 14

1.2.2 Immune system “quality” control 18

1.3 Physiological immunosuppression and immune evasion of malignant cells 32

1.3.1 PD-1 and CTLA-4 mediated immunosuppression 33

1.3.2 Tim-3/galectin-9 mediated immunosuppression 36

1.4 Blood cancer as a fatal systemic malignancy facing permanent interaction with immune system from the very beginning 41

2. AIMS AND OBJECTIVES 47

3. MATERIALS AND METHODS 48

3.1 Materials 48

3.2 Tissue culture 49

3.2.1 Cells lines 49

3.2.2 Primary human cells 50

3.2.3 Primary human blood plasma samples 51

3.2.4 Bone marrow extracts 51

3.2.5 Human breast tissue samples 52

3.3 Cell lysis 52

3.4 Tissue lysis 53

3.5 Protein quantification 53

3.6 Western Blot analysis 54

3.7 Enzyme-linked immunosorbent assay (ELISA) 57

3.7.1 Determination of galectin-9, soluble Tim-3 (sTim-3), TNF-α, IL-1β, SCF, VEGF and IL-2 concentrations released by the cells 57

3.7.2 Determination of phospho-S2448 mTOR in cell lysates 59

3.7.3 Detection of Tim-3-galectin-9 complex in cell and tissue lysates 60

3.7.4 Detection of cortisol in human blood plasma 60

3.8 Determination of LPHN1 fragments in human blood plasma 61

3.9 Detection of Tim-3-galectin-9 complex in tissue culture medium 61

3.10 Cell viability assay 62

3.11 Caspase 3 activity 63

3.12 Granzyme B activity 63

3.13 Mitochondria isolation 64

3.14 Uptake of BH3I-1 by the cells 64

3.15 Galectin-9 and Tim-3 knockdown 65

3.16 Quantitative real-time PCR (qRT-PCR) 66

3.17 Determination of PKC-α activity 67

3.18 Measurement of phospholipase C (PLC) activity 67

3.19 In-cell assay (also known as on-cell assay) 67

3.20 Confocal microscopy and imaging flow cytometry 68

3.20.1 Tim-3 and galectin-9 characterisation in THP-1 cells 69

3.20.2 Tim-3 and galectin-9 characterisation in primary human breast tissues 70

3.21 Fluorescence-activated cell sorting (FACS) 71

3.22 Synchrotron radiation circular dichroism spectroscopy (SRCDS) 71

3.23 Leukaemia cell protection assay 73

3.24 Statistical Analysis 73

4. Tim-3-galectin-9 immunosuppressive pathway and its pathophysiological role 74

4.1 Free and galectin-9-bound Tim-3 are shed differentially from the cell surface 74

4.2 Latrophilin 1, PKC-α and mTOR-dependent translation are crucial for Tim-3 and galectin-9 production and secretion 83

4.3 Galectin-9 protects AML cells from NK cell killing activity 89

4.4 Discussion 97

5. AML cells recruit normal physiological systems to progress the disease by preserving expression of stem cell proteins 105

5.1 Hematopoietic stem cells (HSCs) produce LPHN1, which expression is preserved in malignant AML cells but not in healthy leukocytes 105

5.2 Cortisol induces LPHN1 expression in AML cells and HSCs, but not in healthy leukocytes 107

5.3 Soluble LPHN1 fragments are detectable in AML blood plasma 110

5.4 FLRT3 upregulates galectin-9 secretion in AML cells in a LPHN1-dependent manner 111

5.5 Discussion 114

6. AML cells employ stress and danger signals to support overall malignant cell survival and proliferation 117

6.1 The effects induced in human AML cells by HMGB1 stimulation 117

6.2 HMGB1 stimulates TNF-α secretion by human AML leading to upregulation of SCF production 121

6.3 Discussion 124

7. Activity of Tim-3-galectin-9 pathway in solid tumours 127

7.1 Biochemistry and functions of Tim-3-galectin-9 secretory pathway in human breast cancer cells 127

7.1.1 Expression and activity of the FLRT3/LPHN/Tim3/galectin-9 pathway in breast tumours 127

7.1.2 Galectin-9 protects breast cancer cells against cytotoxic immune attack 135

7.1.3 Discussion 137

7.2 Expression of key components of the FLRT3/LPHN/Tim-3/galectin-9 pathway in solid and liquid tumours 141

8. Classic programmed cell death pathway downregulates Tim-3-galectin-9 immunosuppressive pathway. 146

8.1 Pharmacologically induced mitochondrial defunctionalisation suppresses Tim-3-galectin-9 secretory pathway in human colorectal cancer cells 146

8.2 Discussion 151

9. CONCLUSIONS 152

10. BIBLIOGRAPHY 154

11. APPENDIX 173

11.1 Electrophoresis solutions 173

11.1.1 SDS-polyacrylamide gels 173

11.1.2 1.5 M Tris-HCL pH 8.8 173

11.1.3 0.5 M Tris-HCL pH 6.8 173

11.1.4 10X Running buffer (8.3) 173

11.1.5 Sample buffer 173

11.2 Western blot buffers 174

11.2.1 10X Blotting Buffer (pH 8.3) 174

11.2.2 1X Blotting Buffer (with 20% Methanol) 174

11.2.3 10X TBS buffer (9% NaCl, 100 mM Tris HCl, pH 7.4) 174

11.2.4 1X TBST buffer (pH 7.4) 174

11.3 List of Publications 174

FIGURES

Figure 1: Cancer Global Incidence and Mortality. Incidence and mortality are reported as absolute numbers of new cancer cases and cancer-related deaths, respectively, per annum (Ferlay et al., 2010; Fitzmaurice et al., 2015; IARC, 2018; Parkin et al., 2005; Parkin, 2001; Torre et al., 2016).....2

Figure 2: Schematic model of cancer initiation and progression – from a healthy tissue (a), to the first mutations of a single somatic cell (b and c), able to promote clonal expansion causing benign tumour formation (d), to further mutations, responsible of malignant transformation, and, finally, metastasis development (g).....6

Figure 3: Processes underwent by HIF-1α protein under normal oxygen availability (a) and hypoxic conditions (b) 8

Figure 4: Cell cycle progression (Boyle, 2008) 15

Figure 5: Restriction point – RB phosphorylation, conditioned by the levels of growth-regulating signals, represents the point in which the cell commits to cell-cycle division in extracellular-independent manner.....16

Figure 6: General scheme of the mechanism through which cell cycle checkpoints operate. 17

Figure 7: HMGB1 structure 20

Figure 8: HMGB1 effects in early stages of inflammation.....22

Figure 9: Structure of MCH class I and MICA/B 23

Figure 10: Discrimination between healthy and transformed cells by NK cells 24

Figure 11: NK cell-mediated apoptosis induction in anomalous cells.....27

Figure 12: T cell activation 32

Figure 13: Immune cell physiological inactivation.....34

Figure 14: Cancer cell evasion through surface expression of immunosuppressive molecules. Prolonged stimulation of immune cells by cancer cells can cause upregulated PD-1 and CTLA-4 expression on the surface of CTCs and NK cells. Transformed cells can be still recognised and killed by hyper-activated immune cells, if the latter don't encounter APCs or T regulatory cells, which are able to inhibit over-stimulated lymphocytes or NK cells (a). Cancer cells expressing CD80/CD86 and/or PD-L1/PD-L2 inactivate immune system cells and thus escape host anti-tumour immunity (b). Anti-CTLA-4 and anti-PD-1 antibodies prevent inhibitory interactions of immune cells with cancer cells expressing CD80/CD86 and/or PD-L1/PD-L2 and thus facilitate malignant cells elimination by CTCs and NK cells (c). 35

Figure 15: Tim-3 structure and its interaction with galectin-9 on immune system cells. 38

Figure 16: Classification of galectins into three main groups based on their domain structural organisation (A) (Heusschen, Griffioen, & Thijssen, 2013). Galectin-9 structure: in green – sugar molecules, which can possible interact with a glycoprotein, are situated in proximity to carbohydrate binding sites (B) (Gonçalves Silva et al., 2017) 40

Figure 17: Inhibitory interactions via PD-1 and CTLA-4 receptors lead to immune cells inactivation by direct binding to respective ligands and through suppression of IL-2 secretion 43

Figure 18: Maximum of absorption of CBB alone and in complex with the protein. Protonated CBB has maximum of absorption at 465 nm (A). Deprotonation of CBB by basic amino acids leads to the formation of negatively charged sulfonate groups which can bind the protein through electrostatic interactions. In addition, aromatic residues, such as Trp, Tyr and Phe, can bind CBB through π-interactions. Stabilisation of CBB-protein complex results in the shift of maximum of absorption of the dye from 465 nm to 595 nm (Adapted from Gregoriu, et al., 2008). 54

Figure 19: Schematic representation of gel/membrane/filter papers/filter pads assembly in semi-dry (A) and wet (B) transfers. 55

Figure 20: OPD oxidation catalysed by HRP leads to the formation of DAP, which absorbs wavelengths in the range 400 – 450 nm (corresponding to the violet colour) of visible light spectrum and reflects wavelengths in the range 560 – 590 nm donating the typical yellow colour to the solution. DAP protonation leads to the formation of the compound absorbing the wavelengths from 450 nm to 500 nm and reflecting wavelengths which together donate bright orange colour to the solution [structures were drawn using ChemSpace]. 59

Figure 21: Viable cells contain active dehydrogenases able to reduce NAD^+ in NADH; then, electron coupling reagent phenazine ethosulfate (PES) transfers electrons from NADH in the cytoplasm to reduce MTS in the culture medium into an aqueous soluble formazan (Adapted from Riss et al., 2013). 62

Figure 22: Dibromine (obtained after breaking BH3I-1 compound) reacts with phenol red (λ_{mac}=428 nm) leading to the formation of bromophenol blue (λ_{mac}=585-590 nm). (Adapted from Wever et al., 2018). 65

Figure 23: Beam light 23 at Diamond Light Source Synchrotron and scheme of Synchrotron radiation circular dichroism (SRCD) spectroscopy analysis (Gonçalves Silva et al., 2017)... 72

Figure 24: Tim-3 is shed differentially from the cell surface depending if expressed in complex with galectin-9 or as a free transmembrane protein. Following the treatment of THP-1 cells with 100 nM PMA for 16 h, the media was exchanged with the fresh one containing 100 µM GI254023X (ADAM10/17 inhibitor) or 100 µM BB-94 (matrix metalloproteinase inhibitor) and incubated for 4 h. (A) The media collected after 16 h of incubation was subjected to immunoprecipitation and Western blot analysis for galectin-9 and Tim-3 detection (as outlined in Material and Methods). (B) The media collected after 20 h of incubation (all the samples) was subjected to ELISA for galectin-9, Tim-3 and galectin-9-Tim-3 complex detection. Images

are from one experiment representative of six which gave similar results. Quantitative data are mean values ±SEM (n=6) *p < 0.05; **p < 0.01 vs. control. 76

Figure 25. PMA induces generation and/or release of Tim-3, galectin-9 and Tim-3-galectin-9 complex. Following the treatment of THP-1 cell with 100 nM PMA (16 h incubation), secreted and intracellular levels of galectin-9, Tim-3 and Tim-3-galectin-9 complex were characterised by ELISA and Western blot. Comparative analysis (expressed in % control) of galectin-9 and Tim-3-galectin-9 complex levels secreted by PMA-treated and untreated THP-1 cells are illustrated in the bar diagram on the top. Images are from one experiment representative of three which gave similar results. Quantitative data are mean values ±SEM (n=3) *p < 0.05; **p < 0.01; ***p < 0.001 vs. control. 78

Figure 26: Co-localization of Tim-3 and galectin-9 in THP-1 cells. PMA-activated and paraformaldehyde-fixed cells were analysed using confocal microscopy for the detection of Tim-3 and/or galectin-9. Images are from one experiment representative of six which gave similar results. 79

Figure 27: Co-localization of galectin-9 and Tim-3 in THP-1 cells upon PMA activation. THP-1 cells stimulated with PMA were permeabilized and subjected to imaging flow cytometry as described in Materials and Methods. Images represent six selected single cells. 80

Figure 28: Levels of galectin-9, sTim-3 and soluble Tim-3-galectin-9 complex are significantly higher in blood plasma of AML patients compared to that of healthy donors. Galectin-9 and Tim-3 concentrations in blood plasma of 98 AML patients and of 12 healthy donors were analysed by ELISA (A, B, E and F). Five randomly chosen plasma samples of each group were used for Tim-3-galectin-9 ELISA-based detection (C and G). Five randomly selected blood plasma obtained from AML patients and healthy donors were sonicated, boiled for 5 minutes at 95º C and subjected to Western blot analysis (D). Correlations between the levels of Tim-3 and galectin-9 as well as Tim-3-galectin-9 complex and galectin-9 in blood

plasma were determined for both healthy donors (H and J) and AML patients (I and K). Images are from one experiment representative of five which gave similar results. Quantitative data are mean values ±SEM (n=3) *p < 0.05; **p < 0.01; ***p < 0.001 vs. control.....81

Figure 29: Interaction of Tim-3 with galectin-9 leads to major conformational changes increasing solubility of the protein complex. Galectin-9 (right) and extracellular domain of Tim-3 (left) are schematically represented in panel A. In Tim-3 structure, amino acid residues involved in galectin-9-independent binding are highlighted in green., while those which can be potentially glycosylated are shown in red. In galectin-9 structure, sugar molecules possibly involved in the binding with the glycoprotein and located close to the close to the carbohydrate binding sites are illustrated in green (A). The SRCD spectroscopy of Tim-3, galectin-9 and Tim-3-galectin-9 interaction (both simulated and real curves are presented) (B). 83

Figure 30: LPHN1, PKCαand mTOR pathways are involved in Tim-3 and galectin-9 production and secretion in AML cells. THP-1 cells were exposed to 100 nM PMA or 250 pM LTX for 16 h with or without 1 h pre-treatment with the PKCα inhibitor Gö6983 (A, B, D) or the mTOR inhibitor AZD2014 (C, D). Cellular levels of Tim-3 and galectin-9 were characterised by Western blot. The p-S2448 mTOR was measured by ELISA. Secreted Tim-3 and galectin-9 were detected by ELISA. Images are from one experiment representative of three which gave similar results. Quantitative data are the mean values ± SEM of three independent experiments; *p b 0.05; **p b 0.01; ***p b 0.001 vs. control. Symbols “a” or “b” are used instead of “*” to indicate differences vs. PMA and LTX-treated cells, respectively. 85

Figure 31: LTX induces Tim-3 and galectin-9 release in primary human AML cells. Primary human AML blasts (AML-PB001F) were incubated for 24 h with 250 pM LTX. The media was then subjected to ELISA for galectin-9 and Tim-3 detection (A). Harvested cells after the incubation were lysed and subjected to Western blot analysis and LPHN1 expression was

characterised (B). Images are from one experiment representative of six which gave similar results. Quantitative data are mean values ± SEM of six independent experiments; **p < 0.01 vs. control.....86

Figure 32: FLRT3 induces galectin-9 and Tim-3 secretion in THP-1 cells. (A) THP-1 cells were treated for 16 h with 10 nM extracellular domain of human recombinant FLRT3. The concentrations of galectin-9 and Tim-3 in the media obtained were determined by ELISA. (B) THP-1 cells were incubated with mouse bone marrow (mBM) extracts (10 μg protein/ml) for 16 h with or without 1 h pre-treatment with 5 μg/ml anti-FLRT3 antibody. The presence of FLRT3 in mBM extracts was confirmed by Western blot analysis. The levels of Tim-3 and galectin-9 released in the media were measured by ELISA. (C) The presence of FLRT3 was also confirmed in RCC-FG1 cells by Western blot analysis. RCC-FG1 cells were co-cultured with THP-1 cells at a ratio of 1 THP-1:2 RCC-FG1 with or without 1 h pre-treatment with 5 μg/ml FLRT3 neutralizing antibody. The levels of Tim-3 and galectin-9 released in the media were measured by ELISA. Images are from one experiment representative of three which gave similar results. Quantitative data depict mean values ± SEM of three independent experiments; *p b 0.05; **p b 0.01; ***p b 0.001 vs. control. Symbols “a” or “b” are used instead of “*” to indicate differences vs. cells treated with mBM extracts or co-cultured with RCC-FG1 cells, respectively. 88

Figure 33: PMA, LTX and FLRT3 upregulate PKCα activity in THP-1 cells. (A) PKCα activity was analysed in resting THP-1 cells as well as those exposed for 16 h to 100 nM PMA, 250 pM LTX and 10 nM FLRT-3. (B) PKCα activity was analysed in resting THP-1 cells and those co-cultured with RCC-FG1 cells (ratio 1 THP-1: 2 RCC-FG1) in the absence or presence of 5 μg/ml FLRT-3 neutralising antibody. Images are from one experiment representative of three which gave similar results. Quantitative data are mean values ± SEM of three independent

experiments; *p < 0.05; **p < 0.01 vs. control. Symbol “bb” indicates p<0.01 vs. THP-1/RCC-FG1 co-culture. 89

Figure 34. LAD2 cells express and externalize Tim-3 and galectin-9. Left panel: the levels of cell surface and total Tim-3 and galectin-9 in LAD2 cells were measured using LICOR in cell assay (ICA, non-permeabilized cells) and in cell Western (ICW, permeabilized cells). Right panel: LAD2 cells were cultured in presence or absence of 0.1 μg IgE; Tim-3 and galectin-9 intracellular levels were measured by Western blot analysis, while the amount of secreted galectin-9 was characterised by ELISA. Images are from one experiment representative of three which gave similar results. Quantitative data show mean values ± SEM of three independent experiments; ***p b 0.001 vs. control. 90

Figure 35: Primary human NK cells express Tim-3 but don’t produce detectable amounts of galectin-9 in primary human NK cells. Expressions of both proteins were analysed in whole cell extracts by Western blot. Human recombinant galectin-9 was used as a positive control. Images are from one experiment representative (two donors in each) of three which gave similar results. 91

Figure 36: Galectin-9 participates in the formation of an “immunological synapse” between NK cells and LAD2 cells. Primary human NK cells were immobilized on the surface of Maxisorp plates. Cells were then co-cultured for 30 min with LAD2 cells with or without 30 min pre-treatment of LAD2 cells with 5 μg/ml galectin-9 neutralizing antibody (or the same amount of isotype control antibody). LAD2 cells were then visualized using LI-COR assay as outlined in Materials and Methods. Images are from one experiment representative of five which gave similar results. Quantitative data represent mean values ± SEM of five independent experiments; *p < 0.05; **p < 0.01. 92

Figure 37: Galectin-9 protects myeloid leukaemia K562 cells from being killed by primary human NK cells. K562 cells were incubated for 24 h with PMA in 96-well Maxisorp plates.

(A) After 24 h, PMA-containing media was replaced with the media containing primary human NK cells. K562 and NK cells were then co-cultured (at ratio 1:2) for 16 h in the absence or presence of 5 ng/ml galectin-9. Viability of K562 and NK cells was measured using MTS test. Images are from one experiment representative of three which gave similar results. Quantitative data represent mean values ± SEM (n=3) independent experiments; ***p < 0.001 vs. control. (B) K562 cells co-incubated for 16 h with primary human NK cells, at a 1:2 ratio, in presence or absence of galectin-9 5 ng/ml. Cells were imaged using phase-contrast microscopy. The images are from one representative experiment of six (n = 6), which gave similar results. Scale bar (the same for all images), 50 μm. (C) NK cells induced aggregation of K562 cells was quantified as a function of galectin-9 concentration. Left, the per cent of cells found in aggregates in individual cultures and in the co-culture. Right, the size of cell aggregates in individual cultures and in the co-culture. The data represent the mean values ± SD of six independent experiments; *, p < 0.05; **, p < 0.01; ****, p < 0.0001 93

Figure 38: Cell-derived galectin-9 attenuates AML cell killing activity of primary human NK cells. PMA pre-treated THP-1 cells were co-cultured with primary human NK cells at 1:2 ratio for 6 h. After the incubation, MTS test was performed on isolated THP-1 cells. Granzyme B and caspase 3 activity was also characterised in THP-1 cell lysates as described in Materials and Methods (left panel). Galetin-9 levels in the media were measured using ELISA (left panel). NK cells were subjected to Western blot analysis for specific detection of galectin-9 and Tim-3 (right panel). Images are from one experiment representative of three which gave similar results. Quantitative data show mean values ± SEM of three independent experiments; *p < 0.05; **p < 0.01; ***p < 0.001 vs control.....96

Figure 39: Soluble Tim-3 attenuates IL-2 release. (A and B) The levels of IL-2 in blood plasma obtained from AML patients and healthy donors were measured by ELISA. (C) Jurkat T cells were treated with increasing concentration of Tim-3 for 24 h. After the treatment the media

was subjected to ELISA for IL-2 detection. Data show mean values ± SEM of three independent experiments; *p < 0.05; **p < 0.01.....97

Figure 40: Possible biochemical interactions between AML and NK cells. Triggering of LPHN1 leads to the surface expression and release of galectin-9 by AML cells. Cell surface-associated or secreted galectin-9 binds then to the NK cell receptor (likely – Tim-3). This interaction induces NK cells to release of IFN-γ, which stimulates IDO1 to convert tryptophan (Trp) into formyl-kynurenine (FKU) inside AML cells. FKU is then further degraded into L-kynurenine (KU), which can be released by AML cells. KU attenuates the ability of NK cells to deliver granzyme B into AML cells in perforin/mannose-6-phosphate receptor (MPR)-dependent manner. If successfully delivered, granzyme B catalyses the cleavage of the protein Bid into tBid, which leads to mitochondrial disfunction with consequent release of cytochrome c from the mitochondria into the cytosol of malignant cells. Once liberated in the cytosol, cytochrome c induces apoptosome formation leading to the activation of caspase-3. Furthermore, granzyme B is capable of performing direct proteolytic activation of caspase-3. These effects lead to AML cell apoptosis. However, this process is not taking place in presence of galectin-9, which impairs NK cell cytotoxic activity as described above.....102

Figure 41: Pathobiochemical pathway allowing AML cells to escape host anti-cancer immunity. The interaction of FLRT3, expressed on the surface of endothelial cells (EC), with AML surface receptor, LPHN1, leads to the activation of Gq which then stimulates PLC. Activated PLC catalyses the hydrolysis of phosphatidyl-inositol-bisphosphate (PIP2) into inositol-trisphospate (IP3) and diacylglycerol (DAG). IP-3 is then able to bind ER-associated IP3 receptor (IP3R) leading to Ca2 + mobilization. Released IP3 and DAG activate PKC-α, which triggers mTOR translational pathway through downregulation of TSC1/TSC2. This leads to increased synthesis of galectin-9 and Tim-3. In addition, PKCα phosphorylates protein Munc18 leading to the formation of SNARE complexes, which tether cytosolic vesicles to the

plasma membrane. This pre-activates the release machinery, and elevated cytosolic Ca2 + lead to exocytosis of free and galectin-9-associated Tim-3. Once expressed on the membrane of AML cells, both types of Tim-3 are differentially shed from the cell surface by proteolytic enzymes. Galectin-9 impairs the ability of NK cells to kill AML cells, while sTim-3 attenuates the release of IL-2, cytokine required for the activation of immune cells. 104

Figure 42: Characterisation of expression of LPHN1, Tim-3 and galectin-9 proteins in CD34-positive human stem cells (HSCs) and THP-1 AML cells (positive control). Western blot analysis was employed for the detection of LPHN1, Tim-3 and galectin-9 proteins in CD34-positive HSCs and THP-1 cells. Images are from one experiment representative of three which gave similar results. 106

Figure 43: Comparative analysis of LPHN1 protein expression in primary human AML, THP-1 cells and PHL. Lysates of each cell type were subjected to Western blot analysis. Images are from one experiment representative of three which gave similar results. Data are the mean values ± SEM of three independent experiments; **p < 0.01 vs. AML cells. 107

Figure 44: LPHN1 expression in human AML cells and haematopoietic stem cells, but not in primary healthy human leukocytes, is upregulated by cortisol. Primary human AML, THP-1 and haematopoietic stem cells as well as primary healthy leukocytes (PHL) were treated with 1 μM cortisol for 24 h. The levels of LPHN1 mRNA were measured by quantitative real-time PCR (A). LPHN1 protein levels were characterised by Western blot analysis (B – primary AML cells, C – THP-1 cells and D – PHL). For PHL, lysates of LPHN1 overexpressing NB2A cells were used as a positive control. The concentrations of secreted galectin-9 were measured by ELISA (B, C, D). Images are from one experiment representative of four which gave similar results. Data represent mean values ± SEM for four independent experiments. *p < 0.05; **p < 0.01 vs. control. 108

Figure 45: The levels of cortisol and galectin-9 are significantly higher in blood plasma of AML patients compared to healthy donors one. Blood plasma of ten healthy donors and ten AML patients was collected at the same time of the day to avoid the influence of circadian dynamics ensuring comparability of cortisol levels. The levels of cortisol (left panel) and galectin-9 (right panel) were measured by ELISA, and the correlation between these two proteins was analysed. Data are the mean values ± SEM of ten independent experiments.; *p < 0.05; **p < 0.01; ***p < 0.01 vs control. 109

Figure 46: Soluble LPHN1 fragments are elevated in blood plasma of AML patients. Blood plasma of ten healthy donors and ten AML patients was subjected to immunoprecipitation employing Santa Cruz mouse monoclonal antibody as capture antibody. Obtained extracts were then subjected to Western blot analysis using rabbit anti-LPHN1 antibody (PAL-1 or Abcam anti-LPHN1 antibody) for detection (A). Specific detection of soluble LPHN1 fragments (in the same blood samples) was performed using ELISA as outlined in Material and Methods (B). Images are from one experiment representative of six which gave similar results. Data are the mean values ± SEM of ten independent experiments; *p < 0.05; **p < 0.01; ***p < 0.01 vs control. 111

Figure 47: On cell detection of cell surface presence of rabbit polyclonal antibody recognising LPHN1 (clone name RL1). LPHN1 negative NB2A cells (negative control) and THP-1 cells were subjected to on cell assay using anti-rabbit Li-Cor secondary antibody. Images are from one experiment representative of three which gave similar results. 112

Figure 48: FLRT3, component normally circulating in blood plasma, induces galectin-9 secretion in AML cells in a LPHN1-dependent manner. THP-1 cells and PHL were exposed to 10 nM human recombinant FLRT3 for 16 h followed by detection of secreted galectin-9 levels by ELISA. In THP-1 cells, the treatment was performed with or without 1 h pre-exposure to 1 µg/ml RL1 anti-LPHN1 polyclonal antibody (A). The levels of secreted FLRT3 and its

fragments were analysed in the blood plasma of healthy donors and AML patients using Western blot (B). THP-1 cells were exposed for 16 h to 10% blood plasma either from healthy donors or AML patients with or without pre-treatment with FLRT3 neutralising antibody. Levels of secreted galectin-9 were analysed using ELISA (C). Data are shown as mean values ± SEM from four independent experiments; *p < 0.05; **p < 0.01 vs. control. 113

Figure 49: Interaction of FLRT3 with LPHN1 leads to significant conformational changes. SRCD spectroscopy of FLRT3, LPHN1 FLRT3-LPHN1 interaction (both simulated and real curves are presented).....114

Figure 50: Physiological cross-links leading to cortisol-induced upregulation of LPHN1 expression in AML cells followed by facilitation of galectin-9 secretion in a FLRT3-dependent manner. AML is associated with a decreased blood plasma glucose levels, which normally leads to upregulation of secretion of corticotropin-releasing hormone (CTRH) by hypothalamus. CTRH induces secretion of adrenocorticotropic hormone (ACTH) by pituitary gland. Secreted ACTH upregulates cortisol production by the adrenal cortex, thus leading to cortisol-induced upregulation of LPHN1 levels in AML cells. Galectin-9, secreted in FLRT3-LPHN1-dependent manner attenuates anti-cancer activity of cytotoxic T cells (CTC) and NK cells. 116

Figure 51: Differential receptors are involved in HMGB1-induced biological responses of human AML cells. Total levels of the immune receptor Tim-3 and its surface presence were characterised in THP-1 and primary human AML-PB001F cells by in-cell Western (ICW) and in-cell (on-cell) assay (ICA) respectively. Both cell types were exposed to 1 µg/ml HMGB1 for 4 h with or without 1 h pre-treatment with single chain anti-Tim-3 antibody (aTim-3 (-)) followed by Western blot analysis of phospho-S65 vs total eIF4E-BP1, HIF-1α and RAGE expression as well as by detection of phospho-S2448 mTOR, release of TNF-α and VEGF using ELISA. PI-3 K activity was monitored by colorimetric assay. Images are from one

experiment representative of five which gave similar results. Data is shown as mean values ± SEM of five independent experiments. * p < 0.05; **, p < 0.01 and *** when p < 0.001 vs control; [a] p< 0.05; [aa], p < 0.01 vs HMGB1.....118

Figure 52: HMGB1 binds Tim-3 with a high binding affinity. Recombinant, purified Ig-like V-type domain of human Tim-3 (residues 22–124) and human HMGB1 were employed for these experiments. Interaction of HMGB1 protein with Tim-3 was analysed using SRCD spectroscopy-based titration which was conducted in the far UV region using 0.2 μM HMGB1 and increasing stoichiometric concentrations of Tim-3 (A). Changes in CD signal monitored at 222 nm were plotted against Tim 3 concentration using Hill function. Qualitative binding was verified by analysis of interactions of equimolar concentrations of Tim-3 and HMGB1 using SRCD spectroscopy (B).....120

Figure 53: TLRs 2 and 4, but not RAGE, are involved in HMGB1-induced TNF-α secretion. THP-1 cells were pre-treated for 1 h with the indicated concentrations of TLR2/4 and RAGE-neutralising antibodies followed by 4 h exposure to 1 μ/ml HMGB1. TNF-α concentrations were then measured in the culture medium by ELISA. Data are shown as mean values ± SEM for three independent experiments. * p<0.05; **, p<0.01 vs control; a p<0.05; aa, p<0.01 vs HMGB1.....121

Figure 54: HMGB1 triggers an intercellular signalling cascade leading to SCF secretion. (A) Primary human AML cells (AML-PB-001F) were incubated for 4 h with 1 μg/ml HMGB1 followed by collection of the culture medium (detection of TNF-α was performed in this medium using ELISA), which was used to culture primary human healthy leukocytes for 4 h in the absence or presence of TNF-α-neutralising antibody. Medium was collected (levels of IL-1β were measured by ELISA) and used to culture MCF-7 breast cancer epithelial cells for 4 h in the absence or presence of IL-1β-neutralising antibody. Following this exposure, medium was collected and SCF was measured in it by ELISA. (B) Primary mouse bone marrow

cells (10^6 cells per 3 ml medium) were exposed for 24 h to 1 µg/ml HMGB1 followed by detection of TNF-α, IL-1β and SCF by ELISA. (C – I). Levels of TNF-α, IL-1β and SCF were measured in the blood plasma of healthy donors and AML patients by ELISA. Mean values ± SEM are presented as well as levels of each protein in blood plasma of each analysed donor/patient. *p < 0.05; **p< 0.01 vs control.....123

Figure 55: Correlation between TNF-α, IL-1β and SCF levels in the blood plasma of healthy donors and AML patients. Data were obtained from the blood plasma of healthy donors (n=10) and AML patients (n=30). Correlation analysis was performed using GraphPad Prism (R2 values are presented in Figure 54 C).....124

Figure 56: HMGB1 induces SCF and VEGF production via interaction with differential signalling receptors. The scheme shows that secreted HMGB1 is capable of inducing TNF-α secretion by living AML cells (and possibly healthy leukocytes, based on results obtained in the experiments with mouse bone marrow samples). Secreted TNF-α induces IL-1β production by healthy leukocytes which then induces SCF release in endothelial cells. These processes are Tim-3-independent. HMGB1 also induces VEGF secretion by AML cells in Tim-3-dependent manner.....125

Figure 57: Expression of FLRT3/LPHN/Tim-3/galectin-9 pathway components and activities of PLC/PKCα and mTOR pathways in primary human breast tumours. Expression levels of Tim-3, galectin-9 (A), FLRT3 and LPHN2 (B) were analysed in primary breast malignant tumours and healthy breast tissues (HT) of five patients (n=5) by Western blot. Activities of PLC, PKCα and the levels of phospho-S2448 mTOR were detected as outlined in the Materials and Methods (C). The amounts of phospho-S65 and total eIF4E-BP (mTOR substrate) were analysed using Western blot (D). The levels of CD3 (biomarker of T cells) were also measured using lysate of Jurkat T cells as a positive control (E). Molecular weight markers (MW) are expressed in kDa. Images are from one experiment representative of five which gave similar

results. Other results are shown as mean values ± SEM. * p<0.05; **, p<0.01 and *** when p<0.001 vs control. 129

Figure 58: Expression of galectin-9 in primary human breast tumours and healthy breast tissues. Lysates of primary breast malignant tumours and healthy breast tissues (HT) of five patients (n=5) were subjected to Western blot using 10 % PAGE. Specific detection of galectin-9 was performed employing Abcam rabbit anti-galectin-9 antibody. Images are from one experiment representative of five which gave similar results. Other results are shown as mean values ± SEM. *** p<0.001 vs HT.....130

Figure 59: Expression, interaction and co-localisation of Tim-3 and galectin-9 in primary human breast tumours. (A) Presence of the Tim-3-galectin-9 complex in primary normal and tumour tissue extracts was analysed using ELISA as outlined in the Materials and Methods. (B) Expression and co-localisation of galectin-9 and Tim-3 were analysed in primary human breast tumours and healthy tissues of the same patients using confocal microscopy (see Materials and Methods for further details). Images are from one experiment representative of five which gave similar results. Scale bars correspond to 20 µm.....131

Figure 60: Levels of galectin-9, Tim-3 and IL-2 in blood plasma of human healthy donors and patients suffering from primary and metastatic breast tumours. (A) Concentrations of galectin-9, soluble Tim-3 and IL-2 were analysed in blood plasma of healthy donors and breast cancer patients by ELISA. Data are shown as mean values ± SEM of 20 for healthy donors (HD), 42 for primary breast cancer (PBC) patients and 20 for metastatic breast cancer (MBC) patients. * - p<0.05; **, p<0.01 and vs HD. 132

Figure 61: Expression of crucial components of FLRT3/LPHN/Tim-3/galectin-9 pathway in MCF-7 cells and primary human breast tumours. (A) Expression of a key components of this pathway was characterised in MCF-7 cells and primary breast tumour tissue lysates using Western blot analysis. Beta-actin was used as a housekeeping protein. (B) Levels of galectin-

9 mRNA were compared in normal and healthy breast tissues as well as in MCF-7 cells and normalised against those of β-actin. (C) Expression of LPHN3 was detected in primary human breast tumour tissue lysates and MCF-7 cells. (D) Expression of GαQ was detected in primary human breast tumour tissue lysates and MCF-7 cells. Images are from one experiment representative of at least three which gave similar results. Data are the mean values ± SEM of five independent experiments; **, p<0.01 and *** when p<0.001 vs control (HT). 133

Figure 62: FLRT3 induces translocation of galectin-9 onto the surface of MCF-7 breast cancer cells. (A) MCF-7 cells were exposed for 4 h to 10 nM FLRT3 and activities of PLC, PKCα, the levels of phospho-S2448 mTOR and the amounts of phospho-S65 and total eIF4E-BP (an mTOR substrate) were analysed as described in the Materials and Methods. (B) MCF-7 cells were exposed for 4 h to 10 nM FLRT3 with or without 1 h pre-treatment with 30 µM U73122 (PLC inhibitor) or 70 nM Gö6983 (PKCα inhibitor). Surface presence of galectin-9 was characterised by on-cell assay. (C) Secondary structure and conformational changes of LPHN2 olfacomedin-like domain, FLRT3, and the complex of the two proteins mixed at the equimolar ratio were characterised using SRCD spectroscopy as outlined in the Materials and Methods. An interaction between olfactomedin-like domain of LPHN3 and FLRT3 generated by Swiss PDB viewer (5cmn.pdb file downloaded through PubMed database was used (Prokhorov et al., 2015)) is presented to illustrate the structural basis of this interaction. Images are from one experiment representative of four which gave similar results. Other results are shown as mean values ± SEM of at least three independent experiments. * p<0.05; **, p<0.01 vs control..134

Figure 63: Galectin-9 protects MCF-7 cells against T cell-dependent cytotoxic immune attack. (A) MCF-7 cells were co-cultured with TALL-104 cytotoxic T lymphocytes at a ratio of 4 : 1 for 16 h (the ratio was determined by the aggressive behaviour of TALL-104 cells) in the absence or presence of 5 µg/ml galectin-9 neutralising antibody or 5 µg/ml isotype control antibody. (B) After the experiment TALL-104 cells were lysed and PARP cleavage, as an

indicator of the rate of apoptotic cells, was measured using Western blot analysis. (C) CD8 expressions (reflecting the infiltration of TALL-104 into the MCF-7 layer) were measured by on-cell assay. (D) Galectin-9 surface presence was measured using on-cell assay in resting MCF-7 cells and those co-cultured with TALL-104 cells. (E) Viability of MCF-7 cells was measured by MTS test. Images are from one experiment representative of five which gave similar results. Other results are presented as mean values ± SEM of five independent experiments. * $p<0.05$ vs control. 136

Figure 64: Breast cancer cell-based pathobiochemical pathways showing LPHN-induced activation of PKCα, which triggers the translocation of Tim-3 and galectin-9 onto the cell surface which is required for immune escape. The interaction of FLRT3 with LPHN isoform leads to the activation of PKCα, most likely through the classic Gq/PLC/Ca^{2+}pathway. Ligand-bound LPHN activates Gq, which in turn stimulates PLC. This leads to phosphatidyl-inositol-bisphosphate (PIP_2) degradation and production of inositol-trisphospate (IP_3) and diacylglycerol (DAG). PKCα is then activated by DAG and cytosolic Ca^{2+}. PKCα provokes the formation of SNARE complexes that tether vesicles to the plasma membrane. Galectin-9 impairs the cancer cell killing activity of cytotoxic T cells (and other cytotoxic lymphocytes). Possible (not directly confirmed) interactions of galectin-9 with glycoside component and T cell receptor (TCR)/CD8, with MHC I and antigen are highlighted with question mark "?" to indicate the fact that it is a hypothetic interaction, since TALL-104 cells used in the study kill tumour cells in MHC-independent manner. 140

Figure 65: Molecular weight, isoforms and glycosylation level of the proteins reported in Table 1 and 2. Tim-3: lower band represents non-glycosylated protein, upper band(s), protein with differential levels of glycosylation; Galectin-9: multiple bands represent different isoforms of the same protein; FLRT3 – detectable between 80 and 95 kDa (upper band where applicable or the only visible band); another band (lower band; possibly extracellular domain) often

appears at around 60 most likely reflecting levels of glycosylation in first two cases and proteolytic processing in the third. Traces – detectable expression which requires loading of >100 µg protein per well.....144

Figure 66: Expression of Tim-3, galectin-9, LPHNs 1, 2 and 3 as well as FLRT3 proteins in various human cancer cell lines. Lysates of indicated cells were subjected to Western blot analysis as outlined in Materials and Methods (images are presented in Supplementary table 1). Detected infrared fluorescence of the bands divided by the total protein amounts loaded (measured using Bradford assay) was used as a measure of protein quantity. Levels of Tim-3 & total galectin-9 (A) and LPHNs 1, 2 & 3 (B) were expressed as a % of those levels present in THP-1 cells (expressed as 100%). Since THP-1 cells lack FLRT3 expression, the levels of this protein were expressed as % RCC-FG1 (C), respectively considering FLRT3 level in these cells as 100%. Abbreviations used – Bn – brain, CR – colorectal, Ki – kidney, BBM – blood, bone marrow and mast cells, Li – liver, Br – breast, Pr – prostate, Lu – lung, Sk – skin. Data are presented as mean values ± SEM of three independent experiments. 145

Figure 67: Pro-apoptotic defunctionalisation of mitochondria reduces galectin-9 expression and leads to its redistribution in human Colo-205 colorectal adenocarcinoma cells. Colo-205 cells were exposed to 100 µM BH3I-1 for 24 h followed by (A) detection of cell viability using an MTS test and colorimetric assay of caspase 3 activity. Cell viability was also tested for normal and Tim-3 or galectin-9 knockdown Colo-205 cells. (B) Following 24 h of exposure to BH3I-1 S65-phosphorylation levels of eIF4E-BP were analysed by Western blot. (C) Surface presence and total cellular levels of Tim-3 and galectin-9 were analysed in Colo-205 cells using FACS. (D) Secreted levels of galectin-9 were analysed in Colo-205 cells following 24 h of exposure to BH3I-1 by ELISA. (E) Surface levels of galectin-9 in non-treated and BH3I-1-stimulated Colo-205 cells were compared using an on-cell assay. (F) The presence of Tim-3-galectin-9 complex in Colo-205 cells was confirmed using Western blot analysis (bands were

appearing at around 70 KDa). THP-1 cells were used as a positive and K562 as a negative control. (G) Levels of Tim-3 and galectin-9 were analysed in Colo-205 lysates following 24 h of exposure to BH3I-1 by Western blot. (H) Mitochondrial extracts were obtained from non-treated and BH3I-1-stimulated Colo-205 cells and subjected to Western blot analysis to detect Tim-3 and galectin-9. Total protein levels were measured using a Bradford assay and equal protein amounts were loaded onto the gels. (I) Galectin-9 mRNA levels were analysed in non-treated Colo-205 cells and those exposed to BH3I-1 using qRT-PCR. Images are from one experiment representative of at least four which gave similar results. In the scheme galectin-9 is abbreviated as G9. Quantitative results are shown as mean values ± SEM of 3 - 6 independent experiments. * $p<0.05$; **, $p<0.01$ vs control. 147

Figure 68: Total cellular levels of Tim-3 and galectin-9 and levels of secreted galectin-9 in THP-1 human AML cells. Total Tim-3 and galectin-9 levels were measured by FACS in permeabilised THP-1 cells. The secreted levels of galectin-9 were also measured in culture medium, in which THP-1 cells were kept for 16 h and compared with those of Colo-205 cells cultured under the same conditions. Images are from one experiment representative of at least four which gave similar results. Other results are shown as mean values ± SEM of five independent experiments. ** $p<0.01$ vs control. 149

Figure 69: Mitochondrial defunctionalisation reduces intracellular galectin-9 levels in both healthy (RC-124) and malignant (HepG2) epithelial cells but induces galectin-9 translocation into mitochondria only in malignant (HepG2) cells. Cells were exposed to 1 mM H2O2 for 6 h followed by Western blot analysis of cellular and mitochondrial levels of Tim-3 and galectin-9 in both RC-124 (A) and HepG2 (B) cells. In mitochondria of RC-124 cells Tim-3, galectin-9 and the complex of both proteins (MW ~ 70 KDa) was not detectable, while in mitochondria isolated from HepG2 cells a complex was clearly detectable in H2O2-stimulated cells. Images are from one experiment representative of at least four which gave similar results. Quantitative

results are shown as mean values ± SEM of four independent experiments. ** p<0.01 vs control. 150

TABLES

Table 1 Cancer classification 10

Table 2: List of major DAMPs and their respective PPRs. 19

Table 3: Main functions of HMGB1-induced cytokines in early stages of inflammation 22

Table 4: Virus associated tumours 30

Table 5: Major B7 ligands and their binding partners 33

Table 6: Anti-CTLA-4 and anti-PD-1 monoclonal antibodies approved by European Medicine Agency (EMA) for cancer treatment 35

Table 7: Expression of Tim-3, galectin-9, LPHNs 1, 2 and 3 as well as FLRT3 proteins in brain, colorectal, kidney, blood/bone marrow cell lines. Cell lysates were subjected to Western blot analysis for specific detection of the proteins. The concentration of galectin-9 in the media used to culture these cells was measured by ELISA. 142

Table 8: Expression of Tim-3, galectin-9, LPHNs 1, 2 and 3 as well as FLRT3 proteins in liver, breast, prostate, lung and skin cell lines. Cell lysates were subjected to Western blot analysis for specific detection of the proteins. The concentration of galectin-9 in the media used to culture these cells was measured by ELISA. 143

Table 9: PAGEs preparation 173

Table 10: Sample Buffer preparation 173

ABBREVIATIONS

Ab: Antibody

Abl: Gene Abelson

ADAM: **a** **d**isintegrin **a**nd **m**etalloproteinase domain-containing proteins

AGEs: Advanced glycation end products

ALL: Acute lymphoid leukaemia

AML: Acute myeloid leukaemia

Apaf-1: Apoptotic protease activating factor-1

APC: Antigen presenting cell

Apo-1: Apoptosis antigen 1 (also called Fas)

ATL: Adult T-cell leukaemia

BAK: BCL2-antagonist/killer

Bat3: HLA- B associated transcript 3

Bcl-xL: B-cell lymphoma-extra-large protein

BCR: B cell receptors

BCR: Breakpoint cluster region

BID: BH3 Interacting Domain Death Agonist

BSA: Bovine serum albumin

CDK: Cyclin-dependent kinases

CKI: Cyclin-dependent kinase inhibitors

CML: Chronic myelogenous leukaemia

CRD: Carbohydrate recognition domain

CTC: Cytotoxic T cell

CTL: Cytotoxic T cell

CTLA-4: Cytotoxic T lymphocyte antigen-4

DAG: Diacyl glycerol

DAMPs: Damage-associated molecular patterns

DAP: 2,3-diaminophenazine

DC: Dendritic cell

DD: Death domain

DED: Death effector domain

DISC: Death-inducing signalling complex

DTT: Dithiothreitol

EBV: Epstein–Barr virus

ECM: Extracellular matrix

EDTA: Ethylenediaminetetraacetic acid

eIF4E: Initiation factor 4E

eIF4E-BP: eIF4E binding protein

EMA: European Medicine Agency

ER: Endoplasmic reticulum

ERK: Extracellular signal–regulated kinases

FACS: Fluorescence-activated cell sorting

FADD: Fas-associated protein with death domain

FasL: Fas ligand

FBS: Foetal bovine serum

FKU: Formyl-L-kynurenine

FLRT3: Fibronectin leucine rich transmembrane protein 3

HBV: Hepatitis B virus

HCV: Hepatitis C virus

HD: Healthy donors

HIF-1: Hypoxia-inducible factor 1

HMGB1: High-mobility group box 1

HPA: Hypothalamic-pituitary-adrenal axis

HPV: Human genital papillomavirus

HRP: Horse radish peroxidase

HSC: Hematopoietic stem cell

HTLV-1: Human T-lymphotropic virus-1

IDO1: Indoleamine 2,3-dioxegenase

IFN-γ: Interferon γ

IgV: Immunoglobulin variable domain

IL-1β: Interleukin 1β

IL-6: Interleukin 6

IL-8: Interleukin 8

IP3: Inositol 1,4,5-trisphosphate

KU: L-kynurenine

LPHN: Latrophilin

LRR: Leucin-rich repeats

MDS: Myelodysplastic syndromes

MHC: Major histocompatibility complex

MICA: MHC class I chain-related protein A

MICB: MHC class I chain-related protein B

MSCs: Mesenchymal cells

mTOR: Mammalian target of rapamycin

MW: Molecular weight

NFκB: Nuclear factor kappa-B

NK: Natural Killer

NKG2D: Natural Killer Group 2D

NSCLC: Non-small-cell lung carcinoma

OPD: Orto-phenylenediamine

PARP: Poly ADP ribose polymerase

PBS: Phosphate-buffered saline

PD-1: Protein cell death 1

PDL: Poly-D-lysine

PD-L1: PD ligand 1

PD-L2: PD ligand 2

PES: Phenazine ethosulfate

PHDs: Prolyl hydroxylases

PIP2: Phosphatidylinositol 4,5-bisphosphate

PKCα: Protein kinase Cα

PLC: Phospholipase C

PMA: Phorbol 12-myristate 13-acetate

PMSF: Phenylmethylsulfonyl fluoride

PRRs: Pattern recognition receptors

qRT-PCR: Reverse transcription polymerase chain reaction

RAGE: Receptor for advanced glycation end products

RB: Retinoblastoma

S6K1: Ribosomal protein S6 kinase beta-1 (also called p70S6 kinase)

SCCHN: Squamous cell cancer of the head and neck

SCF: Stem cell factor

SDS: Sodium dodecyl sulphate

SDS-PAGE: Sodium dodecyl sulphate-polyacrylamide gel electrophoresis

SH2: Src homology 2

SRCD: Synchrotron radiation circular dichroism

STS: Soft tissue sarcomas

TBST: Tris-buffered saline, 0.1% Tween 20

TCR: T cell receptor

Tim-3: T cell immunoglobulin and mucin domain 3

TIR: Toll-interleukin 1 (IL-1) receptor domain

TLR: Toll-like receptors

TMB: 3,3′,5,5′-tetramethylbenzidine

TNFR: TNF receptor

TNF-α: Tumour necrosis factor α

TPI: Triosephosphate isomerase

VEGF: Vascular endothelial growth factor

1. INTRODUCTION

Cancer is a wide group of systemic disorders resulting from growth of abnormal cells which have a potential to invade and/or spread to other parts of the body.

Taken together, cancers are the second leading cause of death worldwide and remain a serious medical burden in countries of all income levels (WHO, 2018; IARC, 2018)

Until the middle of XX century cancer incidence and mortality rates were almost the same. Since then, great effort has been made to uncover fundamental mechanisms underlying cancer physiopathology for the development of the treatments for different types of malignancies (Richiardi & Terracini, 2015). Although cancer prognosis is no longer as catastrophic as in the past, there are still a huge number of individuals dying because of the cancer each year.

Approximately 18.1 million cancer diagnoses and 9.1 million cancer-associated deaths were registered in 2018 worldwide (IARC, 2018). Just ten years earlier (2008), these numbers were considerably lower: 12.7 million cancer cases and 7.6 cancer-related deaths (Ferlay et al., 2010). Indeed, cancer incidence and mortality are unceasingly increasing globally as reported in Figure 1 (Ferlay et al., 2010; Fitzmaurice et al., 2015; IARC, 2018; Parkin et al., 2005; Parkin, 2001; Torre et al., 2016). Furthermore, cancers are expected to become the first leading cause of death, principally, as a result of considerable reduction in mortality rates of other major diseases, such as stroke and coronary diseases (Bray et al., 2018).

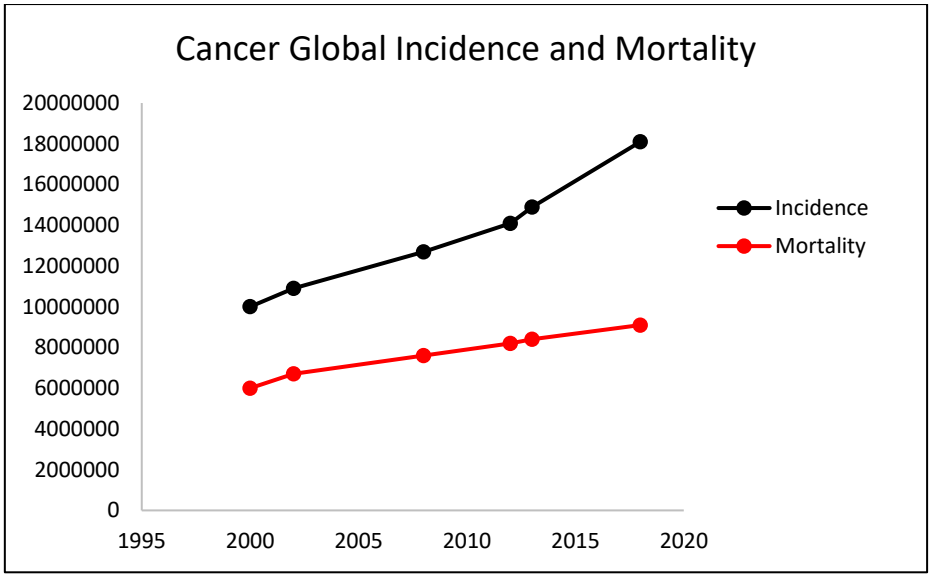


Figure 1: Cancer Global Incidence and Mortality. Incidence and mortality are reported as absolute numbers of new cancer cases and cancer-related deaths, respectively, per annum (Ferlay et al., 2010; Fitzmaurice et al., 2015; IARC, 2018; Parkin et al., 2005; Parkin, 2001; Torre et al., 2016).

Although the absolute number of cancer-related deaths is increasing globally, the mortality rate, expressed as the ratio between the number of deaths and the number of new cancer cases, is plateauing or decreasing for various types of malignancies in higher income countries (HIC) (Fitzmaurice, 2017; Torre et al., 2016). This phenomenon is due to several factors. Firstly, the development of more effective treatments, as a result of massive advances in cancer research, has led to significant improvements in cancer survival rates (Arruebo et al., 2011; Falzone, Salomone, & Libra, 2018). Furthermore, the progress in medical technologies as well as the discovery of specific cancer antigens has given the opportunity to detect earlier and faster diverse malignancies contributing positively on patient life expectancy (Hazelton & Luebeck, 2011; Hofvind, et al., 2013; Landy, et al., 2016; Loud & Murphy, 2017; Marmot et al., 2013; Ouakrim et al., 2015; Paci, Broeders, et al., 2012). Finally, the prevention has an important impact on cancer incidence and has the potential to considerably reduce future cancer burden. Epidemiological studies predict that promoting healthy life style (eliminating the habits of smoking tobacco, decreasing alcohol drinking, practicing regularly physical activity and keeping under control body mass index) could decrease of 30-50% cancer incidence (Arem &

Loftfield, 2018). Moreover, anti-cancer vaccination and effective treatments of cancer-associated infections are expected to play an important role in prevention of neoplasia transformations (Doorakkers, et al., 2018; Howley, 2015; Wroblewski, et al., 2010; Zhao B, et al., 2019).

However, despite great strides in the fight against cancer, much still needs to be achieved. Diagnosis of some types of malignancies, such as pancreatic or lung cancers, is frequently translated in a death sentence (Ansari et al., 2016; Bray et al., 2018; Wong, et al., 2017; Zappa & Mousa, 2016). In addition, current therapies frequently cause short and long term side effects (Devlin, et al., 2017; Nurgali, et al., 2018). Thus, the development of innovative anti-cancer strategies with higher efficiency and lower toxicity is required. Encouraging outcomes obtained from the molecularly targeted therapies suggest that this goal can be achieved through better exploration of the differences between malignant and healthy cells as well as the enhancement of host immune system defences (Arruebo et al., 2011; Falzone et al., 2018).

1.1 Cancer development and metastasis (stages of cancer development)

Most tissues in the human body possess the ability to regenerate (Rue & Martinez Arias, 2015). Older cells are continuously replaced with new ones in the majority of our organs during physiological cell turnover (Pellettieri & Alvarado, 2007; Spalding, et al., 2005). Moreover, damaged tissues or partially or totally removed organs can regenerate reacquiring initial dimensions and functions (Baddour, et al., 2012).

Since the number of the cells has to be usually constant in the adult organism, there has to be a balance between cell proliferation and programmed cell death (tissue homeostasis). Indeed, these processes are tightly controlled in the living beings, ensuring structural and functional stability of the systems forming any organism (Liu, et al., 2001; Rue & Martinez Arias, 2015).

Deregulation of the normal tissue homeostasis can lead to various consequences, including tumorigenesis. Organ or tissue enlargement, as a result of uncontrolled cell proliferation, can turn, initially, in primary tumour development, and then, might contribute to secondary tumour formation (metastasis) (Basanta & Anderson, 2017).

Broadly, oncogenesis is a multistep process starting with a mutational event in a single cell and then progressing through acquisition of further genetic and/or epigenetic alterations, that are transmitted to the progeny of that cell when it divides (Barrett, 1993; Karakosta, 2005). These aberrations, typically, involve three types of genes (Pelengaris & Khan, 2013):

- *Proto-oncogenes* – are the genes, which encode proteins participating in promotion of cell survival, growth and proliferation and thus have a potential to become oncogenic;
- *Tumour suppressor genes* – are the genes responsible for inhibition of cell proliferation and/or activation of programmed cell death;
- *Caretaker genes* – include genes implicated in detection and reparation of DNA damage.

For instance, aberrations of the oncogene *c-MYC*, "master regulator" of cell growth, proliferation and dedifferentiation of pre-malignant cells during tumorigenesis, have been found in many human cancers, which prognosis is frequently conditioned by the rate of *c-MYC* oncoprotein expression (Chen, et al., 2018; Grotzer et al., 2001; Miller, et al., 2012; Schlotter, et al., 2003). Similarly, deregulations of the onco-suppressor *p53*, also called "the guardian of the genome", have been observed in a number of malignancies and are recognised to be essential for cancer progression (Efeyan & Serrano, 2007). The fact that *p53* possesses both, caretaker and tumour suppressor gene capabilities, renders it particularly important for the prevention of genome mutations required for malignant transformations (Ozaki & Nakagawara, 2011).

However, alterations of a single gene are, usually, insufficient for the transformation of a healthy cell into a malignant one. A cell needs to overcome numerous “obstacles” in order to be able (1) to avoid programmed death caused by various factors, (2) to proliferate and (3) to adapt to putative new microenvironments. Therefore, numerous mutations involving a variety of genes are required for tumorigenesis and cancer progression.

In fact, natural selection theory has been widely accepted for cancer development. It assumes that cancer origin and advancement are evolutionary processes driven by acquisition of progressively more advantageous alterations, responsible for selective growth of the cells with better survival characteristics (Arneth, 2018).

Initial genetic or epigenetic alterations are, frequently, phenotypically “silent” implying that the cell remains perfectly differentiated and completely functional within the tissue [Figure 2 b)]. Further mutations affecting key regulatory genes might trigger oncogenic pathways and inhibit tumour suppressor ones [Figure 2 c)]. This results in clonal expansion of the premalignant cells consequentially followed by primary tumour formation (benign tumour) [Figure 2 d)]. An important feature of benign tumours consists in their inability to invade surrounding tissues. Indeed, the mass of cells composing benign tumour is well circumscribed and, usually, grows slowly. Although this type of tumour is generally not life-threatening, it provides a fertile ground for malignant transformation. Indeed, downregulation of DNA repair and tumour suppressive mechanisms, occurring during the early stages of benign tumour development, makes pre-malignant cells more susceptible to acquire new mutations compared to normal cells. Faster and easier accumulation of further alterations results, then, in the creation of various pre-malignant sub-clones with different survival characteristics, which are proportional to their cell population rates within the benign tumour. In addition, some mutations contribute to the acquisition of new properties, which allow those specific subclones

to infiltrate in the surrounding tissues [Figure 2 e)]. This results in malignant tumour formation (cancer) (Pelengaris & Khan, 2013).

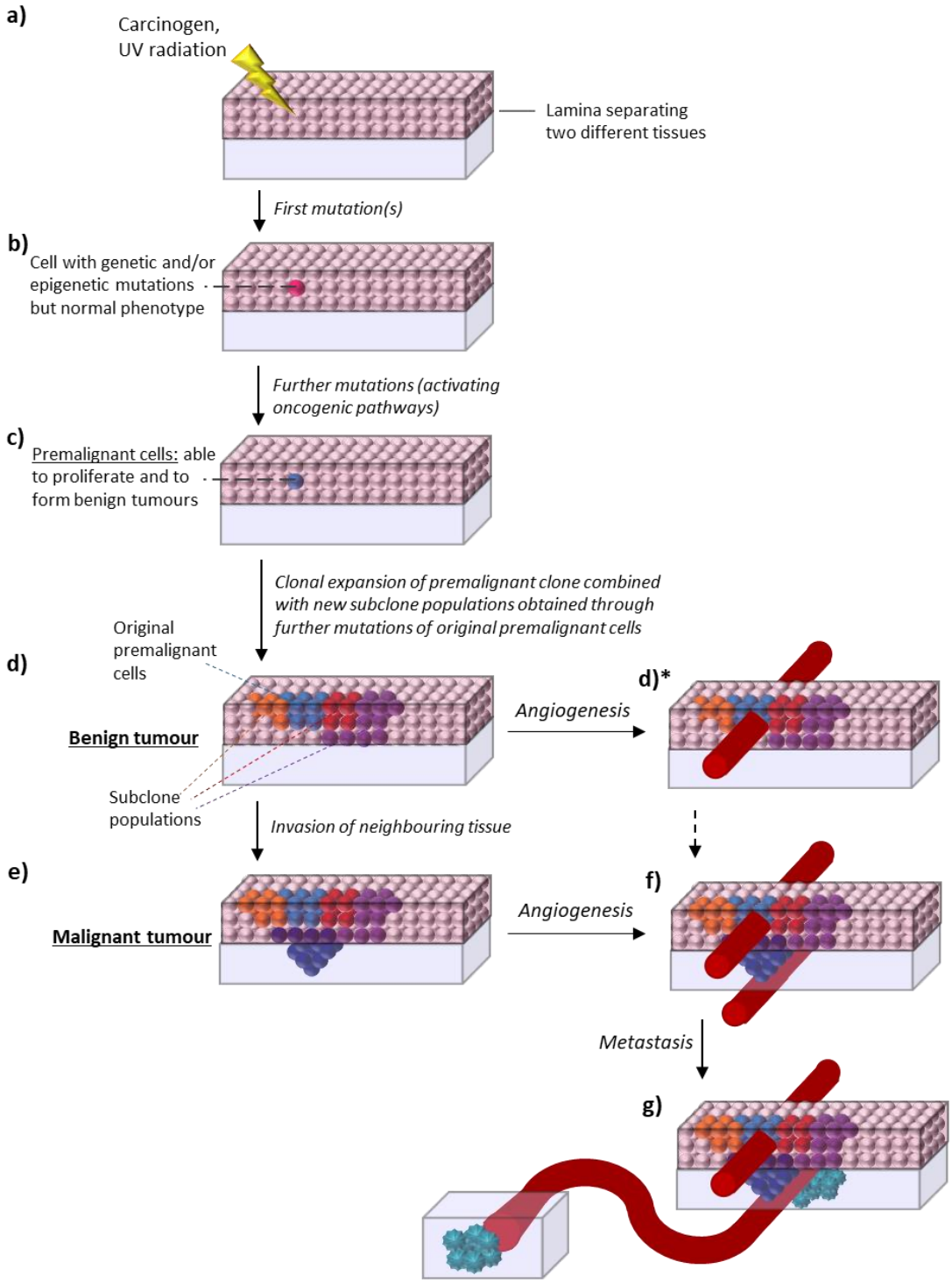


Figure 2: Schematic model of cancer initiation and progression *– from a healthy tissue (a), to the first mutations of a single somatic cell (b and c), able to promote clonal expansion causing benign tumour formation (d), to further mutations, responsible of malignant transformation, and, finally, metastasis development (g).*

Malignant transformation is usually accompanied by cell de-differentiation, which increases progressively during neighbouring tissue invasion. Importantly, malignancies with lower cell differentiation are more aggressive and are associated with poorer cancer survival rates (D. Yang et al., 2011; Yoshida, et al., 2011). Indeed, greater de-differentiation is also correlated with higher proliferation speed, which leads to faster cancer development (Jilkine & Gutenkunst, 2014).

Abnormal proliferation occurring during both, pre-malignant and malignant stages, requires constant provision of oxygen and nutrients from blood vessels. However, energy requirements for effective cell growth and proliferation become insufficient over time, due to inadequate number of capillaries for the increased dimensions of the tumour. Therefore, blood vessels development (angiogenesis) plays a crucial role from the early stages of oncogenesis [Figure 2d[2)] and 2f)]. Taken together, number of the tumour cells rapidly increases, while the number of blood vessels supplying oxygen/nutrients remains unchanged in the first instance. Thus the amount of oxygen delivered to each cell goes down and the way to overcome this issue is to: 1) implement stress signalling relying mainly on glycolysis (oxygen-free glucose degradation resulting in ATP production; 2) build up new blood vessels (induce angiogenesis) in order to meet requirements of each cell in oxygen/nutrients.

Indeed, reduced oxygen availability leads to activation of hypoxic signalling pathways requiring activation of hypoxia-inducible factor 1 (HIF-1). HIF-1 is a heterodimeric protein (transcription complex), composed of two subunits: HIF-1β, which is constitutively expressed, and HIF-1α, which is up-regulated in response to low oxygen concentrations. In normoxia conditions, HIF-1α is continuously hydroxylated by prolyl hydroxylases (PHDs), which employ cellular O_2 as a co-substrate. Hydroxylated HIF-1α is, then, recognised and polyubiquitinated by specific complexes and, subsequently, degraded by proteasomes. This prevents HIF-1 dimerization, requirement necessary for its activation [Figure 3a)]. Hypoxic

environment, instead, leads to down-regulation of oxygen-dependent HIF-1α degradation due to restricted availability of O_2. Activated HIF-1 complex, resulting from of HIF-1α and HIF-1β dimerization, is, then, able to promote transcription of numerous genes, including vascular endothelial growth factor (VEGF). Finally, triggering of VEGF receptors expressed by vascular endothelial cells activates signalling pathways responsible for new blood vessel formation [Figure 3b)] (Krock, Skuli, & Simon, 2011).

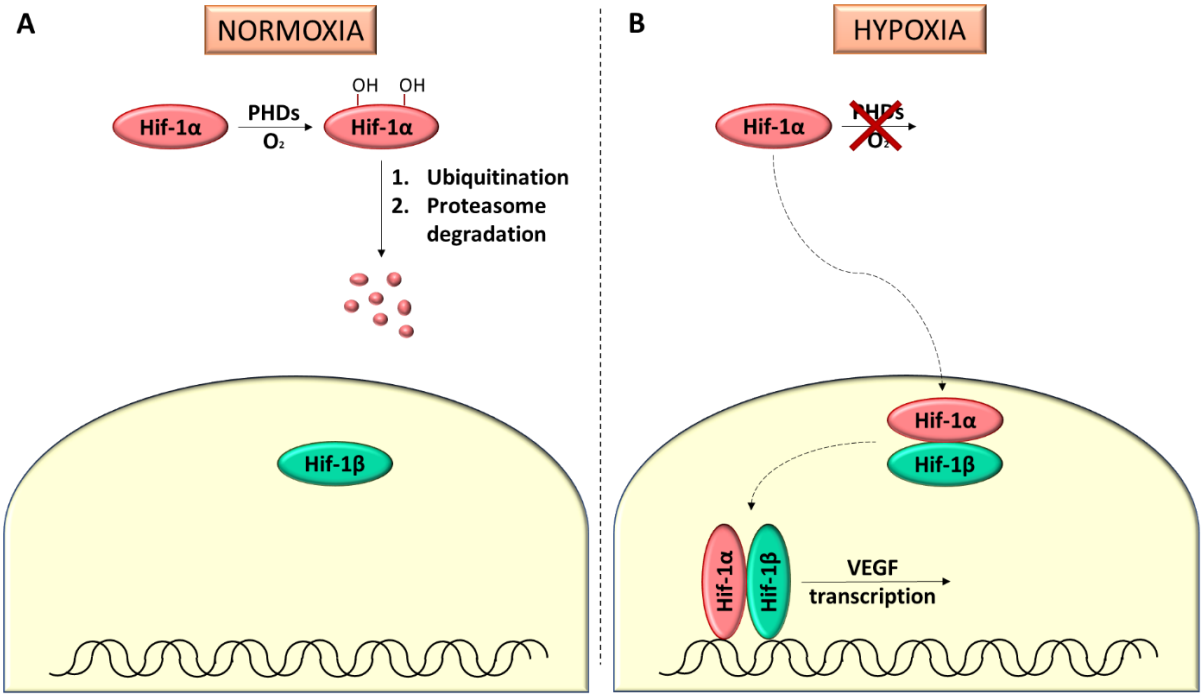


Figure 3: Processes underwent by HIF-1α protein under normal oxygen availability (a) and hypoxic conditions (b)

In addition to the mechanism associated with decreased oxygen levels, neovascularization can be induced, directly, by mutations regarding key regulatory genes of angiogenesis and, indirectly, by oncogenes, such as *RAS* and *Myc*, able to upregulate expression of angiogenic factors (Hanahan & Weinberg, 2011; Uthoff et al., 2002).

Formation of new blood vessels contributes as well to further steps of cancer progression: malignant cell dissemination from the original site of tumour formation to distant organs (metastasis) [Figure 2g)] (Bielenberg & Zetter, 2015).

However, before metastasis occur, malignant cells need to acquire a number of mutations allowing them (1) to win cell-cell and cell-extracellular matrix (ECM) interactions, (2) to survive in blood or lymphatic vessels and, finally, (3) to be able to invade (and to proliferate in) distant organs. Deregulation of metastases suppressor genes plays also a crucial role in cancer spread in different organs (Seyfried & Huysentruyt, 2013).

Indeed, it is hypothesised that a number of various malignant subclones extravasate in lymphatic or blood vessels during cancer progression. Nonetheless, most of them don't survive in the new environments for different reasons (Luzzi et al., 1998). For example, wide population of cytotoxic CD8 T cells affects considerably survival and proliferation of malignant cells entering the lymph nodes (Pelengaris & Khan, 2013). Another factor responsible for the death of migrating cancer cells is represented by their biochemical incompatibility with a potential site of colonization, such as lack of specific adhesive interactions with the new microenvironment (Q. Liu et al., 2017; Pelengaris & Khan, 2013). Thus, only "the fittest" and most aggressive cancer cells are able to metastasise successfully. Indeed, the ability to adapt in the new "habitat" is correlated with improved avoidance of suicide pathways and evasion of host immune attack, rendering malignant cells stronger and capable to proliferate faster (Arneth, 2018). For this reason, metastatic cancers are associated with poorer prognosis and higher mortality rates. Approximately 90% of cancer deaths are due to secondary (metastases) rather than the primary tumours (Seyfried & Huysentruyt, 2013). Therefore, early detection of cancer, before it has spread, is critical for patient life expectancy (Coumans, Siesling, & Terstappen, 2013; Hiom, 2015). In addition, an accurate identification of malignancy type ensures the undertaking of correct therapeutic measurements, and consequently, increases the chances for successful outcome.

1.1.1 Types of cancer – "solid" and "liquid" tumours

Cancers are classified by the type of tissue in which the initial malignant transformation occurs. Indeed, although the epigenetic plasticity and genetic diversity observed for a specific type of cancer in different patients, malignant cells almost always retain some of the peculiar features of the normal cell types from which they have originated. These specific features can be identified by histological and/or cytological examinations, allowing, in this way, to characterise the type of malignant neoplasm (Arneth, 2018; Ramsay, 1990; Weinberg, 2007).

The commonest cancer types and corresponding healthy tissues from which they evolve are outlined in Table 1 (Ramsay, 1990).

Table 1 Cancer classification (Ramsay, 1990)

Tissue or cell derivation	**Malignant neoplasm**
Epithelia	*Carcinoma*
Squamous epithelium	Squamous cell carcinoma
Glandular epithelium	Adenocarcinoma
Mesenchyme	*Sarcoma*
Fibrous tissue	Fibrosarcoma
Adipose tissue	Liposarcoma
Striated muscle	Leiomyosarcoma
Smooth muscle	Rhabdomyosarcoma
Bone	Osteosarcoma
Cartilage	Chondrosarcoma
Nervous tissue	*Neuroectdermal tumours*
Glial cells	Glioma
Primitive neural cells	Neuroblastoma
Astrocytes	Astrocytoma
Oligodendrocytes	Oligodendroglioma
Blood-forming cells	*Hematopoietic malignancies*
Lymphoid cells	Lymphocytic leukaemia
Myeloid cells	Myeloid leukaemia
Melanocytes	Melanoma
Germ cells	Teratoma

Most of human tumours originate in epithelial tissues and are called carcinomas. These malignancies can be further sub-classified according to biological functions associated with epithelia. For instance, malignant transformations of glandular cells, sub-type of epithelial cells responsible for both exocrine and endocrine secretions, generate adenocarcinomas. On the other hand, tumorigenesis of epithelial cells with protective functions of the underlying tissues usually induces squamous cell carcinoma (Weinberg, 2007).

Generally, organ main functions reflect the type of carcinoma that may develop with higher probability. Indeed, most cancers occurring in the organs, such as stomach or pancreas, which predominant role consists in the release of gastric or pancreatic juices by epithelial cells, are adenocarcinomas (Dicken et al., 2005; Smith, et al., 2015). Conversely, tumorigenesis of oropharyngeal epithelia, which provide mechanical barriers protecting from pathogens deriving from air or food, usually lead to squamous cell carcinoma (Panarese et al., 2019).

However, mixed carcinomas, malignancies characterized by coexistence of both, adenocarcinoma and squamous carcinoma cells, have been also reported to develop in some organs, such as lung and cervix (Bastide, et al., 2010; Choo & Naylor, 1984).

Another class of cancers arises from mesenchymal cells (MSCs). These malignancies, called sarcomas, constitute approximately 21% of all paediatric solid malignant cancers and around 1% of all adult solid malignant cancers (Burningham, et al., 2012; Weinberg, 2007). Sarcomas can be also sub-classified into two groups: soft tissue sarcomas (STS) and sarcomas of the bone (Hui, 2016).

The commonest soft tissue sarcomas include liposarcoma, tumour involving adipocyte oncogenesis, leiomyosarcoma and rhabdomyosarcoma, which arise from malignant transformations of striated and smooth muscle tissues, respectively (Hoang, et al., 2018).

Most frequent sarcomas of the bone are, instead, osteosarcoma and chondrosarcoma (Hui, 2016). The former is thought to derive from osteoblastic lineages of cells or undifferentiated MSCs, while the latter develops from cartilage tumorigenesis. Osteosarcoma affects predominantly adolescents and children, while chondrosarcoma is more frequent in elderly population (Abarrategi et al., 2016; Hui, 2016).

Third class of cancers regards oncogenesis of diverse elements composing nervous system (Weinberg, 2007). Glioblastoma, astrocytoma and oligodendroglioma, malignancies originating from various types of glial cells, are among the most frequent cancer types of this class (Patel et al., 2019).

Another group of cancers is represented by haematopoietic malignancies. There are two main blood-forming lineages deriving from the differentiation of hematopoietic stem cells: lymphoid and myeloid lineages. Oncogenesis of these two categories of blood cells can induce four main types of haematopoietic tumours: acute lymphoblastic, acute myelogenous, chronic lymphocytic, and chronic myelogenous leukaemia. Acute lymphoblastic leukaemia is the commonest blood cancer in childhood, while acute myeloid leukaemia occurs more frequently in the adults (Davis, et al., 2014).

This classification, based on the type of tissue/cell in which tumorigenesis initiates, reflects also some specific tissue-dependent gene mutations (Schaefer & Serrano, 2016). For example, aberrations of BRCA1 gene, which product is involved in DNA repair and apoptosis regulation, occur mostly in breast and ovarian cancers (E. Y.-H. P. Lee & Abbondante, 2014). Similarly, aberrations of ABL1, a gene encoding a tyrosine kinase implicated in a variety of cellular process, such as genome reparation and apoptosis regulation, are predominantly associated with leukaemia (Dasgupta et al., 2016; Shaul & Ben-Yehoyada, 2005).

However, despite diverse cell origin, different cancer types can also share some common tissue-independent mutations (Schaefer & Serrano, 2016). Consequently, different categories of malignant neoplasms, might be unified under the same roof based on their mutations. For example, alterations of the genes coding for the tumour suppressor *p53* were reported to occur quite in all the cancer types (Rivlin, et al., 2011). Similarly, aberrations of the oncogene *c-Myc* were found in more than 50% of human tumours (Chen et al., 2018).

High conservation of some gene alterations in different cancer types is a consequence of their involvement in key pathways of cell cycle. Indeed, most oncogenic mutations regard genes implicated in crucial mechanisms enabling the cell to prevent abnormal cell growth and proliferation (Pelengaris & Khan, 2013).

1.2 Normal physiological barriers preventing cancer development

The human body is continuously exposed to a multitude of carcinogens able to promote genetic and/or epigenetic alterations (Pelengaris & Khan, 2013). Moreover, DNA replication is error prone (Tippin, et al., 2004). Nonetheless tumorigenesis is a relatively rare event considering the number of cells undergoing mitosis in the human body every day. Indeed, cells possess multiple quality-control mechanisms allowing them to prevent alterations during cell replication and abnormal cell proliferation. Moreover, an additional "extracellular" quality-control system is available in case previous checkpoints result to be ineffective. This supplementary biological barrier is represented by immune system cells, which are able to eliminate promptly any anomalous cell appearing in the body (Pelengaris & Khan, 2013).

Thus, it is possible to divide cancer biological barriers in two categories:

- Cell-cycle checkpoints;
- Immune system "quality control" or cancer immunosurveillance.

1.2.1 Cell-cycle checkpoints

Each cell receives continuously various intra- and extra-cellular stimuli, which are then integrated to produce an adequate response. One part of the inputs intercepted by the cell is responsible for cell cycle regulation and progression. This part of signals can be broadly divided in inhibitory and stimulatory factors of cell proliferation. Indeed, the commitment of the cell to divide is meticulously regulated by the balance of negative and positive growth factors in the tissue microenvironment (Duronio & Xiong, 2013).

When the proliferative inputs prevail on the inhibitory growth signals, the cell activates pathways which lead to DNA replication and cell division. These processes are part of cell cycle, which progresses through consecutive phases:

1. G_1 – "gap 1" period in which the cell synthetases mRNA and proteins necessary for genome replication;
2. S – stage in which DNA synthesis occurs;
3. G_2 – "gap 2" phase in which the cell grows and prepares for mitosis;
4. M – mitosis.

The cell can stay in a quiescent state (phase G_0) for a relatively indefinite interval of time, until the mixture of inputs favours proliferative signals, forcing such cell to re-enter in G_1 phase, proceed through S and G_2 stages, and, finally, to undergo mitosis (Pelengaris & Khan, 2013).

Intracellularly, this progression is associated with different levels of specific cyclins, proteins termed in this way because of their periodical synthesis and degradation related to the cell cycle. Indeed, the concentrations of three major types of cyclins (G_1/S, S and M cyclins) oscillate during the cell cycle progression.

Growth factors can stimulate the synthesis of G_1 cyclins, which are then able to bind specific cyclin-dependent kinases (CDK). These enzymes are usually inactive in resting cells and their levels are stable throughout the cell cycle. The interaction of specific cyclin with its respective CDK leads to the formation of an active complex able to phosphorylate a variety of proteins, essential for each stage of cell cycle [Figure 4] (Boyle, 2008).

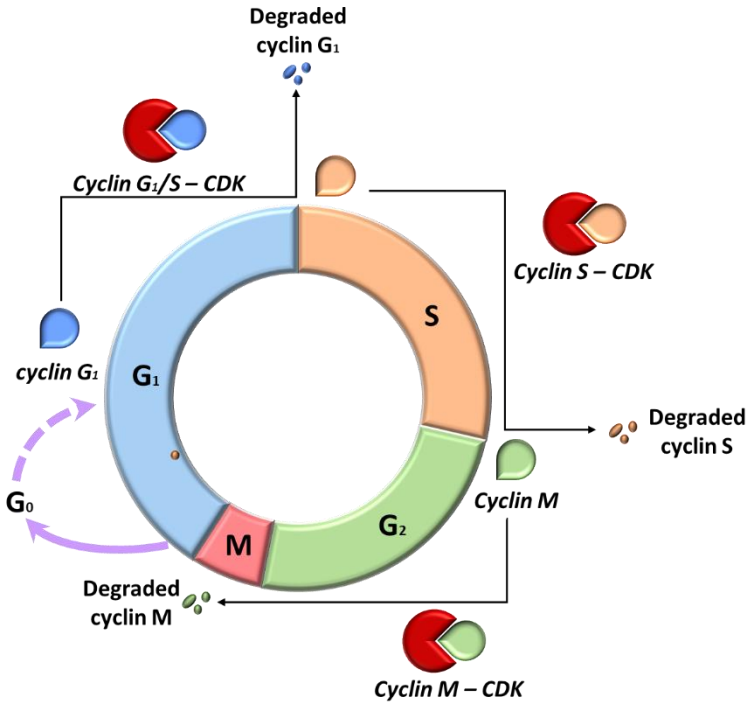


Figure 4: Cell cycle progression (Boyle, 2008)

Upon mitogenic stimulation, one of the first targets of G_1 cyclin/CDK phosphorylation is retinoblastoma (RB) protein, tumour suppressor ubiquitously expressed in human body (Cordon-Cardo & Richont, 1994; Giacinti & Giordano, 2006).

Prior to proliferative signals, unphosphorylated RB proteins are constitutively bound to E2 transcription factors (E2Fs) that are required for expression of S-phase genes [Figure 5a)]. This interaction precludes E2F binding to DNA and, thus, prevents gene transcription.

Phosphorylation of RB protein, upon growth factor downstream signalling, provokes conformational changes that decrease RB affinity to its natural E2F, and thus, cause RB-E2F

dissociation. In this way, E2F transcription factors, released from phosphorylated RB proteins, are able to interact with DNA and initiate specific gene transcription [Figure 5b)].

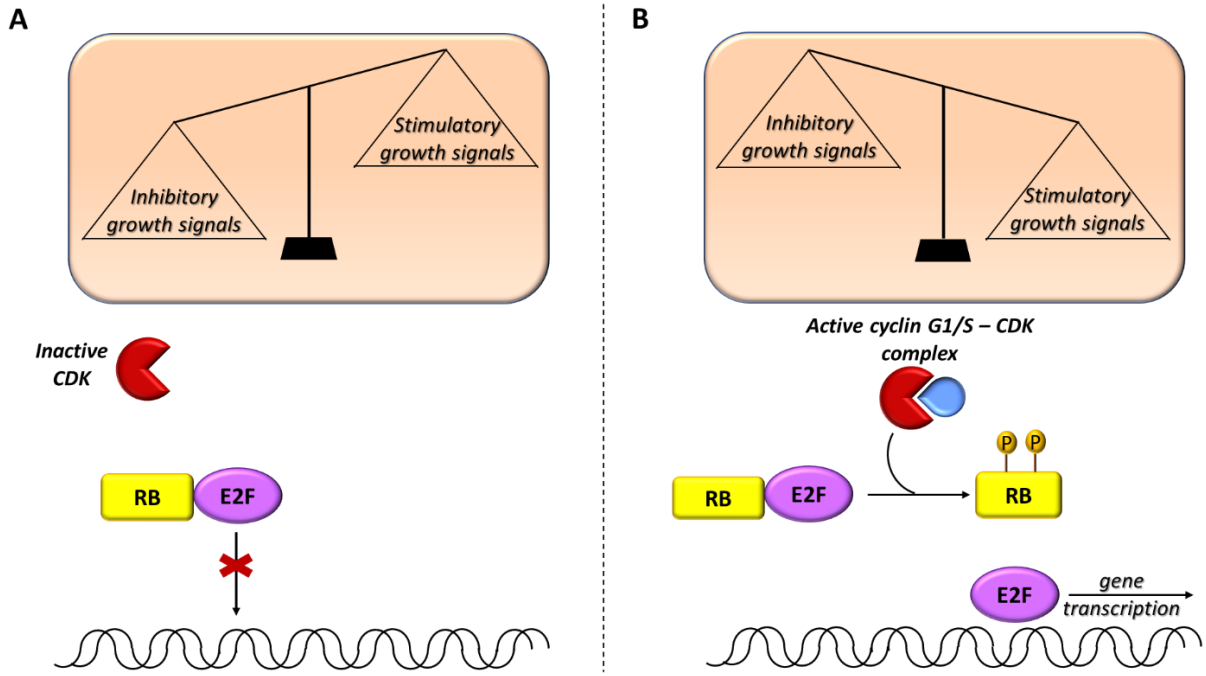


Figure 5: Restriction point *– RB phosphorylation, conditioned by the levels of growth-regulating signals, represents the point in which the cell commits to cell-cycle division in extracellular-independent manner.*

Therefore, the phosphorylation state of RB proteins, tumour suppressors responsive to the balance of growth-stimulatory and inhibitory factors, represents the first restriction point of cell division. After RB phosphorylation, followed by initiation of E2F-mediated transcription, the cell becomes irreversibly committed to enter S phase and to complete cell division without being any longer dependent on stimulation of external growth factors (Lara-Gonzalez, et al., 2012).

However, before genome replication initiates, some intracellular signals, such as "genotoxic stress" (DNA damage), can promote cell cycle arrest in G_1 phase. This occurs generally through inhibition of cyclin/CDK complexes by cyclin-dependent kinase inhibitors (CKI). Indeed, accumulation of specific CKIs, consequent to detection of genome damage, leads to cell cycle arrest providing time "to fix" DNA before its replication. If DNA reparation is successful, the

cell recovers and proceeds in S phase, while if it fails, the cell usually undergoes apoptosis. These regulatory systems, responsible for control of DNA integrity before replication, belong to G_1/S checkpoints.

Importantly, DNA stability is verified during the whole progression of cell cycle through multiple control quality systems, which can be further grouped in intra-S and G_2/M checkpoints. These regulatory mechanisms operate in analogous way to G_1/S checkpoint, upregulating various types of CKI able to inhibit cell cycle-specific effectors necessary for cell cycle arrest and DNA reparation. General scheme of the mechanism through which all these control-quality systems operate is represented in Figure 6 (Pelengaris & Khan, 2013).

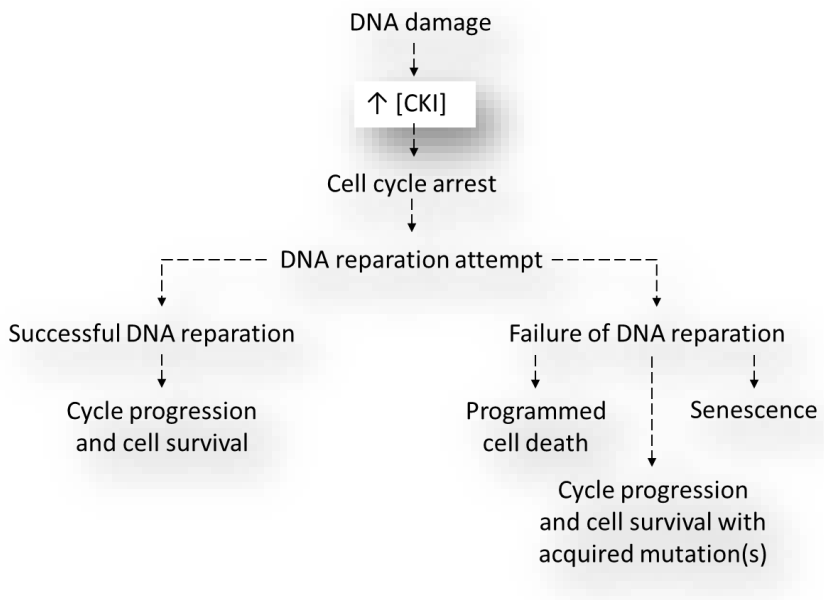


Figure 6: General scheme of the mechanism through which cell cycle checkpoints operate.

Finally, after genome replication, during M phase, chromosome partition between two daughter cells is controlled by so called "spindle" checkpoints. This group of control-quality systems assesses that mitotic spindle, necessary for chromosome partition, is assembled correctly ensuring that each daughter cell gets the right number and configuration of chromosomes (Lara-Gonzalez, et al., 2012).

Despite multiple checkpoints present during all the steps of cell cycle, some genome aberrations can be "missed" by these control-quality systems leading to survival of cells with acquired mutations. In this case host immune system plays a crucial role in detection and elimination of these aberrant cells.

1.2.2 Immune system "quality" control

Although tumours develop from healthy tissues recognised as self by the host immune system, cancer cells can still elicit an immune response through expression of anomalous products and through creation of an inflammatory environment, as a result of tissue disruption consequent to the invasion by malignant cells (Pelengaris & Khan, 2013).

Tumours are complex microenvironments characterised by hypoxia and nutrition deprivation, which cause constant cellular stress. Consequently, despite the high proliferation rate, one part of malignant cells dies continuously because of metabolic adversities encountered during cancer development and progression. In addition, genomic instability, typical of oncogenic cells, may also contribute to the death of cancer clones which acquired disadvantageous mutations. Moreover, malignant cells, not only compete for nutrients with normal cells, but also damage them, when invading healthy tissues. Therefore, opposite processes, such as abnormal growth/proliferation, and apoptosis/necrosis, can be identified in tumorigenic tissues (Coussens & Werb, 2002; Fonseca & Dranoff, 2008; Reuter, et al., 2010).

These events contribute to the generation of damage-associated molecular patterns (DAMPs), molecules released by stressed, dying or injured cells. These chemically unrelated mediators are usually retained intracellularly in healthy cells and released in the extracellular space only in specific circumstances, such as tissue damage and metabolic stress. Their main function, once liberated from the cells, consists in recruitment and activation of innate immune defences in tumorigenesis sites. Indeed, DAMPs elicit host immune response by binding specific pattern

recognition receptors (PRRs), expressed by Natural Killer (NK) cells, macrophages and dendritic cells (He et al., 2017; Roh & Sohn, 2018; Sato, et al., 2009).

Major DAMPs and their respective receptors are reported in Table 2 (He et al., 2017; Roh & Sohn, 2018).

Table 2: List of major DAMPs and their respective PRRs (Roh & Sohn, 2018)**.**

Intracellular location	**DAMP**	**PPR**
cytosol	S100 proteins	TLR2, TLR4, RAGE
	HSP	TLR2, TLR4, RAGE
	ATP	P2X7, P2Y2
Nucleus	Histones	TLR2, TLR4
	HMGB1	TLR2, TLR4, RAGE, TIM-3
	HMGN1	TLR4
	DNA	TLR9, AIM2
	RNA	TLR3, TLR7, TLR8, RIG-I, MDA5
Mitochondria ER	mtDNA	TLR9
	TFAM	RAGE

Importantly, all these molecules binding PRRs have different physiological intracellular roles and act as DAMPs only when released in extracellular space. For example, high-mobility group box 1 (HMGB1), ubiquitously expressed non-histone DNA-binding protein, is normally located in the cell nucleus. HMGB1 is involved in many DNA activities, such as DNA repair and genome stability maintenance, when localised inside the nucleus (He et al., 2017).

The human HMGB1 is a small protein of 245 aa, composed of three distinct domains: A box, B box and acidic C-terminal tail (containing numerous glutamic and aspartic acid residues) [Figure 7]. Nuclearly, HMGB1 binds directly to DNA employing its positively charged A and B boxes, while acidic C-terminal tail enhances the specificity of this interaction (He et al., 2017; Wang, et al., 2007).

In addition to nuclear functions, HMGB1 is involved in the promotion of autophagy in response to oxidative stress, when translocated in cytosol. Increased ROS levels, consequent to hypoxia and cell starvation, cause oxidation of two highly conserved aminoacidic residues, cysteine 23 (C23) and cysteine 45 (C45), leading to formation of disulphide bond in A box of HMGB1. Subsequently, ROS promote also its translocation from nucleus to cytosol, where disulphide bridge (C23/C45) is able to interact with Beclin-1, disrupting its interaction with Bcl-2 and, thus, promoting autophagy (D. Tang et al., 2010).

Finally, in extracellular space, HMGB1 acts as an alarmin, able to recruit and activate the innate immune response. Once released, from dying or injured cell, HMGB1 interacts with following receptors (He et al., 2017):

- the receptor for advanced glycation end products (RAGE), which binds residues 150-183 of HMGB1;
- Toll-like receptors (TLRs), TLR2 and TLR4, which bind residues 89-108 of HMGB1.

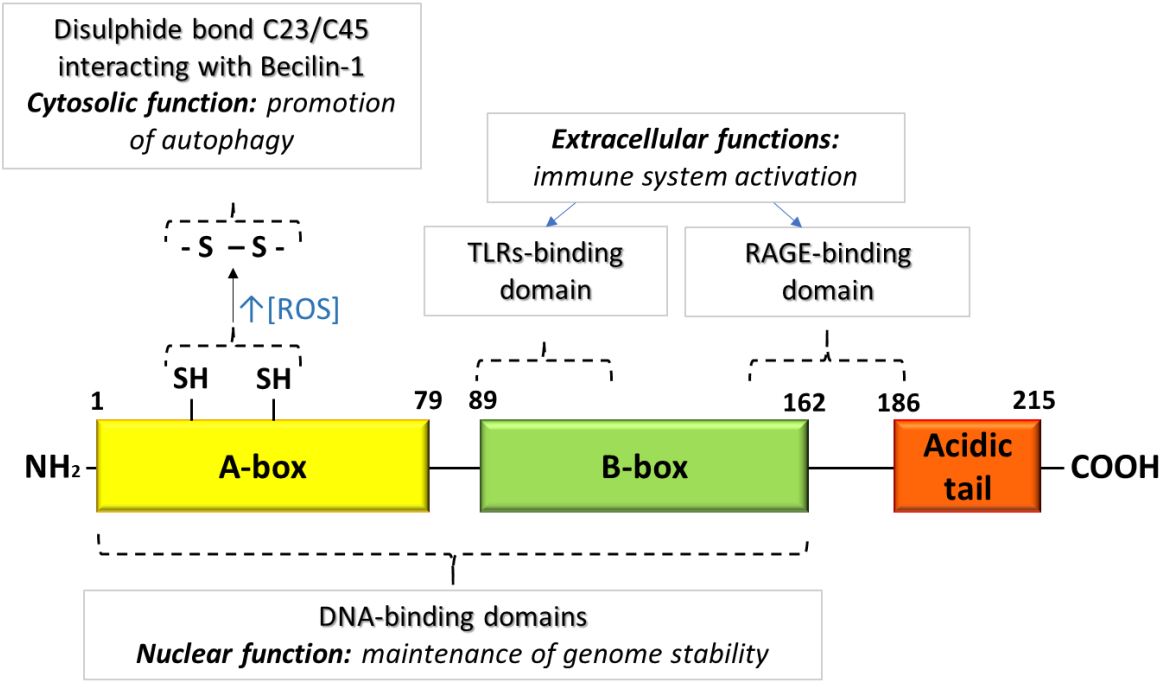


Figure 7: HMGB1 structure

TLRs are transmembrane glycoproteins constituted of three main domains: extracellular domain containing leucine rich repeats (LRR), transmembrane domain and intracellular Toll-interleukin 1 (IL-1) receptor domain (TIR). The interaction of LRR with the ligand induces conformational changes leading to dimerization of two receptors of TLR. This results in the association of two TIR domains, which together form a platform able to interact with specific intracellular adaptor proteins. Downstream signalling following TIR/adaptor protein complex formation leads to gene transcription and translation of different cytokines necessary at various stages of inflammation process (Dajon, et al., 2017).

The TLR family comprises ten members (TLR1-TLR10), two of which, TLR2 and TLR4, have been reported to interact with HMGB1 (He et al., 2017; Moresco, et al., 2017). Main effects of TLR2/TLR4 triggering by this alarmin during the early stages of inflammation is reported in Figure 8 and Table 3 (Dumitriu, et al., 2006; He et al., 2017; G. Li, et al., 2013; J. Li et al., 2003; S. Yang, et al., 2014).

RAGE is a transmembrane protein able to bind a variety of ligands. The first ones to be identified were advanced glycation end products (AGEs), macromolecules obtained through non enzymatic reaction between reducing sugars and proteins, lipids or nucleic acids. Subsequently, RAGE has been reported to bind other ligands, such as HMGB1 and other DAMPs (Gkogkolou & Böhm, 2012; E. J. Lee & Park, 2013; Xie et al., 2008).

RAGE is a member of the immunoglobulin superfamily and is ubiquitously expressed at low levels in adults but is upregulated following cellular stress. Triggering of RAGE stimulates the propagation of various intracellular signalling pathways leading to the activation of the transcription factor nuclear factor kappa-B (NFκB), which promotes expression of numerous genes during the inflammation process [Figure 8 and Table 3] (Kierdorf & Fritz, 2013; Narumi et al., 2015).

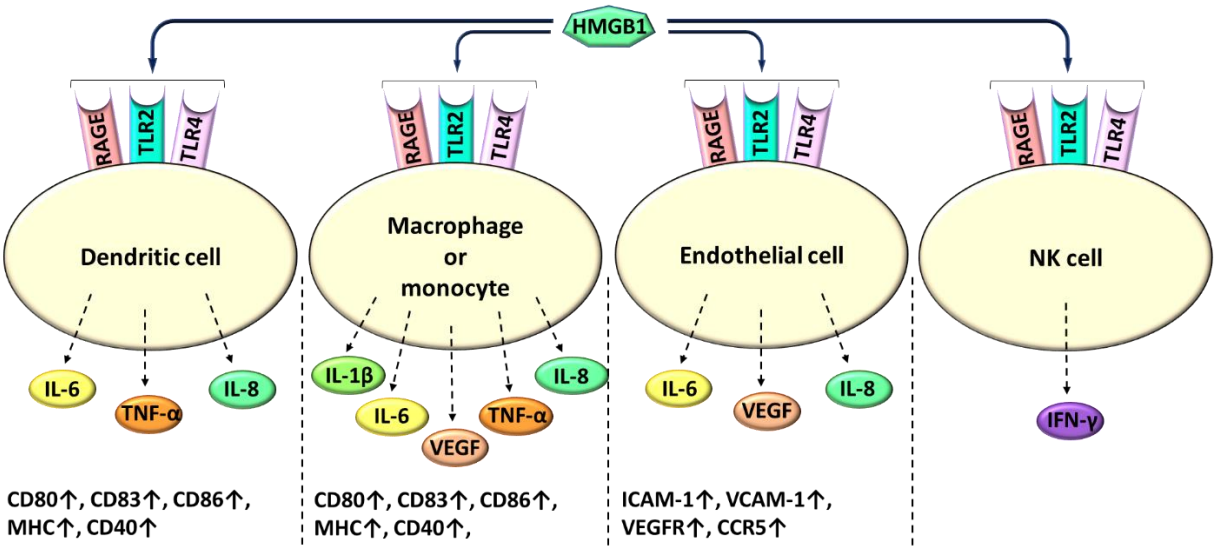


Figure 8: HMGB1 effects in early stages of inflammation

Table 3: Main functions of HMGB1-induced cytokines in early stages of inflammation (Dinarello, 2009; Ding et al., 2011; Kursunel & Esendagli, 2016; Janeway, 2012; Tanaka, et al., 2014; van Horssen, et al., 2006)

IL-6 (interleukin 6)	• promotes differentiation of naïve CD4 T cells into effector cells, of CD8 T cells into cytotoxic T cells and of activated B cells into antibody-producing plasma cells; • inhibits TGF-β-induced T regulatory differentiation; • promotes megakaryocyte maturation required for the platelets production.
TNF-α (tumour necrosis factor α)	• induces programmed cell death of aberrant cells through direct interaction with TNF receptors (TNFR) ubiquitously expressed in different tissues of human body; • promotes dendritic cell maturation (CD80↑, CD83↑, MHC↑, CD40↑); • activates vascular endothelium and increases vascular permeability facilitating accumulation of immune system components in the site of tumorigenesis; • promotes synthesis of numerous pro-inflammatory cytokines.
IL-1β (interleukin 1β)	• activates vascular endothelium and increases vascular permeability • activates immune cells
IFN-γ (interferon γ)	• promotes differentiation of T cells into effector cells; • upregulates MHC expression of antigen presenting cells (APCs); • stimulates further chemotactic factors production and promotes immune cells recruitment.
IL-8 (interleukin 8)	• chemotactic factor
VEGF (vascular endothelial growth factor)	• growth factor inducing new blood vessels formation

Activation and recruitment of NK cells, macrophages and dendritic cells leads usually to a rapid elimination of anomalous cells (H. Yang & Tracey, 2010). Indeed, stressed cells typically express danger-activated signals (DASs) on their surfaces, which can be recognised by innate immune system cells. DASs are self-proteins that are poorly expressed by healthy cells but are upregulated on the surface of stressed and transformed cells. Major histocompatibility complex (MHC) class I chain-related protein A and B (MICA and MICB) are among the commonest DASs, that can bind (Natural Killer Group 2D) NKG2D receptor present on NK cells. This interaction activates NK cells leading to instant death of carcinogenic cells (Corthay, 2014).

MICA and MICB are considered non-classical MHC class I molecules, which are structurally similar to self-MHC-I expressed by almost all the cell types of the human body. Both, MICA/B and self-MHC-I contain one membrane-spanning α chain (heavy chain) consisting of three extracellular immunoglobulin-like domains, a transmembrane domain and intracellular cytoplasmatic tail. Differently from MICA/B, self-MHC-I is also bound to β2 micro-globulin (extracellular light chain) and exhibits a small oligopeptide (8-11 aa) obtained from self-protein proteasomal degradation occurring routinely in healthy cells [Figure 9] (Ghadially et al., 2017; Weinberg, 2007).

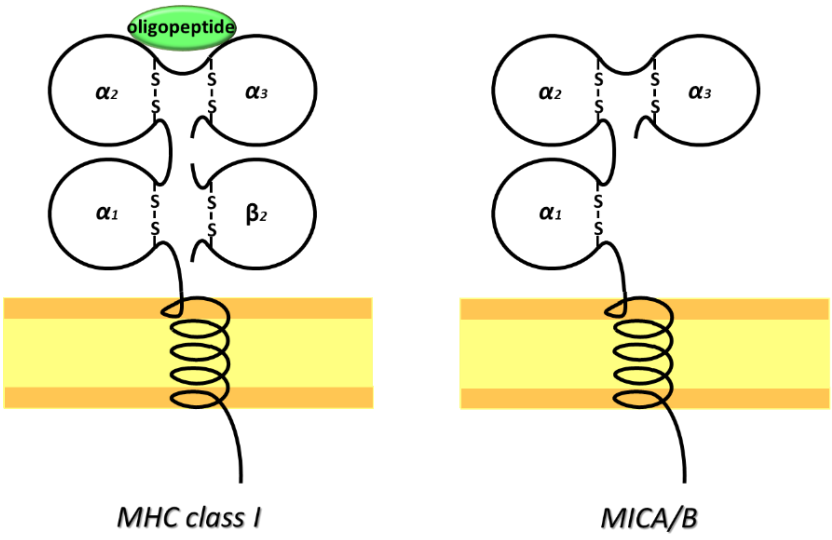


Figure 9: Structure of MCH class I and MICA/B

Healthy cells display relatively high concentration of self-MHC class I molecules able to bind different types of NK inhibitory receptors, such as a subgroup of killer-cell immunoglobulin-like receptors (KIRs). This inhibitory interaction prevents NK cells in destroying normal tissues. Contrarily, transformed cells frequently express significantly lower levels of self-MHC class I molecules or present aberrant oligopeptides, which aren't recognised as self by immune system cells. Downregulation of inhibitory signals in addition to upregulation of activating ligands, such as MICA/B, on aberrant cells shifts the balance toward NK cell activation and consequent elimination of these anomalous cells [Figure 10] (Long, 2002; Pegram, Andrews, Smyth, Darcy, & Kershaw, 2011; Pelengaris & Khan, 2013).

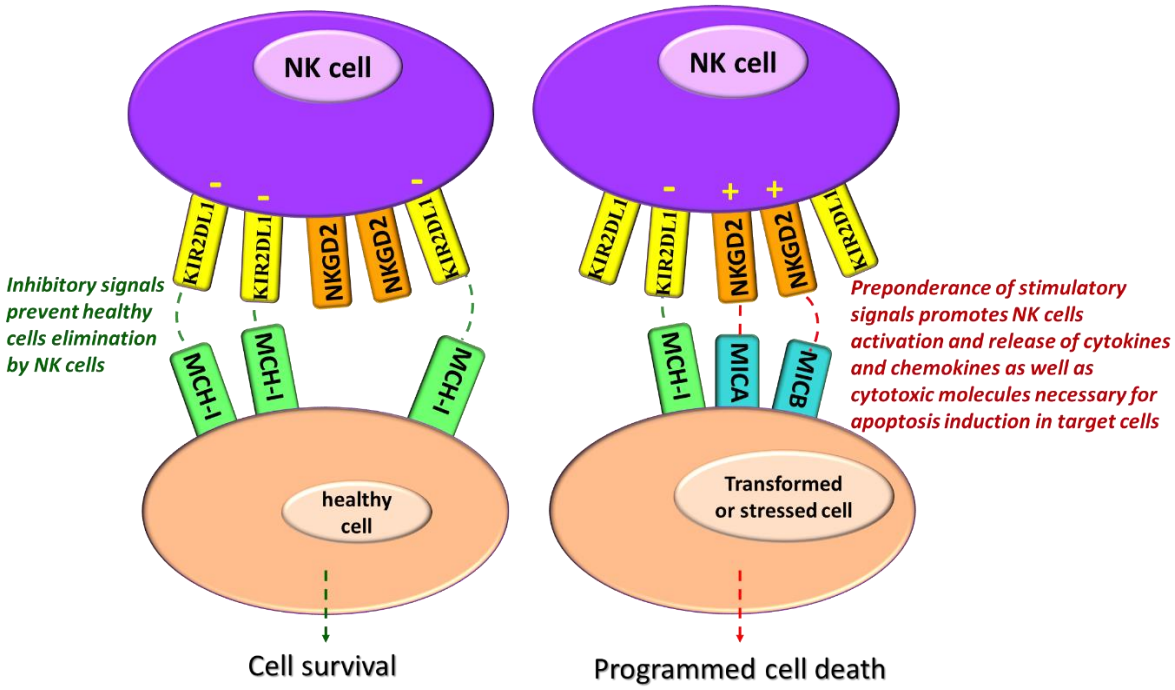


Figure 10: Discrimination between healthy and transformed cells by NK cells

Upon recognition and activation, NK cells can induce apoptosis in transformed cells through (1) degranulation, process inducing release of cytotoxic molecules such as perforin and granzyme, or (2) through interaction of death receptors expressed by aberrant cells and their ligands upregulated in activated immune cells (Paul & Lal, 2017).

Perforin is 60-70-kDa glycoprotein, able to polymerise and form pores in target cells. Resulting disruption of the membrane, consequent to perforin congregation, leads to passive transportation of ions, water, enzymes and other molecules through the pores. Granzymes represent the most important components delivered by NK cells into transformed cells employing these non-selective passages (Osińska, et al., 2014; Paul & Lal, 2017). Granzymes belong to serine-protease family able to cleave specific peptide bonds dependent on the type of granzyme. For instance, granzyme B, the commonest enzyme of cytolytic granules, specifically cleaves peptide bonds after aspartic acid residues of their substrates. Indeed, once delivered into a target cell, granzyme B recognises and cleaves these peptide bonds in several substrates, such as the pro-apoptotic protein Bid and pro-caspase 3. Truncated Bid (tBid) proteins bind then their mitochondrial partners, such as B-cell lymphoma-extra-large (Bcl-xL) proteins, promoting oligomerization of no longer constrained mitochondrial transmembrane macromolecules, such as BAK proteins. Association of BAK proteins results in formation of channels, which allow cytochrome c release from mitochondria. Once liberated in the cytosol, cytochrome c binds apoptotic protease activating factor-1 (Apaf-1). Conformational changes resulting from this interaction uncover specific domains necessary for oligomerization of Apaf-1/cytochrome c complex with consequent formation of apoptosome. This heterogeneous complex binds procaspase-9 molecules and converts them into active caspase 9 enzymes leading to construction of proteolytic platform (active apoptosome) able to catalyse procaspase 3 cleavage. Active caspase 3 triggers proteolytic cascade which finally leads to cell death. In addition, as mentioned above, intrinsic pathway of NK cell-mediated apoptosis can occur through direct cleavage of procaspase 3 by granzyme B (Boyle, 2008; Krzewski & Coligan, 2012; Wei et al., 2000).

Moreover, upregulation of death receptor ligands on NK cells consequent to their activation during inflammation can promote extrinsic pathways of apoptosis in transformed cells.

One of the most studied death receptors expressed by human cells is apoptosis antigen 1 (Apo-1), also called CD95 or Fas. This transmembrane receptor belongs to TNF receptor (TNFR) superfamily and is expressed by majority of human cells in inactive state (as monomer). Its interaction with trimeric Fas ligand (FasL) expressed by activated NK cells induces Fas trimerization in target cells. This provokes clustering of Fas cytoplasmatic death domains (DD) allowing to recruit intracellular adaptor proteins (FADD). Conformational changes resulting from the latter interaction leads to exposure of FADD death effector domains (DED) able to recruit the initiator caspases, such as pro-caspase 8. Following Fas–FADD–caspase 8 complex, called the death-inducing signalling complex (DISC), caspase 8 undergoes self-cleavage with consequent formation of active proteolytic enzyme. Activated caspase 8 is able then to catalyse cleavage of effector pro-apoptotic enzymes, such as caspase 3, leading to initiation of proteolytic cascade, which culminates with death of the transformed cell (Boyle, 2008; Kominami et al., 2012; Krzewski & Coligan, 2012; Susan, 2007).

Schematic representation of NK-cell mediated extrinsic and intrinsic apoptosis pathways is illustrated in Figure 11.

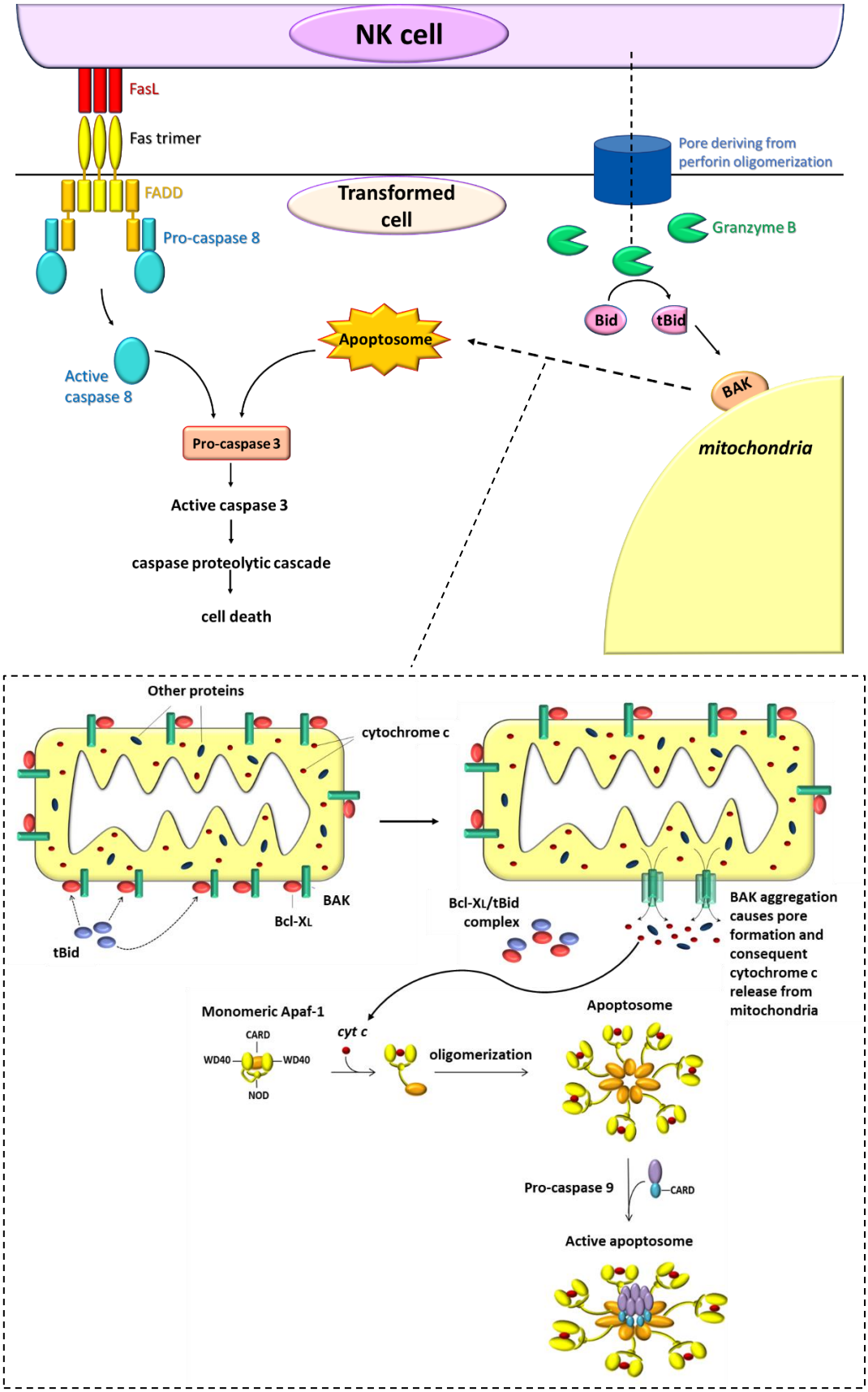


Figure 11: NK cell-mediated apoptosis induction in anomalous cells

In addition to previously described recognition mechanisms typical during the early stages of inflammation (MHC I downregulation and DASs upregulation), NK cells can identify and kill anomalous cells through antibody-dependent cellular cytotoxicity (ADCC) in following stages of inflammation characterised by adaptive immune responses. In this case, NK cell surface receptor CD16 (FcγRIII) interacts with Fc region of the antibody (ab) bound to target antigens expressed by transformed cells. Triggering of CD16 induces the release of cytotoxic granules by NK cells leading to rapid elimination of abnormal cells (W. Wang, et al., 2015).

Adaptive immune responses are initiated after antigen presenting cells (APCs), such as dendritic cells (DCs), migrate to the lymph nodes and interact with specific T and B cell subpopulation contributing to their activation and proliferation(Weinberg, 2007).

APCs recognise transformed cells in similar way to NK cells. Triggering of their PRRs and stimulation by inflammatory cytokines induces DC maturation. This process involves (Pelengaris & Khan, 2013; ten Broeke, et al., 2013):

- upregulation of MHC II molecules, bearing antigens derived from engulfed and phagocytosed anomalous cells;
- upregulation of co-stimulatory T cell molecules, such as CD80, CD83, CD86 and CD40;
- synthesis and release of cytokines facilitating T cell activation, such as IL-7 and IL-12;
- increased potential to migrate from tumorigenic tissues to the neighbouring lymph nodes for the interaction with B and T cells.

Indeed, DCs are amongst the few cell types able to express both MHC I and II class molecules. Once endocytosed soluble and particulate matter of tumorigenic environment or internalised aberrant cells, APCs fragment ingested proteins into small peptides of 18-22 aa, which are assembled intracellularly with MHC II molecules. The complex MHC II/antigen is then

expressed on APCs cell surface. Moreover, DCs possess a unique capacity to display antigens derived from endocytosed material also on MHC I molecules.

Considering that malignant cells arise from healthy tissues, most of these oligopeptides carried on MHC I and MCH II molecules are self-protein and don't evoke immune response. However, some of tumour-derived antigens are recognised as non-self upon interaction with specific B cell receptors (BCR) and T cell receptors (TCR) contributing to the activation and proliferation of featured lymphocytes.

Broadly, cancer-related immunogenic oligopeptides derive from proteins that can be grouped in several classes (Blankenstein, Gilboa, & Jaffee, 2012; Vigneron, 2015):

- phenotypically altered normal proteins;
- virus oncoproteins;
- macromolecules expressed exclusively during embryonic development;
- proteins that are usually expressed at low concentrations but are upregulated during tumorigenesis.

Genetic mutations can lead to altered amino acid sequences in tumour-expressed proteins, that have the potential to be identified as foreign and therefore induce adaptive immune responses. Indeed, numerous cytotoxic T cells (CTLs) and peculiar antibodies for tumour-specific antigens can be identified in the blood of cancer patients. Phenotypically altered protein can arise from modifications of nucleic sequence within one specific gene. For example, DNA alterations of the gene codifying for glycolytic enzyme triosephosphate isomerase (TPI) leads to chemically changed TPI mutant. Oligopeptides obtained from TPI processing by APCs has been reported to be highly immunogenic and represent tumour-specific melanoma antigens (Pieper et al., 1999). Moreover, structurally altered proteins can result also from chromosomal translocations occurring, for example, in chronic myelogenous leukaemia (CML). In the latter case, amino acid sequence of proteins codified by gene Abelson (Abl) normally present on

chromosome 9 and breakpoint cluster region (BCR) located on chromosome 22, are identical to those found in BCR-Abl fusion protein resulting from chromosomal translocation. Nevertheless, the small region where BCR and Abl are fused constitutes novel amino acid sequence that can be possibly recognised as non-self by immune system cells (Salesse & Verfaillie, 2002; Weinberg, 2007).

Tumour-specific antigens can also arise from oncovirus-infected cells. Seven types of viruses have been found to be tumorigenic [Table 4]. Once internalised inside the cell, oncoviruses can stimulate oncogenic pathways inducing overexpression of already existing host proto-oncogenes and/or producing specific oncoproteins codified by viral genes. Fragmentation of viral oncoproteins by APCs can give rise to immunogenic peptides able to stimulate anti-tumour defences through specific T and B cell activation and proliferation (Chang, et al., 2017; Krump & You, 2018).

Table 4: Virus associated tumours (Chang et al., 2017)

Virus	**Main virus-induced malignancies**
Epstein–Barr virus (EBV)	Several lymphoma types, nasopharyngeal and gastric cancers
Hepatitis B virus (HBV)	hepatocellular carcinoma
Human T-lymphotropic virus-1 (HTLV-1)	adult T-cell leukaemia (ATL)
Human genital papillomavirus (HPV)	cervical carcinoma, squamous cell head and neck cancers, squamous cell anal cancer, vulvar cancer
Hepatitis C virus (HCV)	hepatocellular carcinoma

Carcinogenesis is usually associated with dedifferentiation, that somatic cells undergo acquiring proliferative capabilities typical of stem cells. Numerous cancer types have been also reported to activate embryonic pathways (Kelleher, et al., 2006). Some embryonic proteins are physiologically expressed only during early stages of embryonic progression, before immunological tolerance is developed. Therefore, it has been suggested that these proteins might be recognised as non-self if expressed in adults. Indeed, early foetal protein-derived oligopeptides don't interact with specific immune cell receptors necessary for elimination of

autoreactive lymphocytes and thus can be highly immunogenic. Similarly, this concept has been proposed for proteins that are usually expressed at very low concentrations. In this case developing lymphocyte populations hardly encounter these proteins leading to survival of B and T cells, which are able to bind weakly expressed macromolecules. Upregulated levels of proteins, that are silent or expressed at very low levels in healthy tissues, have been found in different types of cancers and reported as possibly immunogenic (Aurisicchio et al., 2013; Criscitiello, 2012; John et al., 2008; Vigneron, 2015).

As mentioned above, oligopeptides deriving from these cancer-specific proteins are displayed by APCs which present them to peculiar lymphocytes in the lymph nodes. This encounter stimulates activation of several types of lymphocytes:

- CD4 or T helper (Th) cells, which are further classified in (1) Th1 lymphocytes responsible for CD8 T cell activation and (2) Th2 lymphocytes that induce B cell differentiation in plasma cells releasing cancer antigen-specific antibodies;
- CD8 T cells, which differentiate in cytotoxic T cells upon their activation.

T cell activation starts with the engagement of MHC-antigen complexes and specific T cell receptor (TCR), which leads to upregulation of CD40 ligand (CD40L) by T_H1 cells. This interaction leads to increased expression of APCs surface molecules, such B7-1 (CD80) or B7-2 (CD86), able to bind T cell receptor CD28 and promote further lymphocyte differentiation. Moreover, CD80/CD86-CD28 interaction enhances T-cell survival upregulating anti-apoptotic proteins, such BcL-xL. In addition, mature DCs release stimulatory cytokines, such as IL-12 and IL-7, which contribute to T cell activation. However, complete CD8 T cell maturation and differentiation in cytotoxic T cells requires a supplementary CD4 T cell "licensing". Indeed, IL-2 and other cytokines expression by activated Th1 cells are required for complete CD8 activation and promotion of proliferation [Figure 12] (Pelengaris & Khan, 2013).

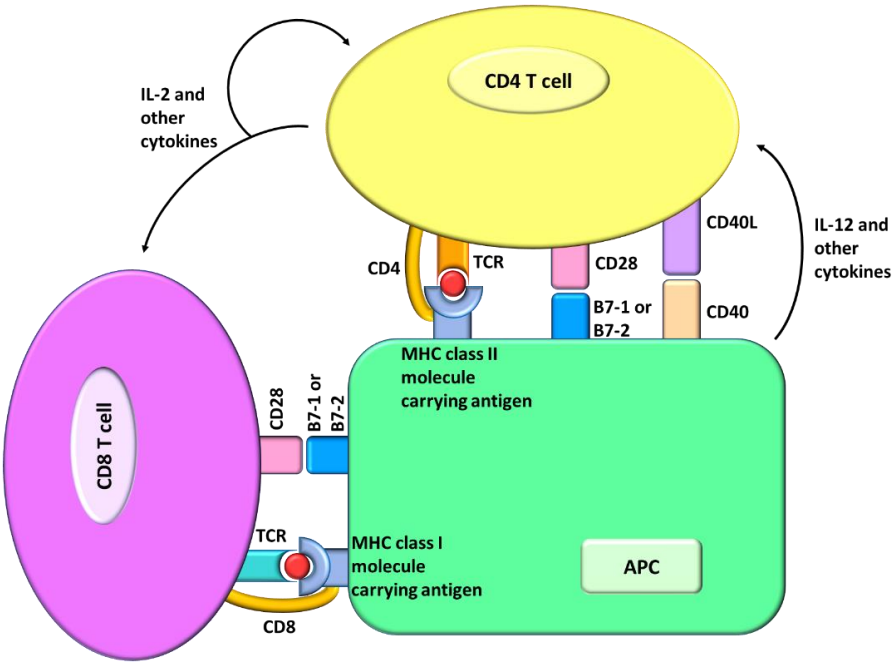


Figure 12: T cell activation

Once activated, cytotoxic T cells (CTCs) migrate in tumorigenic tissues to kill transformed cells. Upon antigen-specific recognition, CTCs can induce apoptosis in cancer cells by triggering their death receptors or releasing cytotoxic granules, similarly to NK cells. In addition to specific recognition of antigens expressed by malignant cells, CTCs can bind also DASs through their constitutively expressed receptors, such as NKGD2.

Once eliminated tumorigenic cells, hyperactivated immune cells have to be "stopped" to prevent excessive tissue damage. Therefore, physiological immunosuppressive systems are activated in the final stages of the inflammation. In addition, tissue regeneration and reparation mechanisms are promoted with the purpose of restoring normal tissue functionality.

1.3 Physiological immunosuppression and immune evasion of malignant cells

Since tumorigenesis is usually accompanied by inflammation, malignant cell growth and development is continuously threatened by host immune systems. For this reason, only the clones that can successfully escape anti-tumour immunity are able to survive and proliferate. Indeed, cancer cells acquire mechanisms allowing them to upregulate immunosuppressive

systems and to shape inflammatory responses for their own growth advantages (Coussens & Werb, 2002).

1.3.1 PD-1 and CTLA-4 mediated immunosuppression

One of the mechanisms employed by cancer cells to escape host immune attack consists in expressing immunosuppressive proteins on their surfaces. Some of these inhibitory macromolecules belong to B7 family ligands and to their partner receptors.

The members of B7 family are usually upregulated during inflammatory responses and can induce both costimulatory and coinhibitory signals in lymphocytes and NK cells. Major B7 molecules and their binding partners are reported in Table 5 (Seliger, et al., 2008).

Table 5: Major B7 ligands and their binding partners (Seliger et al., 2008)

B7 ligand	**Cells expressing B7 ligand**	**Binding partner of B7 molecule**	**Cells expressing B7 binding partner**	**Function**
B7-1 (CD80)	Activated APCs	CD28	T cells	Stimulation
		CTLA4	Activated T cells	Inhibition
B7-2 (CD86)	Activated APCs	CD28	T cells	Stimulation
		CTLA4	Activated T cells	Inhibition
B7-H1 (PD-L1)	APCs, non-lymphoid tissues	PD-1	Activated T cells, B cells, NK cells	Inhibition
B7-DC (PD-L2)	APCs	PD-1	Activated T cells, B cells, NK cells	Inhibition

As mentioned above, B7-1 and B7-2, proteins upregulated on APCs surface after the stimulation by DAMPs or CD40 triggering, can interact with CD28 expressed on naïve T cells contributing to their activation in the initial stages of adaptive immune responses. However, this binding (B7-1 or B7-2 with CD28) triggers also transient surface expression of cytotoxic T lymphocyte antigen-4 (CTLA-4) on activated lymphocytes in delayed manner. CTLA-4 (CD152) interacts with B7-1 and B7-2 with significantly higher affinity compared to CD28. Therefore, once expressed on the membrane, CTLA-4 replaces CD28 in the interaction with B7-1 and B7-2 proteins leading effector T cell inhibition (Chambers, et al., 2001). Indeed,

CTLA-4 downstream signalling blocks T cell proliferation by impeding its entry into cell cycle and downregulates the production of stimulatory cytokines, such as IL-2 (Sansom, 2000).

Similarly, protein cell death 1 (PD-1), also called CD279, is upregulated on the surface of T cells constantly exposed to the antigen and on the membrane of hyper-stimulated NK cells. PD-1 triggering by PD ligands (PD-L1 and PD-L2), small B7 glycoproteins expressed on APCs, causes rapid inactivation of immune cells in analogous way to CTLA-4 signalling (Salmaninejad et al., 2019; Seliger, et al., 2008) [Figure 13].

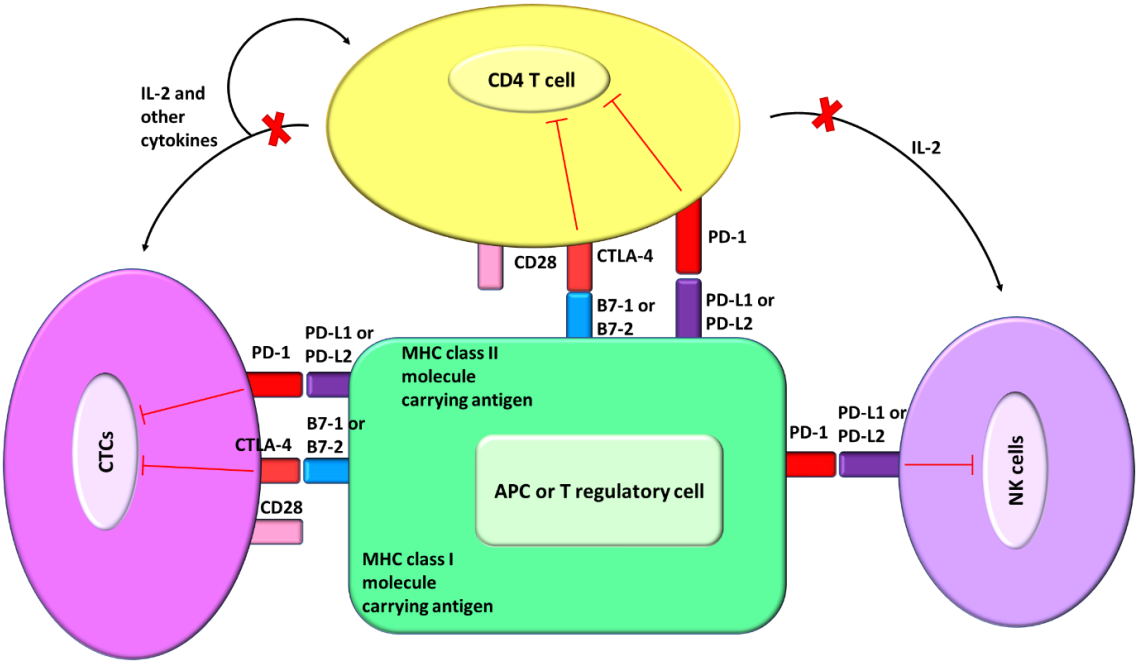


Figure 13: Immune cell physiological inactivation

Frequently, malignant cells employ these physiological pathways to escape the immune attack. Surface expression of PD-1 ligands and CD80/CD86 has been found in various cancer types. Therefore, monoclonal antibodies able to prevent inactivation of immune cells have been developed for this kind of malignancies and have shown efficacy for several types of cancer [Table 6, Figure 14] (Blank & Enk, 2014; Buchbinder & Desai, 2016; European Medicines Agency (EMA); Hsu et al., 2018; Seliger et al., 2008; Thomson, Allison, et al., 2006).

Table 6: Anti-CTLA-4 and anti-PD-1 monoclonal antibodies approved by European Medicine Agency (EMA) for cancer treatment

Antibody (ab)	Ab target	Cancer types, for which the ab has been approved (EMA)
Ipilimumab (Yervoy)	CTLA-4	Melanoma and advanced renal cell carcinoma
Nivolumab (Opdivo)	PD-1	Melanoma, non-small-cell lung carcinoma (NSCLC), advanced renal carcinoma, Hodking lymphoma, squamous cell cancer of the head and neck (SCCHN), urothelial cancer
Atezolizumab (Tecentriq)	PD-1	NSCLC and urothelial cancer
Pembrolizumab (Keytruda)	PD-1	Melanoma, NSCLC, Hodking lymphoma, SCCHN, urothelial cancer
Avelumab (Bavencio)	PD-1	Merkel cell carcinoma

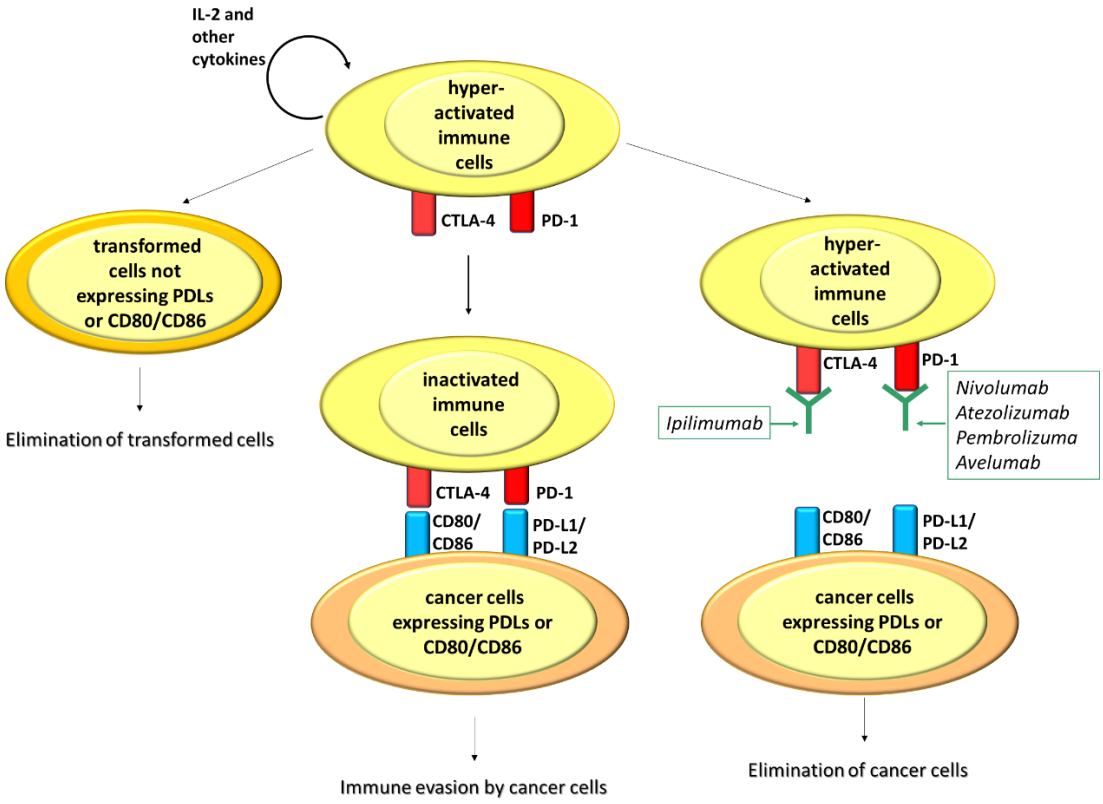


Figure 14: Cancer cell evasion through surface expression of immunosuppressive molecules. *Prolonged stimulation of immune cells by cancer cells can cause upregulated PD-1 and CTLA-4 expression on the surface of CTCs and NK cells. Transformed cells can be still recognised and killed by hyper-activated immune cells, if the latter don't encounter APCs or T regulatory cells, which are able to inhibit over-stimulated lymphocytes or NK cells (a). Cancer cells expressing CD80/CD86 and/or PD-L1/PD-L2 inactivate immune system cells and thus escape host anti-tumour immunity (b). Anti-CTLA-4 and anti-PD-1 antibodies prevent inhibitory interactions of immune cells with cancer cells expressing CD80/CD86 and/or PD-L1/PD-L2 and thus facilitate malignant cells elimination by CTCs and NK cells (c).*

1.3.2 Tim-3/galectin-9 mediated immunosuppression

Another mechanism allowing tumorigenic cells to escape host immune attack consists in their increased surface expression of transmembrane protein T cell immunoglobulin and mucin domain 3 (Tim-3). Indeed, it has been reported that soluble form of Tim-3 (sTim-3) is able to attenuate immune cells proliferation and to reduce the secretion of IL-2, a crucial cytokine necessary for the activation of NK cells and effector T cells (Geng et al., 2006). Presumably, once shed from the membrane of malignant cells, sTim-3 is able to interact with surface receptors expressed by immune system cells and downregulate their anti-tumour responses. Indeed, Tim-3 upregulation by malignant cells is also often correlated with poorer patient prognosis (Du et al., 2017; Peng, Li, & Sun, 2017; Sumbayev et al., 2016; Zhuang et al., 2012).

Human Tim-3 is a type 1 cell-surface glycoprotein containing 302 aa, that are structurally divided in four domains: extracellular N-terminal immunoglobulin variable (IgV) domain and a mucin domain, a transmembrane domain and a cytoplasmic tail containing six tyrosine residues and an Src homology 2 (SH2) binding motif (Kikushige & Miyamoto, 2013).

In absence of Tim-3 binding ligands, the intracellular domain is bound to HLA- B associated transcript 3 (Bat3), which precludes the phosphorylation of Tyr256 and Tyr263 present in the cytoplasmatic tail preventing Tim-3 downstream signalling. The binding of Tim-3 extracellular domain by its endogenous ligands can induce conformational changes that result in the release of Bat-3 allowing the phosphorylation of specific tyrosine residues present in the cytoplasmatic tail of Tim-3. Phosphorylated intracellular Tim-3 domain is then able to recruit specific SH2 domain-containing Src kinases which may lead to distinct downstream signalling depending on the Tim-3-bound ligand and on cell type expressing this transmembrane receptor (Das, et al., 2017; Ocaña-Guzman, et al., 2016) [Figure 15]. Indeed, Tim-3 has been associated with

both inhibitory and co-stimulatory function, depending in part on the specific cell type, in which this receptor is expressed (Banerjee, et al., 2018).

In myeloid AML cells, triggering of membrane-associated Tim-3 by its endogenous ligand, galectin-9, a β-galactoside-binding lectin, induces an activating signalling. Indeed, Tim-3 forms an autocrine loop with galectin-9 in AML cells inducing mammalian target of rapamycin (mTOR) pathway activation and promoting self-renewal and growth (Gonçalves Silva, et al., 2016; Kikushige et al., 2015).

In addition to myeloid cells, Tim-3 has been shown to be expressed in Th1 cells, cytotoxic T cells and NK cells. However, contrarily to myeloid cells, Tim-3 triggering in these lymphocytes and NK cells has been shown to induce inhibitory downstream responses (Das, et al., 2017; Du et al., 2017; Kang et al., 2015). Tim-3 surface upregulation was found in "exhausted" CTCs and in hyper-stimulated NK cells and its triggering can provoke functional inactivation and inhibition of cytokine production (Du et al., 2017; Gallois, et al., 2014, Kang et al., 2015).

This differential signalling in distinct cell types might be explained by the fact that phosphorylated Tim-3 domain recruits different Src kinases in immune system cells and myeloid cells as proposed by Ocaña-Guzman and colleagues (Ocaña-Guzman, et al., 2016).

As mentioned above, one of the endogenous ligands of Tim-3 is galectin-9. Thus, it is reasonable to assume that galectin-9 (and possibly other endogenous ligands) is involved in Tim-3 triggering also CTCs and NK cells.

Importantly, galectin-9 can bind Tim-3 only when IgV domain is glycosylated (Ocaña-Guzman, et al., 2016). Indeed, extracellular domains of Tim-3 can be subjected to O- and N-glycosylation. For this reason, the molecular weight (MW) of Tim-3 can vary depending on the levels of glycosylation. The lowest MW of full-length Tim-3 is 33 kDa, which corresponds

to mono-glycosylated protein. Since the MW of each glycan is around 2-3 kDa, it is possible to estimate the number of sugars bound to Tim-3 considering the MW of the full-length glycoprotein (Clayton et al., 2015) [Figure 15].

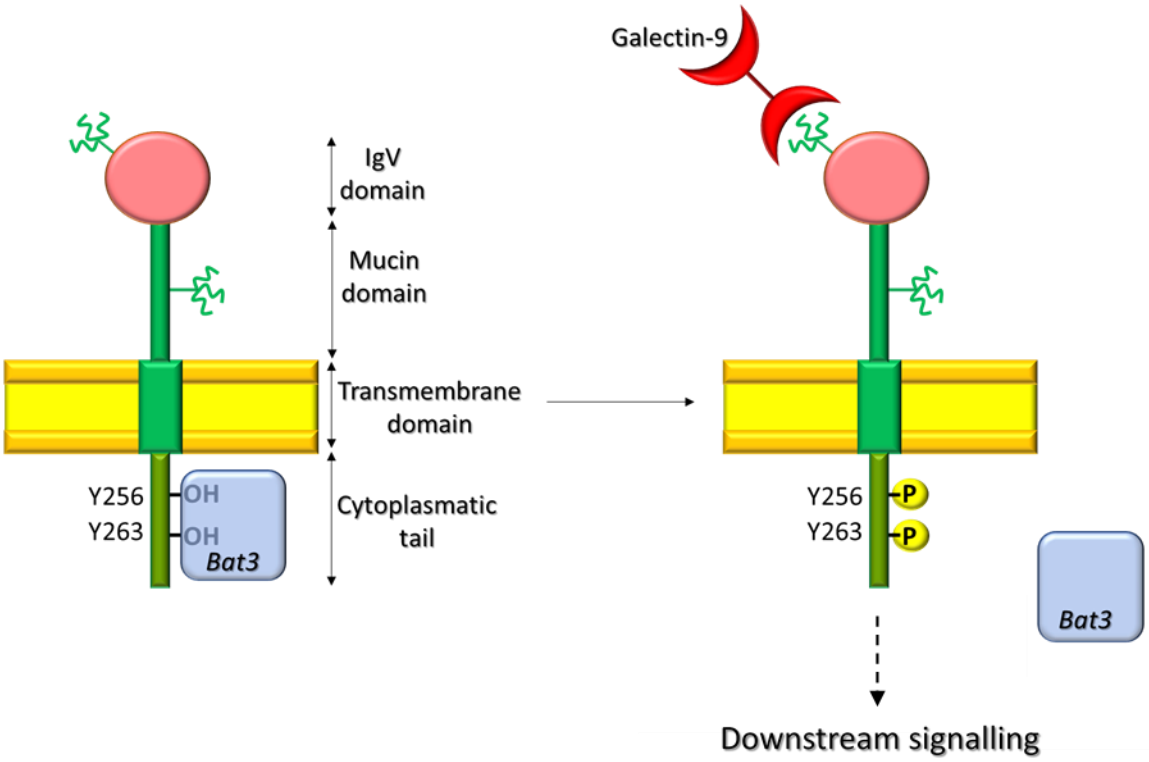


Figure 15: Tim-3 structure and its interaction with galectin-9 on immune system cells.

Since cancer is associated with chronic inflammation, prolonged hyperactivation of lymphocytes and NK cells leads to surface upregulation of Tim-3 during tumorigenesis. This feature is frequently exploited by malignant cells, which suppress anti-tumour immunity through expression of galectin-9 using its intracellular trafficker Tim-3 (Gonçalves Silva, et al., 2016; Z. Liu et al., 2016). Indeed, galectins lack signal sequence necessary for their transport into the endoplasmic reticulum (ER) and thus necessitate a trafficking protein for their surface expression (Gonçalves Silva et al., 2017). It means that Tim-3 acts as both, endogenous receptor and trafficking protein of galectin-9.

To date, 15 mammalian galectins have been identified that all share a conserved carbohydrate recognition domain (CRD) and exhibit high affinity for β-galactosides present on

glycoconjugates. Galectins can be classified into 3 groups according to their structure and number of CRDs:

- Prototype galectins, consisting of a single CRD;
- tandem repeat galectins, consisting of 2 different but homologous CRDs, connected by a linker region;
- chimera galectins, which have a tail of short tandem repeats fused to a single CRD.

The prototype galectins (galectins -1, -2, -5, -7, -10, -11, -13) usually self-associate and form dimers. Tandem-repeat galectins (galectins -4, -6, -8, -9) contain CRDs connected by a variable length linker peptide. Usually, galectin-9 is monomeric. However, galectin-9 has been reported to self-associate and form dimers (in mouse) and multimers (in human). The only chimera Gal-3 has a C-terminal CRD linked to N-terminal tail, that can exist as monomer, dimer or higher order oligomer state, such as tetramer and pentamer [Figure 16] (Dings, et al., 2018; N. et al., 2007; Nagae et al., 2006; Thijssen, et al., 2007).

Galectins are involved in various basic cellular mechanisms, such as cell aggregation, proliferation, migration and apoptosis. Deregulation of galectin levels has been observed in several malignancies. Indeed, galectins have been reported to contribute to tumour progression as a result of their immunosuppressive properties and control of cell proliferation/apoptosis (Thijssen et al., 2007).

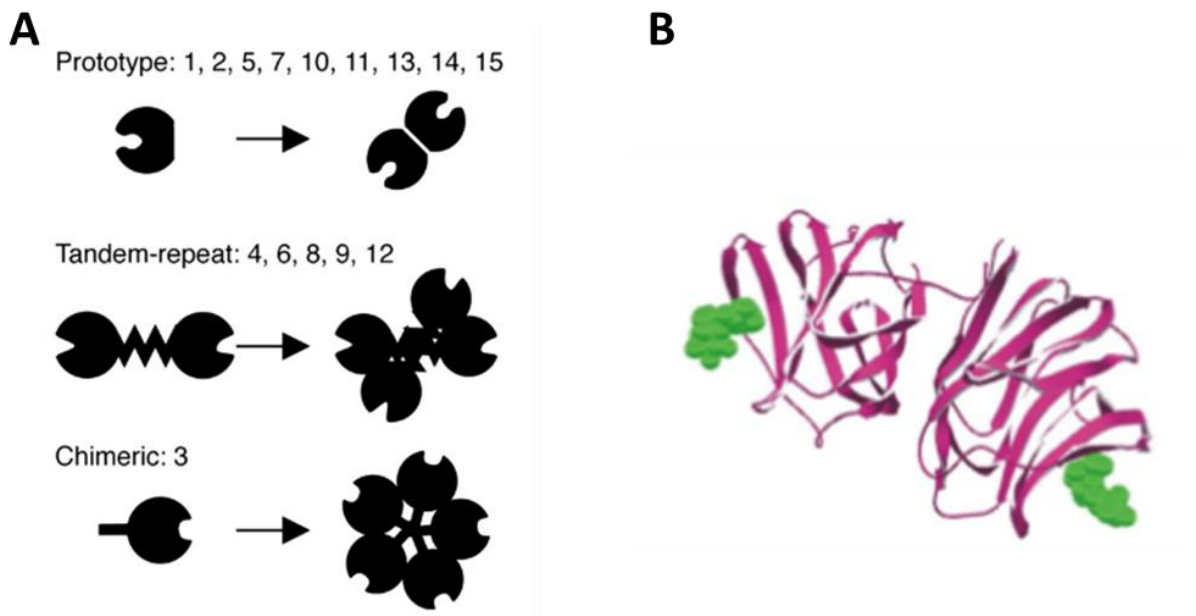


Figure 16: Classification of galectins into three main groups based on their domain structural organisation (A) (Heusschen, Griffioen, & Thijssen, 2013)***. Galectin-9 structure:*** *in green – sugar molecules, which can possible interact with a glycoprotein, are situated in proximity to carbohydrate binding sites (B)* (Gonçalves Silva et al., 2017)

As mentioned above, galectins accumulate intracellularly and are secreted only when bound to their cytoplasmatic traffickers. This suggests that galectins may have also an intracellular role. Recently it has been reported that galectin-3 is able to protect acute myeloid leukaemia (AML), prostate and colorectal cancer cells from anticancer drug-induced apoptosis (Fukumori et al., 2006; Harazono, et al., 2014). Galectin-3 has been shown to sustain mitochondrial integrity possibly through direct binding to BCL2 proteins. Indeed, galectin-3 contains the NWGR anti-death motif of the Bcl-2 family. Galectin-3 can bind to BCL2 proteins, such Bax, through the NWGR motif and inhibit cancer cell death induced by anticancer drugs. In addition, galectin-3 has been reported to be able to decrease Bad expression preventing mitochondrial depolarization. Moreover, phosphorylated galectin-3, formation of which can result from DNA damage induced by anticancer drugs, is able to stimulate extracellular signal–regulated kinases (ERK) pathway and induce Bad phosphorylation, promoting mitochondrial stabilization (Harazono, et al., 2014; Ruvolo, 2016). However, this anti-apoptotic property hasn't been investigated yet in other galectins, such as galectin-9.

In AML cells, it has been shown that galectin-9, in addition to immunosuppressive properties, forms an autocrine loop with its endogenous receptor and trafficker Tim-3, leading to the promotion of NF-κB and β-catenin signalling, which are critical for AML self-renewal and survival (Gonçalves Silva, et al., 2016; Yasinska, et al., 2018).

Understanding the mechanisms implemented by malignant cells in order to escape host immune surveillance can be best achieved by the investigation of biochemical pathways implemented by blood cancer cells. Cells causing these systemic malignancies are under constant exposure to cytotoxic lymphoid cells and thus become a subject for immune attack.

1.4 Blood cancer as a systemic malignancy facing permanent interaction with the immune system from the very beginning

Intensive production of immunosuppressive molecules is pivotal for the progression of hematopoietic malignancies. Indeed, transformed blood cells are circulating in close contact to immune system cells, which can potentially eliminate cancer cells in absence of immunosuppressive mechanisms (Gonçalves Silva, et al., 2016; Yasinska, et al., 2018).

It is assumed that leukaemia arises from accumulation of mutations in hematopoietic stem cells (HSCs) rather than in mature blood cells. This hypothesis is supported by the fact that leukaemia cells usually preserve the capacity to express the Kit receptor (stem cell factor receptor), which is responsible for cell self-renewal. Contrarily, differentiation of HSCs into specialised blood cells results in the loss of their ability in Kit receptor expression. For this reason mature blood cells can’t proliferate ensuring relatively constant number of specialised haematopoietic cells in the human body (Passegué, et al., 2003).

Initial differentiation of HSCs can lead to myeloid stem cell or to lymphoid stem cell, both still expressing Kit receptor. The myeloid stem cells can then differentiate into myeloid leukocytes

(monocytes, neutrophils, eosinophils and basophils), erythrocytes and platelets. On the other hand, the maturation of lymphoid stem cells can lead to lymphocytes and NK cells development (Janeway et al., 2012).

Based on the type of haematopoietic stem cell undergoing malignant transformation and on the velocity of progression (acute or chronic), leukaemia is classified in four main groups: acute myeloid leukaemia (AML), chronic myeloid leukaemia (CML), acute lymphoid leukaemia (ALL) and chronic lymphoid leukaemia (CLL) (Szczepański, et al., 2003).

Among these four types of leukaemia, AML is the commonest one in the adults. Each year a significant number of new AML cases is registered all over the world. Unfortunately, the survival rates for this malignancy remain very low. Rapid progression and multiple immunosuppressive mechanisms characterising AML result, indeed, in poor prognosis and high mortality rates (Estey & Döhner, 2006; WHO, 2018).

High proliferation rate and survival of AML cells is a consequence of specialised mechanisms acquisition by malignant cells, which leads to continuous self-renewal and protect from host immune attack. Indeed, AML cells express immunosuppressive ligands, such as CD86, PD-L1 and PD-L2, able to inactivate lymphocytes and NK cells as described before [Figure 17] (Yasinska, et al., 2018).

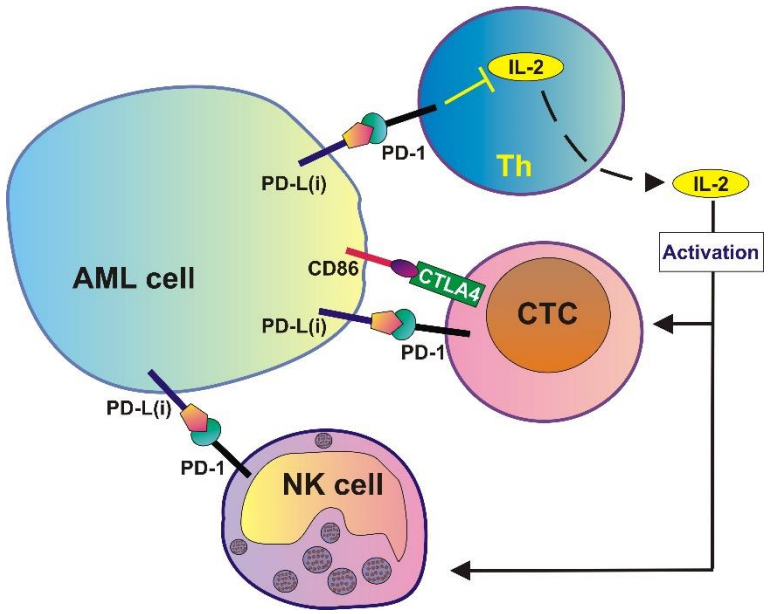


Figure 17: Inhibitory interactions via PD-1 and CTLA-4 receptors lead to immune cells inactivation by direct binding to respective ligands and through suppression of IL-2 secretion

Moreover, as previously described, AML cells express high surface levels of Tim-3/galectin-9 complex, that can be shed leading to the release of Tim-3 and galectin-9, which can induce apoptosis in T cells and inactivates NK cells circulating in the bloodstream (Yasinska, et al., 2018).

Moreover, it has been recently reported that galectin-9 can promote downstream signalling when interacting with its endogenous Tim-3 receptor on AML cells. Indeed, this complex formation on the surface of AML cells stimulates the phosphorylation in Ser2448 residue of mammalian target of rapamycin (mTOR) (Gonçalves Silva, I., et al., 2016). Active mTOR (phosphorylated in Ser2448) is then able to promote phosphorylation of various substrates, such as eukaryotic translation initiation factor 4E (eIF4E) binding protein (BP). Indeed, hypo-phosphorylated eIF4E-BPs interacts avidly with eIF4E protein preventing its interaction with cap structure at 5' end of specific mRNAs (Jossé, et al., 2016). Phosphorylation of Ser65, Thr70 and possibly other aa residues of eIF4E-BP by active mTOR induces conformational changes in eIF4E-BPs that lead to the loss of affinity for eIF4E. Released eIF4E is then able to bind mRNAs and promote translation of various proteins necessary for AML cell survival and

proliferation. Another important target of active mTOR is the ribosomal protein S6 kinase beta-1 (S6K1), also called p70S6 kinase. Active S6K1 promotes the phosphorylation of e S6 ribosomal protein, which leads to specific protein synthesis. The mTOR induced protein synthesis leads to increased levels of various proteins, including Hif-1α, thus promoting VEGF transcription and future angiogenesis. Moreover, active mTOR positively affects glycolysis rendering it more efficient (Gonçalves Silva, et al., 2016, Prokhorov et al., 2015).

Consequently, galectin-9/Tim-3 signalling is pivotal for AML progression. However, the mechanisms underlying its surface expression remains still unclear. Neuronal receptor neuronal receptor latrophilin 1 (LPHN1) has been proposed to be responsible for galectin-9 secretion.

LPHN1 is G-protein-coupled receptor physiologically expressed in neurons, where it is involved in neurotransmitter release in Ca^{2+} dependent manner. Recently, it was discovered that the neuronal receptor latrophilin 1 (LPHN1) is expressed in human monocytic cells (THP-1) and in primary human AML cells, but is absent in mature healthy leukocytes. It has been shown that its triggering by latrotoxin, compound present in the venom of black widow spider, leads to Ca^{2+} mobilisation and cytokine exocytosis by AML cells (Sumbayev et al., 2016).

Moreover, since these cells are circulating in the blood, it is obvious that LPHN1 ligands should be present as well in the vessels or expressed by endothelial cells. To date, two LPHN endogenous ligands of nervous tissue have been identified: Lasso/teneurin-2 and fibronectin leucine rich transmembrane protein 3 (FLRT3) (O'Sullivan et al. 2012; Silva et al. 2011). Western blot analysis of in myeloid leukaemia cell lines (THP-1 and U-937), primary healthy leukocytes or blood plasma obtained from healthy donors showed that teneurin-2 was absent (Sumbayev et al. 2016). For this reason, our second candidate as possible stimulatory LPHN1

ligand on AML cells was FLRT3. However, its presence in the blood or on circulating cells haven't been examined yet. Also, FLRT3 effects on AML cells haven't been studied yet.

FLRTs are transmembrane proteins containing an extracellular leucine-rich repeat (LRR) domain, able to interact with proteins containing olfactomedin domain. Structural studies of LPHNs revealed the presence of an external olfactomedin domain in all the three isoforms of this receptor (LPHN1-3). Indeed, the interaction between FLRT3 LRR domain and LPHNs olfactomedin domain has been reported (Krasnoperov, et al. 1999; Lelianova, et al. 1997; O'Sullivan, et al. 2012).

Additionally, the transcription factor(s) associated with LPHN1 expression in AML cells remain(s) still unknown.

We hypothesised, that cortisol could be involved in LPHN1 regulation. Indeed, abnormal cortisol levels were detected in several cancer types, but these have never been reported for AML (Mazzoccoli, et al., 2003; Sephton, et al., 2013; Schrepf, et al., 2015).

Cortisol is a glucocorticoid hormone produced by adrenal gland. The hypothalamic-pituitary-adrenal (HPA) axis tightly controls cortisol levels, which increase in response to numerous stimuli such as stress and energetic deficiency (Bamberger, 1996).

Cancer cells use high amounts of glucose, main energy source of the body, in order to proliferate rapidly. Therefore, anomalous reduction of hematic glucose occurs during cancer development. Hypoglycaemia, resulting from this process, stimulates HPA axis with consequent cortisol release by adrenal gland (Greenwood, et al., 1966; Koenig, et al., 2005). One of the cortisol functions, indeed, is to increase glucose levels in the blood, mainly by promoting glycogenolysis and gluconeogenesis (Garber, et al., 1976).

Although its concentration in the blood oscillates during the day, cortisol is an always circulating hormone and, thus, can regularly interact with glucocorticoid receptors present in myeloid and other blood cells. Depending on the cell type, this hormone can promote differential gene transcription leading to cell-specific responses. For instance, T cells activity and proliferation was found to be suppressed by glucocorticoid treatment (Herold, et al., 2006; Davis, et al., 2014). Contrarily, white blood cells proliferation was shown to be significantly upregulated by glucocorticoids. Indeed, it was found that glucocorticoids are able induce haematopoiesis of myeloid lineage cells (Rinehart, 1997).

Thus, cortisol could potentially support AML cell progression by suppressing anti-tumour immunity and by stimulating malignant cells proliferation. In addition, as mentioned above, cortisol is able to stimulate the expression of numerous proteins inside the cells.

For all these reasons, we thought to test cortisol also as a potential regulator of LPHN1 expression.

Finally, Tim-3 and galectin-9 proteins have been characterised in different solid tumours, but mechanisms underlying regulation of their biochemical activities remain unknown.

2. AIMS AND OBJECTIVES

The aim of this PhD programme was to investigate the Tim-3-galectin-9 immunosuppressive pathway in human malignant cells and the biochemical functions of its crucial components.

The following objectives were addressed in order to achieve this aim:

1) To investigate the biochemistry and function of the Tim-3-galectin-9 secretory pathway in human AML cells which are in permanent contact with cytotoxic lymphoid cells.

2) To investigate the ability of human AML cells to recruit crucial components of normal metabolism to escape immune surveillance and progress the disease. In particular:

A) To study the effects of cortisol (hormone of adrenal cortex with crucial physiological function) on the activation of galectin-9 secretion by AML cells and possible recruitment of this hormone as an AML cell survival/immune escape factor.

B) To investigate the biochemical mechanisms underlying recruitment of stem cell factor (SCF, main normal haematopoietic growth factor) by human AML cells for the purposes of survival, proliferation and immune escape. In particular, the study focuses on the role of danger signal HMGB1 produced by AML cells in activation of SCF production by healthy tissues.

3) To study the expression and activity of the Tim-3-galectin-9 immunosuppressive pathway in human solid tumour cells in order to understand whether is unique for AML or ubiquitous and common for a variety of malignant tumours.

4) To investigate the behaviour of Tim-3-galectin-9 immunosuppressive pathway in healthy and malignant human cells in the case of mitochondrial dysfunction followed by apoptotic cell death and to understand whether galectin-9 could also plays intracellular anti-apoptotic role as some other members of the galectin family (for example galectin-3).

3. MATERIALS AND METHODS

3.1 Materials

Tissue culture medium and supplements were purchased from Sigma-Aldrich (Sufflock, UK).

Mouse monoclonal antibodies directed against mTOR and β-actin, and rabbit polyclonal antibodies against phospho-S2448 mTOR, RAGE, galectin-9, HRP-labelled rabbit anti-mouse secondary antibody were purchased from Abcam (Cambridge, UK). Rabbit polyclonal antibodies against LPHN1 (PAL1 and RL1) as well as rabbit polyclonal antibody against LPHN2 (PAL2) were previously described (Davydov et al., 2009; Volynski et al., 2000). Other two anti-LPHN1 antibodies, rabbit antibody against native form and mouse monoclonal antibody, were purchased respectively from Abcam and Santa Cruz Biotechnology (Dallas, Texas, USA). Another rabbit antibody against LPHN2 was obtained from Abcam. Human recombinant FLRT3 and mouse monoclonal anti-FLRT3 antibody were purchased from Santa Cruz Biotechnology. Antibodies against phospho-S65 and total eukaryotic initiation factor 4E binding protein 1 (eIF4E-BP1) were obtained from Cell Signalling Technology (Danvers, MA, USA). Goat anti-mouse and goat anti-rabbit fluorescence dye-labelled antibodies were purchased from LI-COR (Lincoln, Nebraska USA).

Anti-Tim-3 mouse monoclonal antibody, its single chain variant, human Ig-like V-type domain of Tim-3 (amino acid residues 22–124), human HMGB1 and human SCF were a kind gift of Dr Luca Varani (Gonçalves Silva et al., 2017; Prokhorov et al., 2015; Yasinska, et al., 2018).

A soluble extracellular fragment of LPHN1, LPH-51, was produced and purified as previously described (Volynski et al., 2000).

DOPAT transfection reagent, primers and galectin-9 silencing RNA (siRNA) were obtained from Sigma-Aldrich. Tim-3 silencing RNA (siRNA) was purchased from Santa Cruz Biotecnology.

Maxisorp™ microtitre plates were provided either by Nunc (Roskilde, Denmark) an Oxley Hughes Ltd. (London, UK). ELISA-based assay kits for the detection of galectin-9, Tim-3, IL-2, TNF-α, IL-1β, SCF and VEGF were purchased from Bio-Techne (R&D Systems, Abingdon, UK).

Secondary antibodies for confocal laser microscopy, TRITC labelled antibody (goat anti-mouse IgG) and t FITC labelled antibody (goat anti-rabbit IgG), were obtained from Abcam. Imaging flow cytometry (goat anti-mouse and goat anti-rabbit Alexa 488, Alexa 555 and Alexa 647) were purchased from Invitrogen (Carlsbad, USA).

All other chemicals purchased were of highest grade of purity and obtained from Fischer Scientific (Loughborough, UK) or Sigma (Sufflock, UK).

3.2 Tissue culture

3.2.1 Cells lines

THP-1 human myeloid leukaemia monocytes, K562 chronic myelogenous leukaemia cells, Jurkat T cells, MCF-7 human epithelial breast cancer cells, Colo-205 human colorectal adenocarcinoma cells of epithelial origin, HEP G2 human hepatocarcinoma cells were obtained from the European Collection of Authenticated Cell Cultures (ECACC, Salisbury, UK). RC-124 non-malignant human kidney cells of epithelial origin and renal clear cell carcinoma RCC-FG1 cells were obtained from CLS Cell Lines Service GmbH (Eppelheim, Germany). Cells were cultured in RPMI 1640 medium (R8758 – Sigma-Aldrich) with L-glutamine and sodium bicarbonate and supplemented with 10% foetal bovine serum (FBS), penicillin (50 IU/ml) and

streptomycin sulphate (50 µg/ml). LAD2 mast cells were kindly provided by A. Kirshenbaum and D. Metcalfe (NIH, USA). Cells were cultured in StemPro-34 serum-free media in the presence of 100 ng/ml SCF (Kirshenbaum et al., 2003). Untransfected mouse neuroblastoma cells (NB2A) and those overexpressing the full-size LPHN1 (LPH-42) were cultured as previously described (Volynski et al., 2000). TALL-104 cytotoxic T lymphocytes derived from human acute lymphoblastic leukaemia were obtained from the American Tissue Culture Collection (ATCC). TALL-104 were cultured in ATCC-formulated Iscove's Modified Dulbecco's Medium supplemented with 100 units/ml recombinant IL-2, 2.5 µg/ml human albumin, 0.5 µg/ml D-mannitol and FBS to a final concentration of 20%. LN401 human glioblastoma cells, BC-8701 human breast cancer cells, MDA-MB-231 human breast adenocarcinoma cells, PC3 prostate adenocarcinoma cells, Calu 6 human pulmonary non-small cell carcinoma cells, BEAS-2B human bronchial epithelium cells, D10 human malignant melanoma and HaCaT human keratinocytes were obtained from ECACC, ATCC or CLS Cell Lines Service GmbH. All the cells were cultured at 37 ºC and 5% CO_2.

Cell lines were accompanied by identification test certificates and were cultured according to specific tissue culture protocols. The cells were cultured for maximum 25-30 passages.

3.2.2 Primary human cells

Primary human AML mononuclear blasts (AML-PB001F, newly diagnosed/untreated) were purchased from AllCells (Alameda, CA, USA) and handled in accordance with the manufacturer's instructions following ethical approval (REC reference: 16-SS-033). Other primary human AML cells were obtained from the sample bank of the University Medical Centre Hamburg-Eppendorf (Ethik-Kommission der Ärztekammer Hamburg, reference: PV3469). Cells were incubated in IMDM medium containing 15% BIT 9500 serum substitute,

100 μM mercaptoethanol, 100 ng/ml stem cell factor (SCF), 50 ng/ml FLT3, 20 ng/ml G-CSF, 20 ng/ml IL-3, 1 μM UM729 and 500 nM stemregenin 1 (SR1).

Primary human NK cells and primary human healthy leukocytes were purified from buffy coat blood (prepared from healthy donors) obtained from the National Health Blood and Transfusion Service (NHSBT, UK) following ethical approval (REC reference: 16-SS-033).

Primary CD34-positive HSCs were obtained from Lonza (Basel, Switzerland).

Primary cells were cultured for maximum 2-3 passages before being used for the experiments.

3.2.3 Primary human blood plasma samples

Blood plasma from healthy donors was provided by the National Health Blood and Transfusion Service (NHSBT, UK) following ethical approval (REC reference: 16-SS-033).

Primary human AML plasma samples were obtained from the sample bank of University Medical Centre Hamburg-Eppendorf (Ethik-Kommission der Ärztekammer Hamburg, reference: PV3469).

3.2.4 Bone marrow extracts

Femur bones of six-week-old C57 BL16 mice (25 ± 2.5 g, kindly provided by Dr. Gurprit Lall, School of Pharmacy, University of Kent) were used for the experiments following approval by the Institutional Animal Welfare and Ethics Review Body. Animals were handled by authorized personnel in accordance with the Declaration of Helsinki protocols. Bone marrow was isolated from femur bone heads as described before (Swamydas & Lionakis, 2013). Cells were kept in RPMI 1640 medium supplemented with 10% FBS, penicillin (50 IU/ml) and streptomycin sulphate (50 μg/ml). In addition, whole extracts were obtained from isolated bone marrow with final protein concentration 1 mg/ml.

3.2.5 Human breast tissue samples

Primary human tumour tissue samples paired together with peripheral tissues (also called "normal" or "healthy" of the same patients) were collected surgically from breast cancer patients treated at the Colchester General Hospital, following written consent taken before surgery. Paired normal (healthy) peripheral tissues were removed during macroscopic examination of a tumour by pathologists. Blood samples were collected before breast surgery from patients with primary breast cancer and before treatment from patients with metastatic breast cancer. Samples were also collected from healthy donors (individuals with no diagnosed pathology), which were used as control samples. Blood separation was performed using buoyancy density method employing Histopaque 1119-1 (Sigma, St. Louis, MO) according to the manufacturer's protocol. Ethical approval documentation for these studies was obtained from the NRES Essex Research Ethics Committee and the Research & Innovation Department of the Colchester Hospitals University, NHS Foundation Trust [MH 363 (AM03) and 09/H0301/37].

3.3 Cell lysis

Cell pellets obtained after the centrifugation were re-suspended in lysis buffer (50 mM Tris-HCl, 5 mM Ethylenediaminetetraacetic acid (EDTA), 150 mM NaCl, 0.5% Nonidet-40, 1 mM phenylmethylsulfonyl fluoride (PMSF), pH 8.0) and kept on the ice for 60-90 minutes. After the incubation on the ice, the samples were centrifuged. The supernatants containing protein extracts obtained after centrifugation were used straight after or stored at -80°C until future use.

3.4 Tissue lysis

The lysates were prepared using 100 mg of each frozen tissue, which was initially grounded into a powder and then, homogenised with 100 µL of the tissue lysis buffer (20mM Tris/HEPES pH 8.0, 2 mm EDTA, 0.5 M NaCl, 0.5% sodium deoxycholate, 0.5% Triton X-100, 0.25 M Sucrose, supplemented with 50 mM 2-mercaptoethanol, 50 µM PMSF, 1 µM pepstatin supplied just before use). Tissues were homogenised using Polytron Homogenizer (Capitol Scientific, USA) and a syringe was used to obtain homogeneous cell suspension. These tissue suspension were then filtered through medical gauzes and centrifuged at +4ºC at 10,000 g for 15 minutes. After the centrifugation, proteins present in supernatants were precipitated by incubation of the samples on ice for 30 minutes with equal volumes of ice-cold acetone. Protein pellets were obtained by centrifugation (4ºC, 10,000 g, 15 minutes) followed by air drying at room temperature and then suspended in the SDS-lysis buffer described in the section 3.3 (D'Arcy et al., 2008).

3.5 Protein quantification

Protein concentration in the samples was measured using Bradford assay, which involves the addition of an acidic dye (Coomassie Brilliant Blue G-250) to the protein solutions.

At the assay pH (under acidic conditions) the dye molecules are protonated and present the maximum of absorption at 465 nm (brownish colour) [Figure 18A]. When added to protein solutions, the Coomassie Brilliant Blue G-250 (CBB) can bind proteins via π-interactions (aromatic ring of CBB with aromatic aa residues of the protein) and via electrostatic attraction (negatively charged sulfonate groups of CBB with protonated basic aa residues of the protein). Protein-CBB complex formation leads to the shift of the dye maximum absorption from 465 nm to 595 nm (blue colour) [Figure 18B] (Georgiou, et al., 2008).

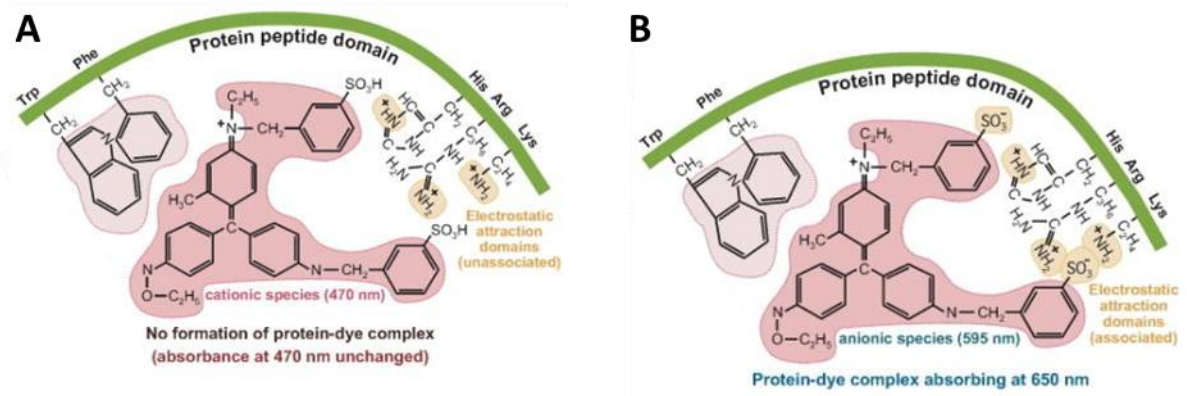


Figure 18: Maximum of absorption of CBB alone and in complex with the protein. Protonated CBB has maximum of absorption at 465 nm (A). Deprotonation of CBB by basic amino acids leads to the formation of negatively charged sulfonate groups which can bind the protein through electrostatic interactions. In addition, aromatic residues, such as Trp, Tyr and Phe, can bind CBB through π-interactions. Stabilisation of CBB-protein complex results in the shift of maximum of absorption of the dye from 465 nm to 595 nm (Adapted from Gregoriu, et al., 2008).

For protein quantification, 5 µl of cell lysate were mixed with 150 µl of Bradford reagent (0.01% (w/v) Coomassie Brilliant Blue G-250, 4.7% (w/v) ethanol and 8.5% (w/v) phosphoric acid) in a microwell plate. Following 5 minutes of incubation, the optical density at 620 nm was read in the plate reader.

3.6 Western Blot analysis[1]

Tissue o cell lysates were mixed with 2X or 4X sample buffer (125 mM Tris-HCL, 2% sodium dodecyl sulphate (SDS), 10% glycine, 1 mM dithiothreitol (DTT), 0.002% bromophenol blue, pH6.9) and boiled 5 min at 95°C.

The mixture of proteins was then separated according to their MW using sodium dodecyl sulphate-polyacrylamide gel electrophoresis (SDS-PAGE). SDS is an anionic detergent that denatures (together with DTT) the proteins and "wraps" the obtained polypeptide chains. This binding results in the formation of negatively charged complexes with equal charge densities per unit length of protein, thereby eliminating the ionic charges of individual amino acids. In

[1] Buffers and other solutions used in this paragraph are reported in section 7.1 and 7.2 in Appendix

this way the proteins can be resolved on the SDS-PAGE gel according to their MW and not to their three-dimensional size or their individual charges.

After loading the protein mixtures in the wells of the gel kept in the running buffer (described in Appendix), an electric field was applied to force negatively charged polypeptides to migrate from cathode (negative pole) to anode (positive pole) leading to the separation of proteins according to their MW. Constant voltage of 150-200 V was applied until the dye front was about 1 cm from the bottom of the gel. Proteins were resolved on 7.5%, 10% or 12% SDS-polyacrylamide gels, prepared as described in section 7.1 in Appendix. Polyacrylamide gel percentage was chosen according to the molecular weight of the target protein:

Protein target, (KDa)	>250	90-250	50-90	20-50	<20
Gel%	5	7.5	10	12	15

After performing SDS-PAGE, the separated proteins in the gel were transferred to a nitrocellulose membrane using semi-dry (BioRad system) or wet (Invitrogen system) blotting. Filter paper and/or filter pads, together with nitrocellulose membrane were soaked in blotting buffer and assembled with obtained gel in the transfer cassette as illustrated in Figure 19.

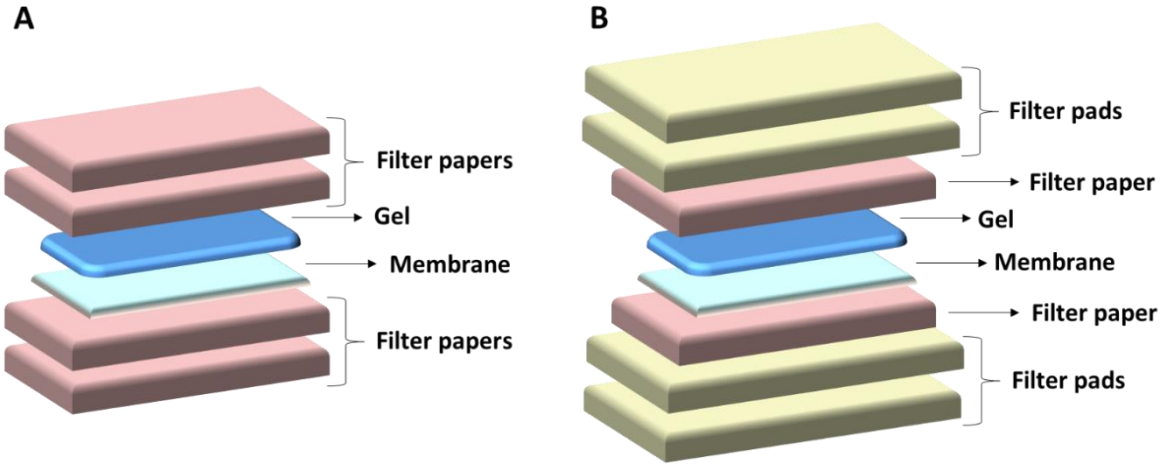


Figure 19: Schematic representation of gel/membrane/filter papers/filter pads assembly in semi-dry (A) and wet (B) transfers.

The blotting was performed in a semi-dry (BioRad system) or wet (Invitrogen system) environment at constant voltage and 0.07 Amp (semi-dry transfer) or 0.1 Amp (wet transfer), one to two hours, according to the gel and system used.

After the blotting, the membranes were blocked with blocking buffer (tris-buffered saline, 0.1% Tween 20 (TBST), 2% bovine serum albumin (BSA)) for at least 1 h under constant agitation at room temperature to minimise unspecific binding of the antibodies on the membrane.

Blocked membranes were then incubated with the antibodies for target proteins for at least two hours at room temperature. For all primary antibodies a 1:1000 dilution in blocking buffer was used, except those against LPHNs, FLRT3 (where a 1:500 dilution was used) and CD3 (where a 1:100 dilution was used).

Following the incubation with primary antibodies, the membranes were washed with TBST buffer for at least 15 min, under constant agitation at room temperature and then incubated with Li-Cor goat secondary antibodies, conjugated with fluorescent dyes, diluted in TBST buffer (1: 2000 dilution). After the incubation with secondary antibodies (1h, room temperature), the membranes were washed with TBST buffer as described above and visualised using a Li-Cor Odyssey imaging system. The detection of the bands corresponding to target proteins is possible because of the fluorescent tags bound to the secondary antibodies. These fluorescent dyes, when excited with specific wavelengths of light in the near infrared spectrum, emit at different wavelengths, which can be detected by Odyssey Imaging System. In particular, this imaging system has two channels which can be employed for the detection of fluorescence corresponding to one of two specific monochromatic wave lengths (680 nm and 800 nm).

Western blot data were qualitatively and quantitatively analysed using Odyssey software and values obtained were normalised against those of β-actin, employed to ascertain equal protein

loading into the wells of the gel. Molecular weights of target proteins were calibrated in proportion to the running distance of protein standard markers.

Western blot analysis was employed to detect the components of the Tim-3, galectin-9, FLRT3, LPHNs 1-3, Gαq, CD3, Hif-1α and RAGE in cell or tissue lysates.

In order to quantitatively analyse mTOR-dependent phosphorylation of eIF4E-BP using Western Blot analysis, levels of phospho-S65-eIF4E-BP and total eIF4E-BP were detected on different membranes to avoid the overlap of protein bands due to possible incomplete membrane stripping. Values obtained after densitometry analysis of the bands corresponding to phospho-S65-eIF4E-BP and total eIF4E-BP were normalised against those of β-actin for respective membranes. The levels of eIF4E-BP phosphorylation were then calculated using the ratio between normalised phospho-S65-eIF4E-BP and total eIF4E-BP as described in the following equation:

$$\mathbf{pS65-eIF4E-BP\ level} = \frac{[\mathbf{pS65-eIF4E-BP}]}{[\mathbf{Actin}]} \div \frac{[\mathbf{eIF4E-BP\ total}]}{[\mathbf{Actin}]}$$

This ratio in control samples was considered as 100%.

3.7 Enzyme-linked immunosorbent assay (ELISA)

ELISA was used for the detection and quantification of target proteins in the cell culture media, human plasma, and cell and tissue lysates.

3.7.1 Determination of galectin-9, soluble Tim-3 (sTim-3), TNF-α, IL-1β, SCF, VEGF and IL-2 concentrations released by the cells

Levels of galectin-9, soluble Tim-3 (sTim-3), TNF-α, IL-1β, SCF, VEGF and IL-2 in cell culture media or in human blood plasma were determined by solid phase sandwich ELISA (R&D Systems assay kits) according to the manufacturer's protocol. Briefly, 100 µL of capture

antibody for specific target protein were added to each well of 96-well microplate coated with poly-D-lysine (PDL), which was then incubated overnight at room temperature. Prior to the well-loading, capture antibody was diluted in phosphate-buffered saline (PBS) solution obtaining an optimal concentration for ELISA performance as recommended in the manufacturer's protocol. After the incubation with the capture antibody, the wells were blocked with ELISA blocking buffer (PBS/BSA 1%) for at least one hour under constant agitation at room temperature. 100 µL of sample (culture media or human blood plasma) were then added to each well and left for at least two hours under constant agitation at room temperature. Following the incubation with the samples, the wells were washed with TBST buffer and incubated with 100 µL of specific biotinylated detection antibody diluted in PBS/BSA 1% for at least two hours under constant agitation at room temperature. After the incubation with the detection antibody, the wells were washed with TBST buffer and incubated with 100 µL of streptavidin labelled with horse radish peroxidase (HRP) diluted in PBS/BSA 1% for at least 30 minutes under constant agitation at room temperature. The wells were then washed with TBST buffer and then incubated with 100 µL of substrate solution (0.2% H_2O_2, 56 Mm orto-phenylenediamine (OPD)) for maximum 10 minutes at room temperature protecting from light. The reaction was stopped by adding 100 µL of 1.8 M H_2SO_4 in each well when change colour was observed. Indeed, HRP catalyses the oxidation of OPD in presence of H_2O_2 leading to the formation of 2,3-diaminophenazine (DAP), which maximum absorbance wavelength depends on the pH of the solution. The pH lowering after the addition of H_2SO_4 leads to irreversible inactivation of HRP and to the formation of protonated form of DAP which absorbance can be measured between 450 nm and 500 nm [Figure 20] (Bovaird, Ngo, & Lenhoff, 1982; Fornera & Walde, 2010; Vanessa et al., 2018).

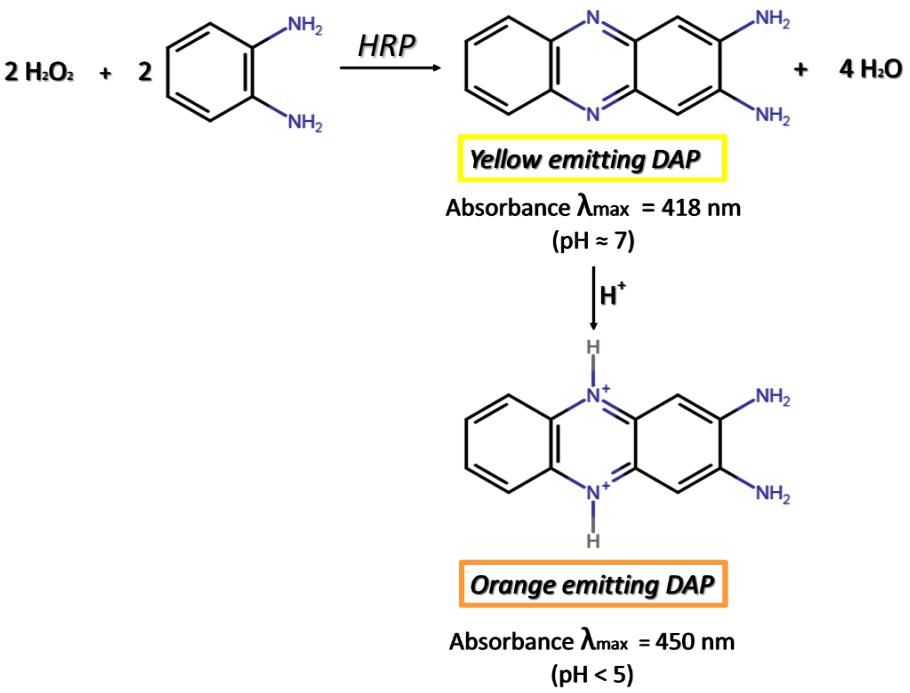


***Figure 20*:** OPD oxidation catalysed by HRP leads to the formation of DAP, which absorbs wavelengths in the range 400 – 450 nm (corresponding to the violet colour) of visible light spectrum and reflects wavelengths in the range 560 – 590 nm donating the typical yellow colour to the solution. DAP protonation leads to the formation of the compound absorbing the wavelengths from 450 nm to 500 nm and reflecting wavelengths which together donate bright orange colour to the solution [structures were drawn using ChemSpace].

Since DAP concentrations are directly proportional to the levels of HRP-labelled streptavidin in the well, obtained absorbance values are directly proportional to the concentration of the protein of interest contained in the sample.

3.7.2 Determination of phospho-S2448 mTOR in cell lysates

ELISA plate was initially coated with mouse anti-mTOR antibody and then blocked with PBS/BSA 2%. Subsequently, the wells were incubated with the cell lysates at room temperature for at least two hours. After washing the plate with TBST buffer, the wells were incubated with anti-phospho-S2448 mTOR antibody at room temperature for at least 2 h. The plate was then washed with TBST again and HRP-labelled goat anti-rabbit IgG (Abcam) was added to the wells and left to react for at least 30 min at room temperature. After washing the plate with

TBST, bound secondary antibodies were detected by the peroxidase reaction (OPD/H2O2) as described above.

3.7.3 Detection of Tim-3-galectin-9 complex in cell and tissue lysates

Mouse single-chain antibody against Tim-3 was employed as capture antibody, instead of using the full-length anti-Tim3 antibody from R&D ELISA kit. The wells were then incubated with cell or tissue lysates at room temperature for at least two hours. After washing the plate with TBST, biotinylated goat antibody against galectin-9 (detection antibody of R&D Systems ELISA kit) was added to the wells and kept for at least two hours at room temperature. The plate was then washed and incubated with HRP-labelled streptavidin for at least 30 minutes. This step was followed by the development of peroxidase reaction and its visualization as described above.

3.7.4 Detection of cortisol in human blood plasma

Plasma cortisol was measured by ELISA using the Salimetrics assay kit according to the manufacturer's protocols (Salimetrics, Suffolk, UK). Briefly, plasma samples were added to microtitre plate coated with monoclonal anti-cortisol antibodies. Cortisol enzyme conjugates (cortisol bound to HRP) were then added to the samples and incubated for at least one hour at room temperature. After the incubation the plate was washed and the chromogenic substrate 3,3′,5,5′-tetramethylbenzidine (TMB) is added. The oxidation of TMB by HRP causes the development of the blue colour in the wells of microtiter plate. The reaction is stopped by adding an acidic solution, which leads to the yellow colour formation. The optical density can be then read at 450 nm.

In this competitive immunoassay, plasma cortisol competes with cortisol conjugated to HRP for the antibody binding sites on a microtitre plate. Therefore, the levels of cortisol HRP conjugates are inversely proportional to the amount of cortisol present in the sample.

3.8 Determination of LPHN1 fragments in human blood plasma

ELISA plates were initially coated with mouse monoclonal LPHN1 antibody and blocked with TBST/BSA 2%. Human plasma samples were then added to the wells of the microtitre plate and kept under constant agitation for 4 hour at room temperature. After the incubation the plate was washed with TBST. Bound proteins were then extracted using glycine-HCl pH lowering buffer (pH 2.0) and mixed with lysis buffer (pH 7.5) at ratio 1:1 and with 4x sample buffer (described previously). Following Western Blot analysis of the samples obtained, LPHN1 fragments were detected using rabbit PAL1 anti-LPHN1 antibody.

In addition to protein immunoprecipitation followed by Western Blot detection, LPHN1 in human plasma was determined by ELISA. Mouse monoclonal LPHN1 antibody was used as capture antibody, while PAL1 antibody was employed as detection antibody. After the incubation with PAL1 antibody, the plate was incubated with HRP-labelled anti-rabbit secondary antibody. LPHN1 fragments were then visualised through the development of the peroxidase reaction as previously described.

3.9 Detection of Tim-3-galectin-9 complex in tissue culture medium

ELISA plates were coated with mouse single-chain antibody against Tim-3and blocked with PBS/BSA 2%. RPMI-1640 medium, in which THP-1 cells were cultured, was then added to the wells of the plate. After 4 hour of incubation with the samples, the plate was washed with TBST and the proteins were extracted employing 0.2 M glycine-buffer. Obtained extracts were then neutralised with lysis buffer, mixed with lysis buffer and subjected to Western Blot analysis, as described above. The bands corresponding to Tim-3-galectin-9 complex were visualised using mouse anti-Tim-3 antibody and galectin-9 antibodies-.

3.10 Cell viability assay

Promega (Southampton, UK) MTS (3-(4,5-dimethylthiazol-2-yl)-5(3-carboxymethoxyphenyl)-2-(4-sulfophenyl)-2H-tetrazolium) assay kit was used to evaluate cell viability. In this assay, MTS tetrazolium compound is converted to a coloured formazan product by dehydrogenases in metabolically active cells. This conversion is proportional to the amount of living cells and can be assessed by measuring the maximum absorbance of the reaction product at 490 nm (Riss et al., 2013) [Figure 21].

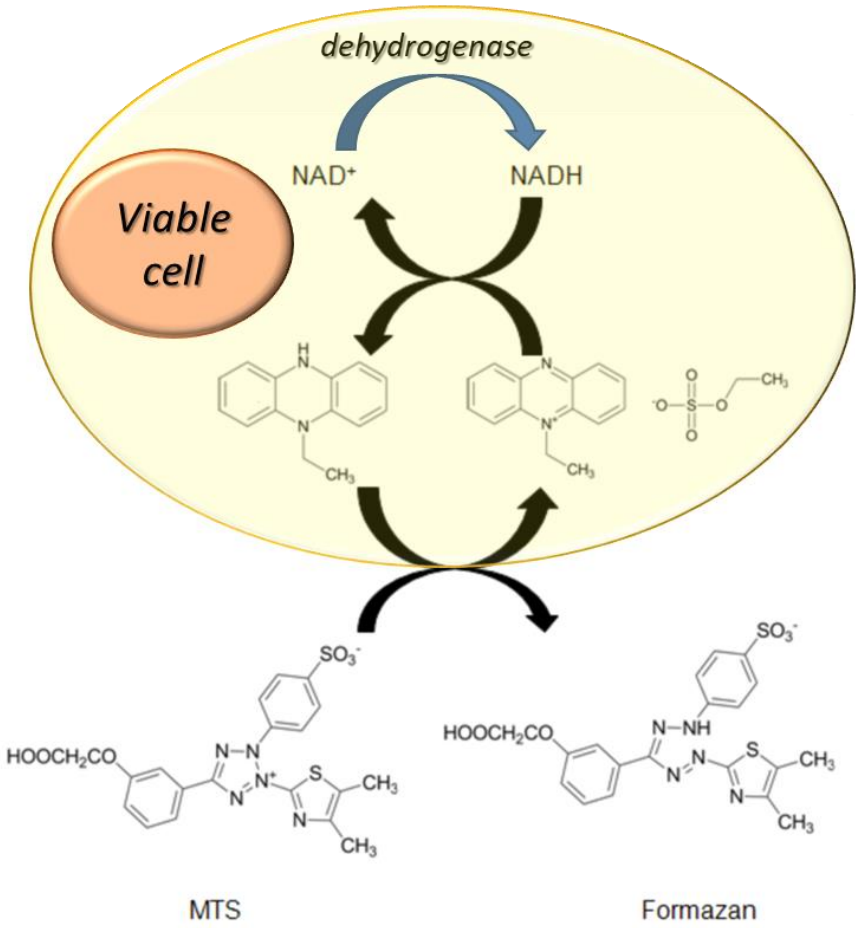


Figure 21: Viable cells contain active dehydrogenases able to reduce NAD^+ in NADH; then, electron coupling reagent phenazine ethosulfate (PES) transfers electrons from NADH in the cytoplasm to reduce MTS in the culture medium into an aqueous soluble formazan (Adapted from Riss et al., 2013).

To assess cell viability, 20 µl of "One Solution Reagent" containing MTS and an electron coupling reagent (phenazine ethosulfate (PES)) were added to 100 µl of cell suspension into a

microwell of 96-well plate. After mixing, the plate was placed in the incubator at 37°C for 1-4 hours, and the absorbance at 490 nm was then measured in accordance to the manufacturer's protocol.

3.11 Caspase 3 activity

Caspase 3 activity was determined employing colorimetric assay kit (R&D Systems). This assay is based on the ability of the activated caspase 3 to cleave molecules that contain the amino acid motif DEVD such as poly ADP ribose polymerase (PARP).

Indeed, in this colorimetric assay, caspase-specific peptide (containing DEVD motif) conjugated to the colour reporter molecule p-nitroaniline (pNA) is added to sample to verify caspase 3 activity. The cleavage of the peptide by the caspase leads to the release of the chromophore pNA, which can be quantitated spectrophotometrically at a wavelength of 405 nm. The intensity of colour reaction is directly proportional to the level of caspase enzymatic activity in the cell lysate.

Once added caspase lysis buffer to the cell pellets, the samples are incubated on the ice for 10 minutes. After the incubation on the ice, the samples are centrifuged (10,000 x g for 1 minute) and the supernatants are transferred in the new tubes and kept on the ice. To 50 µL of sample are added 0.5 µL of 1 M solution of dithiothreitol (DTT), 50 µL of Reaction Buffer and 5 µL of Caspase-3 colorimetric substrate (DEVD-pNA) into a microwell of the 96-well plate. The plate is then incubated at 37 °C for 1-2 hours. After the incubation, the absorbance at 405 is measured in accordance to the manufacturer's protocol.

3.12 Granzyme B activity

Granzyme B activity was determined using a fluorimetric assay kit (BioVision). This assay is based on the employment of synthetic substrate, containing the Granzyme B recognition

sequence along with a fluorescent label 7-Amino-4-trifluoromethylcoumarin (AFC). The cleavage of this specific recognition sequence by Granzyme B leads to the release of AFC, which then can be fluorometrically determined (Excitation wavelength = 380 nm; Emission wavelength = 500 nm).

After homogenising the cells in specific assay buffer, the samples were kept on the ice for 10 minutes and then centrifuged. Obtained supernatants were then transferred in the new tubes and placed on the ice. To 1 – 50 µL of sample supernatants were added 50 µL of the mixture Granzyme B substrate/Granzyme B Assay Buffer (1:10) into each well of 96-well plate. After the incubation for 30-60 min at 37^0C (protected from light), the fluorescence was measured at Ex/Em = 380/500 nm.

3.13 Mitochondria isolation

Cellular mitochondria were isolated employing differential centrifugation (Nicholas, Coughlan, et al., 2011). The cells were initially homogenised in an isolation buffer containing 0.32 M sucrose, 1 mM EDTA (K+ salt), and 10 mm Tris-HCl (pH 7.4). Homogenates were then centrifugated (1330 x g, 3 minutes) and obtained supernatants were further subjected to centrifugation (21,200 x g, 10 minutes). After the centrifugation, pellets (isolated mitochondria) were lysed in the cell lysis buffer. Protein content of the samples were then analysed using Bradford assay.

3.14 Uptake of BH3I-1 by the cells

Cells treated and untreated with 5-[(4-bromophenyl)methylene]-a-(1-methylethyl)-4-oxo-2-thioxo-3-thiazolidineacetic acid (BH3I-1), a synthetic apoptosis inducer, were harvested and then centrifuged. After applying harsh reaction conditions (high temperature and low pH) to the obtained pellet, 125 µL of RPMI 1640 medium were added to Eppendorf tubes containing

the sample. Dibromine (Br_2) resulting from the molecular disruption of BH3I-1, as a consequence of harsh conditions applied to the sample, can react with phenol red (λ_{mac}=428 nm) contained in RPMI 1640 medium leading to the formation of bromophenol, which has the maximum of absorbance at 585 nm (Sollo, et al., 1971; Wever, et al., 2018). Therefore, it is possible to estimate amount of BH3I-1 molecules which entered the cell by measuring the absorbance of the sample containing bromophenol at 585 nm [Figure 22]. Indeed, quantity of bromophenol molecules resulting from bromination of phenol red are directly proportional to BH3I-1 molecules present inside the cell after the incubation with this apoptosis inducer.

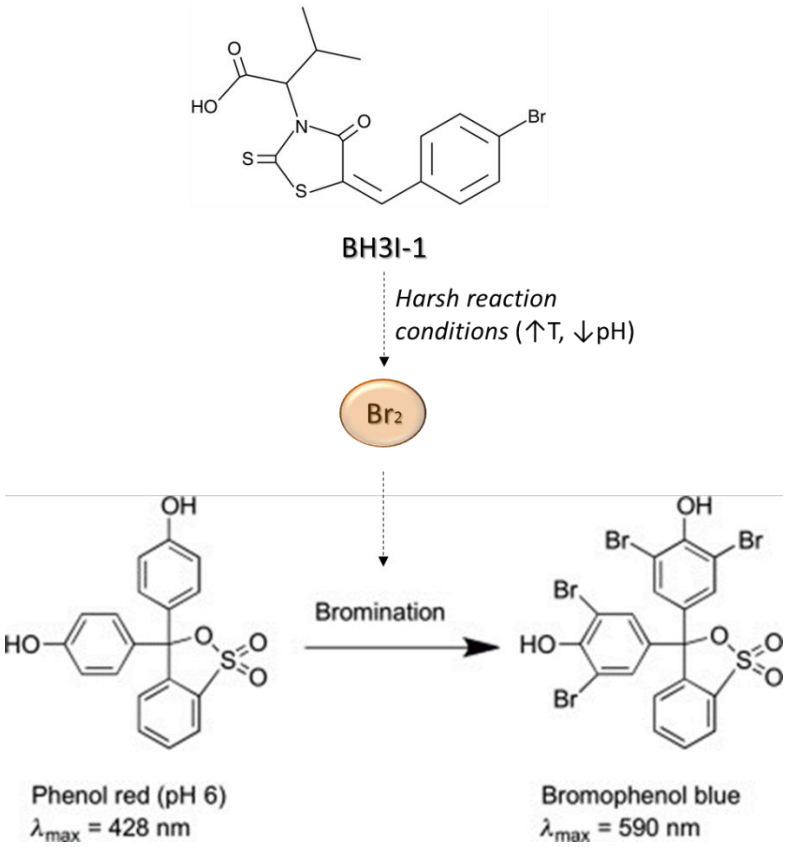


Figure 22: Dibromine (obtained after breaking BH3I-1 compound) reacts with phenol red (λ_{mac}=428 nm) leading to the formation of bromophenol blue (λ_{mac}=585-590 nm). (Adapted from Wever et al., 2018).

3.15 Galectin-9 and Tim-3 knockdown

For galectin-9 gene expression silencing, a specific siRNA target sequence (uga ggu gga cga ugu ggu ucc c) was employed. For Tim-3 knockdown, a commercially available siRNA

obtained from Santa Cruz Biotechnology, CA, USA, was used. Corresponding random siRNA (uac acc guu agc aga cac c dtd) was employed as a negative control.

The cells were transfected with specific siRNAs using cationic liposome-forming compound DOTAP as recommended in manufacturer's instructions. Briefly, the liposomes were prepared using 7 μg of siRNA, 20 μL of DOTAP and 74 μL of HEPES. After incubating these reagents for 30-60 minutes on the ice (to allow the formation of the liposomes), 15 μl of the mixture obtained were added to 3 ml of the culture media containing Colo-205 cells.

3.16 Quantitative real-time PCR (qRT-PCR)

Quantitative real-time PCR (qRT-PCR) was employed to monitor mRNA levels corresponding to target proteins.

Total RNA was isolated from the cells using a GenElute^{TM} mammalian total RNA preparation kit (Sigma-Aldrich). Target mRNAs was then converted into DNA sequences and amplified through reverse transcriptase-polymerase chain reaction (RT-PCR) in accordance with manufacturer's protocol. This was followed by quantitative real-time PCR. For Galectin-9 following primers were employed: 5'-CTTTCATCACCACCATTCTG-3' and 5'-ATGTGGAACCTCTGAGCACTG-3'. For Tim-3 was used 5'-CATGTTTTCAC-ATCTTCCC-3' primer and for actin were employed 5'-TGACGGGGTCACCCACACTG-TGCCCATCTA-3' and 5'-CTAGAAGCATTTGCGGTCGACGATGGAGGG-3' primers. For LPHN1 following primers were exploited: 5′-AGCCGCCCCGAGGCCGGAACCTA-3′ and 5′-AGGTTGGCCCCGCTGGCATAGAGGGAGTC-3′. Reactions were performed using a LightCycler® 480 real-time PCR system and respective SYBR Green I Master kit (Roche, Burgess Hill, UK). Analysis was performed according to the manufacturer's protocol. Values representing galectin-9, Tim-3 and LPHN1 mRNA levels were normalised against β-actin.

3.17 Determination of PKC-α activity

The catalytic activity of PKC-α was measured based on its ability to phosphorylate specific substrate (such as Histone IIIS) (Micol, et al., 1999). Briefly, ELISA plates were initially coated with 0.2 mg/ml Histone IIIS. Then the samples mixed with reaction buffer (20 mM Tris-HCl (pH 7.5), 200 µM $CaCl_2$, 5 mM $MgCl_2$ and 20 µM ATP) at ratio 1:5 were added to the wells and the plate was incubated for 30 minutes at 37°C. After washing with TBST, Histone IIIS phosphorylation was determined spectrophotometrically employing molybdenum blue reaction (Nagul, 2015). The values obtained from this colorimetric assay were then normalised against total protein present in each sample.

3.18 Measurement of phospholipase C (PLC) activity

The activity of PLC was determined based on the ability of this enzyme to catalyse hydrolysis of the phospholipid phosphatidylinositol 4,5-bisphosphate (PIP2) with consequent formation of diacyl glycerol (DAG) and inositol 1,4,5-trisphosphate (IP3).

30 µL of cell or tissue lysates were mixed with 70 µL of assay buffer containing PIP2 (20 mM Tris-HCl buffer (pH 7.2), 0.1% sodium deoxycholate, 300 µM $CaCl_2$, 100 µM EDTA, 100 mM NaCl) and incubated for 60 minutes at 37°C. After the incubation, to 100 µL of the sample obtained were added 100 µL of organic phase (heptane/isopropanol in ratio 13:7). The mixtures obtained were then left to reform the biphasic system. Extracted organic phase was then combined with lysis buffer and sample buffer and subjected to gel electrophoresis on 33% PAGE. PIP2 and its cleaved components were the visualised on PAGE employing blue toluidine staining.

3.19 In-cell assay (also known as on-cell assay)

The in-cell assay (ICA) was employed to characterise surface presence of Tim-3, galectin-9 and CD8. Briefly, the cells were suspended in the culturing medium containing primary

antibodies against one of the target proteins and left to react for at least 3 h under constant agitation at room temperature. After washing with PBS or tissue culture medium, the cells were re-suspended in the fresh media containing Li-Cor goat secondary antibodies and incubated for at least 2 hours under constant agitation at room temperature. The cells were then washed and placed in a microtitre plate, which was scanned using Li-Cor Odyssey imaging system. Cells incubated only in presence of specific secondary antibody were employed as negative control.

Li-COR on cell assay was also used to characterise the interaction of RL-1 antibody with the surface of THP-1 cells.

3.20 Confocal microscopy and imaging flow cytometry

THP-1 cells were grown on 12 mm cover slips in 24-well plates. Cells were treated overnight with PMA and then fixed/permeabilised for 20 min with ice-cold methanol (MeOH) or MeOH/acetone (purissimus). Alternatively, cells were fixed in a freshly prepared 2% paraformaldehyde, washed 3 times with PBS and then permeabilised with 0.1% triton X-100. Cover slips were then blocked for 1h at RT with 10% goat serum in PBS. 1 µg/ml anti-Tim-3 antibody and anti-galectin-9 antibody were used as primary antibodies and incubated overnight at 4°C. Goat-anti-mouse Alexa Fluor 488 and goat-anti-rabbit Alexa Fluor 555 were used as secondary antibodies. Cells were incubated with secondary antibodies for 45 min at RT. The preparations were examined on Olympus laser scanning confocal microscope as described (**Prokhorov et al., 2015; Fasler-Kan et al., 2010**). Images were then collected and analysed using proprietary image acquisition software. Imaging flow cytometry was performed in accordance with a previously described protocol (Fasler-Kan et al., 2016). Briefly, permeabilised cells were stained with mouse anti-Tim-3 and rabbit anti-galectin-9 antibodies for 1 hour at room temperature. Goat anti-mouse Alexa Fluor 647 and goat-anti-rabbit Alexa Fluor 488 were used as secondary antibodies. Images were collected and analysed using

IDEAS analytical software on ImageStream X mark II (Amnis-EMD-Millipore, USA). This method described in Gonçalves Silva et al., 2017.

For Tim-3-galectin-9 co-localisation assay in breast tissue slices, image acquisition, a Nikon A1si laser scanning confocal microscope was allied with a Plan Fluor DIC 40x magnifying, 1.3-numerical aperture (N.A.) oil-immersion objective. NIS Elements software (version 3.21.03, Nikon, Tokyo, Japan) was used to analyse the data. Cell images were acquired in three channels for DAPI (excitation at 399 nm with laser power 10 arbitrary units [AU], emission collection at 450 nm; nuclei labelling), Alexa Fluor 488 (excitation wavelength 488 nm with laser power 10 AU and, emission wavelength at 525 nm (corresponds to a green channel, galectin-9), Alexa Fluor 555 (excitation 561 nm with laser power 10 AU, emission collection at 595nm, red channel, Tim-3), with a photomultiplier tube gain of 100 AU. No offset was used, and pinhole size was set between 1.2 and 2 times the Airy disk size of the used objective, depending on the strength of a signal. This method is described in Yasinska et al., 2019.

3.20.1 Tim-3 and galectin-9 characterisation in THP-1 cells

THP-1 cells were cultivated in 12 mm cover glasses in 24-well plates. Cells were treated with phorbol 12-myristate 13-acetate (PMA) and fixed/permeabilised for 20 min with ice-cold methanol or a mixture methanol/acetone. Alternatively, cells were fixed in a freshly prepared 2% paraformaldehyde, washed 3 times with PBS and permeabilised with 0.1%TX-100.

Cover glasses were blocked for 1 hour at room temperature with 10% goat serum in PBS. The plates were then incubated overnight at 4°C with 1 µg/ml of anti-Tim-3 and anti-galectin-9 antibodies. After washing, the cells were incubated for 45 min at room temperature with goat-anti-mouse Alexa Fluor 488 and goat-anti-rabbit Alexa Fluor 555 secondary antibodies.

The preparations were examined using the Olympus laser scanning confocal microscope as described previously (Prokhorov et al., 2015). Obtained images analysed using the proprietary image acquisition software.

3.20.2 Tim-3 and galectin-9 characterisation in primary human breast tissues

Tissue sections were obtained using a freezing microtome with the cutting thickness of 5-6 µm. Each tissue section was sliced onto a poly-D-lysine-coated microscope slide (BDH). Acquired slides were then incubated in 3% H_2O_2 for 15 minutes to block endogenous peroxidase activity.

Subsequently, the slides were permeabilised using PBS containing 0.26% Triton for 20 minutes at room temperature and blocked for at least 30 minutes in the blocking buffer (PBS, 0.05% Tween, 2% serum, 1% BSA). After blocking, the slides were incubated with anti-Tim-3 and anti-galectin-9 antibodies diluted in the blocking buffer (1:2000 dilution) for 2 h at room temperature. Then, the slides were washed three times with PBS and incubated in the dark for 1 h with anti-IgG-FITC-labelled secondary antibody (1:400 dilution). Slide washing was then followed by Fluoro-Gel mounting media containing DAPI nuclei-staining reagent. Negative controls were prepared by incubating the slides with secondary antibody alone. Images were obtained employing Confocal Laser Scanning Microscopy (BioRad Hercules).

For image acquisition, a Nikon A1si laser scanning confocal microscope was used with a Plan Fluor DIC 40x magnifying, 1.3-numerical aperture (N.A.) oil-immersion objective. NIS Elements software (version 3.21.03, Nikon, Tokyo, Japan) was employed for data analysis. Cell images were acquired in three channels for DAPI (excitation at 399 nm with laser power 10 arbitrary units [AU], emission collection at 450 nm; nuclei labelling), Alexa Fluor 488 (excitation wavelength 488 nm with laser power 10 AU and, emission wavelength at 525 nm (corresponds to a green channel, galectin-9), Alexa Fluor 555 (excitation 561 nm with laser power 10 AU, emission collection at 595nm, red channel, Tim-3), with a photomultiplier tube

gain of 100 AU. No offset was used, and pinhole size was set between 1.2 and 2 times the Airy disk size of the used objective, depending on signal strength.

3.21 Fluorescence-activated cell sorting (FACS)

Surface presence and total cellular levels of Tim-3 and galectin-9 were characterised using FACS. The cells were initially fixed with freshly prepared 2% paraformaldehyde, washed 3 times with PBS and permeabilised with 0.1% TX-100. The cells were then incubated with mouse anti-Tim-3 and rabbit anti-galectin-9 antibodies overnight at 4ºC. Goat anti-mouse Alexa Fluor 647 and goat-anti-rabbit Alexa Fluor 488 were employed as secondary antibodies. Target protein characterisation was then analysed using FACS Calibur cytometer with CellQuestPro software (Becton Dickinson, USA).

3.22 Synchrotron radiation circular dichroism spectroscopy (SRCDS)

The interactions of Tim-3 with galectin-9 as well as the binding of LPHN1 and LPHN2 with FLRT3 were characterised employing SRCD spectroscopy at beamline B23, Diamond Light Source (Didcot, UK) [Figure 23].

SRCD measurements of human recombinant Tim-3 and human recombinant galectin-9 were performed using 0.2 μg/ml of samples in 10 cm path length cell, 3 mm aperture diameter and 800 μl capacity using Module B with 1 nm increment, 1 s integration time, 1.2 nm bandwidth at 23 °C (Hussain, et al., 2012; Siligardi & Hussain, 2015). These macromolecules were analysed alone and as a mixture (with stoichiometry of 1:1 molar ratio).

SRCD measurements of soluble extracellular fragment of LPHN1, LPH-51, alone or in combination with human recombinant FLRT3 (equimolar ratio) were carried out using 0.01 μM sample of soluble LPH-51 in a 1 cm path length cell of 3 mm aperture diameter and 60 μl capacity using a Module B instrument with 1 nm increment, 1 s integration time and 1.2 nm

bandwidth at 23 ºC. Similarly, human recombinant LPHN2 (olfactomedin-like domain, MyBioSource, San Diego, Ca, USA) was analysed alone or mixed with FLRT3 by SRCD spectroscopy. In this case SRCD measurements were performed using 0.7 µM samples.

The results obtained were processed using CDApps (Hussain et al., 2015) and OriginLab™.

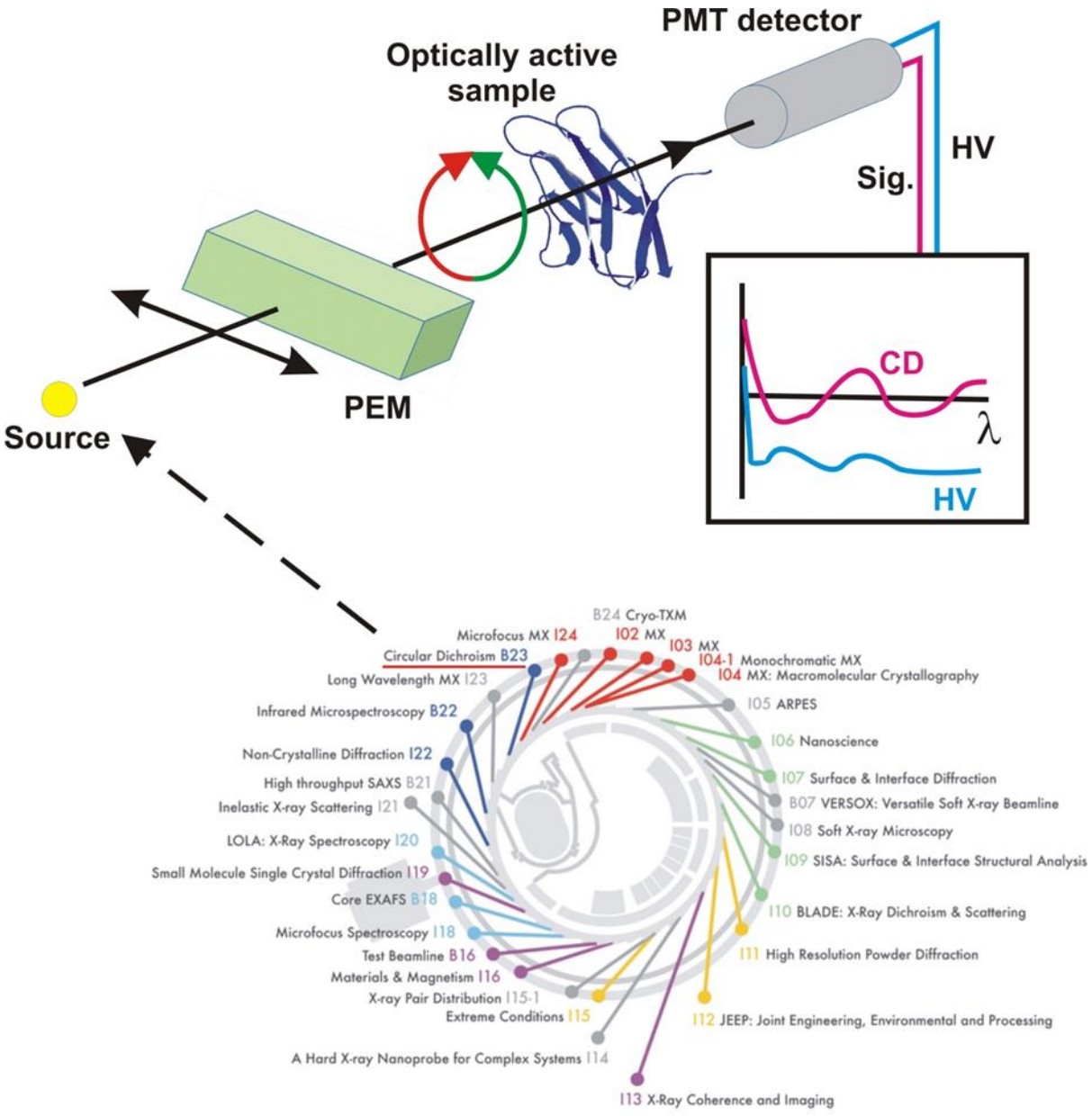


Figure 23: Beam light 23 at Diamond Light Source Synchrotron and scheme of Synchrotron radiation circular dichroism (SRCD) spectroscopy analysis *(Gonçalves Silva et al., 2017).*

3.23 Leukaemia cell protection assay

K562 (chronic myeloid leukaemia cells not releasing galectin-9) and NK cells were cultivated separately or as a 1:2 co-culture (K562: NK) for 16 h, at 37°C, in the presence or absence of 0.5 - 5 ng/ml of galectin-9. The unfixed cell cultures were then imaged under an inverted microscope (TE200, Nikon), using phase-contrast lighting, a digital camera and the WinFluor image acquisition software (J. Dempster, University of Strathclyde).

Images were acquired at different focal planes and analysed using the ImageJ software. Since K562 cells are significantly larger than NK cells, it was possible to identify each cell type both in mono-cultures and in co-cultures, by optimising the ranges of particle sizes during automatic particle counting. Additionally, illumination correction, background substraction, overlapping cell separation, and particle size optimization were applied using ImageJ software.

3.24 Statistical Analysis

Each experiment was performed at least three times. Statistical analysis of the results obtained was performed using two-tailed Student's t-test, when comparing two events at a time. One-way ANOVA test was employed instead for multiple comparisons. Where applicable, a post-hoc Bonferroni correction was used. Statistical probabilities (p) reflecting significant differences between individual events were expressed as * where $p<0.05$, ** where $p<0.01$ and *** where $p<0.001$.

4. Tim-3-galectin-9 immunosuppressive pathway and its pathophysiological role

Recently it has been discovered that Tim-3-galectin-9 pathway is involved in the immune system suppression (Golden-Mason et al., 2013; Gonçalves Silva, Rüegg, Gibbs, Bardelli, Fruewirth, et al., 2016; Kikushige et al., 2015; F. Wang et al., 2007). However, the mechanisms implicated in the activation of biosynthesis of the components of the Tim-3-galectin-9 pathway, galectin-9 secretion and its effects on cytotoxic lymphocytes (NK cells and T cells) remain unclear.

4.1 Free and galectin-9-bound Tim-3 are shed differentially from the cell surface

It has been previously reported that Tim-3 can be shed from the cell surface by proteolytic enzymes, such as **a** **d**isintegrin **a**nd **m**etalloproteinase domain-containing proteins (ADAM) 10/17 (Clayton et al., 2015; Möller-Hackbarth et al., 2013). Therefore, proteolytic shedding was proposed as possible mechanism of secretion of both Tim-3 and Tim-3-galectin-9 complex by AML cells.

For this reason, THP-1 cells were cultured for 16 h in presence or in absence of 100 nM phorbol 12-myristate 13-acetate (PMA), compound known to induce proteolytical shedding of Tim-3 from the cell surface and galectin-9 release (possibly consequent to the proteolysis of Tim-3-galectin-9 complex expressed on the membrane) (Chabot et al., 2002; Möller-Hackbarth et al., 2013). After the incubation, immunoprecipitation from the culture media was performed employing 96-well plates coated with mouse single-chain antibody against Tim-3 and the precipitate was extracted as described in Materials and Methods. Obtained extracts were then subjected to Western blot analysis. Following the incubation with anti- galectin-9 antibody, specific bands were detected at ~32 kDa (the molecular weight of galectin-9) and ~52 kDa

[Figure 24 A]. Following the incubation with anti-Tim-3 antibody, specific bands appeared at ~33 kDa (the molecular weight of soluble Tim-3 – sTim-3), ~20 kDa and ~52 kDa [Figure 24 A]. The fact that the band at 52 kDa is detectable by both antibodies suggests that it corresponds to the unbroken Tim-3-galectin-9 complex. Moreover, Tim-3 fragment of 20 kDa is likely to be shed in complex with galectin-9 (~32 kDa) from the cell surface and then disassociated from its ligand during the Western blot procedure. Therefore, Tim-3 is probably shed at different cleavage sites when bound to galectin-9 (Tim-3 band at 20 kDa) and when expressed on the cell surface in absence of its natural ligand (Tim-3 band at 33 kDa). Consequently, different enzymes should be involved in its surface shedding.

To verify this hypothesis, ADAM 10/17 were investigated. The aim was to find out whether these proteases are involved in the release of free Tim-3 fragment and/or galectin-9-Tim-3 complex. Thus, THP-1 cells were cultured for 16 h with or without 100 nM PMA, a compound known to upregulate the expression of proteolytic enzymes and other proteins. After 16 h of incubation, PMA-containing medium was removed and replaced with the fresh medium containing 100 µM GI254023X (ADAM 10 and 17 inhibitor) or 100 µM BB-94 (a matrix metalloproteinase inhibitor) and the cells were incubated for further 4 h. The levels of galectin-9 and Tim-3 released in the media were then determined by ELISA kits as described in manufacturer's protocol, while the concentration of soluble Tim-3-galectin-9 complex was measured using a single-chain anti-Tim-3 antibody for capturing and biotinylated anti-galectin-9 antibody for detecting as outlined in Materials and Methods. Obtained data showed that PMA treatment significantly increased the release of Tim-3, galectin-9 and Tim-3-galectin-9 complex [Figure 24 B]. However, subsequent treatment with protease inhibitors, GI254023X and BB-94, reduced the levels of soluble Tim-3 in the media but did not influence the release of galectin-9 and Tim-3-galectin-9 complex [Figure 24 B]. This suggests that different mechanisms are involved in the release of Tim-3-galectin-9 from the cell surface.

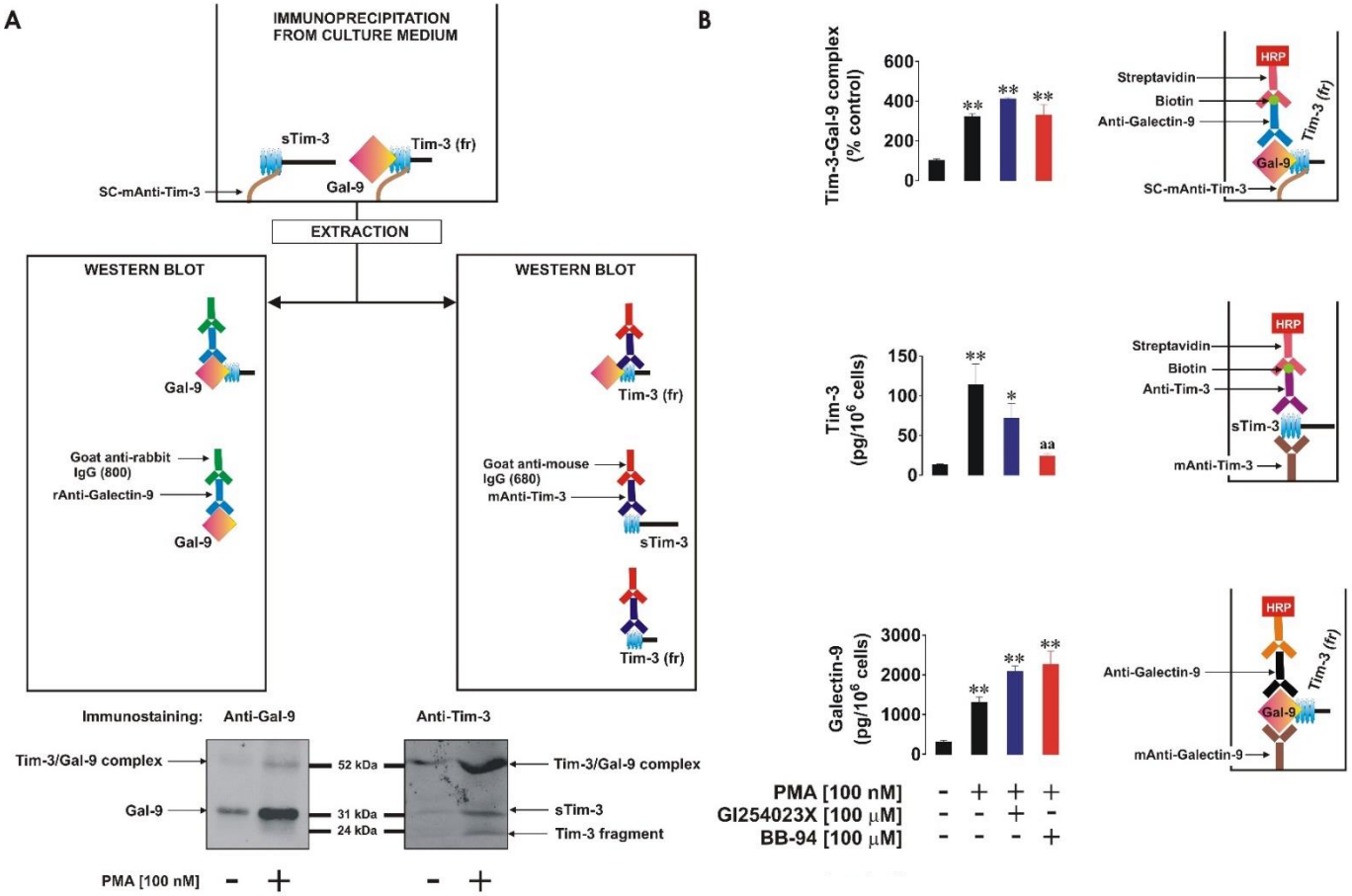


Figure 24: Tim-3 is shed differentially from the cell surface depending if expressed in complex with galectin-9 or as a free transmembrane protein. Following the treatment of THP-1 cells with 100 nM PMA for 16 h, the media was exchanged with the fresh one containing 100 µM GI254023X (ADAM10/17 inhibitor) or 100 µM BB-94 (matrix metalloproteinase inhibitor) and incubated for 4 h. (A) The media collected after 16 h of incubation was subjected to immunoprecipitation and Western blot analysis for galectin-9 and Tim-3 detection (as outlined in Material and Methods). (B) The media collected after 20 h of incubation (all the samples) was subjected to ELISA for galectin-9, Tim-3 and galectin-9-Tim-3 complex detection. Images are from one experiment representative of six which gave similar results. Quantitative data are mean values ±SEM (n=6) *p < 0.05; **p < 0.01 vs. control.

Intracellular levels of Tim-3 and galectin-9 in THP-1 cells untreated and treated with PMA were also characterised employing Western blot analysis. The data obtained showed that despite the increase in the release of sTim-3, galectin-9 and Tim-3-galectin-9 complex by THP-1 cells, the intracellular levels of these proteins decreased [Figure 25]. In addition, a specific band detectable by both anti-Tim-3 and anti-galectin-9 antibodies appeared at ~70 kDa (molecular weight corresponding to the sum of uncleaved Tim-3 and galectin-9) [Figure 25]. These results suggest that the complex between full Tim-3 and galectin-9 (~70 kDa) is first formed intracellularly and undergoes proteolytical shedding only after being expressed on the cell membrane leading to the release of soluble form of this complex (~52 kDa).

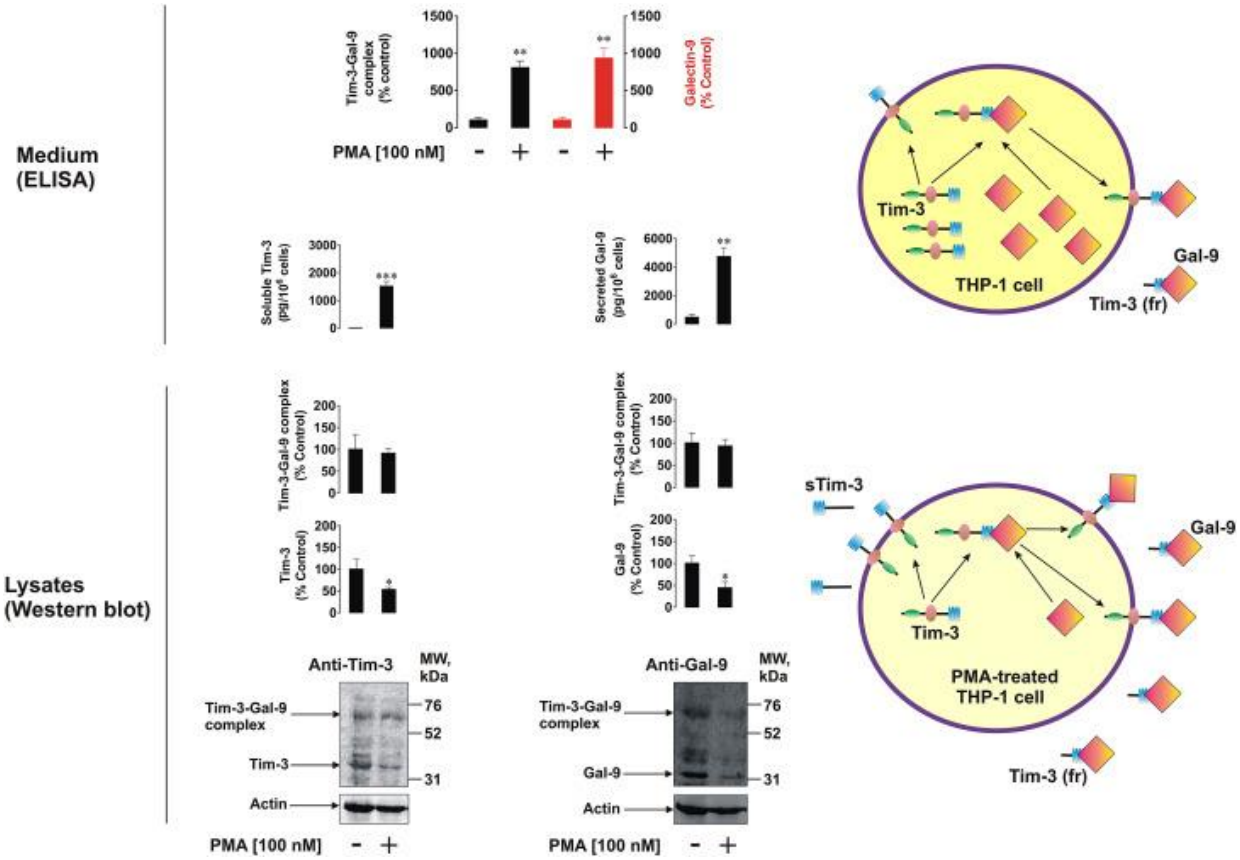


Figure 25. PMA induces generation and/or release of Tim-3, galectin-9 and Tim-3-galectin-9 complex. Following the treatment of THP-1 cell with 100 nM PMA (16 h incubation), secreted and intracellular levels of galectin-9, Tim-3 and Tim-3-galectin-9 complex were characterised by ELISA and Western blot. Comparative analysis (expressed in % control) of galectin-9 and Tim-3-galectin-9 complex levels secreted by PMA-treated and untreated THP-1 cells are illustrated in the bar diagram on the top. Images are from one experiment representative of three which gave similar results. Quantitative data are mean values ±SEM (n=3) *$p < 0.05$; **$p < 0.01$; ***$p < 0.001$ vs. control.

The presence of Tim-3-galectin-9 complex in THP-1 cells was also verified by co-localization assays using confocal microscopy [Figure 26]. Following PMA treatment and paraformaldehyde fixation, non-permeabilised and methanol-permeabilised THP-1 cells were analysed. Areas full of either Tim-3 or galectin-9 were detected on non-permeabilised cells. However, no substantial co-localisation of these two proteins was observed on THP-1 cell surface. On the other hand, clear evidence of Tim-3 and galectin-9 co-localization was found in permeabilised cells [Figure 26].

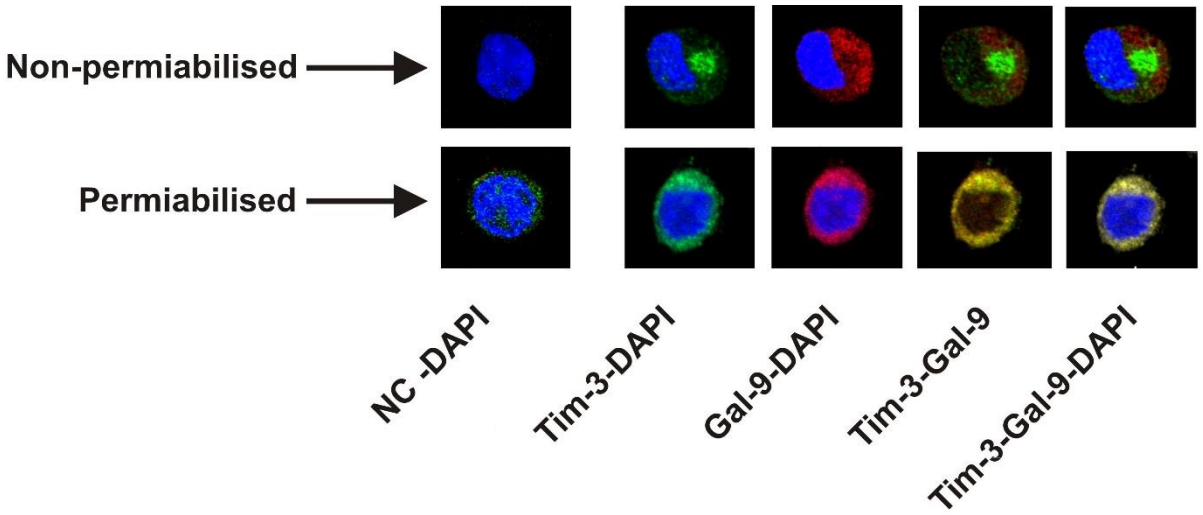


Figure 26: Co-localization of Tim-3 and galectin-9 in THP-1 cells. PMA-activated and paraformaldehyde-fixed cells were analysed using confocal microscopy for the detection of Tim-3 and/or galectin-9. Images are from one experiment representative of six which gave similar results.

The results obtained by confocal microscopy were also confirmed using imaging flow cytometry: Tim-3 and galectin-9 were found co-localised in PMA-treated and permeabilised THP-1 cells [Figure 27].

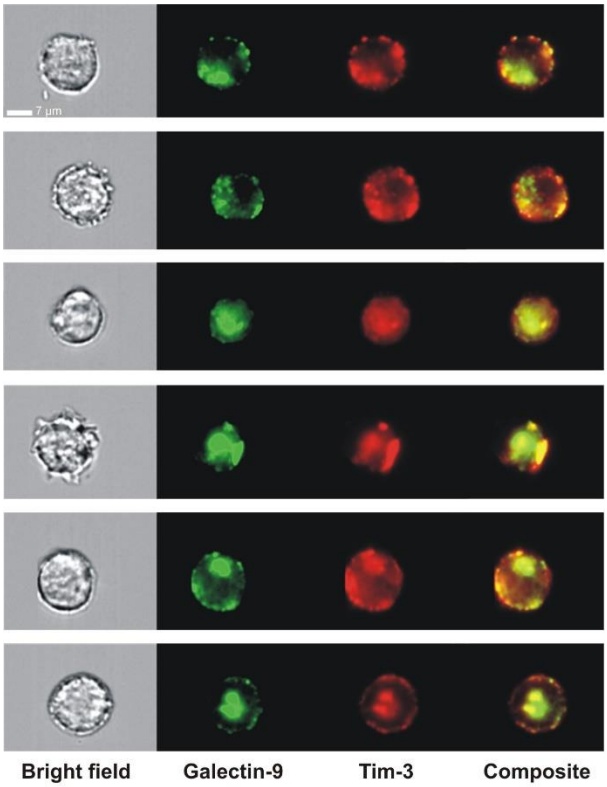


Figure 27: Co-localization of galectin-9 and Tim-3 in THP-1 cells upon PMA activation. THP-1 cells stimulated with PMA were permeabilized and subjected to imaging flow cytometry as described in Materials and Methods. Images represent six selected single cells.

The fact that the Tim-3-galectin-9 complex is detectable intracellularly, but not on the cell surface can be explained by the incapacity of the antibody to interact with the extracellular part of Tim-3 when it is bound to galectin-9 due to steric hindrance. Indeed, since galectin-9 is soluble, it is reasonable to assume that it must be bound to a transmembrane protein (such as Tim-3) in order to remain on the cell surface.

Taken together these results indicate that Tim-3 can be externalised on its own or can act as a trafficker for galectin-9, which does not have the signal domain necessary for secretion and thus requires a trafficker for its surface expression.

Tim-3 and galectin-9 were then analysed in plasma samples obtained from 98 AML patients and from 12 healthy donors. It was found that the levels of galectin-9 and Tim-3 were significantly higher in AML patients' blood plasma compared to healthy donors' ones [Figure 28 A, B, E and F].

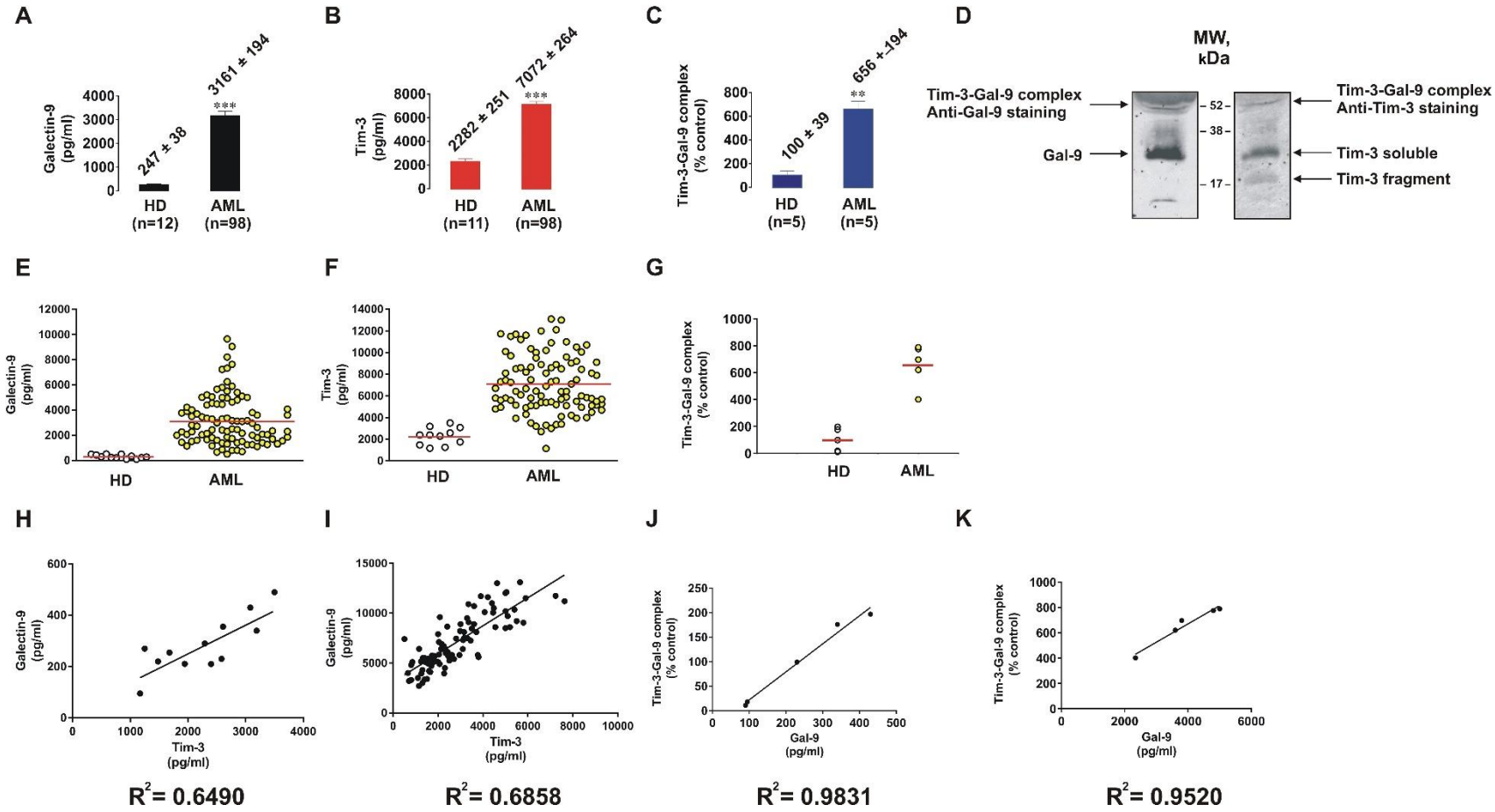


Figure 28: Levels of galectin-9, sTim-3 and soluble Tim-3-galectin-9 complex are significantly higher in blood plasma of AML patients compared to that of healthy donors. Galectin-9 and Tim-3 concentrations in blood plasma of 98 AML patients and of 12 healthy donors were analysed by ELISA (A, B, E and F). Five randomly chosen plasma samples of each group were used for Tim-3-galectin-9 ELISA-based detection (C and G). Five randomly selected blood plasma obtained from AML patients and healthy donors were sonicated, boiled for 5 minutes at 95º C and subjected to Western blot analysis (D). Correlations between the levels of Tim-3 and galectin-9 as well as Tim-3-galectin-9 complex and galectin-9 in blood plasma were determined for both healthy donors (H and J) and AML patients (I and K). Images are from one experiment representative of five which gave similar results. Quantitative data are mean values ±SEM (n=3) *$p < 0.05$; **$p < 0.01$; ***$p < 0.001$ vs. control.

Tim-3-galectin-9 complex was also characterised employing ELISA (as previously described) using five randomly selected plasma samples from the group of studied AML patients and five from the group of healthy donors. It was found that the levels of Tim-3-galectin-9 complex were significantly greater in AML patients and the grade of this elevation was similar to that of galectin-9 [Figure 28 C and G]. In addition to ELISA-based detection, Tim-3 and galectin-9 were characterised by Western blot analysis using five randomly chosen plasma samples from each group. The bands corresponding to galectin-9 (32 kDa), Tim-3 fragment (20 kDa) and sTim-3 (33 kDa) appeared following the incubation with anti-Tim-3 or anti-galectin-9 antibodies. A clear band at ~52 kDa was detected by both anti-Tim-3 and anti-galectin-9 antibody. These results match those obtained with THP-1 cells and reinforce the theory according to which soluble Tim-3 and Tim-3 complexed with galectin-9 are differentially shed from plasma membranes of AML cells. Additionally, the correlations obtained between Tim-3 and galectin-9 concentrations as well as Tim-3-galectin-9 complex and galectin-9 levels in blood plasma of both healthy donors and AML patients suggest a co-release of both proteins in both cohorts [Figure 28 H, I, J and K].

Recently, it has been shown by surface plasmon resonance (SPR) analysis that galectin-9 can bind non-glycosylated Tim-3 with nanomolar affinity (Kd= $2.8x10^{8}$ M). However, this interaction is even greater if Tim-3 is glycosylated (Prokhorov et al., 2015). This is in line with the fact that galectin-9 is a β-galactoside binding protein and thus interacts strongly with glycosylated proteins, such as Tim-3. Schematic representation of Tim-3 and galectin-9 structures is illustrated in Figure 29A.

Galectin-9-Tim-3 interaction was also analysed by synchrotron radiation circular dichroism (SRCD) spectroscopy at Diamond Light Source. Galectin-9 and Tim-3 were mixed to a stoichiometry of 1:1 molar ratio [Figure 29 B].

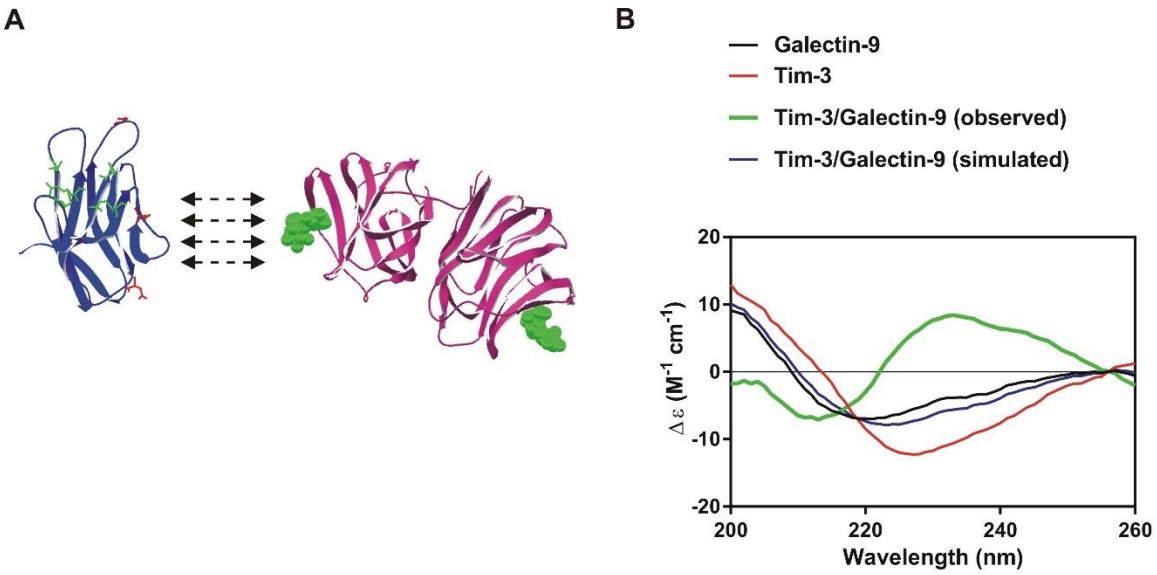


Figure 29: Interaction of Tim-3 with galectin-9 leads to major conformational changes increasing solubility of the protein complex. Galectin-9 (right) and extracellular domain of Tim-3 (left) are schematically represented in panel A. In Tim-3 structure, amino acid residues involved in galectin-9-independent binding are highlighted in green., while those which can be potentially glycosylated are shown in red. In galectin-9 structure, sugar molecules possibly involved in the binding with the glycoprotein and located close to the close to the carbohydrate binding sites are illustrated in green (A). The SRCD spectroscopy of Tim-3, galectin-9 and Tim-3-galectin-9 interaction (both simulated and real curves are presented) (B).

CD spectrum obtained after mixing galectin-9 with Tim-3 was significantly different from the simulated spectrum. This indicates that significant conformational changes occur in these proteins upon the binding. In particular, a clear increase in β-strand component was observed. These results suggest that Tim-3 may alter the conformation of galectin-9 leading to its increased ability to interact with other receptors in target cells. Indeed, galectin-9 is tandem protein containing two carbohydrate recognition domains (CRDs) and thus one sugar-binding domain could bind Tim-3 (or other proteins) leaving the other CRD free to interact with another transmembrane receptor of a target cell.

4.2 Latrophilin 1, PKC-α and mTOR-dependent translation are crucial for Tim-3 and galectin-9 production and secretion

Recently it was discovered that the neuronal receptor LPHN1 is expressed in AML cells, but is absent in healthy leukocytes (Sumbayev et al., 2016).

To investigate whether LPHN1 triggering is involved in Tim-3 and galectin-9 expression, THP-1 cells were exposed to 250 pM α-latrotoxin (α-LTX), a highly specific and potent ligand of LPHN1, for 16 hours. Obtained lysates were then subjected to Western blot and the media was analysed by ELISA. It was found that the levels of intracellular galectin-9 and Tim-3 were downregulated (though not significantly), while the secretion of these proteins was drastically increased [Figure 30 B and D].

Similar results were also obtained when THP-1 cells were exposed to 100 nM PMA, specific PKC-α activator [Figure 30 A and D]. Therefore, one-hour pre-treatment with 70 nM Gö6983 (PKC-α inhibitor) before the exposure to PMA or LTX was performed. It was found that 70 nM Gö6983 treatment following the exposure to PMA or LTX downregulated both secreted and intracellular levels of Tim-3 and galectin-9 [Figure 30 A, B and D]. However, basic release of galectin-9 and Tim-3 wasn't affected by Gö6983 suggesting that it is PKCα independent [Figure 30 D].

It has been also shown that PMA promotes the activation of mTOR, a kinase essential for AML cell survival and proliferation (Gonçalves Silva et al., 2016; Prokhorov et al., 2015; Roux, et al., 2004). Therefore, the phosphorylation rate of mTOR in position Ser2448 (active form) was also investigated in these cell lysates. It was found that both PMA and LTX significantly increased the phosphorylation of mTOR at 2448. This stimulus-induced mTOR activation was attenuated when THP-1 cells were pre-treated with Gö6983 following the exposure to PMA or LTX. Interestingly, the level of phosphor-S2448-mTOR after the incubation with just Gö6983 wasn't different from the control one [Figure 30 A and B].

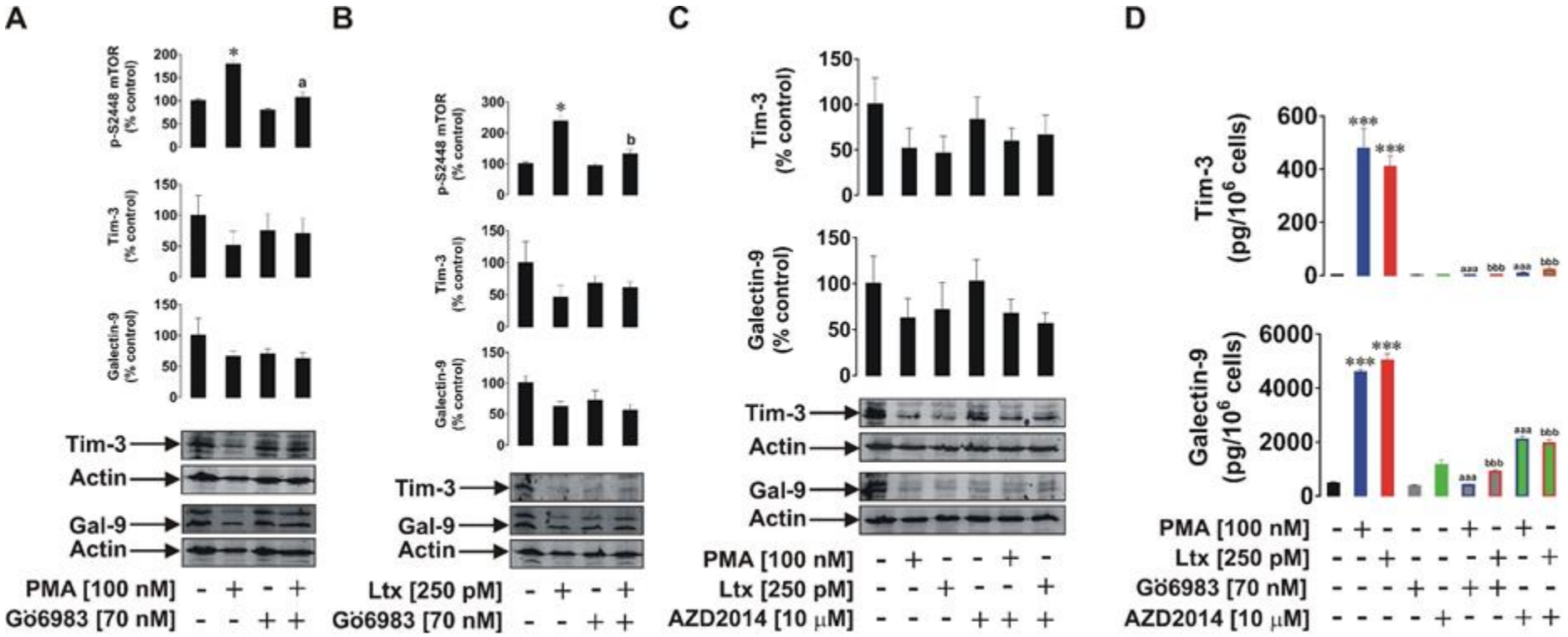


Figure 30: LPHN1, PKCαand mTOR pathways are involved in Tim-3 and galectin-9 production and secretion in AML cells. THP-1 cells were exposed to 100 nM PMA or 250 pM LTX for 16 h with or without 1 h pre-treatment with the PKCα inhibitor Gö6983 (A, B, D) or the mTOR inhibitor AZD2014 (C, D). Cellular levels of Tim-3 and galectin-9 were characterised by Western blot. The p-S2448 mTOR was measured by ELISA. Secreted Tim-3 and galectin-9 were detected by ELISA. Images are from one experiment representative of three which gave similar results. Quantitative data are the mean values ± SEM of three independent experiments; *p b 0.05; **p b 0.01; ***p b 0.001 vs. control. Symbols “a” or “b” are used instead of “*” to indicate differences vs. PMA and LTX-treated cells, respectively.

To prove mTOR involvement in galectin-9 and Tim-3 production, THP-1 cells were pre-treated with 10 μM AZD2014 (a highly selective mTOR inhibitor), before the exposure to 100 nM PMA or to 250 μM α-LTX. It was found that 1 h pre-treatment of THP-1 cells with mTOR inhibitor followed by the exposure to PMA or LTX, reduced intracellular Tim-3 and galectin-9 levels as well as release of both proteins [Figure 30 C and D]. This suggests that PMA or LTX-induced translation of galectin-9 and Tim-3 depends on the mTOR pathway. Importantly, the solvents employed to dissolve pharmacological inhibitors had no effect on any of the studied protein levels or their secretion (data not shown).

To validate obtained results, primary human AML mononuclear blasts AML-PB001F were exposed for 24 h to 250 pM LTX. Western blot analysis showed that AML-PB0011F expressed LPHN1, which production wasn't changing upon the incubation with LTX [Figure 31 B]. Secreted levels of galectin-9 and Tim-3 were significantly increased in LTX-treated AML cells [Figure 31 A] confirming the findings obtained in THP-1 cells.

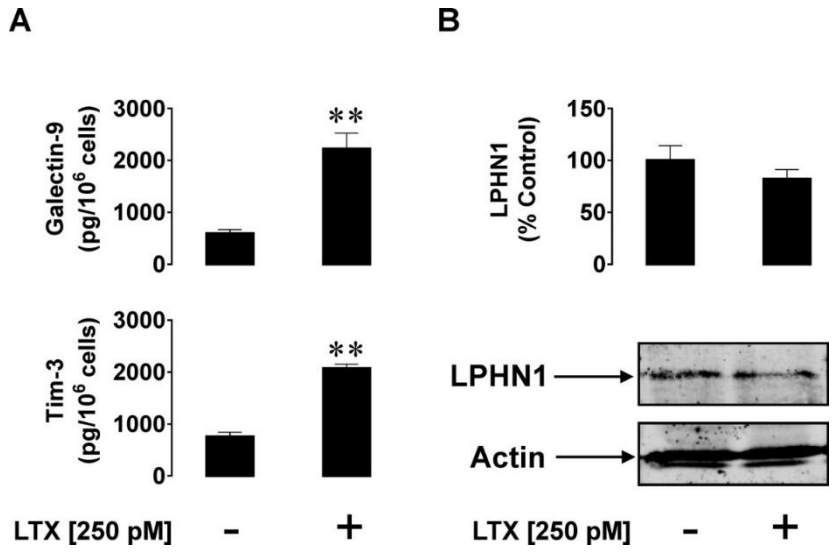


Figure 31: LTX induces Tim-3 and galectin-9 release in primary human AML cells. Primary human AML blasts (AML-PB001F) were incubated for 24 h with 250 pM LTX. The media was then subjected to ELISA for galectin-9 and Tim-3 detection (A). Harvested cells after the incubation were lysed and subjected to Western blot analysis and LPHN1 expression was characterised (B). Images are from one experiment representative of six which gave similar results. Quantitative data are mean values ± SEM of six independent experiments; **$p < 0.01$ vs. control.

Recently it was found that FLRT3 is one of the physiological ligands of LPHN1 (Boucard, 2014). Thus, THP-1 cells were incubated with 10 nM FLRT3 for 16 h. It was found that FLRT3 induced significant upregulation of galectin-9 and sTim-3 release [Figure 32 A]. To confirm that this effect was physiologically relevant, THP-1 cells were also exposed for 16 h to mouse bone marrow (mBM) extracts (containing FLRT3) [Fig. 32 B] with or without 1h pre-treatment with 5 μg/ml FLRT3 neutralizing mouse antibody. It was found that galectin-9 and sTim-3 secretion by THP-1 cells was significantly increased after the exposure to mBM extract. However, this upregulation was attenuated, but not completely blocked, by FLRT3 neutralising antibody [Figure 32 B]. This suggests that BM contains, in addition to FLRT3, other inducers of galectin-9 secretion by AML cells.

THP-1 cells were also co-cultured with FLRT3-expressing RCC-FG1 renal carcinoma cells in the ratio 1 **:** 2, respectively [Figure 32 C]. The cells were incubated for 16 h in the absence or presence of 5 μg/ml FLRT3 neutralizing antibody. The levels of galectin-9 and sTim-3 secreted in the media were measured by ELISA. It was found that the presence of RCC-FG1 cells significantly increased galectin-9 and sTim-3 release and FLRT3 neutralization attenuated these effects [Figure 32 C]. Since RCC-FG1 cells release almost undetectable amounts of galectin-9 and Tim3, the concentrations of these proteins in the media can be attributed quite exclusively to their secretion by THP-1 cells. These results confirm that FLRT3 stimulates the release of galectin-9 in AML cells.

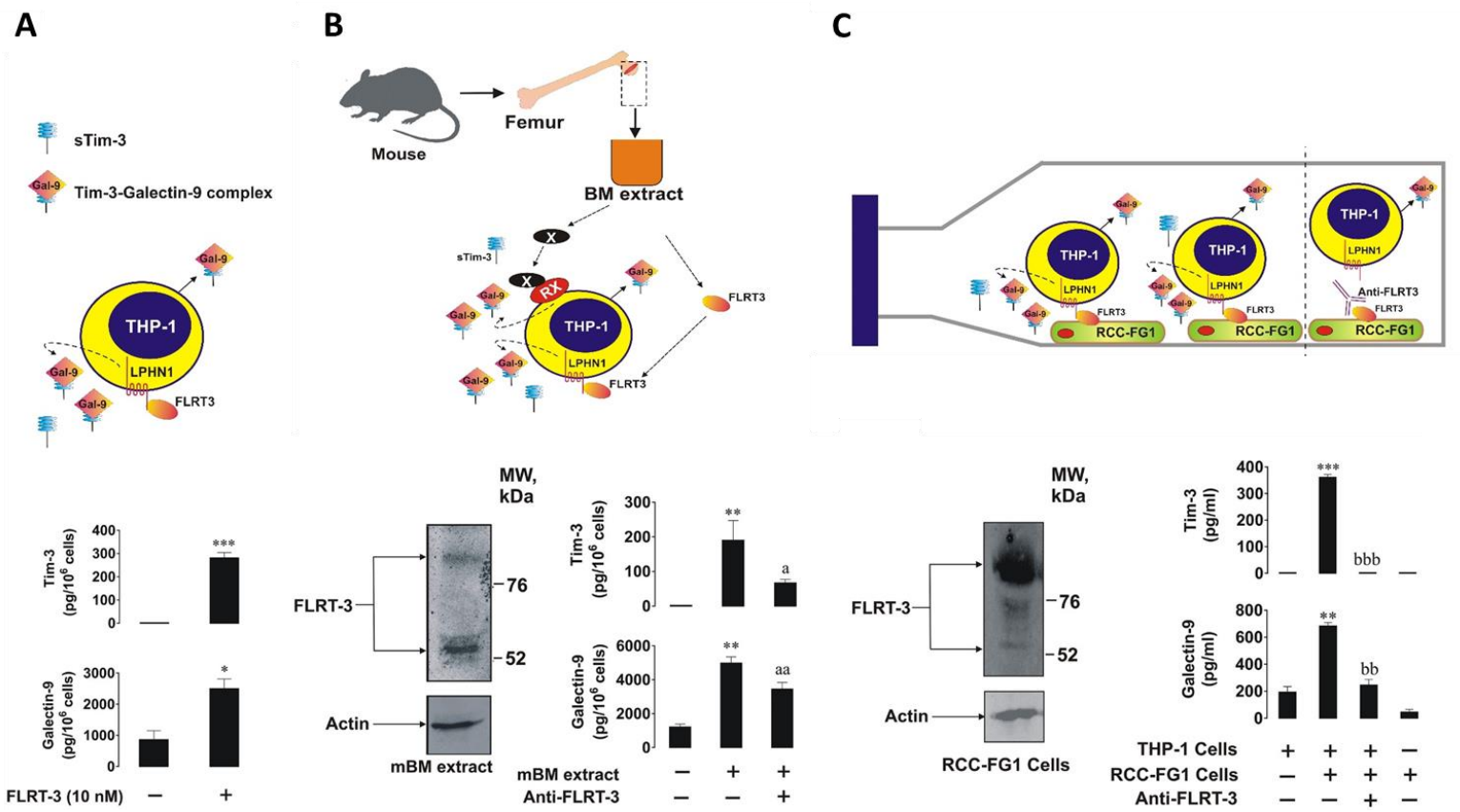


Figure 32: FLRT3 induces galectin-9 and Tim-3 secretion in THP-1 cells. (A) THP-1 cells were treated for 16 h with 10 nM extracellular domain of human recombinant FLRT3. The concentrations of galectin-9 and Tim-3 in the media obtained were determined by ELISA. **(B)** THP-1 cells were incubated with mouse bone marrow (mBM) extracts (10 μg protein/ml) for 16 h with or without 1 h pre-treatment with 5 μg/ml anti-FLRT3 antibody. The presence of FLRT3 in mBM extracts was confirmed by Western blot analysis. The levels of Tim-3 and galectin-9 released in the media were measured by ELISA. **(C)** The presence of FLRT3 was also confirmed in RCC-FG1 cells by Western blot analysis. RCC-FG1 cells were co-cultured with THP-1 cells at a ratio of 1 THP-1:2 RCC-FG1 with or without 1 h pre-treatment with 5 μg/ml FLRT3 neutralizing antibody. The levels of Tim-3 and galectin-9 released in the media were measured by ELISA. Images are from one experiment representative of three which gave similar results. Quantitative data depict mean values ± SEM of three independent experiments; *p b 0.05; **p b 0.01; ***p b 0.001 vs. control. Symbols “a” or “b” are used instead of “*” to indicate differences vs. cells treated with mBM extracts or co-cultured with RCC-FG1 cells, respectively.

In addition, PKCα activity was determined (as outlined in materials and methods) in THP-1 cells treated as described above. It was found that PMA, LTX and FLRT3 significantly upregulated PKCα activity [Figure 33 A]. Similarly, PKCα activity was increased in THP-1 cells when co-cultured with RCC-FG1 cells; this effect was attenuated in presence of anti-FLRT3 neutralising antibody [Figure 33 B]. These results indicate that FLRT3 induces galectin-9 secretion in THP-1 cells in PKCα-dependent manner.

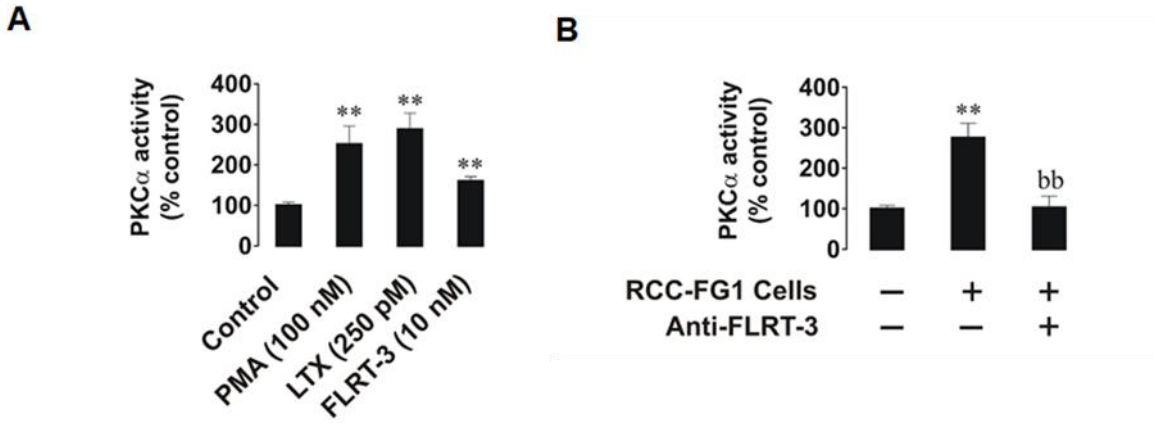


Figure 33: PMA, LTX and FLRT3 upregulate PKCα activity in THP-1 cells. (A) PKCα activity was analysed in resting THP-1 cells as well as those exposed for 16 h to 100 nM PMA, 250 pM LTX and 10 nM FLRT-3. **(B)** PKCα activity was analysed in resting THP-1 cells and those co-cultured with RCC-FG1 cells (ratio 1 THP-1: 2 RCC-FG1) in the absence or presence of 5 µg/ml FLRT-3 neutralising antibody. Images are from one experiment representative of three which gave similar results. Quantitative data are mean values ± SEM of three independent experiments; *$p < 0.05$; **$p < 0.01$ vs. control. Symbol "bb" indicates $p<0.01$ vs. THP-1/RCC-FG1 co-culture.

4.3 Galectin-9 protects AML cells from NK cell killing activity

Recently, Tim-3 was found to be expressed in NK cells. In addition, it was shown that the exposure to galectin-9 (soluble or cell-surface associated) in presence or absence of anti-Tim-3 antibody influences IFN-γ release by NK cells (Gleason et al., 2012). Thus, it has been speculated that Tim-3-galectin-9 interaction might be involved in the creation of immunological synapses between target cells and cytotoxic lymphoid cells.

To investigate this hypothesis, LAD2 human mast cell sarcoma cells (expressing both Tim-3 and galectin-9) and primary human NK cells were employed.

Comparative analysis of total and cell-surface levels of Tim-3 and galectin-9 suggest that these proteins are predominantly expressed on the membrane rather than inside LAD2 cells [Figure 34]. In addition, it was found that resting LAD2 cells don't secrete detectable amounts of galectin-9 but its release can be induced by IgE. Contrarily, intracellular levels of galectin-9 and Tim-3 don't change considerably when LAD2 cells are exposed to IgE [Figure 34].

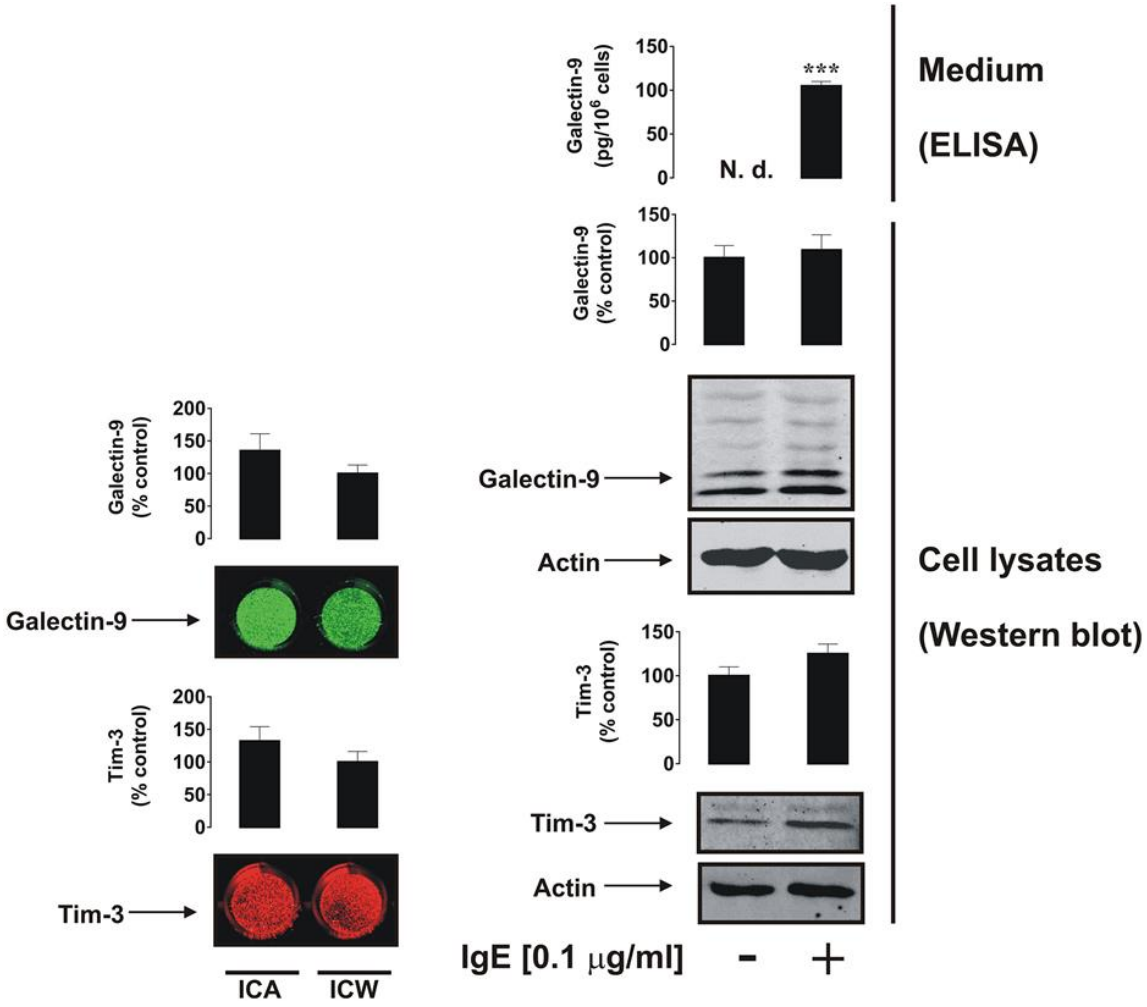


Figure 34. LAD2 cells express and externalize Tim-3 and galectin-9. Left panel: the levels of cell surface and total Tim-3 and galectin-9 in LAD2 cells were measured using LICOR in cell assay (ICA, non-permeabilized cells) and in cell Western (ICW, permeabilized cells). Right panel: LAD2 cells were cultured in presence or absence of 0.1 μg IgE; Tim-3 and galectin-9 intracellular levels were measured by Western blot analysis, while the amount of secreted galectin-9 was characterised by ELISA. Images are from one experiment representative of three which gave similar results. Quantitative data show mean values ± SEM of three independent experiments; ***p b 0.001 vs. control.

Primary human NK cells instead express Tim-3 (several glycosylation variants) but do not produce detectable amounts of galectin-9 protein [Figure 35].

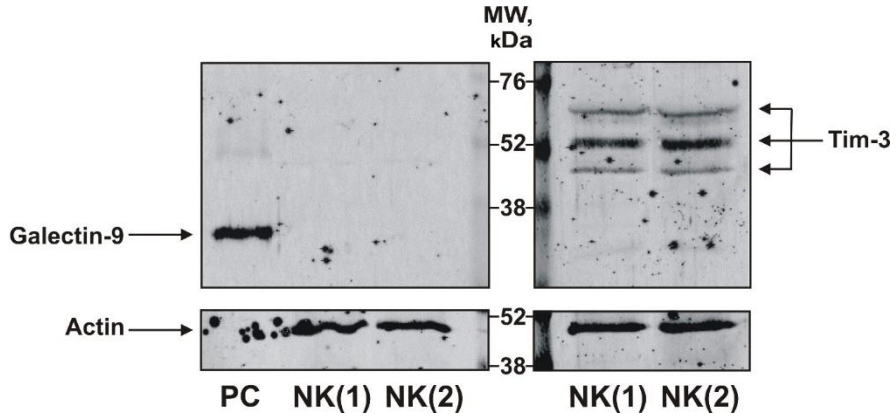


Figure 35: Primary human NK cells express Tim-3 but don't produce detectable amounts of galectin-9 in primary human NK cells. Expressions of both proteins were analysed in whole cell extracts by Western blot. Human recombinant galectin-9 was used as a positive control (PC). Images are from one experiment representative (two donors in each) of three which gave similar results.

Primary human NK cells were immobilised on ELISA plates and co-cultured in presence or absence of IgE-sensitized LAD2 cells (Sumbayev, et al., 2012) at a ratio of 1:1 with or without 15 min pre-incubation with galectin-9 neutralizing antibody. To exclude IgG involvement in synapsis formation, LAD2 and NK cells were also incubated with isotype control antibody instead of anti-galectin-9 one [Figure 35].

Since LAD2 cells, express high affinity IgE receptors (FcεRI), which are not present in NK cells, specific detection of LAD2 cells was possible by incubating the plate with IgE, and following incubations with mouse IgM anti-IgE and then anti-mouse LI-COR secondary antibody (the scheme of the experiment is illustrated in Figure 36).

It was found that LAD2 cells bind NK cells and the presence of galectin-9 neutralizing antibody (but not isotype control antibody) abolished this effect [Figure 36]. These results confirm that galectin-9 expressed by LAD2 cells participates in the interaction with NK cells.

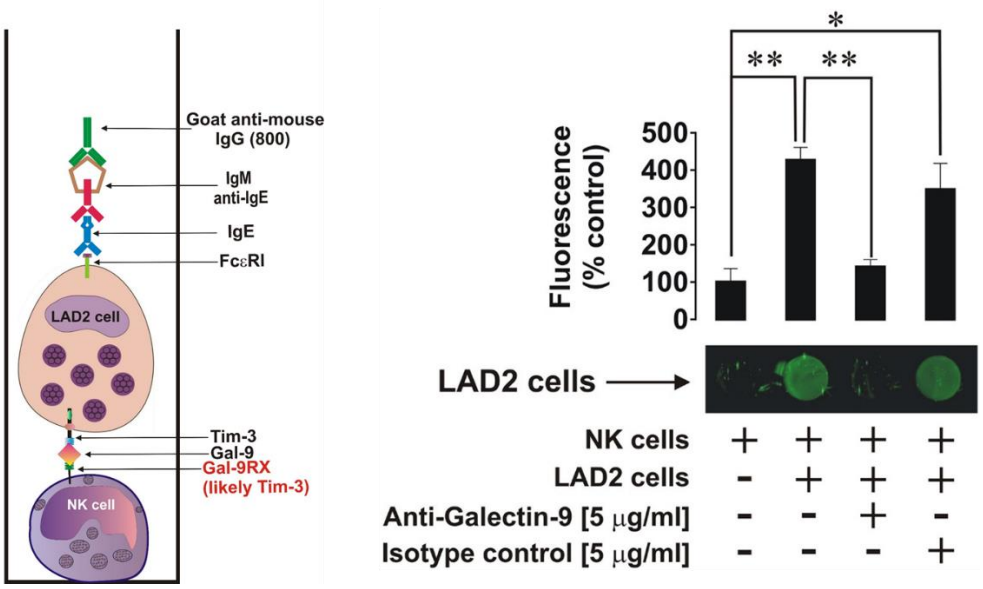


Figure 36: Galectin-9 participates in the formation of an "immunological synapse" between NK cells and LAD2 cells. Primary human NK cells were immobilized on the surface of Maxisorp plates. Cells were then co-cultured for 30 min with LAD2 cells with or without 30 min pre-treatment of LAD2 cells with 5 μg/ml galectin-9 neutralizing antibody (or the same amount of isotype control antibody). LAD2 cells were then visualized using LI-COR assay as outlined in Materials and Methods. Images are from one experiment representative of five which gave similar results. Quantitative data represent mean values ± SEM of five independent experiments; *$p < 0.05$; **$p < 0.01$.

To attest whether these immunological synapses participate or not in the prevention of AML cell killing by cytotoxic immune cells, the co-culture of K562 (chronic myeloid leukaemia cells, not secreting galectin-9) with NK cells was analysed.

K562 cells were grown for 24 h in RPMI media containing 100 nM PMA. After the treatment of K562 cells with PMA (24 h), the media was replaced with the fresh one containing primary human NK cells at ratio of 1 K562:2 NK in the absence or presence of 5 ng/ml human recombinant galectin-9. Following 16 h of co-incubation, MTS test was performed to determine the cell viability of both cell lines. It was found that K562 viability was significantly decreased when co-cultured with NK cells in absence of galectin-9. This reduction was attenuated in presence of galectin-9 [Figure 37 A]. On the other hand, NK cells viability wasn't affected by any of the described conditions [Figure 37 A].

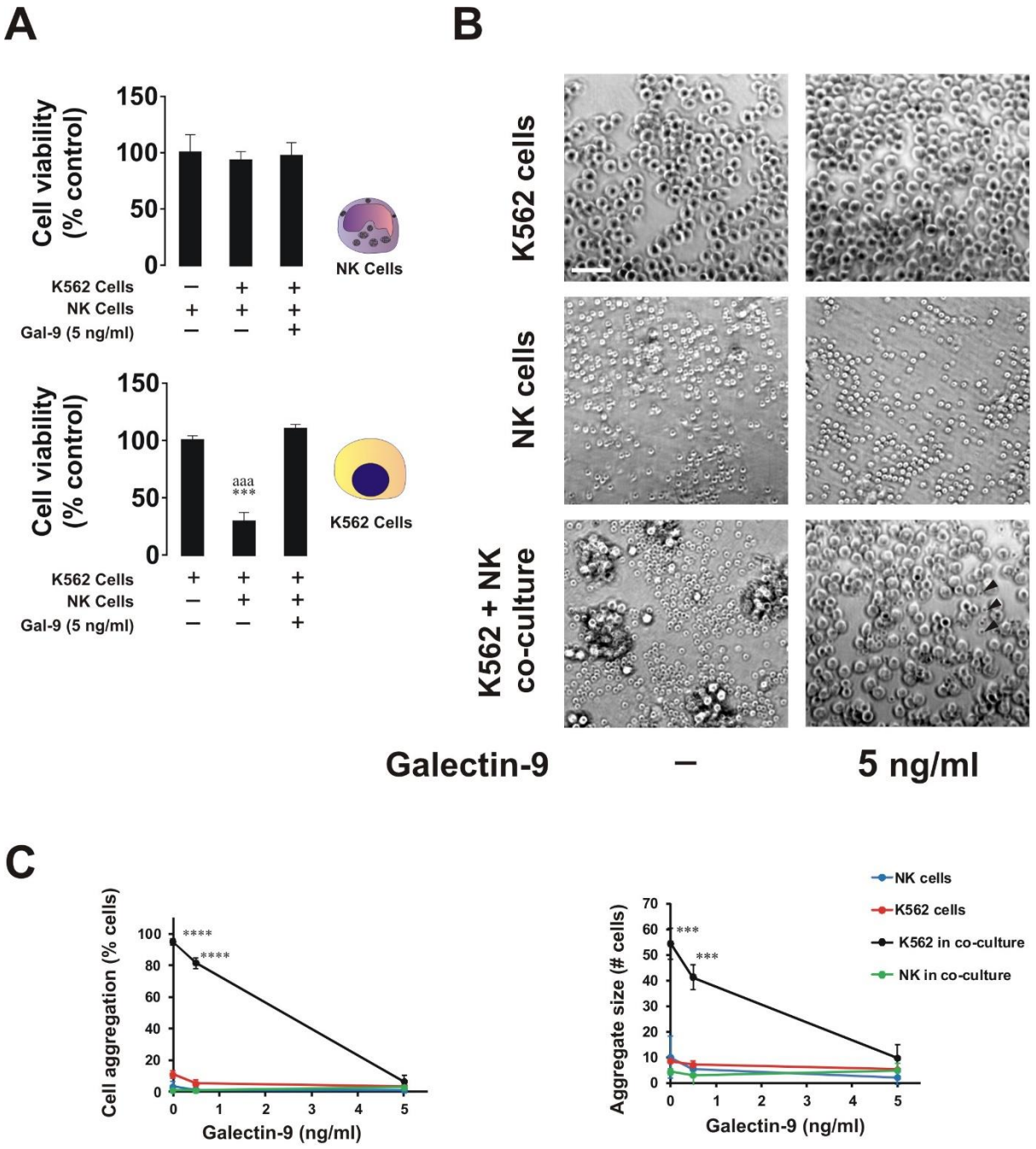


Figure 37: Galectin-9 protects myeloid leukaemia K562 cells from being killed by primary human NK cells. K562 cells were incubated for 24 h with PMA in 96-well Maxisorp plates. (A) After 24 h, PMA-containing media was replaced with the media containing primary human NK cells. K562 and NK cells were then co-cultured (at ratio 1:2) for 16 h in the absence or presence of 5 ng/ml galectin-9. Viability of K562 and NK cells was measured using MTS test. Images are from one experiment representative of three which gave similar results. Quantitative data represent mean values ± SEM (n=3) independent experiments; ***p < 0.001 vs. control. (B) K562 cells co-incubated for 16 h with primary human NK cells, at a 1:2 ratio, in presence or absence of galectin-9 5 ng/ml. Cells were imaged using phase-contrast microscopy. The images are from one representative experiment of six (n = 6), which gave similar results. Scale bar (the same for all images), 50 μm. (C) NK cells induced aggregation of K562 cells was quantified as a function of galectin-9 concentration. Left, the per cent of cells found in aggregates in individual cultures and in the co-culture. Right, the size of cell aggregates in individual cultures and in the co-culture. The data represent the mean values ± SD of six independent experiments; *, p < 0.05; **, p < 0.01; ****, p < 0.0001

In addition, the cells (grown alone and in co-culture) with or without 5 ng/ml galectin-9 were visualised using phase contrast microscopy. Images obtained showed that NK cells induce the formation of massive K562 aggregates in absence of galectin-9. Indeed, none of the cell lines formed visible aggregates if cultured alone with or without galectin-9 [Figure 37 B]. Also, NK cell-induced aggregation of K562 cells was abrogated when the cells were co-cultured in presence of 5 ng/ml galectin-9 [Figure 37 B]. This effect was quantified using increasing concentrations of galectin-9 (in the range 0 – 5 ng/ml) in the co-culture. The data obtained showed that K562 aggregation induced by NK cells decreased in presence of galectin-9 in dose-dependent manner until no K562 cell aggregation was detectable when galectin-9 concentration reached 5 ng/ml [Figure 37 C]. Thus, galectin-9 clearly protects myeloid leukaemia cells from being killed by NK cells.

The interactions between AML THP-1 cells and NK cells were then investigated. THP-1 cells were treated with 100 nM PMA for 16 h. After the pre-treatment of THP-1 cells, their culture medium was replaced with PMA-free medium containing NK cells (ratio of 2 NK cells:1 THP-1 cells) and the cells were co-incubated for 6 h with or without 5 μg/ml galectin-9-neutralising antibody. After the incubation, granzyme B and caspase-3 activities as well as the cell viability of THP-1 cells were characterised as described in Materials and Methods. It was found that the viability of THP-1 cells was significantly reduced when co-cultured with NK cells in presence of anti-galectin-9 neutralising antibody. The stimulation of AML cell death by NK cells was also confirmed by increased granzyme B and caspase-3 activities in THP-1 cells when co-incubated in presence of anti-galectin-9 neutralising antibody [Figure 38]. However, the levels of galectin-9 secreted by THP-1 cells (measured by ELISA) didn’t change considerably in any of described conditions (galectin-9 bound to neutralising antibody was also detectable by ELISA) [Figure 38].

In addition, cell lysates of isolated NK cells were subjected to Western blot analysis for specific detection of Tim-3 and galectin-9. It was confirmed that resting NK cells don't produce detectable amounts of galectin-9. However, this protein on its own, and in the form of unbroken Tim-3-galectin-9 complex, was detectable in NK cells co-cultured with THP-1 cells. Furthermore, the levels of both, galectin-9 alone and in complex with Tim-3, were significantly reduced when the cells were co-incubated in the presence of galectin-9 neutralising antibody [Figure 38]. These results suggest that galectin-9 detected in NK cell lysates is most likely to derive from THP-1 cells, which release high amounts of this protein in the culture media. Once secreted, galectin-9 is able to bind to Tim-3 present on NK cell surface preventing granzyme B delivery in THP-1 cells, and thus inhibiting the caspase-3-dependent apoptotic pathway.

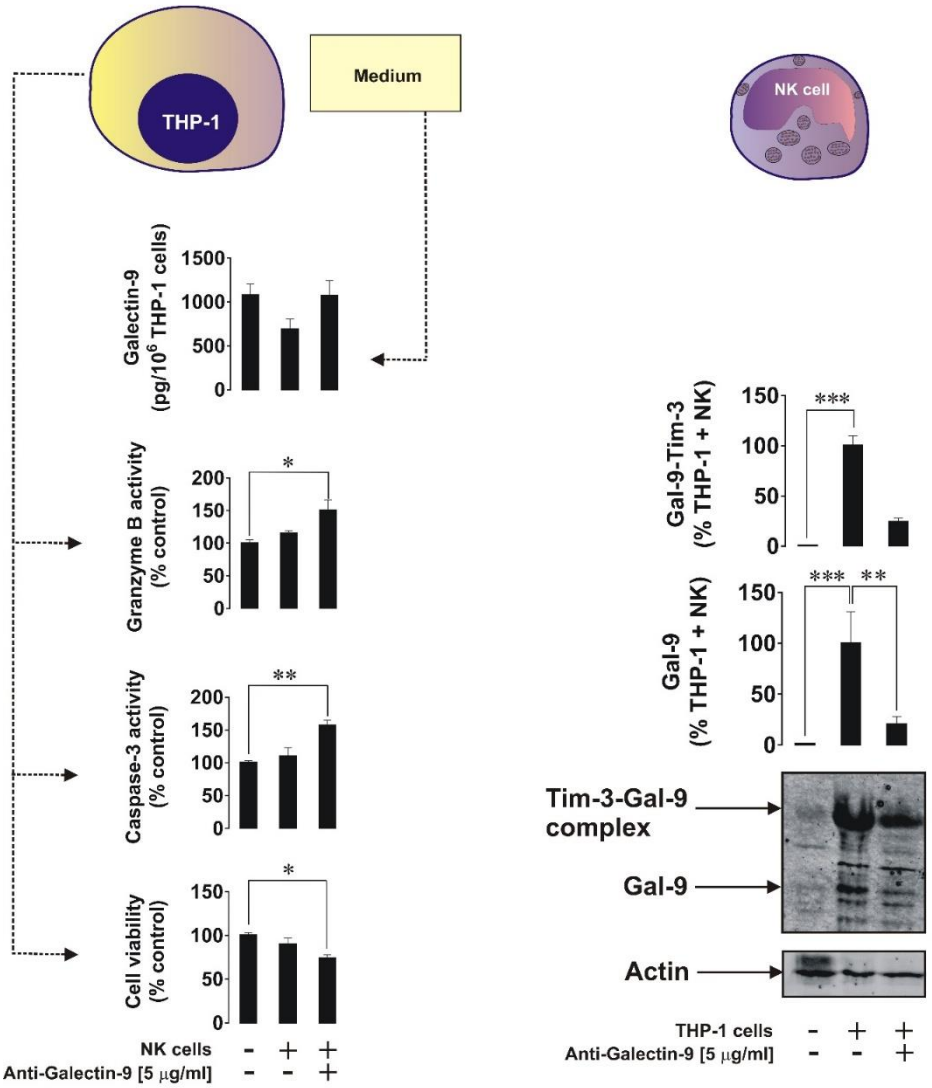


Figure 38: Cell-derived galectin-9 attenuates AML cell killing activity of primary human NK cells. PMA pre-treated THP-1 cells were co-cultured with primary human NK cells at 1:2 ratio for 6 h. After the incubation, MTS test was performed on isolated THP-1 cells. Granzyme B and caspase 3 activity was also characterised in THP-1 cell lysates as described in Materials and Methods (left panel). Galetin-9 levels in the media were measured using ELISA (left panel). NK cells were subjected to Western blot analysis for specific detection of galectin-9 and Tim-3 (right panel). Images are from one experiment representative of three which gave similar results. Quantitative data show mean values ± SEM of three independent experiments; *$p < 0.05$; **$p < 0.01$; ***$p < 0.001$ vs control.

In addition to galectin-9 function in inhibition of cytotoxic activity of NK cells (as described above), sTim-3 has been suggested to participate in the attenuation of cell-mediated immune response (Geng et al., 2006). Indeed, it was found that sTim-3 is able to attenuate immune cells proliferation and to reduce the secretion of IL-2, a cytokine, which activates cytotoxic activity of NK cells and T cells (Geng et al., 2006).

Since the levels of sTim-3 are considerably higher in the plasma AML patients compared to healthy donors [Figure 28 B], comparative analysis of IL-2 concentration between two groups was also performed. It was found that IL-2 levels are significantly lower in AML patients compared to healthy donors [Figure 39 A and B]. To confirm Tim-3 involvement in the reduction of IL-2 secretion by the immune cells, Jurkat T cells (producing detectable amounts of IL-2) were treated with increasing concentrations of sTim-3 for 24h. It was found significant downregulation of IL-2 secretion by Jurkat T cells in presence of increasing concentrations of sTim-3. These results suggest that sTim-3 is also involved in the immune escape of AML cells.

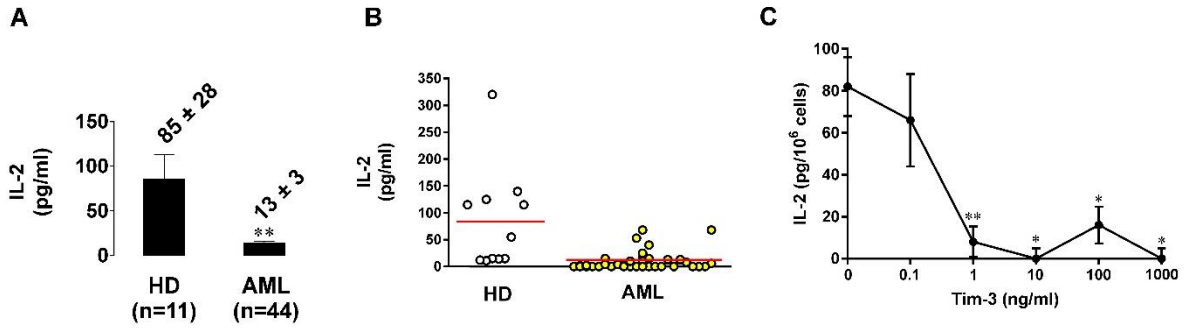


Figure 39: Soluble Tim-3 attenuates IL-2 release. (A and B) The levels of IL-2 in blood plasma obtained from AML patients and healthy donors were measured by ELISA. (C) Jurkat T cells were treated with increasing concentration of Tim-3 for 24 h. After the treatment the media was subjected to ELISA for IL-2 detection. Data show mean values ± SEM of three independent experiments; *$p < 0.05$; **$p < 0.01$.

4.4 Discussion

AML cells are able to suppress anti-tumour immunity, but the biochemical mechanisms involved in this immune escape remain unclear. Recent evidences suggest that Tim-3 and galectin-9, two proteins highly secreted by AML cells, may participate in attenuation of NK and T cell cytotoxic activities (Golden-Mason et al., 2013; Gonçalves Silva, et al., 2016; Kikushige et al., 2015). However, stimuli required for Tim-3 and galectin-9 expression by AML cells as well as their release from the cell surface are poorly understood.

It is known that galectin-9 lacks the signalling sequence necessary for its secretion and thus requires a trafficker in order to be expressed on the membrane or released by the cell (Delacour,

et al., 2009).Tim-3 has been proposed as a possible trafficker of galectin-9 (Gonçalves Silva, et al., 2016).

Our results reinforced the assumption according to which Tim-3 is a galectin-9 trafficker. Tim-3-galectin-9 complex was detected inside the cell (70 kDa) and in the culture media (52 kDa) [Figure 24 and 25]. Indeed, the bands at 70 kDa (cell lysates) and at 52 kDa (media) were recognised by both anti-Tim-3 and anti-galectin-9 antibodies. However, when the same blot was incubated sequentially with both antibodies, the second antibody failed to detect the respective protein in the same band (unless the first antibody is stripped off) due to steric hinderance. Moreover, confocal microscopy co-localisation analysis confirmed the presence of Tim-3-galectin-9 complex inside permeabilised THP-1 cells. Contrarily, surface presence of the complex wasn't detectable by both antibodies using confocal microscopy co-localisation analysis [Figure 26]. This is in line with the previous observation (impossibility to detect the same band by sequential incubation with anti-Tim-3 and anti-galectin-9 antibodies and vice versa). In fact, when the complex is expressed on the cell surface, Tim-3 is covered by galectin-9 and thus can't bind anti-Tim-3 antibody (steric hinderance).

The interaction of Tim-3 with galectin-9 was also characterised by SRCD spectroscopy. We found that the interaction between Tim-3 and galectin-9 leads to major conformational changes in these proteins [Figure 29]. In particular, a clear increase in β-strand has been observed. This suggests that Tim-3 binding alters galectin-9 conformation, possibly increasing its ability to interact with the target proteins. Since galectin-9 is a tandem protein containing two sugar-binding domains, one of them could bind Tim-3 expressed on the membrane of AML cell, leaving the other sugar-binding domain free to interact with Tim-3 (or another receptor) present on the membrane of the target cell (e.g., NK cell).

Previously it was also reported that PKC-α is involved in the secretion of both Tim-3 and galectin-9 (Chabot et al., 2002). We confirmed these findings. PKC-α activation led to mTOR-dependent synthesis of galectin-9 and Tim-3 as well as their increased release by THP-1 cells [Figure 24, 25 and 30]. The release of Tim-3-galectin-9 complex was also found to be considerably augmented following PKC-α activation in THP-1 cells [Figure 34, 25 and 30].

Tim-3 has been reported to be shed from the cell surface by ADAM 10/17 (Möller-Hackbarth et al., 2013). Therefore, we investigated whether these proteolytic enzymes are involved in the shedding of Tim-3 in its free form and/or in complex with galectin-9. We found that ADAM 10/17 contribute to considerably increased secretion of free Tim-3 (sTim-3), but don't induce any significant changes in Tim-3-galectin-9 release from THP-1 cell surface [Figure 24]. Therefore, different proteolytic enzymes are involved in the shedding of Tim-3 depending whether it is bound or not to galectin-9. This deduction was also confirmed by the fact that two distinct bands were specifically detected by anti-Tim-3 antibody at 20 kDa and at 33 kDa in the blot containing immunoprecipitated media used for THP-1 cell culture. Since the band at ~52 kDa was recognised by both anti-Tim-3 and anti-galectin-9 antibodies and the molecular weight of galectin-9 is ~32 kDa, the band at 20 kDa is likely to represent the fragment of Tim-3 that is shed from the cell surface when this Ig is associated with galectin-9. Diversely, when Tim-3 is expressed on the membrane without galectin-9, it is shed at a different site and thus has a different molecular weight (~33 kDa) when compared to the fragment (frTim-3) partially dissociated from the complex during gel electrophoresis [Figure 24].

Recently it was discovered that LPHN1, a G-protein coupled neuronal receptor, is expressed in AML cells but is absent in healthy leukocytes. Moreover, triggering of LPHN1 in myeloid leukaemia cells was found to induce the secretion of IL-6, cytokine promoting survival and

proliferation of AML cells (Sumbayev et al., 2016). Therefore, the involvement of LPHN1 in galectin-9 and Tim-3 exocytosis was investigated.

We found that both natural (FLRT3) and exogenous (LTX-α) ligands of LPHN1 induced mTOR-dependent synthesis of Tim-3 and galectin-9 as well as their exocytosis in AML cells [Figure 30, 31 and 32]. Moreover, LPHN1 triggering increased also PKC-α activity in AML cells [Figure 33]. PKC-α has been reported to induce the formation of SNARE complex responsible for exocytosis (Morgan et al., 2005; Stöckli, et al., 2011). Therefore, our results suggest that FLRT3, found to be physiologically expressed in the bone marrow [Figure 32], can interact with LPHN1 expressed by AML cells inducing galectin-9 and Tim-3 synthesis and their abundant secretion consequent to PKC-α activation. Thus, the presence of LPHN1 in AML cells, but not in healthy leukocytes, may explain considerably higher levels of Tim-3, galectin-9 and of the complex formed by these proteins in the blood plasma of AML patients when compared to healthy donors' ones [Figure 28]. Importantly, high galectin-9 plasma levels have been correlated with lower overall survival rates in patients affected by myelodysplastic syndromes (MDS), a group of blood disorders frequently progressing to AML (Asayama et al., 2017). In addition, AML cells expressing constitutively active PKC-α were also associated with poor prognosis and high mortality rate (Kurinna et al., 2006).

Interestingly, increased PKC-α activation in THP-1 co-cultured with RCC-FG1 cells (expressing FLRT3) was abolished by FLRT3 neutralising antibody [Figure 33]. This is in line with the fact that FLRT3-induced increase of secreted galectin-9 and Tim-3 by THP-1 cells when co-incubated with RCC-FG1 cells was also abolished by FLRT3 neutralising antibody [Figure 32 C]. Diversely, FLRT3 neutralising antibody significantly reduced, but not abolished, PKC-α-induced increase of secreted galectin-9 and Tim-3 by THP-1 cells incubated with bone marrow [Figure 32 B]. This suggests that bone marrow may contain, in addition to

FLRT3, other PKC-α activating proteins, which can bind AML membrane receptors (LPHN1 or others) and induce synthesis and exocytosis of Tim-3 and galectin-9.

Once expressed on the cell surface or released in the culture media, galectin-9 protects AML cells from the immune attack. Indeed, the cell viability of K562 cells (chronic myeloid leukaemia cells not releasing detectable amounts of galectin-9) was significantly reduced by NK cells. On the other hand, cytotoxic activity of NK cells was abolished when the co-culture was performed in the presence of human recombinant galectin-9 [Figure 37].

Galectin-9 involvement in the protection of AML cells from the immune attack was then confirmed using THP-1 cells co-cultured with NK cells in presence or absence of neutralising anti-galectin-9 antibody [Figure 38]. Indeed, the cell viability of THP-1 cells (expressing on their surface and releasing high amounts of galectin-9) was significantly decreased in presence of anti-galectin-9 neutralising antibody.

It is known that NK cell cytotoxic activity consists mainly in the release of the granules containing granzyme B, which leads to the activation of caspase 3 inside the target cell and thus provokes apoptosis of malignant cells (as described in the Introduction). We found that the activities of both enzymes were significantly augmented in THP-1 cells when the co-culture was performed in presence of anti-galectin-9 neutralising antibody. This confirms that NK cells kill AML cells through the delivery of granzyme B inside the malignant cells. Our results suggest also that galectin-9 interacts with Tim-3 exposed on the membrane of NK cells (which don’t express galectin-9) preventing granzyme B delivery into AML cells.

Possible mechanism through which galectin-9 binding to Tim-3 expressed on NK cell surface prevents the release of cytotoxic granules containing Granzyme B is illustrated in Figure 40. It is based on the recent finding regarding the capability of galectin-9 to induce NK cells to release IFN-γ (Gleason et al., 2012). The binding of IFN-γ with its respective receptor expressed on

the surface of AML cells leads to the activation of indoleamine 2,3-dioxegenase (IDO1), an enzyme which converts L-tryptophan into formyl-L-kynurenine, which is then converted into L-kynurenine (Corm et al., 2009; Folgiero et al., 2015; Mabuchi et al., 2016). This intermediate of tryptophan catabolism is then converted to L-kynurenine, which attenuates cytotoxic NK cell activity through the prevention of granzyme B delivery into AML cells.

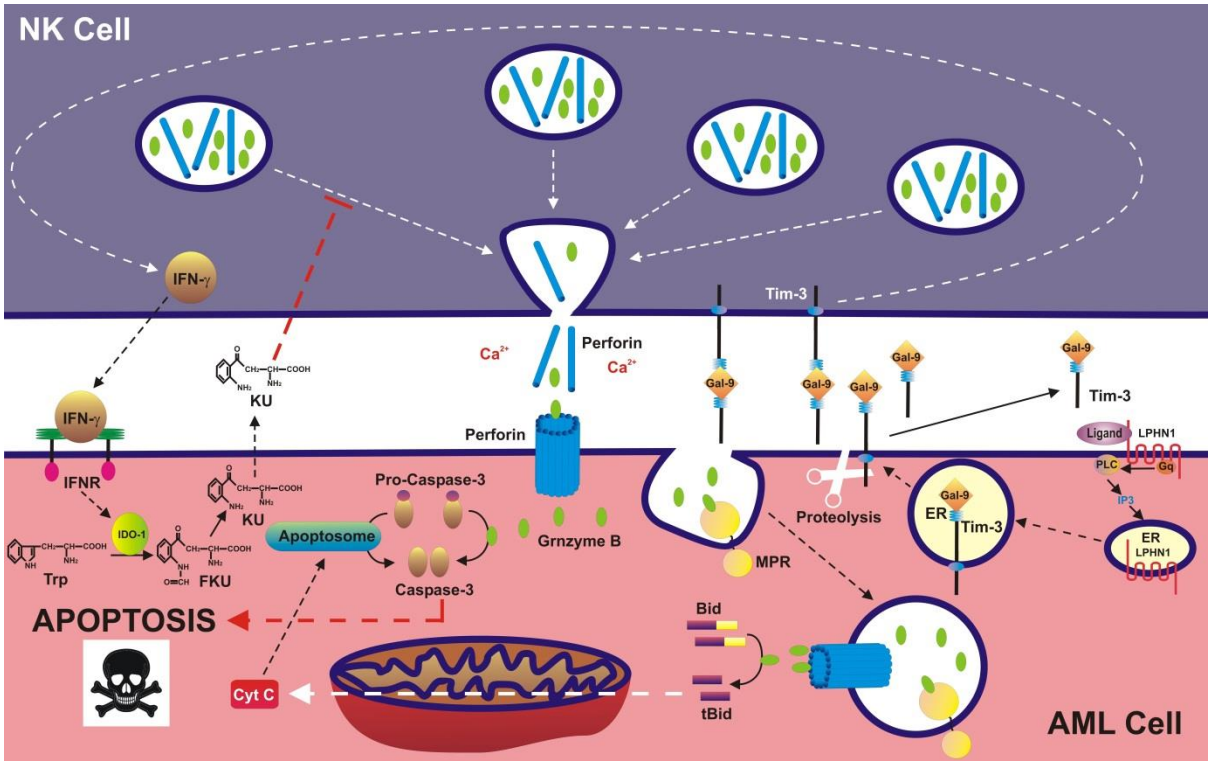


Figure 40: Possible biochemical interactions between AML and NK cells. Triggering of LPHN1 leads to the surface expression and release of galectin-9 by AML cells. Cell surface-associated or secreted galectin-9 binds then to the NK cell receptor (likely – Tim-3). This interaction induces NK cells to release of IFN-γ, which stimulates IDO1 to convert tryptophan (Trp) into formyl-kynurenine (FKU) inside AML cells. FKU is then further degraded into L-kynurenine (KU), which can be released by AML cells. KU attenuates the ability of NK cells to deliver granzyme B into AML cells in perforin/mannose-6-phosphate receptor (MPR)-dependent manner. If successfully delivered, granzyme B catalyses the cleavage of the protein Bid into tBid, which leads to mitochondrial disfunction with consequent release of cytochrome c from the mitochondria into the cytosol of malignant cells. Once liberated in the cytosol, cytochrome c induces apoptosome formation leading to the activation of caspase-3. Furthermore, granzyme B is capable of performing direct proteolytic activation of caspase-3. These effects lead to AML cell apoptosis. However, this process is not taking place in presence of galectin-9, which impairs NK cell cytotoxic activity as described above.

In addition to galectin-9-associated immune escape, we found that AML cells protect themselves from cytotoxic attack through the secretion of Tim-3. Our results suggest that soluble Tim-3 is capable of binding a target protein (or a group of target proteins) expressed

by T cells leading to their decreased secretion of IL-2, a cytokine required for activation of NK cells and cytotoxic T lymphocytes. This is in line with the results obtained from comparative analysis of sTim-3 and IL-2 levels in blood plasma of AML patients and healthy donors (HD). Indeed, we found considerably higher levels of sTim-3 and significantly lower concentration of IL-2 in the blood plasma of AML patients when compared to HD [Figure 28 and 39].

Schematic representation of the pathway derived from previously described findings is illustrated in Figure 41.

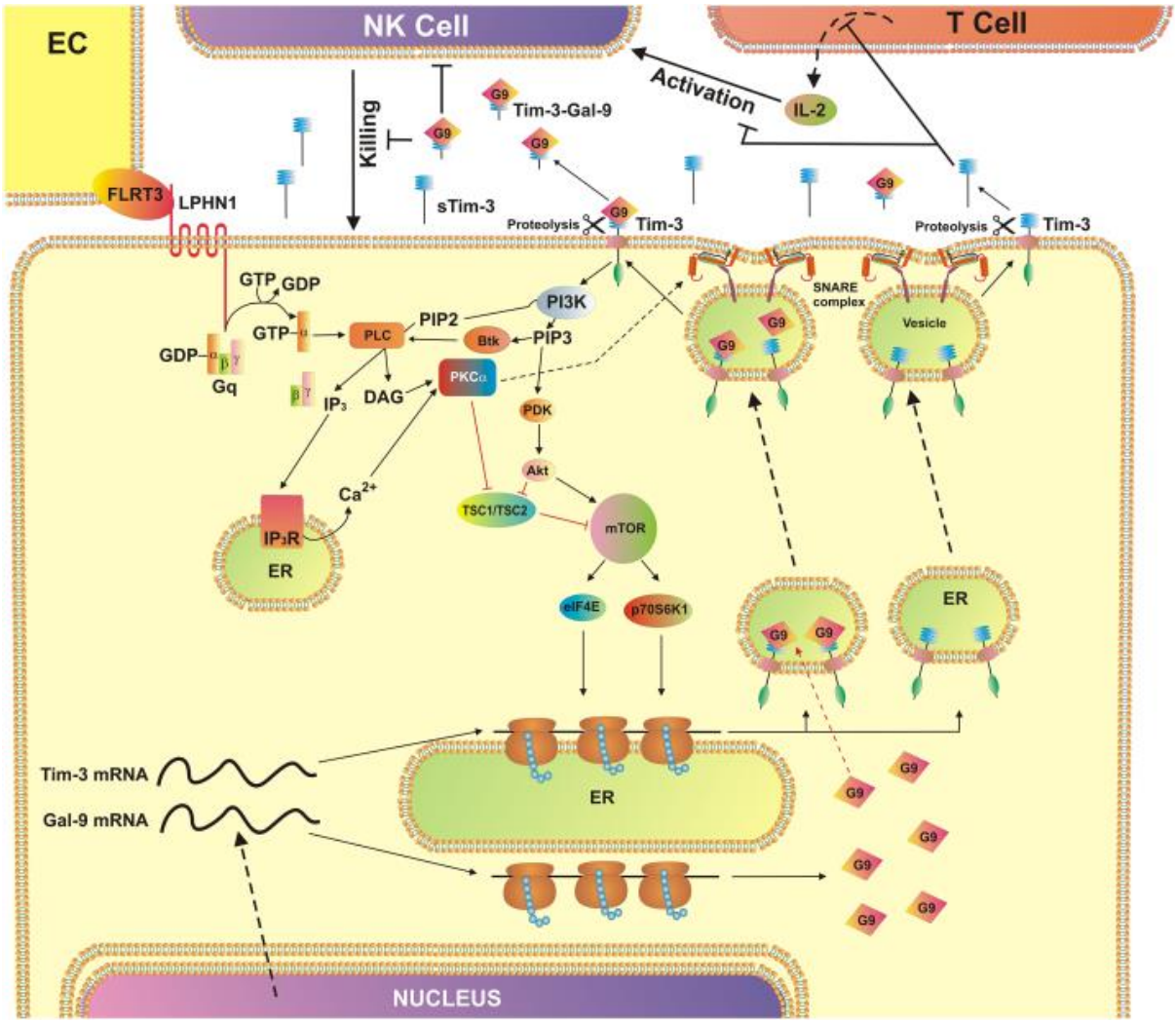


Figure 41: Pathobiochemical pathway allowing AML cells to escape host anti-cancer immunity. The interaction of FLRT3, expressed on the surface of endothelial cells (EC), with AML surface receptor, LPHN1, leads to the activation of Gq which then stimulates PLC. Activated PLC catalyses the hydrolysis of phosphatidyl-inositol-bisphosphate (PIP2) into inositol-trisphospate (IP3) and diacylglycerol (DAG). IP-3 is then able to bind ER-associated IP3 receptor (IP3R) leading to Ca2 + mobilization. Released IP3 and DAG activate PKC-α, which triggers mTOR translational pathway through downregulation of TSC1/TSC2. This leads to increased synthesis of galectin-9 and Tim-3. In addition, PKCα phosphorylates protein Munc18 leading to the formation of SNARE complexes, which tether cytosolic vesicles to the plasma membrane. This pre-activates the release machinery, and elevated cytosolic Ca2 + lead to exocytosis of free and galectin-9-associated Tim-3. Once expressed on the membrane of AML cells, both types of Tim-3 are differentially shed from the cell surface by proteolytic enzymes. Galectin-9 impairs the ability of NK cells to kill AML cells, while sTim-3 attenuates the release of IL-2, cytokine required for the activation of immune cells.

5. AML cells recruit normal physiological systems to progress the disease by preserving expression of stem cell proteins

As previously described (Section 4.2), triggering of LPHN1, expressed in AML cells but not in healthy leukocytes, upregulates the expression and the secretion of Tim-3 and galectin-9 in AML cells allowing these malignant cells to escape host immune attack. However, the mechanisms underlying the regulation of LPHN1 expression in AML cells remain unclear. In addition, the presence of LPHN1 natural ligand (FLRT3) in blood hasn't been investigated yet.

5.1 Hematopoietic stem cells (HSCs) produce LPHN1, expression of which is preserved in malignant AML cells but not in healthy leukocytes

Recently, LPHN1 mRNA was detected in primary human CD34-positive stem cells (Maiga et al., 2016). Thus, LPHN1 protein expression was also investigated in them. Western blot analysis confirmed the presence of LPHN1 in hematopoietic stem cells (HSCs) [Figure 42]. Interestingly, the molecular weight of LPHN1 found in HSCs was slightly higher (~140 kDa) compared to the one detected in THP-1 cells (~130 kDa) [Figure 42] or in primary AML cells (~130 kDa) (Sumbayev et al., 2016).

Since triggering of LPHN1 induces Tim-3 and galectin-9 synthesis in AML cells, the expression of these proteins was also investigated in HSCs. Contrarily to THP-1, neither Tim-3 nor galectin-9 were detectable in primary human CD34-positive stem cells [Figure 42].

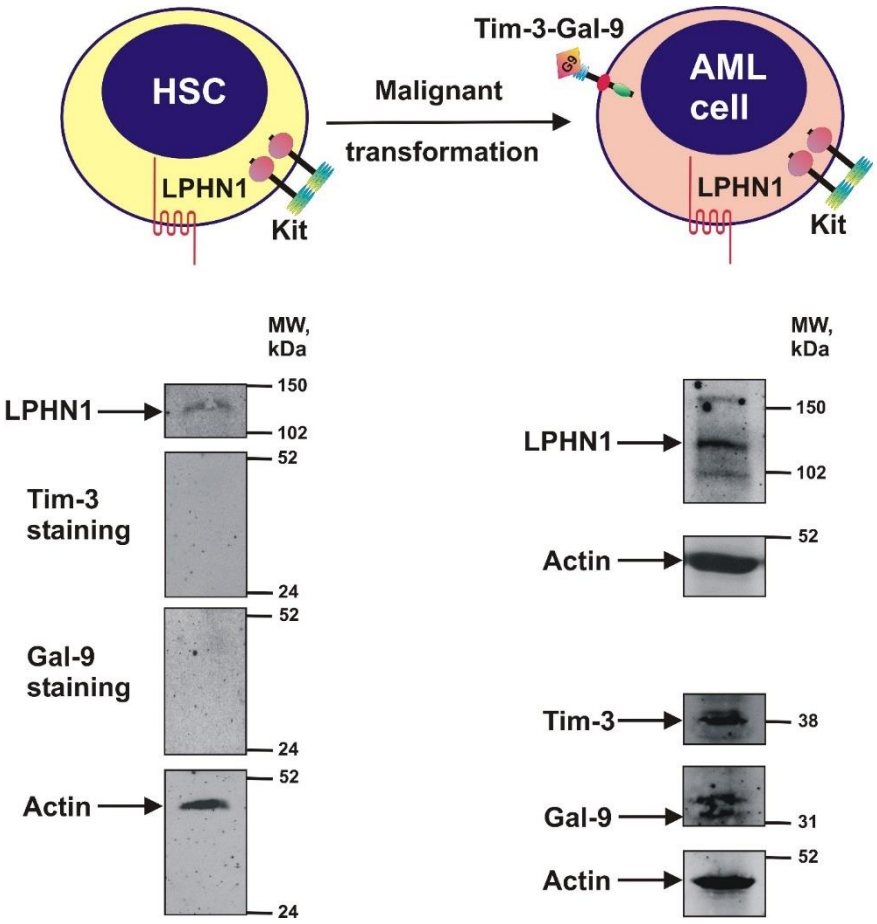


Figure 42: Characterisation of expression of LPHN1, Tim-3 and galectin-9 proteins in CD34-positive human stem cells (HSCs) and THP-1 AML cells (positive control). Western blot analysis was employed for the detection of LPHN1, Tim-3 and galectin-9 proteins in CD34-positive HSCs and THP-1 cells. Images are from one experiment representative of three which gave similar results.

Comparative analysis of LPHN1 protein expression was then characterised in primary human AML cells, THP-1 cells and primary human leukocytes by Western blot analysis. As previously reported, LPHN1 wasn't detectable by Western blot analysis in primary healthy leukocytes (Sumbayev et al., 2016). Clear bands were instead observed in the other two cell types and it was found that LPHN1 levels are considerably higher in primary human AML cells than in THP-1 cells [Figure 43].

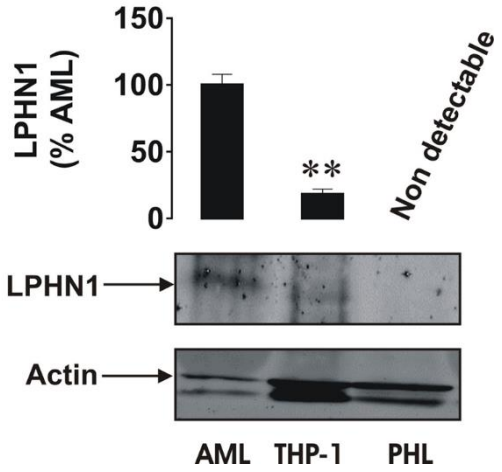


Figure 43: Comparative analysis of LPHN1 protein expression in primary human AML, THP-1 cells and PHL. Lysates of each cell type were subjected to Western blot analysis. Images are from one experiment representative of three which gave similar results. Data are the mean values ± SEM of three independent experiments; **p < 0.01 vs. AML cells.

5.2 Cortisol induces LPHN1 expression in AML cells and HSCs, but not in healthy leukocytes

Since AML cells and HSCs are typically present in the blood vessels or in bone marrow, the components normally circulating in the blood were taken under consideration as potential LPHN1 expression inducers. Cortisol, steroid hormone secreted in the bloodstream by adrenal glands, was proposed to stimulate LPHN1 expression in these cells.

To investigate the effects of cortisol on LPHN1 transcription and translation, primary and THP-1 human AML cells, primary human HSCs and primary healthy human leukocytes were incubated with 1 µM cortisol for 24 h. RNA extracts were then subjected to quantitative real-time PCR (qRT-PCR) to characterise any changes in LPHN1 gene expression in the cells upon the exposure to 1 µM cortisol. Detectable amounts of LPHN1 mRNA were found in all the tested cell types, except primary healthy leukocytes, and in all these cases the levels were significantly upregulated by cortisol treatment [Figure 44].

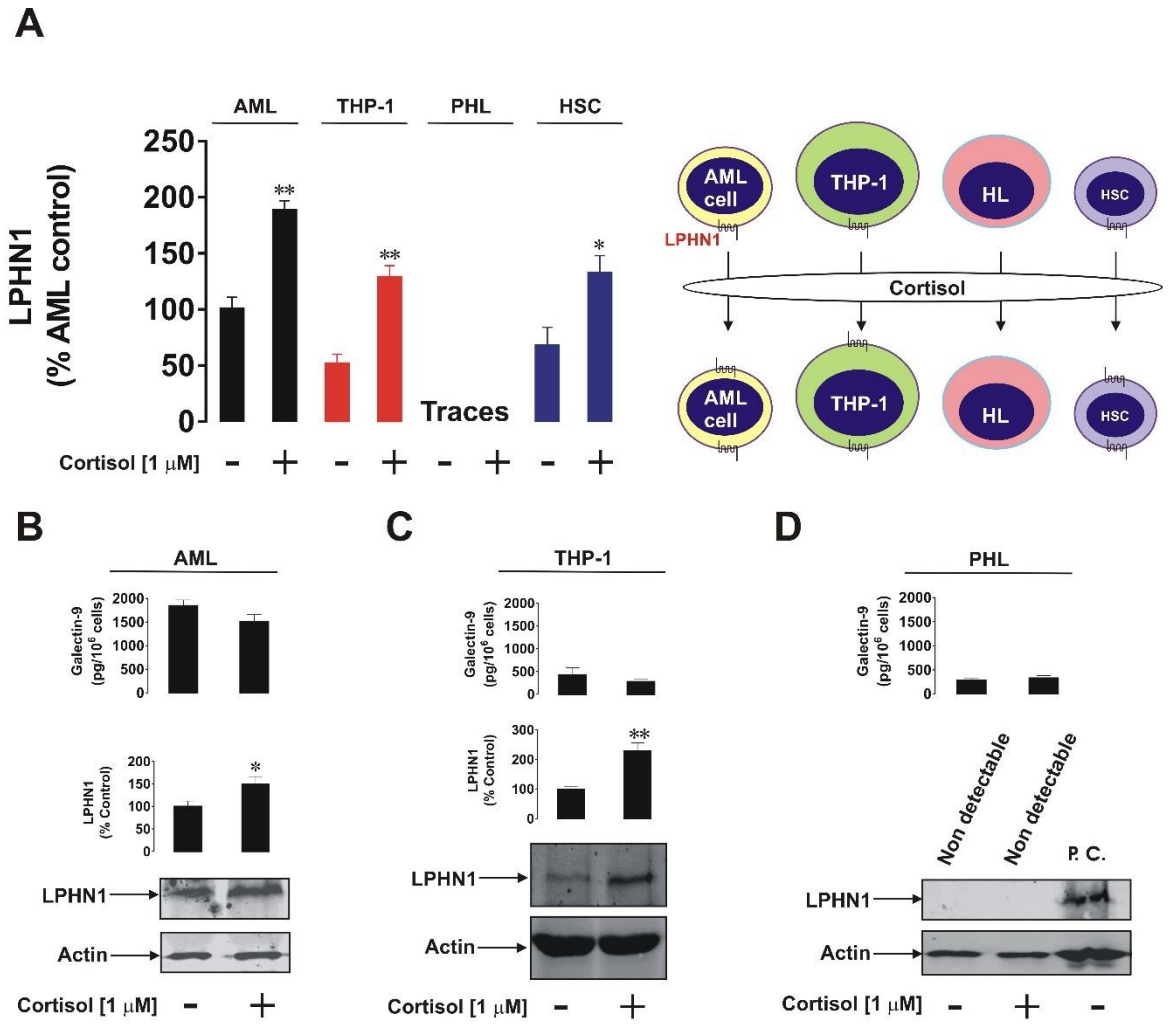


Figure 44: LPHN1 expression in human AML cells and haematopoietic stem cells, but not in primary healthy human leukocytes, is upregulated by cortisol. Primary human AML, THP-1 and haematopoietic stem cells as well as primary healthy leukocytes (PHL) were treated with 1 μM cortisol for 24 h. The levels of LPHN1 mRNA were measured by quantitative real-time PCR (A). LPHN1 protein levels were characterised by Western blot analysis (B – primary AML cells, C – THP-1 cells and D – PHL). For PHL, lysates of LPHN1 overexpressing NB2A cells were used as a positive control. The concentrations of secreted galectin-9 were measured by ELISA (B, C, D). Images are from one experiment representative of four which gave similar results. Data represent mean values ± SEM for four independent experiments. *$p < 0.05$; **$p < 0.01$ vs. control.

In addition, cell lysates of primary and THP-1 human AML cells, PHLs incubated for 24 h in presence or absence of 1 μM cortisol were subjected to Western blot analysis. It was found that LPHN1 protein levels were also upregulated by cortisol in primary and THP-1 human AML cells [Figure 44 B and C]. Contrarily, LPHN1 wasn't detectable in PHLs by Western blot analysis (as shown previously) and its expression wasn't induced by cortisol treatment [Figure 44 D].

The influence of cortisol in galectin-9 release by these three cell types was also investigated. ELISA analysis showed that cortisol treatment didn't provoke any changes in galectin-9 secretion by any of these cell types [Figure 44 B, C and D]. This suggests that LPHN1 needs to be activated by a ligand to induce galectin-9 release by AML cells.

Cortisol and galectin-9 concentrations were then measured in blood plasma of AML patients and healthy donors. It was found that both, cortisol and galectin-9, were significantly higher in blood plasma of AML patients compared to healthy donors one [Figure 45].

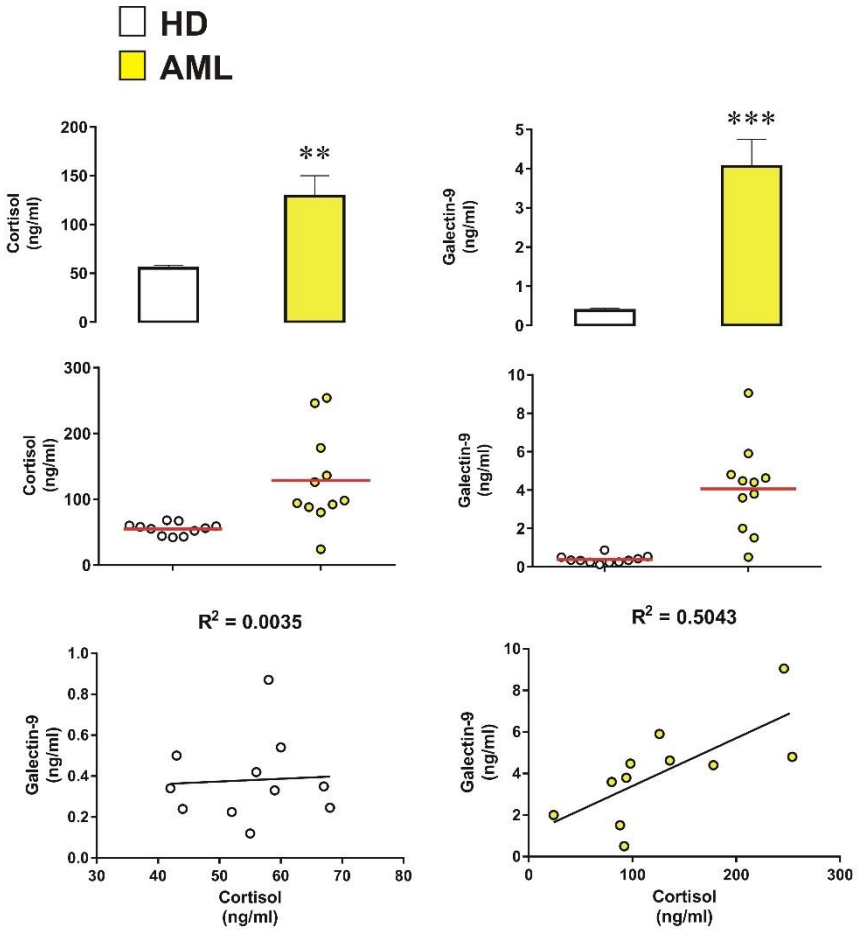


Figure 45: The levels of cortisol and galectin-9 are significantly higher in blood plasma of AML patients compared to healthy donors one. Blood plasma of ten healthy donors and ten AML patients was collected at the same time of the day to avoid the influence of circadian dynamics ensuring comparability of cortisol levels. The levels of cortisol (left panel) and galectin-9 (right panel) were measured by ELISA, and the correlation between these two proteins was analysed. Data are the mean values ± SEM of ten independent experiments.; *p < 0.05; **p < 0.01; ***p < 0.01 vs control.

In addition, no correlation between cortisol and galectin-9 levels was observed in the blood plasma of healthy donors. Contrarily, a clear correlation between the levels of these two proteins was found in the blood plasma of AML patients suggesting that galectin-9 secretion might be linked to LPHN1 expression in this circumstance.

5.3 Soluble LPHN1 fragments are detectable in AML blood plasma

Since LPHN1 is expressed on the membrane of blood cells, it can possibly undergo proteolytical shedding and be released in the bloodstream. To investigate this, blood plasma of AML patients was subjected to immunoprecipitation followed by Western blot analysis using several LPHN1 antibodies. A clear band at ~67-68 kDa was detectable by anti-LPHN1 antibody [Figure 46 A]. Also, the bands having lower molecular weight were observed after the incubation with these antibodies. Thus, once expressed on AML cell membrane, LPHN1 (~120 kDa) can be subjected to proteolytical shedding, which leads to the release of LPHN1 fragments (of ~67-68 kDa and of lower molecular weight) in the bloodstream. None of these bands was, instead, detectable by Western blot analysis in the immunoprecipitated extracts obtained from the blood plasma of healthy donors [Figure 46 A].

The presence of soluble LPHN1 fragments in the blood of AML patients, but not in the one of healthy donors, was also confirmed by ELISA (as described in Materials and Methods) [Figure 46 B].

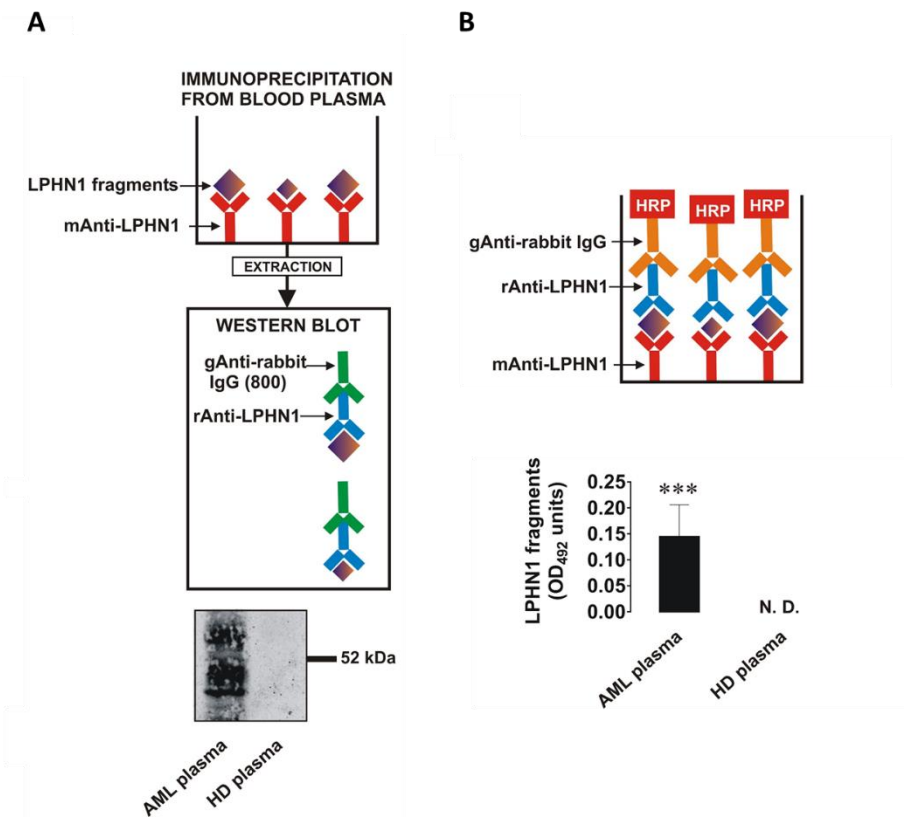


Figure 46: Soluble LPHN1 fragments are elevated in blood plasma of AML patients. Blood plasma of ten healthy donors and ten AML patients was subjected to immunoprecipitation employing Santa Cruz mouse monoclonal antibody as capture antibody. Obtained extracts were then subjected to Western blot analysis using rabbit anti-LPHN1 antibody (PAL-1 or Abcam anti-LPHN1 antibody) for detection (A). Specific detection of soluble LPHN1 fragments (in the same blood samples) was performed using ELISA as outlined in Material and Methods (B). Images are from one experiment representative of six which gave similar results. Data are the mean values ± SEM of ten independent experiments; *$p < 0.05$; **$p < 0.01$; ***$p < 0.01$ vs control.

5.4 FLRT3 upregulates galectin-9 secretion in AML cells in a LPHN1-dependent manner

As reported in Figure 32, FLRT3 induces galectin-9 secretion in THP-1 AML cells. To investigate whether this effect is LPHN1-associated or not, specific anti-LPHN1 neutralising antibody (clone name RL1) was employed.

The specificity of this antibody was determined using THP-1 cells (expressing high amounts of LPHN1 on their surfaces) and NB2A cells, which don't express LPHN1, as a negative control. The interaction of the antibody with THP-1 cell surface receptors, but with NB2A

ones, was characterised by Li-Cor on-cell assay (as described in Materials and Methods) [Figure 47].

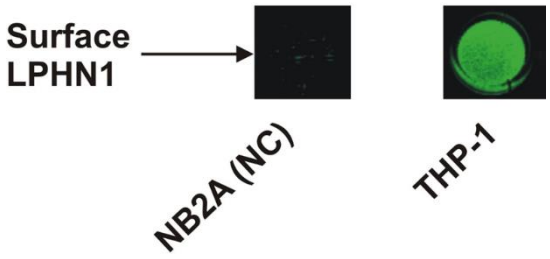


Figure 47: On cell detection of cell surface presence of rabbit polyclonal antibody recognising LPHN1 (clone name RL1). *LPHN1 negative NB2A cells (negative control) and THP-1 cells were subjected to on cell assay using anti-rabbit Li-Cor secondary antibody. Images are from one experiment representative of three which gave similar results.*

To confirm neutralising properties of RL1, THP-1 cells were incubated in presence and absence of 1 µg/ml RL1 antibody for 16 h. After the incubation, the levels of secreted galectin-9 were measured by ELISA. It was found that galectin-9 secretion levels weren't affected by RL-1 antibody (data not shown), suggesting that this antibody doesn't exert an LPHN1 agonistic effect.

After assessing the specificity and neutralising properties of RL1 antibody, the involvement of LPHN1 in galectin-9 secretion by THP-1 AML cells was explored. THP-1 cells were incubated for 16 h with or without 10 nM FLRT3. This treatment was performed with or without 1 h pre-exposure to 1 µg/ml RL1 antibody. After the incubation the levels of galectin-9 released in the culture media were measured by ELISA. It was found that RL1 antibody attenuated FLRT3-induced galectin-9 release in THP-1 cells [Figure 48 A], confirming the involvement of LPHN1 in this process. In addition, this assumption was further reinforced by the fact that FLRT3 treatment didn't upregulate galectin-9 release in primary healthy leukocytes (cells not expressing LPHN1, as shown in Figure 43) [Figure 48 A].

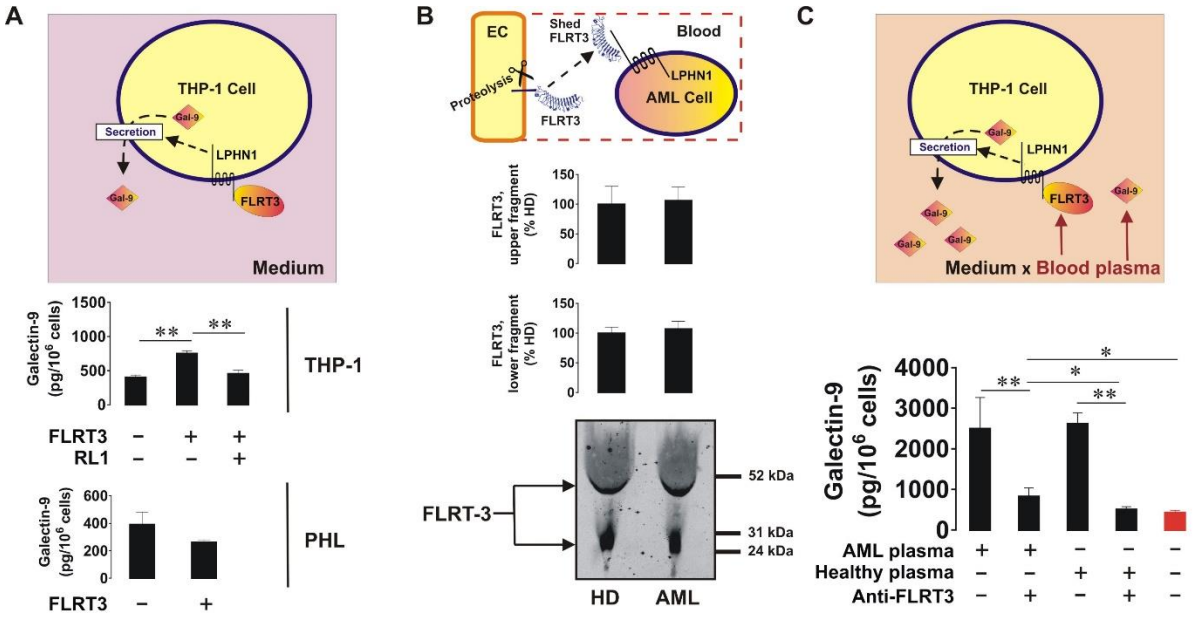


Figure 48: FLRT3, component normally circulating in blood plasma, induces galectin-9 secretion in AML cells in a LPHN1-dependent manner. THP-1 cells and PHL were exposed to 10 nM human recombinant FLRT3 for 16 h followed by detection of secreted galectin-9 levels by ELISA. In THP-1 cells, the treatment was performed with or without 1 h pre-exposure to 1 µg/ml RL1 anti-LPHN1 polyclonal antibody (A). The levels of secreted FLRT3 and its fragments were analysed in the blood plasma of healthy donors and AML patients using Western blot (B). THP-1 cells were exposed for 16 h to 10% blood plasma either from healthy donors or AML patients with or without pre-treatment with FLRT3 neutralising antibody. Levels of secreted galectin-9 were analysed using ELISA (C). Data are shown as mean values ± SEM from four independent experiments; *$p < 0.05$; **$p < 0.01$ vs. control.

Blood plasma obtained from both, AML patients and healthy donors, was then subjected to Western blot analysis for specific detection of FLRT3. The bands at ~55 kDa and ~27-28 kDa were specifically detected by anti-FLRT3 antibody in both groups [Figure 48 B]. These bands correspond to soluble fragments of FLRT3, which are likely to be shed from the cell surface by proteolytic enzymes. Interestingly, the blood plasma from both, AML patients and healthy donors, contained approximately equal amounts of both FLRT3 fragments [Figure 48 B].

To investigate whether these blood-associated FLRT3 fragments are able to stimulate galectin-9 secretion by AML cells in a LPHN1-dependent manner, THP-1 cells were cultured in RPMI 1640 media containing antibiotics (as outlined in Materials and Methods) and 10 % blood plasma from either AML patients or healthy donors (instead of 10% FBS). THP-1 cells were incubated for 16 h with or without a 30 min pre-exposure to anti-FLRT3 neutralising antibody.

The concentration of galectin-9 released in culture media was then measured by ELISA. It was found that the levels of galectin-9 secreted by THP-1 cells were significantly higher when the cells were cultured with 10 % blood plasma than in presence of 10 % FBS (negative control). In addition, anti-FLRT3 neutralising antibody attenuated galectin-9 secretion [Figure 48 C].

FLRT3-LPHN1 interaction was also characterised using SRCD spectroscopy. CD spectrum obtained after mixing FLRT3 with LPHN1 was significantly different from the simulated spectrum suggesting that considerable conformational changes occur in these proteins upon the binding [Figure 49].

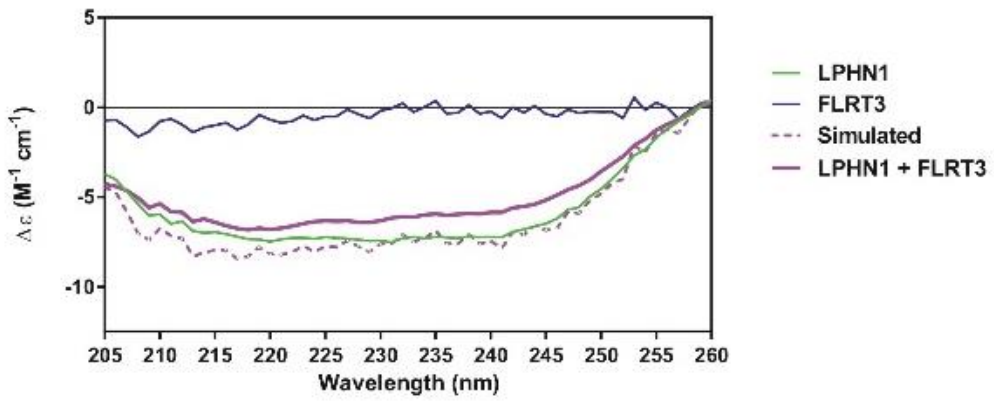


Figure 49: Interaction of FLRT3 with LPHN1 leads to significant conformational changes. SRCD spectroscopy of FLRT3, LPHN1 FLRT3-LPHN1 interaction (both simulated and real curves are presented).

5.5 Discussion

Taken together, our results demonstrate that cortisol upregulates LPHN1 expression in AML cells. Cortisol is a glucocorticoid hormone produced by the adrenal gland in response to numerous stimuli such as stress and energetic deficiency (Torpy & Chrousos, 1996).

In AML, rapid progression of this malignancy leads to decreased glucose levels (Gonçalves Silva, Rüegg, Gibbs, Bardelli, Fruewirth, et al., 2016) and thus the HPA axis is continuously stimulated to release high amounts of cortisol in the bloodstream. This is in line with the fact that significantly higher cortisol levels were found in the blood of AML patients compared to

healthy donors one [Figure 45]. After being released, cortisol is employed by AML cells to upregulate their surface expression of LPHN1, which can then interact with FLRT3, an endogenous ligand of LPHN1 widely available in blood plasma, leading to the upregulation of galectin-9 release. The latter protects AML cells from cytotoxic immune cells (as outlined in Chapter 4) [Figure 50]. Thus, AML cells use crucial components of functional systems within the body to support their survival and attenuate anti-cancer activities of cytotoxic lymphoid cells.

Interestingly, hematopoietic stem cells contain detectable amounts of LPHN1 mRNA and its transcription is also upregulated by cortisol [Figure 44]. Protein expression of LPHN1 was also detected in HSCs [Figure 42]. However, HSCs-associated LPHN1 has a higher MW (~140 kDa) than AML-associated one (~120 kDa). Moreover, contrarily to AML cells, HSCs don't express detectable amounts of galectin-9 and Tim-3 [Figure 42]. Thus, in HSCs, LPHN1 should be involved in different biochemical mechanisms.

PHLs, instead, are able to synthesise and release detectable amounts of galectin-9, but this process occurs in a LPHN1-independent manner. Indeed, neither mRNA nor protein expression of LPHN1 were detectable in PHLs. In addition, cortisol didn't induce LPHN1 transcription/translation, possibly because of gene repression.

Importantly, LPHN1 fragments were clearly detectable by both, Western blot and ELISA, in the blood plasma of AML patients but not in healthy donors. This difference in the composition of blood plasma can be exploited in the future for a faster AML diagnosis, although differential verification tests have yet to be performed.

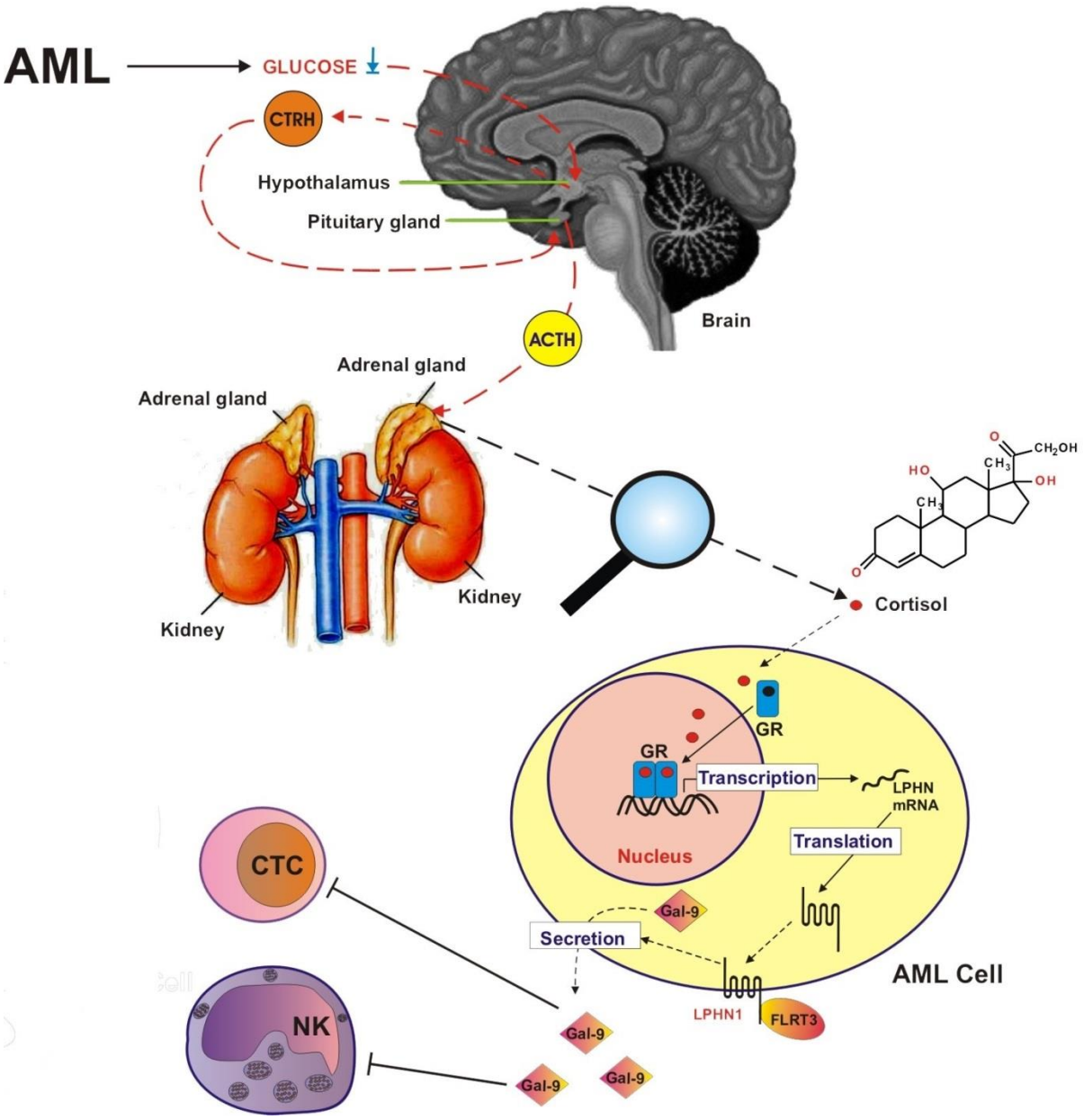


Figure 50: Physiological cross-links leading to cortisol-induced upregulation of LPHN1 expression in AML cells followed by facilitation of galectin-9 secretion in a FLRT3-dependent manner. AML is associated with a decreased blood plasma glucose levels, which normally leads to upregulation of secretion of corticotropin-releasing hormone (CTRH) by hypothalamus. CTRH induces secretion of adrenocorticotropic hormone (ACTH) by pituitary gland. Secreted ACTH upregulates cortisol production by the adrenal cortex, thus leading to cortisol-induced upregulation of LPHN1 levels in AML cells. Galectin-9, secreted in FLRT3-LPHN1-dependent manner attenuates anti-cancer activity of cytotoxic T cells (CTC) and NK cells.

6. AML cells employ stress and danger signals to support overall malignant cell survival and proliferation

Recently, it was found that the blood of AML patients contains significantly higher HMGB1 concentration when compared to healthy donors. Moreover, AML cells were shown to express high levels of HMGB1, possibly because of the conditions associated with AML progression, which support its secretion (such as hypoxia and death of the cells in the tumour microenvironment) (Tang et al., 2017; Yu et al., 2012; Zhang, et al., 2017).

As previously described (in the introduction), released HMGB1 can interact with several surface receptors, including TLR2, TLR4, RAGE and Tim-3 (highly expressed in AML cells). However, the role of HMGB1 in AML progression remains unclear.

6.1 The effects induced in human AML cells by HMGB1 stimulation

It has been reported that triggering of TLR2, TLR4, RAGE and Tim-3 induces the activation of several pathways including PI-3K/mTOR pathway in AML cells. Moreover, activation of this pathway has been shown (1) to upregulate production and secretion of a variety of cytokines including TNF-α and (2) to induce HIF-1α accumulation, which leads to increased glycolysis and angiogenesis (Nicholas, et al., 2011; Prokhorov et al., 2015; Silva, et al., 2015; Sumbayev & Nicholas, 2010; Yasinska, et al., 2014). However, the involvement of HMGB1 on signalling events above described remains hypothetic and it hasn't been investigated yet in AML cells.

To explore this, THP-1 cells, expressing Tim-3 mostly at intracellular level rather than on the membrane [Figure 51, left panel], and primary human AML cells (AML-PB001F), expressing Tim-3 mostly on the cell surface [Figure 51, right panel], were employed.

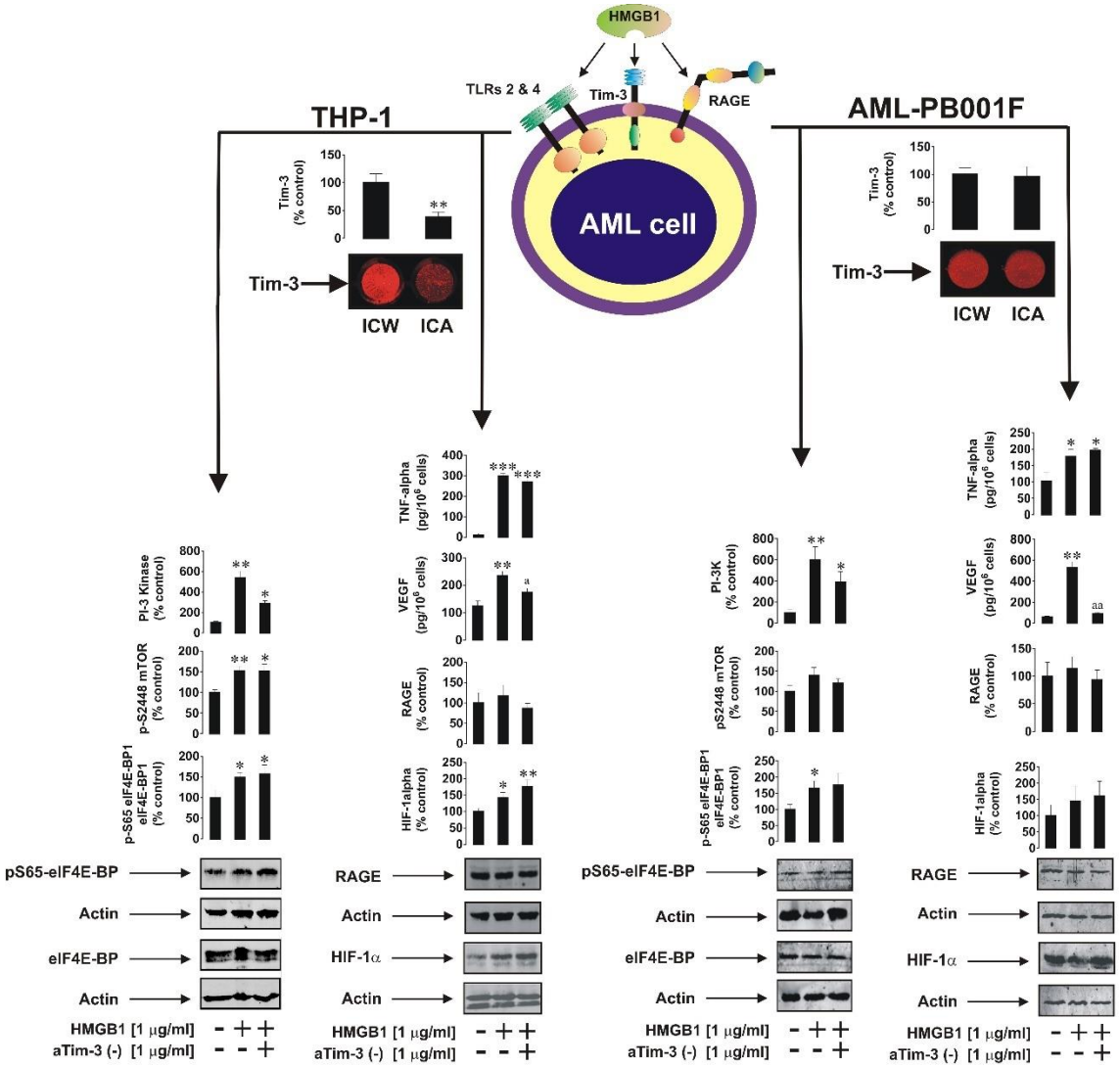


Figure 51**: **Differential receptors are involved in HMGB1-induced biological responses of human AML cells. Total levels of the immune receptor Tim-3 and its surface presence were characterised in THP-1 and primary human AML-PB001F cells by in-cell Western (ICW) and in-cell (on-cell) assay (ICA) respectively**.** Both cell types were exposed to 1 µg/ml HMGB1 for 4 h with or without 1 h pre-treatment with single chain anti-Tim-3 antibody (aTim-3 (-)) followed by Western blot analysis of phospho-S65 vs total eIF4E-BP1, HIF-1α and RAGE expression as well as by detection of phospho-S2448 mTOR, release of TNF-α and VEGF using ELISA. PI-3 K activity was monitored by colorimetric assay. Images are from one experiment representative of five which gave similar results. Data is shown as mean values ± SEM of five independent experiments. * $p < 0.05$; **, $p < 0.01$ and *** when $p < 0.001$ vs control; ^{a} $p< 0.05$; ^{aa}, $p < 0.01$ vs HMGB1.

To investigate specifically Tim-3-associated effects, the cells were exposed for 4 h to 1 µg/ml HMGB1 with or without 1 h pre-treatment with single-chain anti-Tim-3 neutralising antibody. Increased activation of PI-3K was found in both, THP-1 and primary human AML cells, upon HMGB1 stimulation and this effect was non-significantly downregulated by anti-Tim-3 neutralising antibody [Figure 51]. Moderate activation of mTOR (phosphorylation at S2448)

and increased phosphorylation of mTOR substrate eukaryotic initiation factor 4 E binding protein 1 (eIF4E-BP1) were observed in both cell types following the incubation with HMGB1. Pre-treatment with anti-Tim-3 neutralising antibody didn't provoke any changes in these processes.

A moderate increase in mTOR phosphorylation in Ser2448 residue (active form) was also observed in both cell types after the treatment with HMGB1. In line with this finding, augmented phosphorylation of eIF4E-BP (one of mTOR substrates) was found in AML cells after the incubation with HMGB1. Moreover, significant increase in TNF-α secretion by both cell types was induced by HMGB1. The pre-treatment with anti-Tim-3 neutralising antibody didn't affect any of these HMGB1-induced processes, suggesting that these effects are Tim-3-independent [Figure 51].

In addition, HMGB1 induced the upregulation of Hif-1α accumulation in THP-1 cells but not in primary human AML cells [Figure 51]. This difference in Hif-1α accumulation can be explained by the fact that primary human AML cells possess high background levels of this transcription factor subunit and thus are incapable to respond to HMGB1. Despite this, a significant upregulation in VEGF secretion was observed in both cell types after HMGB1 treatment. Interestingly, anti-Tim-3 neutralising antibody significantly attenuated HMGB1-induced VEGF secretion, but did not reduce Hif-1α accumulation in AML cells. The level of downregulation in VEGF secretion was proportional to the amount of Tim-3 present on the surface of each cell type [Figure 51]. Intracellular levels of VEGF weren't affected by anti-Tim-3 neutralising antibody as confirmed by ELISA performed on the cell lysates (data not shown). These results suggest that HMGB1 induces VEGF release in AML cells by triggering Tim-3 receptor expressed on their surface.

Highly sensitive spectroscopic analysis of HMGB1-Tim-3 interactions confirmed that these two proteins interact with each other specifically. The SRCD spectrum of Tim-3/HMGB1 mixture (at ratio 1 : 1) was significantly different from the simulated spectrum (obtained by summing SRCD spectra of the individual components), suggesting that complex formation causes considerable conformational change of the proteins with a clear increase in α-helical content [Figure 52 B]. SRCD spectroscopy was also employed to determine its binding affinity. 200 nM HMGB1 was titrated with increasing amounts of Tim-3 and the changes in CD signal were monitored at 222 nm. The values of obtained CD signals were plotted against increasing Tim-3 concentrations and it was found that HMGB1 binds Tim-3 with high affinity (Kd is coming at nanomolar level 10^{-7} M) [Figure 52 A].

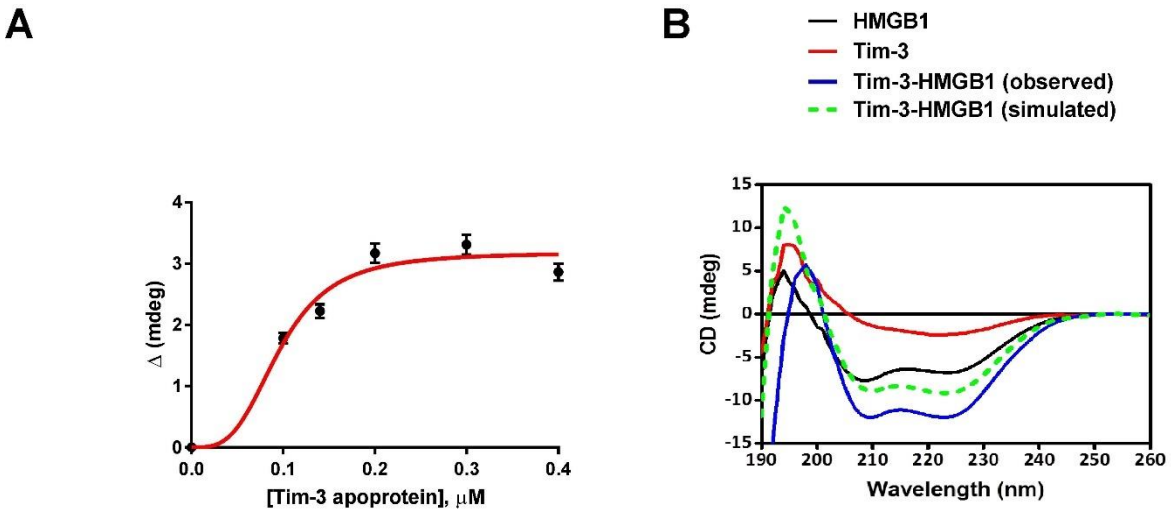


Figure 52: HMGB1 binds Tim-3 with a high binding affinity. Recombinant, purified Ig-like V-type domain of human Tim-3 (residues 22–124) and human HMGB1 were employed for these experiments**.** Interaction of HMGB1 protein with Tim-3 was analysed using SRCD spectroscopy-based titration which was conducted in the far UV region using 0.2 μM HMGB1 and increasing stoichiometric concentrations of Tim-3 (A). Changes in CD signal monitored at 222 nm were plotted against Tim 3 concentration using Hill function. Qualitative binding was verified by analysis of interactions of equimolar concentrations of Tim-3 and HMGB1 using SRCD spectroscopy (B).

As shown above, HMGB1-induced TNF-α secretion by AML cells doesn't occur via Tim-3 receptor [Figure 51]. Thus, other AML receptors binding HMGB1 were explored as possible inducers of TNF-α secretion. As previously described, AML cells express TLR2 and TLR4.

RAGE expression in AML cells was confirmed by Western blot analysis. Thus, THP-1 cells were exposed for 4 h to 1 µg/ml HMGB1 with or without 1 h pre-treatment with 2 µg/ml neutralising antibodies directed against TLR2, TLR4 and RAGE. It was found that TLR2 and TLR4, but not RAGE, are involved in HMGB1-induced TNF-α secretion [Figure 53]. However, it does not rule out the fact that during long-term exposure RAGE might contribute to HMGB1-induced intracellular TNF-α expression which can be upregulated by RAGE ligands (Rashid, et al., 2004).

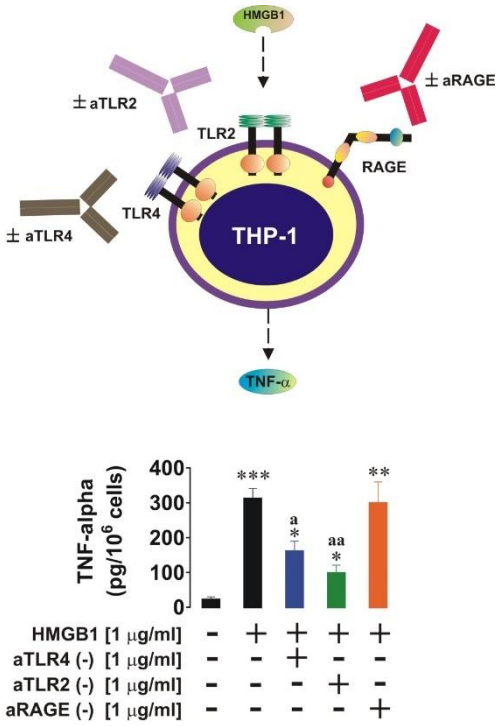


Figure 53: TLRs 2 and 4, but not RAGE, are involved in HMGB1-induced TNF-α secretion. THP-1 cells were pre-treated for 1 h with the indicated concentrations of TLR2/4 and RAGE-neutralising antibodies followed by 4 h exposure to 1 µ/ml HMGB1. TNF-α concentrations were then measured in the culture medium by ELISA. Data are shown as mean values ± SEM for three independent experiments. * $p<0.05$; **, $p<0.01$ vs control; a $p<0.05$; aa, $p<0.01$ vs HMGB1.

6.2 HMGB1 stimulates TNF-α secretion by human AML leading to upregulation of SCF production

The effects of HMGB1-induced TNF-α were studied in primary healthy human leukocytes (PHLs). Cell culture medium containing TNF-α (obtained after the stimulation of THP-1 cells

with 1 µg/ml HMGB1) was employed to treat PHLs for 4 h with or without 1 h pre-treatment with 2 µg/ml TNF-α-neutralising antibody. After the incubation, IL-1β concentration was measured in the media by ELISA. It was found that in the absence of TNF-α-neutralising antibody, PHL released IL-1β, while in the presence of TNF-α-neutralising antibody PHL did not release detectable amounts of IL-1β [Figure 54 A].

Recently, it was reported that MCF-7 breast cancer epithelial cells express IL-1 receptor type 1 and its triggering induces these cells to release stem cell factor (SCF) (Wyszynski, et al., 2016). Therefore, MCF-7 cells were cultured for 24 h in the media containing IL-1β (obtained after culturing PHL in presence of TNF-α) with or without 2 µg/ml of IL-1β-neutralising antibody. After the incubation, collected media was subjected to ELISA for SCF detection. It was found that, in the presence of IL-1β-neutralising antibody, MCF-7 did not release detectable amounts of SCF, while in the absence of it SCF release was clearly detectable [Figure 54 A].

Taken together, these results suggest HMGB1 induces the release of TNF-α by AML cells. TNF-α stimulates IL-1β secretion by PHL. Released IL-1β binds IL-1 receptor expressed by endothelial/epithelial cells and induces the release of SCF is required for proliferation of AML cells and thus supports leukaemia progression.

To confirm that this effect was physiologically relevant, mouse bone marrow cells (*ex vivo*) were culture for 24 h in presence or absence of 1 µg/ml HMGB1. It was found that HMGB1 significantly upregulated the release of TNF-α, IL-1β and SCF in mouse bone marrow cells [Figure 54 B].

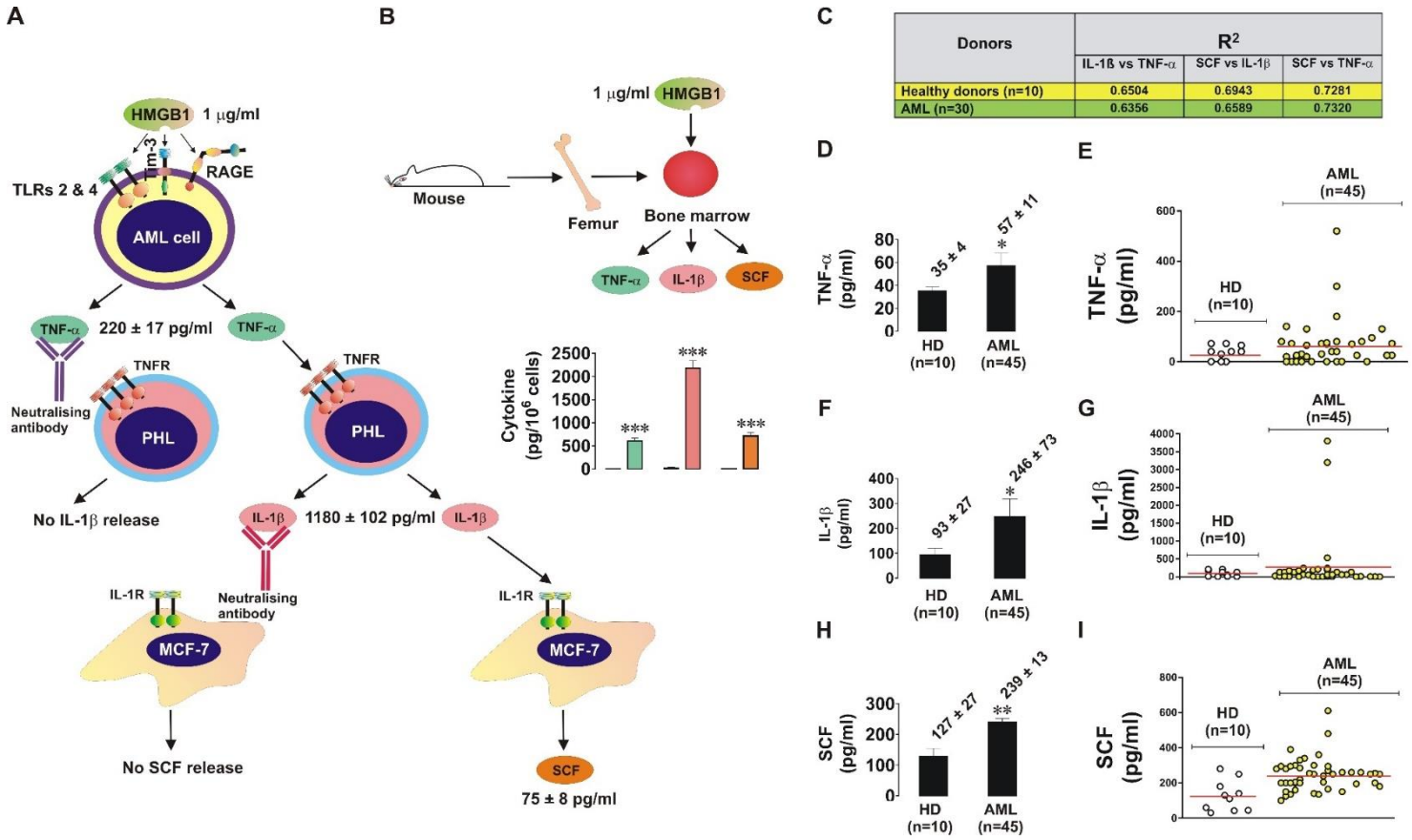


***Figure 54*:*HMGB1 triggers an intercellular signalling cascade leading to SCF secretion*.** (A) Primary human AML cells (AML-PB-001F) were incubated for 4 h with 1 μg/ml HMGB1 followed by collection of the culture medium (detection of TNF-α was performed in this medium using ELISA), which was used to culture primary human healthy leukocytes for 4 h in the absence or presence of TNF-α-neutralising antibody. Medium was collected (levels of IL-1β were measured by ELISA) and used to culture MCF-7 breast cancer epithelial cells for 4 h in the absence or presence of IL-1β-neutralising antibody. Following this exposure, medium was collected and SCF was measured in it by ELISA. (B) Primary mouse bone marrow cells (10^6 cells per 3 ml medium) were exposed for 24 h to 1 μg/ml HMGB1 followed by detection of TNF-α, IL-1β and SCF by ELISA. (C – I). Levels of TNF-α, IL-1β and SCF were measured in the blood plasma of healthy donors and AML patients by ELISA. Mean values ± SEM are presented as well as levels of each protein in blood plasma of each analysed donor/patient. *$p < 0.05$; **$p < 0.01$ vs control.

The concentrations of TNF-α, IL-1β and SCF were then also measured in blood plasma of 10 healthy human donors and 45 AML patients. It was found the levels of all three factors were significantly higher in the blood plasma of AML patients compared to healthy donors [Figure 54 C – I]. In addition, a clear evidence of correlation between IL-1β *vs* TNF-α, SCF vs IL-1β and SCF vs TNF-α was observed in the blood plasma of both healthy donors and AML patients which contained detectable amounts of all the studied cytokines/SCF [Figure 54 C and 55].

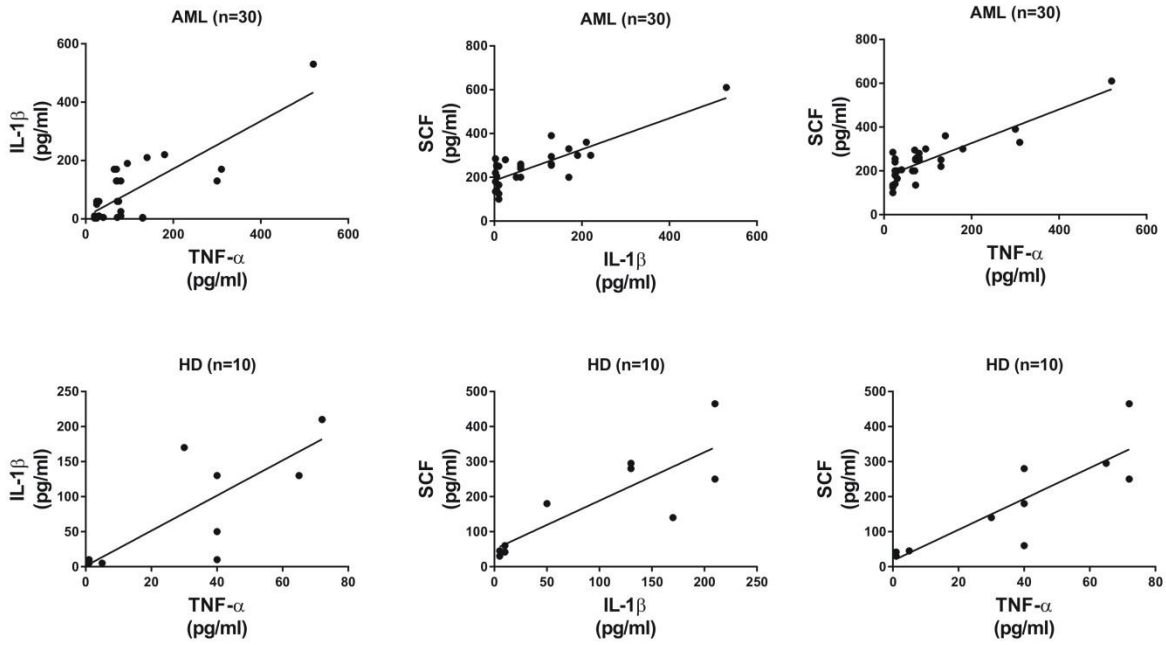


Figure 55: Correlation between TNF-α, IL-1β and SCF levels in the blood plasma of healthy donors and AML patients. Data were obtained from the blood plasma of healthy donors (n=10) and AML patients (n=30). Correlation analysis was performed using GraphPad Prism (R2 values are presented in Figure 54 C).

6.3 Discussion

Our results show that HMGB1 stimulates the activity of the PI-3 K/mTOR pathway in both, a human AML cell line (THP-1 cells) and primary AML cells (AML-PB001F). This HMGB1-induced activation leads to increased TNF-α secretion and accumulation of HIF-1α as well as VEGF release. However, except VEGF secretion, these effects are Tim-3-independent. Also, upregulation of VEGF secretion *via* Tim-3 receptor is HIF-1α-independent. Indeed, HMGB1-

induced HIF-1α accumulation wasn't attenuated by anti-Tim-3 neutralising antibody in AML cells.

SRCD spectroscopic analysis showed that HMGB1 binds Tim-3 with nanomolar affinity (K_d = 10^{-7} M). However, this affinity can be potentially increased by glycosides which normally bind to Tim-3 (the protein used in the studies was sugar-free). Interestingly, the formation of the HMGB1-Tim-3 complex was accompanied by an increase in α-helical content and consequent reduction in β-strand component. This considerable loss in β-strand structures is likely to occur in the Tim-3 protein.

Our results showed also that TNF-α released from HMGB1-stimulated AML cells induce PHL to secrete IL-1β, which in turn stimulated epithelial/endothelial cells to produce/secrete SCF, factor able to bind Kit receptor and induce the survival/proliferation of AML cells [Figure 56].

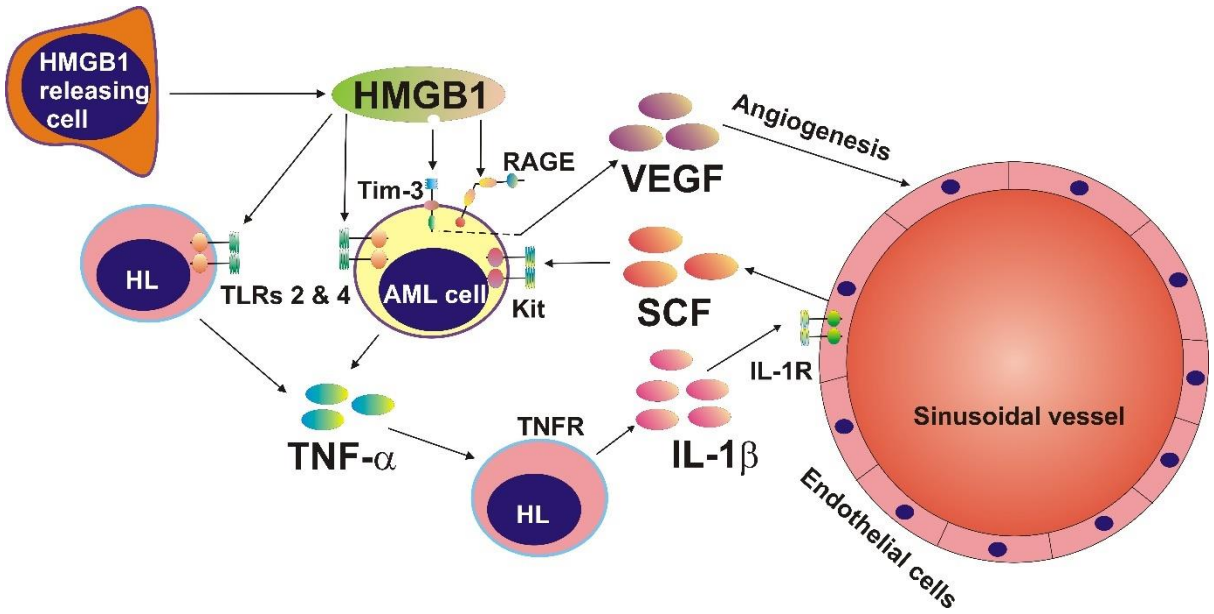


Figure 56: HMGB1 induces SCF and VEGF production via interaction with differential signalling receptors. The scheme shows that secreted HMGB1 is capable of inducing TNF-α secretion by living AML cells (and possibly healthy leukocytes, based on results obtained in the experiments with mouse bone marrow samples). Secreted TNF-α induces IL-1β production by healthy leukocytes which then induces SCF release in endothelial cells. These processes are Tim-3-independent. HMGB1 also induces VEGF secretion by AML cells in Tim-3-dependent manner.

In addition, a clear evidence of correlation between TNF-α, IL-1β and SCF levels was observed in the blood plasma of AML patients and healthy donors, but the concentrations of these signalling proteins were significantly higher in the blood plasma of AML patients than in healthy donors. This in line with the fact that HMGB1 concentration in the blood plasma of AML patients is significantly higher than in healthy donors (Fucikova et al., 2016). However, since the levels of circulating HMGB1 in healthy donors are usually close to zero or anyway very low (Fucikova et al., 2016; Vicentino et al., 2018), other mechanisms (HMGB-1-independent) could be involved in this intercellular signalling cascade. In addition, healthy bone marrow is unlikely to contain HMGB1, an "alarmin" secreted by stressed/dying or injured cells. Indeed, trypan blue exclusion assay showed that 95% of the cells in mouse bone marrow (sample used for our experiments) were viable (data not shown). Contrarily, in leukemic bone marrow (or in AML blood) stressing conditions, such as lack of oxygen, contribute to continuous release of HMGB1, that is able to activate this intercellular cascade (illustrated in Figure 56), which leads to increased levels of SCF, and thus supports leukaemia progression.

HMGB1 has already been proposed as a possible therapeutic target for leukaemia treatment (Yu et al., 2012). In addition, inhibition of HMGB1 has recently been shown to increase drug sensitivity in AML (Lu et al., 2014). Our findings demonstrate additional insights that HMGB1 could be considered as a possible therapeutic target in AML and further confirm the efficiency of targeting Tim-3 (here to specifically block AML-induced angiogenesis) in anti-AML therapy.

7. Activity of Tim-3-galectin-9 pathway in solid tumours

7.1 Biochemistry and functions of Tim-3-galectin-9 secretory pathway in human breast cancer cells

Recently, breast cancer tissues were shown to be capable of expressing some of the key components of above described immunosuppressive pathway. In particular, LPHN2, one of LPHN isoforms, was found to be upregulated in breast tissues (White, et al., 1998). In addition, it was found that breast cancer cells express galectin-9, which was shown to be involved in cell aggregation, thus preventing metastasis (Yamauchi et al., 2006).

Therefore, we decided to investigate whether the Tim-3-galectin-9 immunosuppressive pathway was specific solely to AML or was operating also in breast cancer, and possibly other solid tumours.

7.1.1 Expression and activity of the FLRT3/LPHN/Tim3/galectin-9 pathway in breast tumours

Breast cancer tissues lysates were subjected to Western blot analysis for specific detection of galectin-9, Tim-3, LPHN2, LPHN3 and FLRT3. It was found that all these proteins were expressed in breast cancer tissues [Figure 57 A&B, and 61 C]. Two bands were detected by anti-FLRT3 at ~75 kDa (full protein) and ~55 kDa (highlighted by a question mark). The latter may represent FLRT3 which underwent proteolytical processing. A clear band specifically detectable by anti-galectin-9 antibody appeared at ~55 kDa [Figure 57 A], when gel electrophoresis for protein separation was performed using 12% PAGE (concentration normally used to detect proteins having molecular weight of 20-50 kDa). Since the molecular weight of galectin-9 is ~31-32 kDa, we hypothesized that the band at ~55 kDa could correspond to Tim-3-galectin-9 complex. However, since this band wasn't detectable by anti-Tim-3

antibody, it doesn't represent Tim-3-galectin-9 complex, but probably a galectin-9 isoform bound to carbohydrates. Indeed, when the same sample was subjected to Western blot analysis using 10% PAGE, a specific band detectable by anti-galectin-9 antibody appeared slightly above 31 kDa [Figure 58]. This suggests that, in a 12 % gel, protein running was "delayed" possibly due to the presence of traces of glycosides or other post-translational modifications affecting the protein properties/shape but not the molecular weight.

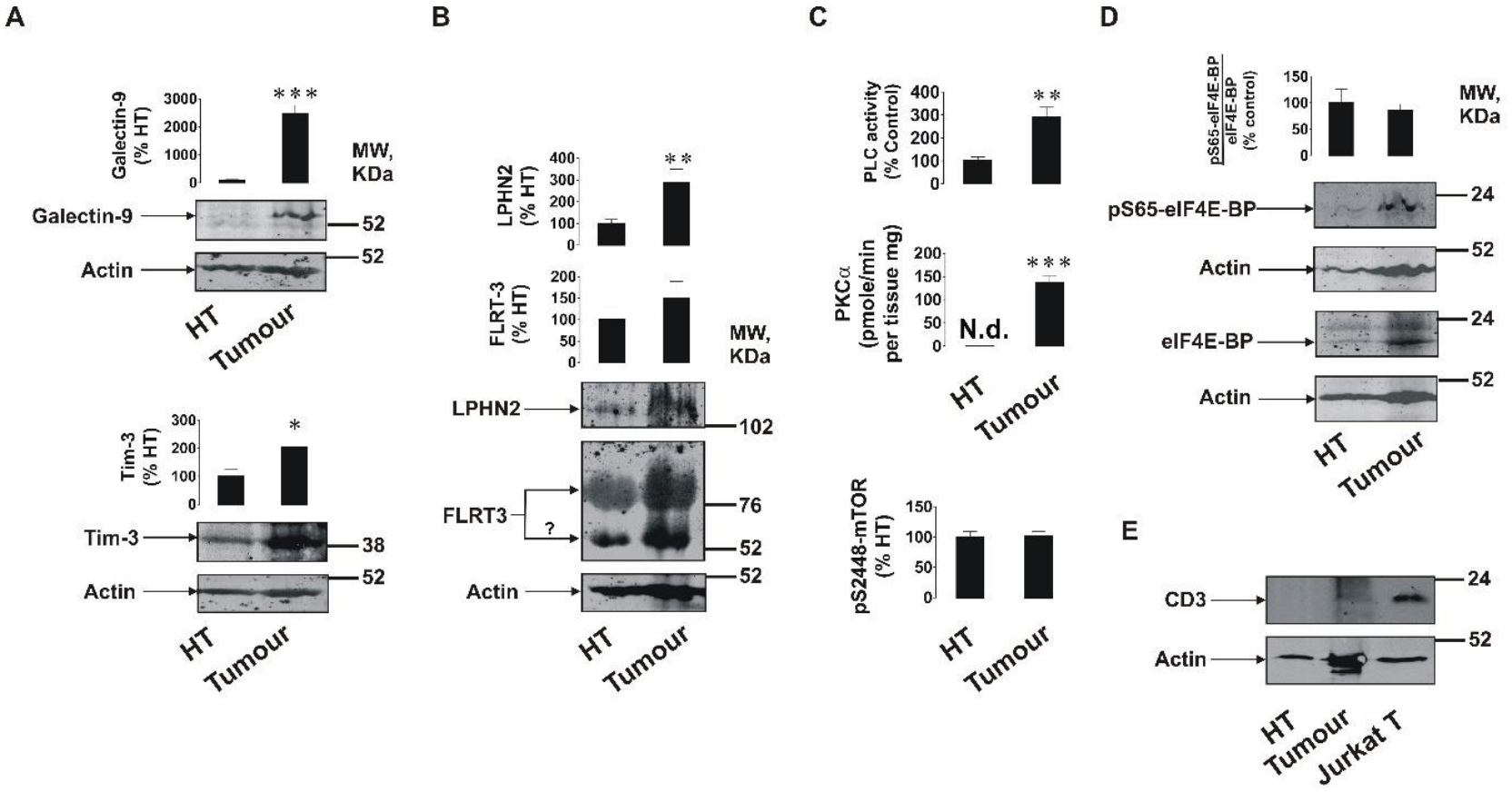


Figure 57: Expression of FLRT3/LPHN/Tim-3/galectin-9 pathway components and activities of PLC/PKCα and mTOR pathways in primary human breast tumours. Expression levels of Tim-3, galectin-9 (A), FLRT3 and LPHN2 (B) were analysed in primary breast malignant tumours and healthy breast tissues (HT) of five patients (n=5) by Western blot. Activities of PLC, PKCα and the levels of phospho-S2448 mTOR were detected as outlined in the Materials and Methods (C). The amounts of phospho-S65 and total eIF4E-BP (mTOR substrate) were analysed using Western blot (D). The levels of CD3 (biomarker of T cells) were also measured using lysate of Jurkat T cells as a positive control (E). Molecular weight markers (MW) are expressed in kDa. Images are from one experiment representative of five which gave similar results. Other results are shown as mean values ± SEM. * $p<0.05$; **, $p<0.01$ and *** when $p<0.001$ vs control.

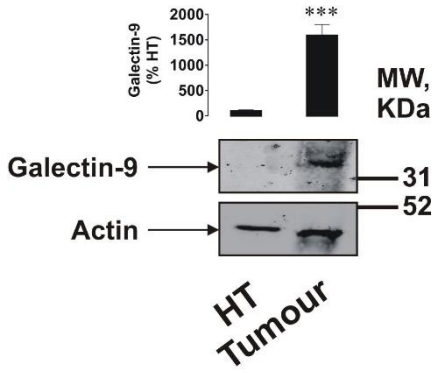


Figure 58: Expression of galectin-9 in primary human breast tumours and healthy breast tissues. Lysates of primary breast malignant tumours and healthy breast tissues (HT) of five patients (n=5) were subjected to Western blot using 10 % PAGE. Specific detection of galectin-9 was performed employing Abcam rabbit anti-galectin-9 antibody. Images are from one experiment representative of five which gave similar results. Other results are shown as mean values ± SEM. *** $p<0.001$ vs HT.

The levels of Tim-3, galectin-9, LPHN2 and FLRT3 found in primary breast malignant tumours were then compared to heathy tissues isolated from the same patients. Western blot analysis showed that the amounts of these components, except FLRT3, were significantly higher in malignant tissues compared to healthy ones [Figure 57 A, B and Figure 58].

The activities of PLC, PKC-α and mTOR were also measured in tumour and healthy breast homogenates. It was found that the activities of PLC and PKC-α were significantly higher in breast cancer tissues compared to healthy ones. The amounts of active mTOR form (mTOR phosphorylated at S2448) were similar in these tissue types [Figure 57 C]. The ratio between phospho-S65 eIF4E-BP and its total amount was also similar in both tissue types, although the amount of both phospho-S65 and total eIF4E-BP was higher in tumour tissues [Figure 57 D].

To confirm that all the protein characterised above are expressed by breast tumour cells and not by tumour-infiltrating lymphocytes, the samples were subjected to Western blot analysis for specific detection of CD3 (a marker of T cells). It was found that CD3 was undetectable in healthy and barely detectable in tumour tissue lysates, proving that the proteins characterised are associated with breast cells [Figure 58 E].

The presence of Tim-3-galectin-9 complex was also verified in both tissue types (as described in material and methods). It was found that the complex was barely detectable in healthy tissue homogenates but was clearly detectable in malignant tissue extracts [Figure 59 A]. The presence of Tim-3-galectin-9 complex was also confirmed by confocal microscopy co-localization analysis [Figure 59 B].

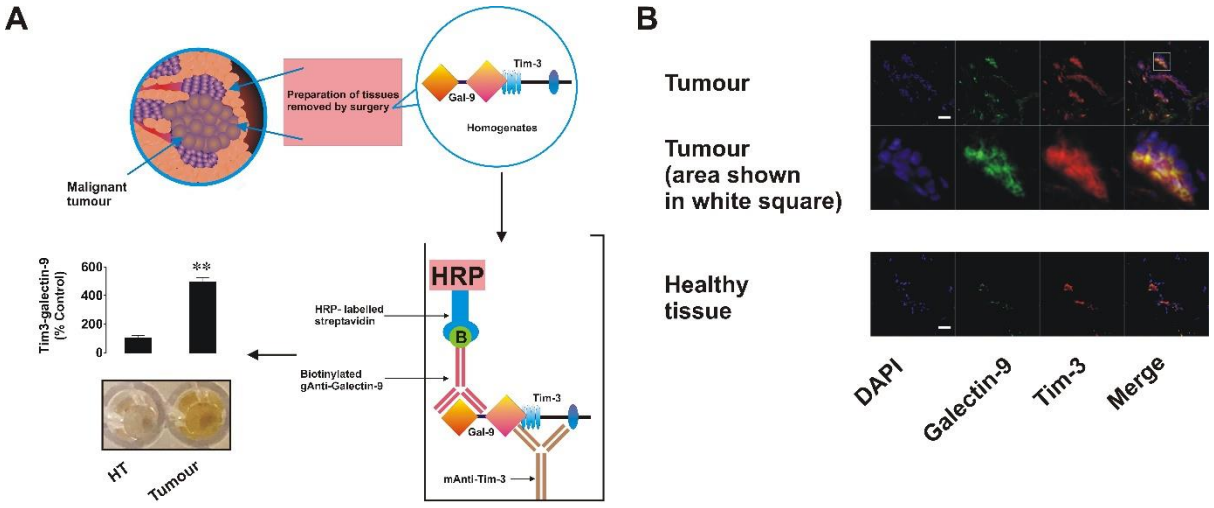


Figure 59: Expression, interaction and co-localisation of Tim-3 and galectin-9 in primary human breast tumours. (A) Presence of the Tim-3-galectin-9 complex in primary normal and tumour tissue extracts was analysed using ELISA as outlined in the Materials and Methods. (B) Expression and co-localisation of galectin-9 and Tim-3 were analysed in primary human breast tumours and healthy tissues of the same patients using confocal microscopy (see Materials and Methods for further details). Images are from one experiment representative of five which gave similar results. Scale bars correspond to 20 µm.

Next, the levels of galectin-9, Tim-3 and IL-2 were measured in blood plasma of healthy donors (HD), primary (PBC) and metastatic breast cancer (MBC) patients. It was found that the levels of Tim-3 and galectin-9 were significantly lower in both, PBC and MBC, than in HD. The concentration of IL-2 was, instead, non-significantly higher in PBC and MBC compared to HD [Figure 60].

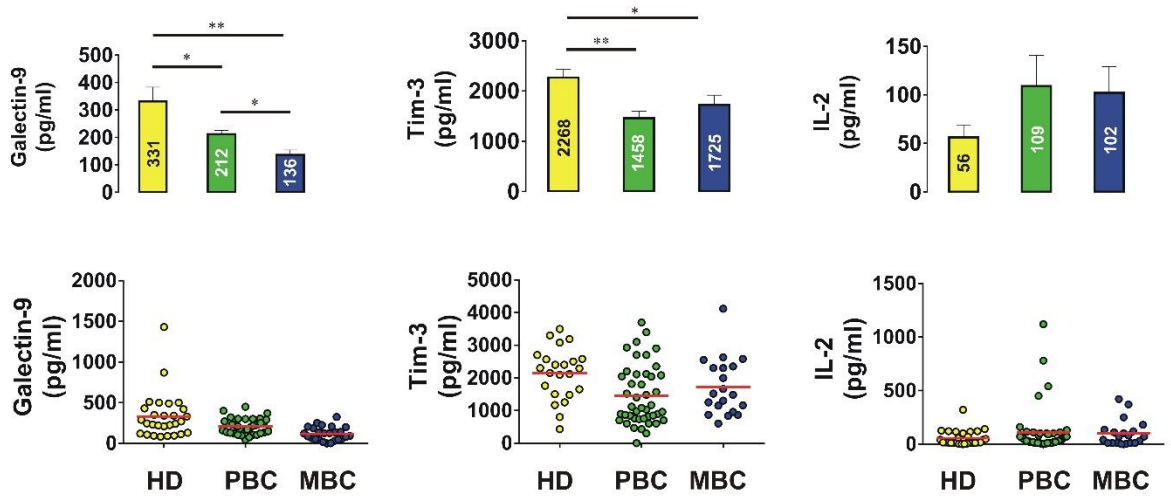


Figure 60: Levels of galectin-9, Tim-3 and IL-2 in blood plasma of human healthy donors and patients suffering from primary and metastatic breast tumours. (A) Concentrations of galectin-9, soluble Tim-3 and IL-2 were analysed in blood plasma of healthy donors and breast cancer patients by ELISA. Data are shown as mean values ± SEM of 20 for healthy donors (HD), 42 for primary breast cancer (PBC) patients and 20 for metastatic breast cancer (MBC) patients. * - $p<0.05$; **, $p<0.01$ and vs HD.

To explore whether the immunosuppressive mechanism described for AML cells can be also activated in breast tumour tissues, MCF-7 breast cancer cells were selected for the further investigations. Among the other breast cancer cell lines analysed [Table 7 and 8], MCF-7 cells were the only ones to express detectable amounts of both LPHNs 2 and 3 and the levels of these proteins were similar to their amounts found in primary breast tumours [Figure 57 B, 61 A and C]. We also confirmed that MCF-7 cells, as primary breast tumours, express detectable amounts of Tim-3, galectin-9 and the complex formed by these proteins [Figure 61 A]. Comparative analysis of galectin-9 mRNA levels between healthy and tumour breast tissues, and MCF-7 cells was performed using qRT-PCR. It was found that the levels of galectin-9 mRNA were significantly higher in both, MCF-7 cells and primary breast tumours, when compared to primary healthy breast tissues [Figure 61 B]. Importantly, the ratio of galectin-9 mRNA in tumour and normal tissues was similar to the respective levels of protein detected [Figure 57 A and 61 B]. Taken together, these results suggest that MCF-7 cells as well as primary healthy and malignant cells express identical galectin-9, thus re-confirming that the same protein was detected by Western blot [Figure 57 A, 58, 61 A and B].

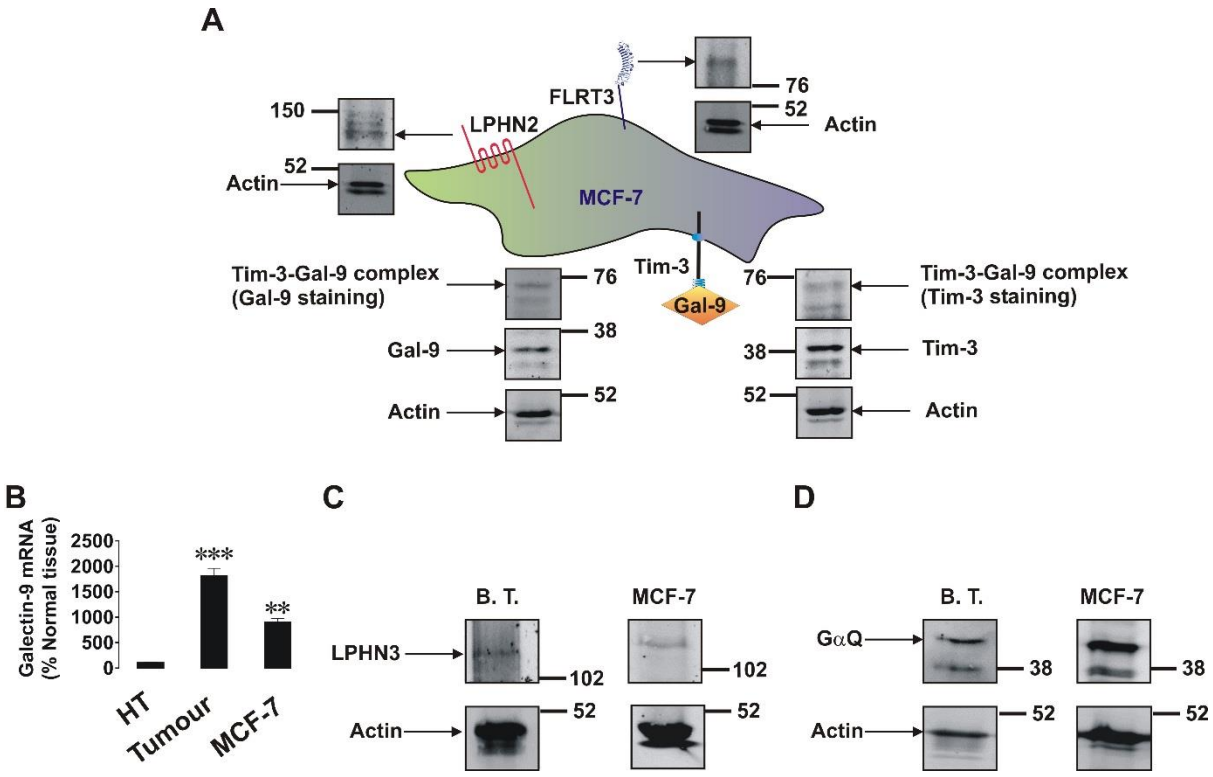


***Figure 61: Expression of crucial components of FLRT3/LPHN/Tim-3/galectin-9 pathway in MCF-7 cells and primary human breast tumours*. (A)** Expression of a key components of this pathway was characterised in MCF-7 cells and primary breast tumour tissue lysates using Western blot analysis. Beta-actin was used as a housekeeping protein. **(B)** Levels of galectin-9 mRNA were compared in normal and healthy breast tissues as well as in MCF-7 cells and normalised against those of β-actin. **(C)** Expression of LPHN3 was detected in primary human breast tumour tissue lysates and MCF-7 cells. **(D)** Expression of GαQ was detected in primary human breast tumour tissue lysates and MCF-7 cells. Images are from one experiment representative of at least three which gave similar results. Data are the mean values ± SEM of five independent experiments; **, $p<0.01$ and *** when $p<0.001$ vs control (HT).

Since LPHN is a G-coupled receptor and thus requires an adaptor protein for the transduction of the signal, cells and tissue lysates were subjected to Western blot analysis for GαQ detection. It was confirmed that both, MCF cells and primary breast tumours, express GαQ [Figure 61 B].

Once assessed that all the key components of FLRT3/LPHN/Tim-3/galectin-9 pathway are present in MCF-7 cells, the activation of this signalling system was investigated by exposing these cells to FLRT3, protein able to bind olfactomedin-like domain expressed by all three LPHN isoforms (as described in the Introduction).

MCF-7 cells were cultured in presence or absence of 10 nM human recombinant FLRT3 for 4 h. After the incubation, PLC and PKC-α activities were measured as described in Materials and Methods. Cell lysates were also subjected to Western blot analysis for the detection of phospho-S2448 mTOR and phospho-S65/total eIF4E-BP. It was found that FLRT3 significantly upregulated PLC and PKC-α activities but did not provoke any changes in the intracellular concentration of phosphor-S2440 mTOR and thus didn't affect the phosphorylation eIF4E-BP (mTOR substrate) [Figure 62 A].

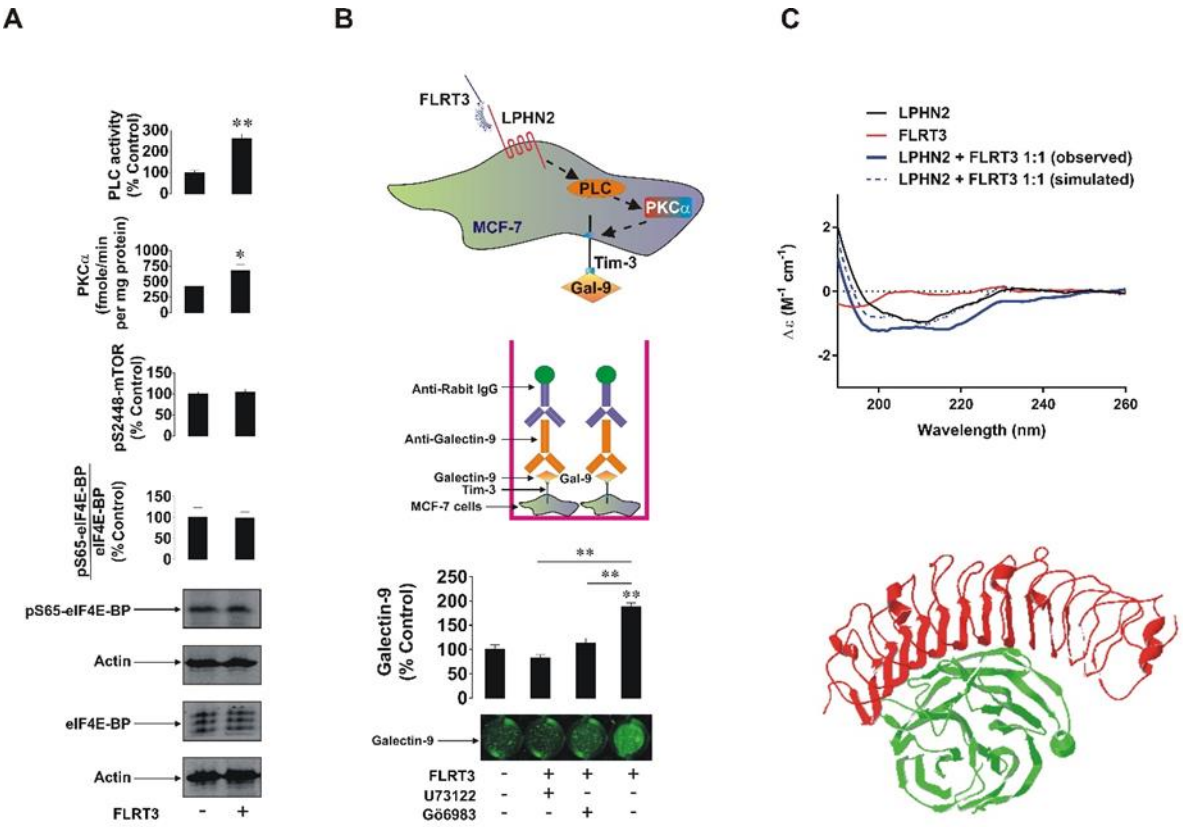


Figure 62: FLRT3 induces translocation of galectin-9 onto the surface of MCF-7 breast cancer cells. (A) MCF-7 cells were exposed for 4 h to 10 nM FLRT3 and activities of PLC, PKCα, the levels of phospho-S2448 mTOR and the amounts of phospho-S65 and total eIF4E-BP (an mTOR substrate) were analysed as described in the Materials and Methods. (B) MCF-7 cells were exposed for 4 h to 10 nM FLRT3 with or without 1 h pre-treatment with 30 μM U73122 (PLC inhibitor) or 70 nM Gö6983 (PKCα inhibitor). Surface presence of galectin-9 was characterised by on-cell assay. (C) Secondary structure and conformational changes of LPHN2 olfacomedin-like domain, FLRT3, and the complex of the two proteins mixed at the equimolar ratio were characterised using SRCD spectroscopy as outlined in the Materials and Methods. An interaction between olfactomedin-like domain of LPHN3 and FLRT3 generated by Swiss PDB viewer (5cmn.pdb file downloaded through PubMed database was used (Prokhorov et al., 2015)) is presented to illustrate the structural basis of this interaction. Images are from one experiment representative of four which gave similar results. Other results are shown as mean values ± SEM of at least three independent experiments. * $p<0.05$; **, $p<0.01$ vs control.

Since MCF-7 cells don't release detectable amounts of galectin-9 to the culture media and its secretion is not induced by FLRT3 (data not shown), surface presence of this protein was characterised as illustrated in Figure 39 B. It was found that the levels of surface-based galectin-9 were significantly upregulated by FLRT3 and this effect was considerably attenuated by U73122 (PLC inhibitor) or Gö6983 (PKCα inhibitor) [Figure 62 B]. This indicates that FLRT3-induced translocation of galectin-9 onto the cell surface of MCF-7 cells is controlled by PLC/PKCα pathway.

To confirm FLRT3-LPHN2 interaction, SRCD spectroscopy analysis of the olfactomedin-like domain of LPHN2 and FLRT3 alone and in their equimolar combination was performed. It was found that conformational changes occurring during FLRT3-LPHN2 interaction are similar to the ones taking place during FLRT3-LPHN1 complex formation [Figure 62 C]. This is in line with the fact that FLRT3 binds specifically olfactomedin-like domain, highly conserved extracellular domain common to all LPHNs. A 3D interaction of LPHN3 olfactomedin-like domain with FLRT3 leucine-rich repeat (LRR) domain is illustrated in Figure 62 C.

7.1.2 Galectin-9 protects breast cancer cells against cytotoxic immune attack

We found that galectin-9 (both secreted and surface-based) was able to attenuate AML cell killing by cytotoxic NK cells [Figure 37 and 38]. Thus, we decided to assess this effect also in breast cancer cell lines. Since solid tumours are mainly infiltrated by T cells rather than NK cells, cytotoxic ALL-derived TALL-104 CD8 lymphocytes were employed to verify this effect. Indeed, MCF-7 cells (adherent) were co-cultured with TALL-104 cells (expressing Tim-3 but not galectin-9) for 16 h at ratio of 4 : 1 in presence or absence of 5 μg/ml galectin-9 neutralising antibody. After the incubation, TALL-104 cells were collected, lysed and subjected to Western blot analysis for the detection of full-length and cleaved PARP (marker of apoptosis).

It was found that PARP cleavage in TALL-104 cells was significantly increased when co-cultured with MCF-7 cells and this effect was attenuated by anti-galectin-9 neutralising antibody [Figure 63 B]. Increased level of PARP cleavage indicates a higher number of apoptotic cells.

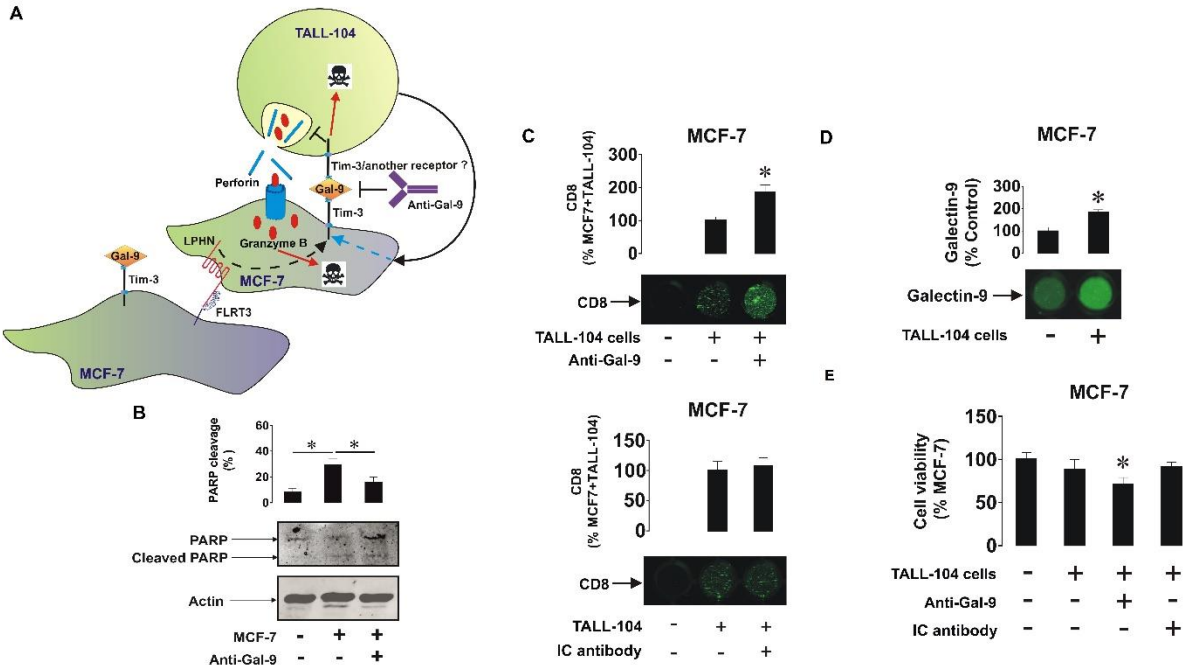


Figure 63: Galectin-9 protects MCF-7 cells against T cell-dependent cytotoxic immune attack. (A) MCF-7 cells were co-cultured with TALL-104 cytotoxic T lymphocytes at a ratio of 4 : 1 for 16 h (the ratio was determined by the aggressive behaviour of TALL-104 cells) in the absence or presence of 5 µg/ml galectin-9 neutralising antibody or 5 µg/ml isotype control antibody. (B) After the experiment TALL-104 cells were lysed and PARP cleavage, as an indicator of the rate of apoptotic cells, was measured using Western blot analysis. (C) CD8 expressions (reflecting the infiltration of TALL-104 into the MCF-7 layer) were measured by on-cell assay. (D) Galectin-9 surface presence was measured using on-cell assay in resting MCF-7 cells and those co-cultured with TALL-104 cells. (E) Viability of MCF-7 cells was measured by MTS test. Images are from one experiment representative of five which gave similar results. Other results are presented as mean values ± SEM of five independent experiments. * $p<0.05$ vs control.

To investigate the effect of galectin-9 on the ability of cytotoxic lymphocytes to bind breast malignant cell (and thus kill them), on-cell assay of MCF-7 cells co-cultured with TALL-104 in presence or absence of galectin-9 neutralising antibody was performed. It was confirmed that MCF-7 cells don't express CD8, since it wasn't detectable when these cells were cultured on their own. CD8 was instead detectable when MCF-7 were co-incubated with TALL-104 and the levels of CD8 were significantly increased when the co-culture was performed in

presence of anti-galectin-9 neutralising antibody [Figure 63 C]. This suggests that the ability of cytotoxic T lymphocytes to bind breast malignant cells increases when galectin-9 activity is disabled, and thus their potential to kill cancer cells augments. Indeed, cell viability of MCF-7 cells was significantly decreased when the co-culture was performed in presence of anti-galectin-9 neutralising antibody (as measured by MTS test) [Figure 63 D]. Importantly, neither binding ability of TALL-104 cells neither cell viability of MCF-7 cells was affected by isotype control antibody [Figures 63 C and D], confirming that these effects are galectin-9 -specific. Interestingly, galectin-9 surface expression was significantly upregulated in MCF-7 cells when co-cultured with TALL-104 cells.

Previously described results represent a strong indication that galectin-9 is capable of protecting breast tumour cells against cytotoxic cell-dependent killing.

7.1.3 Discussion

Our results demonstrate that FLRT3/LPHN/Tim-3/galectin-9 immunosuppressive pathway is activated in breast cancer tissues and protects malignant cells from cytotoxic immune attack. We found that FLRT3 binds LPHN (2 or 3) expressed on the surface of MCF-7 cells and upregulates PLC and PKCα activities, which induce a significant increase in galectin-9 surface expression. We confirmed that, as in AML, also in breast cancer cells, galectin-9 attenuates cytotoxic activity of immune cells. In addition, we found that galectin-9 surface expression was significantly increased by the presence of TALL-104 cells, suggesting that there are other pathways employed by MCF-7 cells to escape cytotoxic attack. Indeed, the biochemical pathway underlying this phenomenon remains to be identified.

We found also that, contrarily to AML, mTOR activity wasn’t upregulated by FLRT3 4 h treatment. This can be explained by the fact that breast cancer cells don’t secrete galectin-9 in contrast to AML cells. Indeed, since AML is blood/bone marrow cancer, its malignant cells

are in constant contact with cytotoxic immune cells and thus require high amounts of galectin-9 to be released and express on the surface in order to escape host immune attack, survive and proliferate. For this reason, mTOR activity is upregulated in AML cells and is continuously stimulated by blood-available endogenous ligand FLRT3. Contrarily, breast cancer is a solid tumour and thus needs "to fight" only with tissue-infiltrating T cells (significantly lower number than in the blood). Therefore, FLRT3-induced moderate PLC and PKC-α activation, which result in the translocation of Tim-3-galectin-9 complex on the surface of breast cancer cells is sufficient to attenuate anti-cancer immunity of cytotoxic lymphocytes.

These results are in line with those obtained in breast tumours compared with healthy breast tissues obtained from the same patients. Indeed, LPHN2, Tim-3 and galectin-9 expression was significantly higher in breast tumours compared to healthy tissues. Tim-3-galectin-9 complex was also detectable by Western blot analysis and co-localisation confocal microscopy in breast tissues. Importantly, its levels were significantly higher in breast cancer tissues than in healthy ones. We found also that PLC and PKCα activities were significantly increased in breast cancer tissues, while mTOR phosphorylation levels were comparable in both tissue types. Also, in line with the results obtained in MCF-7 cells, galectin-9 levels were significantly lower in patients affected by breast cancer than in healthy donors. This confirms that galectin-9 is not released by breast cancer cells but is kept on the cell surface to protect themselves from host immune attack. Tim-3 blood plasma levels were also significantly lower in breast cancer patients compared to healthy donors. The levels of IL-2 were instead non-significantly upregulated in cancer patients compared to healthy donors. Indeed, lower levels of Tim-3 allow higher production of IL-2, which has been shown to be downregulated by sTim-3. This suggests that induction of the cytotoxic activity of NK cells and cytotoxic T cells can still take place.

The presence of active cytotoxic cells could explain also the anti-metastatic potential of galectin-9 previously reported (Yamauchi et al., 2006). Indeed, galectin-9, expressed on the breast cancer cells may induce NK cells to release IFN-γ, which could activate cytotoxic lymphoid cells located in the area of the tumour microenvironment. Activated cytotoxic lymphocytes could then attack and kill malignant cells breaking off from the tumour thus preventing their circulation and metastasis. Overall, it appears that galectin-9 could protect the tumour which produces it in order to evade host immune attack, but this may not promote metastasis.

Schematic representation of Tim-3-galectin-9 pathway operating in breast cancer cells is represented in Figure 64.

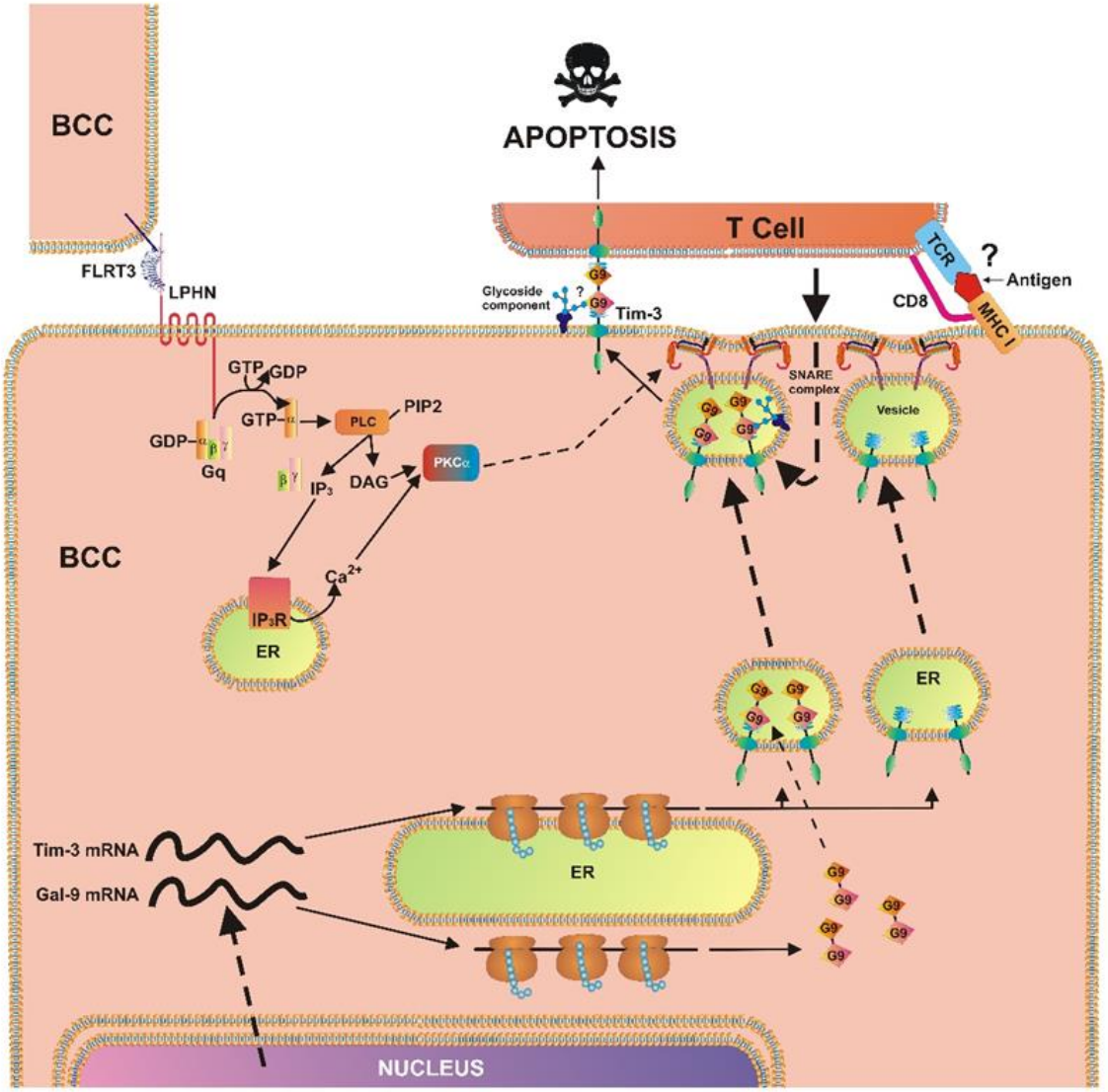


Figure 64: Breast cancer cell-based pathobiochemical pathways showing LPHN-induced activation of PKCα, which triggers the translocation of Tim-3 and galectin-9 onto the cell surface which is required for immune escape. The interaction of FLRT3 with LPHN isoform leads to the activation of PKCα, most likely through the classic Gq/PLC/Ca^{2+}pathway. Ligand-bound LPHN activates Gq, which in turn stimulates PLC. This leads to phosphatidyl-inositol-bisphosphate (PIP_2) degradation and production of inositol-trisphospate (IP_3) and diacylglycerol (DAG). PKCα is then activated by DAG and cytosolic Ca^{2+}. PKCα provokes the formation of SNARE complexes that tether vesicles to the plasma membrane. Galectin-9 impairs the cancer cell killing activity of cytotoxic T cells (and other cytotoxic lymphocytes). Possible (not directly confirmed) interactions of galectin-9 with glycoside component and T cell receptor (TCR)/CD8, with MHC I and antigen are highlighted with question mark "?" to indicate the fact that it is a hypothetic interaction, since TALL-104 cells used in the study kill tumour cells in MHC-independent manner.

7.2 Expression of key components of the FLRT3/LPHN/Tim-3/galectin-9 pathway in solid and liquid tumours

In addition to AML and breast cancer, Tim-3-galectin-9 pathway was shown to suppress anti-cancer immunity in solid tumours, such as colon cancer (Kang et al., 2015). Therefore, we decided to investigate the expression of FLRT3, LPHNs, Tim-3 and galectin-9 (both cell-based and secreted) in various human cancer cell lines (derived from brain, colorectal, kidney, blood/mast cell, liver, breast, prostate, lung and skin tumours) and various non-malignant cell lines and primary cells.

Cell lysates of various cell lines were subjected to Western blot analysis for specific detection of Tim-3, galectin-9, LPHNs 1, 2 and 3 as well as FLRT3 proteins, while galectin-9 released by these cells in the media was measured using ELISA. We found that most of the key components of this immunosuppressive pathway were present in cancer cell lines [Table 7 and Table 8]. The majority of the studied cells expressed at least one LPHN isoform. In some of the cells, in which was present at least on LPHN isoform, FLRT3 wasn't detectable by Western blot analysis. We hypothesised that in this case LPHN-expressing cells can use blood-based soluble FLRT3 to trigger Tim-3-galectin-9 pathway. Indeed, Tim-3 and galectin-9 were found to be expressed in all the studied cancer cell lines, except for the chronic myeloid leukaemia (CML) cell line, K562, which expressed Tim-3 but only traces of cell-associated galectin-9. This could be one of the reasons why CML cells entering the circulation are rapidly eliminated by cytotoxic immune cells.

Additional clarification regarding molecular weight, isoforms and glycosylation level of different proteins studied are illustrated in Figure 65.

Table 7: Expression of Tim-3, galectin-9, LPHNs 1, 2 and 3 as well as FLRT3 proteins in brain, colorectal, kidney, blood/bone marrow cell lines. Cell lysates were subjected to Western blot analysis for specific detection of the proteins. The concentration of galectin-9 in the media used to culture these cells was measured by ELISA.

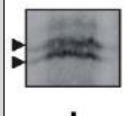
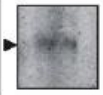
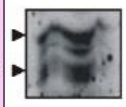
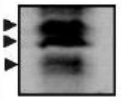
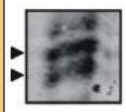
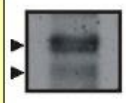
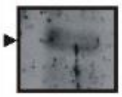
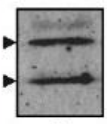
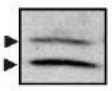
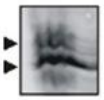
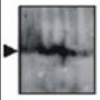
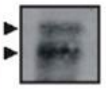
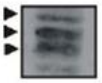
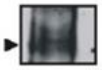
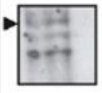
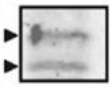
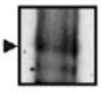
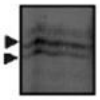
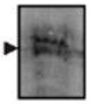
TYPE OF CANCER	CELL LINE	Tim-3	Galectin-9	LPHN1	LPHN2	LPHN3	FLRT3	Galectin-9 secretion (pg/10^5 cells)
BRAIN	LN401 Human glioblastoma	 +	 +	 N. D.	 +	 N. D.	 +	110 ± 24
COLORECTAL	Colo 205 Human colon adenocarcinoma type D	 +	 +	 N. D.	 +	 N. D.	 +	210 ± 36
KIDNEY	RCC-FG1 Clear cell carcinoma	 +	 +	 N.D.	 +	 N.D.	 +	<100
	RC-124 Established from **non-tumour** tissue of a 63-years-old man diagnosed with kidney carcinoma	 +	 +	 N.D.	 +	 N.D.	 N.D.	N.D.
Blood/bone marrow and mast cell cancer	THP-1 Acute myeloid leukaemia	 +	 +	 +	 +	 +	 N. D.	480 ± 58
	K562 Chronic myelogenous leukaemia	 +	 Traces	 N. D.	 N. D.	 N. D.	 N. D.	N. D.
	LAD2 Mast cell sarcoma	 +	 +	 +	 N. D.	+	N. D.	N. D.
	Primary human healthy mononuclear leukocytes	+	+	N. D.	N. D.	N. D.	N. D.	<100

Table 8: Expression of Tim-3, galectin-9, LPHNs 1, 2 and 3 as well as FLRT3 proteins in liver, breast, prostate, lung and skin cell lines. Cell lysates were subjected to Western blot analysis for specific detection of the proteins. The concentration of galectin-9 in the media used to culture these cells was measured by ELISA.

TYPE OF CANCER	CELL LINE	Tim-3	Galectin-9	LPHN1	LPHN2	LPHN3	FLRT3	Galectin-9 secretion (pg/10^6 cells)
LIVER	**Hep G2** Human Hepatocellular carcinoma	 +	 +	 N. D.	 +	 Traces	 +	<100
BREAST	**BC-8701** Human breast cancer	 +	 +	 N. D.	 N. D	 +	 +	N. D.
	MDA-MB-231 Human breast adenocarcinoma	 +	 +	 N. D.	 +	 N. D	 +	N. D.
PROSTATE	**PC3** Prostate adenocarcinoma grade IV (cells derived from metastatic site – bone)	 +	 +	 N. D.	 +	 +	 +	N. D.
LUNG	**Calu 6** Human pulmonary non-small cell carcinoma	 +	 +	 N. D.	 N.D.	 +	 +	N. D.
	BEAS-2B Human bronchial epithelium, **normal**	 +	 +	 N. D.	 N. D.	 N. D.	 N. D.	N. D.
SKIN	**D10** Human malignant melanoma	 +	 +	 N. D.	 Traces	N. D.	Traces	N. D.
	HaCaT *In vitro* spontaneously transformed keratinocytes from histologically **normal skin**	+	Traces	N. D.	+	N. D.	+	N. D.

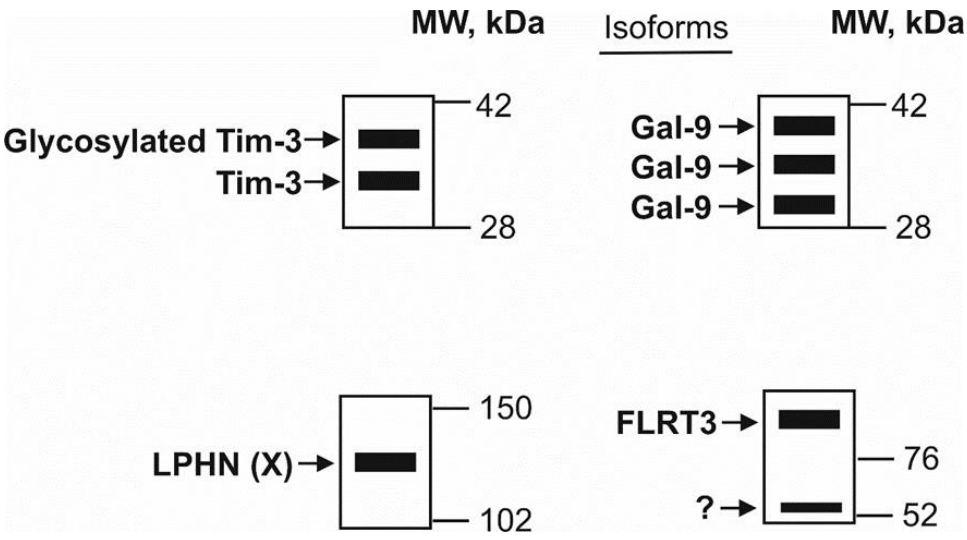


Figure 65: Molecular weight, isoforms and glycosylation level of the proteins reported in Table 1 and 2. Tim-3: lower band represents non-glycosylated protein, upper band(s), protein with differential levels of glycosylation; Galectin-9: multiple bands represent different isoforms of the same protein; FLRT3 – detectable between 80 and 95 kDa (upper band where applicable or the only visible band); another band (lower band; possibly extracellular domain) often appears at around 60 most likely reflecting levels of glycosylation in first two cases and proteolytic processing in the third. Traces – detectable expression which requires loading of >100 µg protein per well**.**

Comparative analysis of the studied proteins in different cell lines shown in Table 1 and 2 were performed by measuring infrared fluorescence of the bands divided by the total quantity of the loaded proteins. All the results of this quantitative analysis are illustrated in Figure 66. Importantly, this comparative analysis evidenced that non-malignant cells expressed lower amounts of galectin-9 and Tim-3 compared to cancerous cells of similar origins.

Taken together, our results suggest that FLRT3/LPHN/Tim-3/galectin-9 pathway could be operating in other cancer cell types in order to avoid host immune attack. However, further investigations are required to confirm this hypothesis.

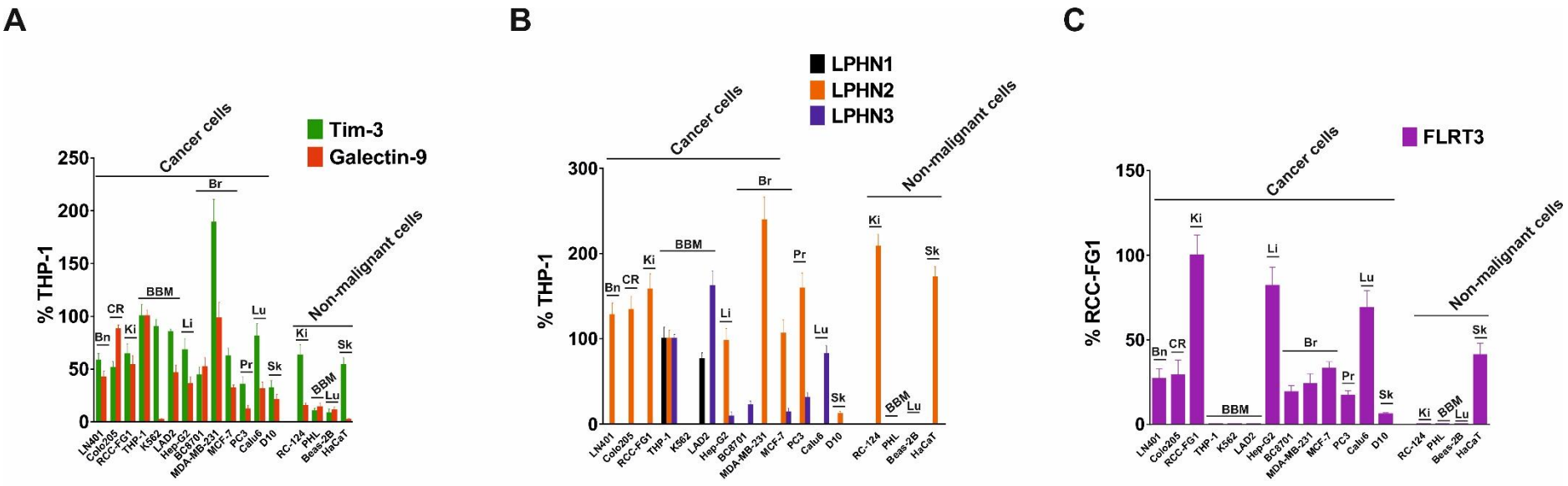


Figure 66: Expression of Tim-3, galectin-9, LPHNs 1, 2 and 3 as well as FLRT3 proteins in various human cancer cell lines. Lysates of indicated cells were subjected to Western blot analysis as outlined in Materials and Methods (images are presented in Supplementary table 1). Detected infrared fluorescence of the bands divided by the total protein amounts loaded (measured using Bradford assay) was used as a measure of protein quantity. Levels of Tim-3 & total galectin-9 (A) and LPHNs 1, 2 & 3 (B) were expressed as a % of those levels present in THP-1 cells (expressed as 100%). Since THP-1 cells lack FLRT3 expression, the levels of this protein were expressed as % RCC-FG1 (C), respectively considering FLRT3 level in these cells as 100%. Abbreviations used – Bn – brain, CR – colorectal, Ki – kidney, BBM – blood, bone marrow and mast cells, Li – liver, Br – breast, Pr – prostate, Lu – lung, Sk – skin. Data are presented as mean values ± SEM of three independent experiments.

8. Classic programmed cell death pathway downregulates Tim-3-galectin-9 immunosuppressive pathway.

Recently it was found some of the galectin family members, such as galectin-3, were able to protect AML and colorectal cancer cells against apoptosis through mitochondrial stabilisation in a B cell lymphoma protein (Bcl) 2-dependent manner (Lee, et al., 2013; Ruvolo, et al., 2016). Thus, we decided to investigate whether galectin-9 possesses this intracellular anti-apoptotic activity too.

8.1 Pharmacologically induced mitochondrial defunctionalisation suppresses Tim-3-galectin-9 secretory pathway in human colorectal cancer cells

To conduct these studies, a pharmacological inhibitor 5-[(4-bromophenyl)methylene]-a-(1-methylethyl)-4-oxo-2-thioxo-3-thiazolidineacetic acid (BH3I-1, Figure 67 A), a synthetic cell permeable Bcl-X_L antagonist was employed as a pharmacological inducer of apoptosis. This compound induces apoptosis *via* inhibition of interactions between the BH3 domain and Bcl-X_L thus defunctionalysing mitochondria.

Colorectal adenocarcinoma cells of epithelial origin, Colo-205, found to employ Tim-3/galectin-9 to escape host immune attack, were incubated for 24 h with or without 100 μM BH3I-1. After the incubation, cell viability and caspase 3 activity were measured as described in material and methods. It was confirmed that BH3I-1 was capable of inducing apoptosis in Colo-205 (based on increased caspase-3 activity and decreased viability of the cell, Figure 67 A).

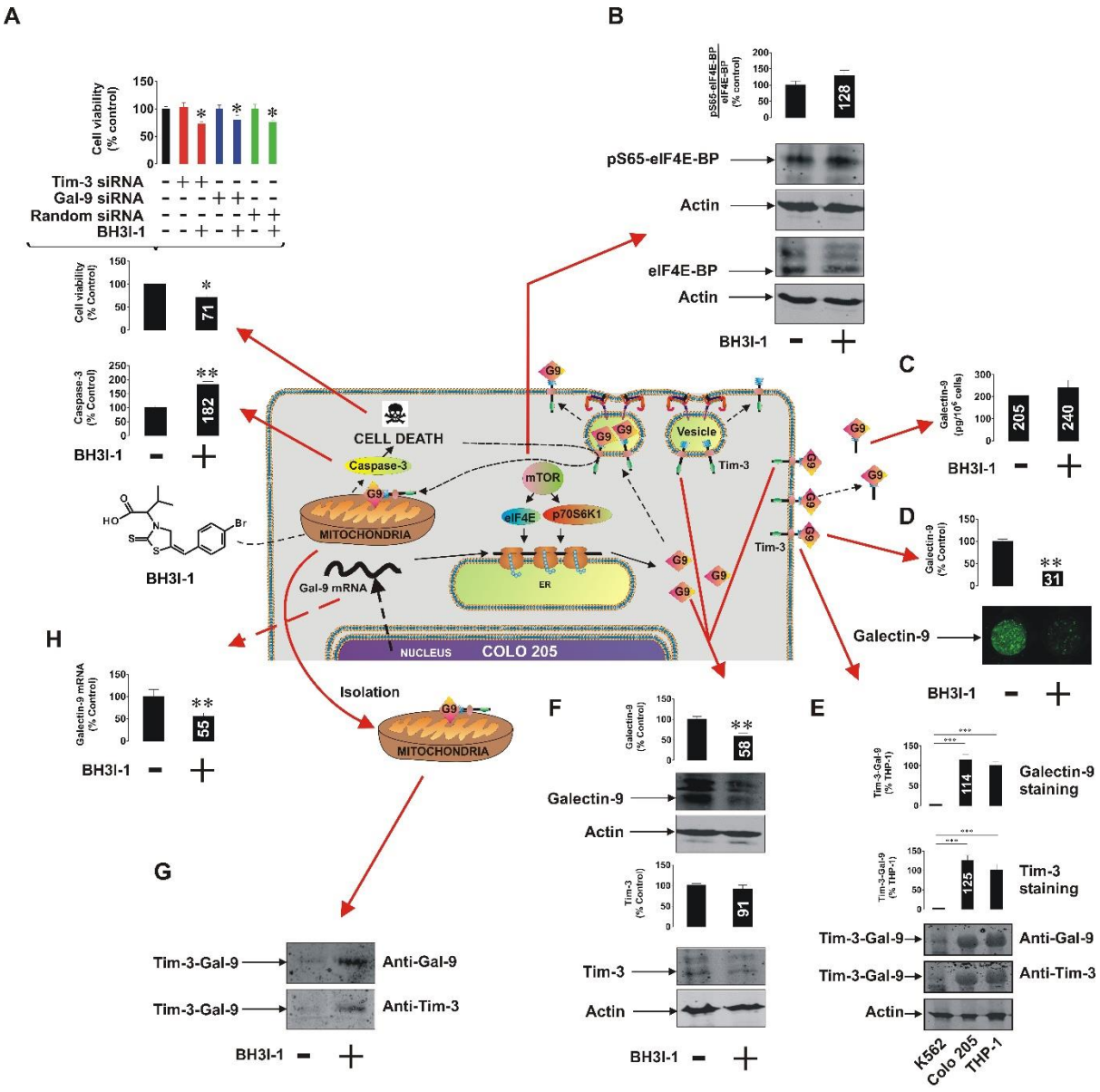


Figure 67: Pro-apoptotic defunctionalisation of mitochondria reduces galectin-9 expression and leads to its redistribution in human Colo-205 colorectal adenocarcinoma cells. Colo-205 cells were exposed to 100 µM BH3I-1 for 24 h followed by **(A)** detection of cell viability using an MTS test and colorimetric assay of caspase 3 activity. Cell viability was also tested for normal and Tim-3 or galectin-9 knockdown Colo-205 cells. **(B)** Following 24 h of exposure to BH3I-1 S65-phosphorylation levels of eIF4E-BP were analysed by Western blot. **(C)** Surface presence and total cellular levels of Tim-3 and galectin-9 were analysed in Colo-205 cells using FACS. **(D)** Secreted levels of galectin-9 were analysed in Colo-205 cells following 24 h of exposure to BH3I-1 by ELISA. **(E)** Surface levels of galectin-9 in non-treated and BH3I-1-stimulated Colo-205 cells were compared using an on-cell assay. **(F)** The presence of Tim-3-galectin-9 complex in Colo-205 cells was confirmed using Western blot analysis (bands were appearing at around 70 KDa). THP-1 cells were used as a positive and K562 as a negative control. **(G)** Levels of Tim-3 and galectin-9 were analysed in Colo-205 lysates following 24 h of exposure to BH3I-1 by Western blot. **(H)** Mitochondrial extracts were obtained from non-treated and BH3I-1-stimulated Colo-205 cells and subjected to Western blot analysis to detect Tim-3 and galectin-9. Total protein levels were measured using a Bradford assay and equal protein amounts were loaded onto the gels. **(I)** Galectin-9 mRNA levels were analysed in non-treated Colo-205 cells and those exposed to BH3I-1 using qRT-PCR. Images are from one experiment representative of at least four which gave similar results. In the scheme galectin-9 is abbreviated as G9. Quantitative results are shown as mean values ± SEM of 3 - 6 independent experiments. * $p<0.05$; **, $p<0.01$ vs control.

To investigate whether galectin-9 (or possibly its receptor Tim-3) could protect the cells from apoptosis, knockdown either of galectin-9 either of Tim-3 was performed prior to BH3I-1 exposure for 24 h. The efficiency of the knockdown was checked by qRT-PCR. It was found that silencing either galectin-9 or its receptor/trafficker Tim-3 did not affect the pro-apoptotic activity of BH3I-1 suggesting that galectin-9 is unlikely to be involved in cell protection in this case [Figure 67 A].

Cell lysates from Colo-205 cultured in presence or absence of BH3I-1 were also subjected to Western blot analysis for specific detection of pS65-eIF4E-BP/ eIF4E-BP proteins. It was found that BH3I-1 didn't affect the phosphorylation levels of eIF4E-BP [Figure 67 B]. Thus, BH3I-1 had no effect on the activity of mTOR, important for galectin-9/Tim-3 synthesis and secretion. Obviously, one could suggest that Colo-205 cells accumulate galectin-9 on their surface and inside the cells based on FACS analysis (Figure 67 C). Decreased levels of surface-based Tim-3 might indicate its masking by galectin-9 (Yasinska et al., 2018).

Next, galectin-9 release by Colo-205 with or without 24 h exposure to BH3I-1 was performed by ELISA. It was found that the BH3I-1 didn't affect Colo-205 ability to secrete galectin-9 [Figure 67 D]. Therefore, on-cell assay was performed to verify whether galectin-9 surface levels are affected by this compound. It was found that BH3I-1 significantly decreased galectin-9 surface expression in Colo-205 cells [Figure 67 E].

Then, we investigated whether Colo-205 cells are able to accumulate Tim-3-galectin-9 complex at a level comparable to THP-1 AML cells. K562 were used as negative control. Thus, lysates of K562, Colo-205 and THP-1 cells were subjected to Western blot analysis. Bands detectable by both anti-Tim-3 and anti-galectin-9 antibodies confirmed that the presence of Tim-3-galectin-9 complex in Colo-205. In addition, we found that it was highly expressed in Colo-205 cells, at the level comparable to THP-1 AML cells [Figure 67 F].

Treatment with BH3I-1 significantly decreased galectin-9 intracellular level but didn't affect Tim-3 concentration inside the cell (as confirmed by Western blot analysis) [Figure 67 G].

Next, mitochondria of Colo-205 cells cultured in presence or in absence of BH3I-1 were isolated as described in material and methods. Isolated mitochondria lysates were then subjected to western blot analysis for Tim-3 and galectin-9 detection. Obtained results showed that the Tim-3-galectin-9 complex is accumulated in mitochondria upon stimulation with BH3I-1 [Figure 67 H].

Quantitative real-time PCR on Colo-205 untreated and treated with BH3I-1 showed that galectin-9 mRNA levels were significantly reduced in presence of this compound [Figure 67 I].

In addition, we observed that Colo-205 cells release lower amounts of galectin-9 in comparison to THP-1 cells. Importantly, these amounts are proportional to cellular Tim-3 levels [Figure 68], supporting the conclusion regarding the involvement of Tim-3 in galectin-9 secretion.

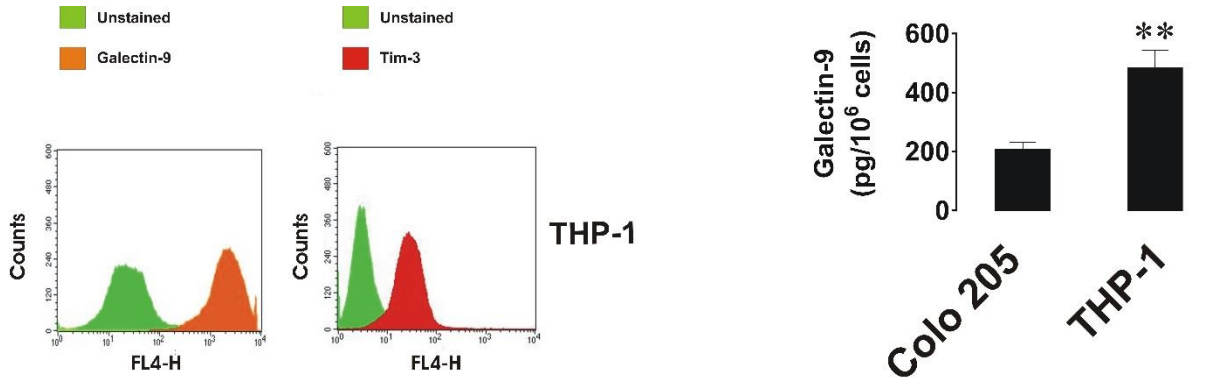


Figure 68: Total cellular levels of Tim-3 and galectin-9 and levels of secreted galectin-9 in THP-1 human AML cells. Total Tim-3 and galectin-9 levels were measured by FACS in permeabilised THP-1 cells. The secreted levels of galectin-9 were also measured in culture medium, in which THP-1 cells were kept for 16 h and compared with those of Colo-205 cells cultured under the same conditions. Images are from one experiment representative of at least four which gave similar results. Other results are shown as mean values ± SEM of five independent experiments. ** $p<0.01$ vs control.

The accumulation of Tim-3-galectin-9 complex upon mitochondrial defunctionalisation was then investigated in two other types of epithelial cells – non-malignant kidney RC-124 and malignant HepG2 hepatoma cells (both abundant in mitochondria levels). However, we found that apoptosis stimulation by BH3I-1 in non-malignant kidney RC-124 cells wasn't as efficient as in Colo-205 cells (data not shown). Indeed, we found that RC-124 cells were less permeable to this inhibitor in comparison to Colo-205 (as confirmed by direct chemical measurement of drug-associated uptake of bromine, data not shown). Therefore, H_2O_2 was used to defunctionalize mitochondria in these cells. HepG2 and RC-124 cells were incubated for 6h in presence or absence of 1 mM H_2O_2. It was found that galectin-9 levels were significantly reduced in both cell types, but the Tim-3-galectin-9 complex was only accumulated in the mitochondria of HepG2 cells and not in RC-124 [Figure 69].

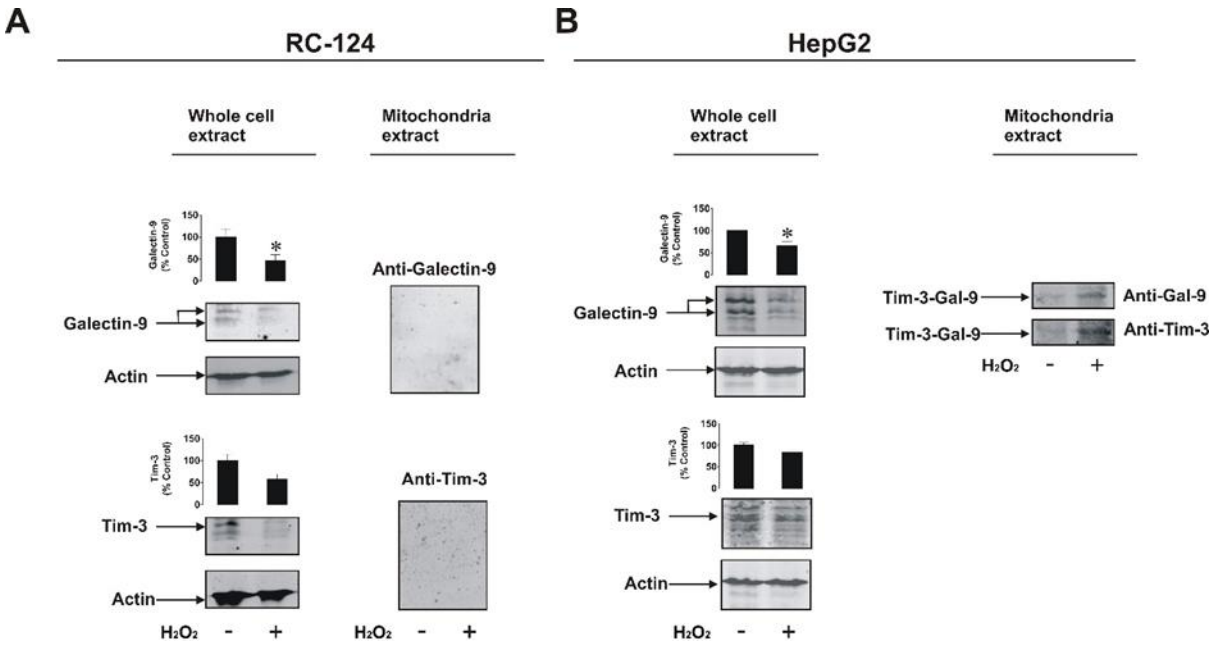


Figure 69: Mitochondrial defunctionalisation reduces intracellular galectin-9 levels in both healthy (RC-124) and malignant (HepG2) epithelial cells but induces galectin-9 translocation into mitochondria only in malignant (HepG2) cells. Cells were exposed to 1 mM H2O2 for 6 h followed by Western blot analysis of cellular and mitochondrial levels of Tim-3 and galectin-9 in both RC-124 (A) and HepG2 (B) cells. In mitochondria of RC-124 cells Tim-3, galectin-9 and the complex of both proteins (MW ~ 70 KDa) was not detectable, while in mitochondria isolated from HepG2 cells a complex was clearly detectable in H2O2-stimulated cells. Images are from one experiment representative of at least four which gave similar results. Quantitative results are shown as mean values ± SEM of four independent experiments. ** $p<0.01$ vs control.

8.2 Discussion

Taken together, our results indicate pro-apoptotic mitochondrial dysfunction leads to a decreased transcription of galectin-9 mRNA leading to its reduced translation. In addition, this pharmacologically induced leads to a re-distribution of the Tim-3-galectin-9 complex into mitochondria where galectin-9 possibly interacts with mitochondrial glycoproteins. The physiological relevance is still unclear. We proposed that galectin-9 transfer in mitochondria and its decrease on the cell surface might be part of a regulated cell suicide program. Indeed, decrease in surface-associated galectin-9 would lead to a decreased protection of a dying cell thus allowing its smooth elimination. Importantly, this phenomenon was observed in both cancer cell line studied but not in non-malignant cells, suggesting that this mechanism could be cancer-specific. Therefore, targeted defunctionalisation of mitochondria in malignant cells may help cytotoxic lymphoid cells to eliminate more efficiently cancer cells since it would reduce cell surface presence of galectin-9 capable of suppressing anti-cancer activity of the immune system cells.

Currently, several drugs targeting mitochondrial defunctionalisation have been shown to enhance conventional chemotherapy and radiotherapy treatment in haematological and solid tumours (Oltersdorf, et al., 2005; Konopleva, et al. 2006; Kang, et al., 2007; Hann, et al., 2008; Tse, et al., 2008; Lock, et al., 2008; Gandhi, et al., 2011; Liu, et al, 2009). We suggest that improved responses in patients undergoing this combinatorial treatment might be partly due to the mechanism here shown.

.

9. CONCLUSIONS

The following conclusions can be made from this research programme:

1. Triggering of LPHN1, expressed in AML cells but absent in healthy leukocytes, activates Gαq/PLC/PKC and mTOR pathways leading to biosynthesis and exocytosis of Tim-3 and galectin-9. Both proteins, Tim-3 and galectin-9 suppress anti-cancer immunity allowing AML cells to survive and proliferate.

2. AML cells recruit crucial components of normal metabolism to escape surveillance and progress the disease. In particular:

   a) Human adrenal cortex hormone cortisol upregulates LPHN1 expression in AML cells; blood-available FLRT3 interacts with LPHN1 leading to galetin-9/Tim-3 synthesis and exocytosis in AML cells.

   b) HMGB1, released by dying or stressed cells, induces SCF and VEGF production *via* interaction with differential signalling receptors. Therefore, targeting HMGB1 in the treatment of AML may reduce SCF and VEGF, both factors pivotal for AML progression.

3. Crucial components of FLRT3/LPHN/Tim-3/galectin-9 pathway are expressed in the majority of cancer cell lines and thus may be common for a variety of malignant tumours. Tim-3-galectin-9 pathway is active in breast cancer cells and is used to protect malignant cells from host immune attack.

4. Galectin-9 doesn't protect cancer cells against apoptosis *via* mitochondrial defunctionalisation. However, mitochondrial defunctionalisation reduces galectin-9 surface expression and leads to its accumulation in mitochondria in malignant cells but not in healthy ones. Therefore, targeted mitochondrial defunctionalisation may be a novel strategy for anti-

cancer immunotherapy, since it would reduce galectin-9 surface expression allowing smooth elimination of cancer cells by immune system cells.

5. Taken together our work demonstrates that Tim-3-galectin-9 immunosuppressive pathway plays a pivotal role in protection of AML and various solid tumour cells towards host immune surveillance operated by cytotoxic lymphoid cells.

10. BIBLIOGRAPHY

Abarrategi, A., Tornin, J., Martinez-Cruzado, L., Hamilton, A., Martinez-Campos, E., Rodrigo, J. P., González, M. V., Baldini, N., Garcia-Castro, J., Rodriguez, R. (2016). Osteosarcoma: Cells-of-Origin, Cancer stem cells, and targeted therapies. *Stem Cells International*, *2016*, 3631764.

Ansari, D., Tingstedt, B., Andersson, B., Holmquist, F., Sturesson, C., Williamsson, C., Sasor, A., Borg, D., Bauden, M., Andersson, R. (2016). Pancreatic cancer: Yesterday, today and tomorrow. *Future Oncology*, *12*, 16, 1929-46.

Arem, H., & Loftfield, E. (2018). Cancer Epidemiology: A Survey of Modifiable Risk Factors for Prevention and Survivorship. *American Journal of Lifestyle Medicine*, *12*, 3, 200–210.

Arneth, B. (2018). Comparison of Burnet's clonal selection theory with tumor cell-clone development. *Theranostics*, *8*, 12, 3392–3399.

Arruebo, M., Vilaboa, N., Sáez-Gutierrez, B., Lambea, J., Tres, A., Valladares, M., & González-Fernández, Á. (2011). Assessment of the evolution of cancer treatment therapies. *Cancers*, *3*, 3, 3279–3330.

Asayama, T., Tamura, H., Ishibashi, M., Kuribayashi-Hamada, Y., Onodera-Kondo, A., Okuyama, N., Yamada A., Shimizu, M., Moriya, K., Takahashi, H., Inokuchi, K. (2017). Functional expression of Tim-3 on blasts and clinical impact of its ligand galectin-9 in myelodysplastic syndromes. *Oncotarget*, *8*, 51, 88904–88917.

Aurisicchio, L., Peruzzi, D., Koo, G., Wei, W.-Z., La Monica, N., & Ciliberto, G. (2013). Immunogenicity and Therapeutic Efficacy of a Dual-Component Genetic Cancer Vaccine Cotargeting Carcinoembryonic Antigen and HER2/ neu in Preclinical Models. *Human Gene Therapy*, *25*, 2, 121–131.

Baddour, J. A., Sousounis, K., & Tsonis, P. A. (2012). Organ repair and regeneration: An overview. *Birth Defects Research Part C - Embryo Today: Reviews*, *96*, 1, 1-29.

Bamberger, C. M. 1., Schulte, H. M, Chrousos, G. P. (1996) Molecular determinants of glucocorticoid receptor function and tissue sensitivity to glucocorticoids. *Endocr Rev. 17*, 3, 245-61.

Barrett, J. C. (1993). Mechanisms of Multistep Carcinogenesis and Carcinogen Risk Assessment. *Environmental Health Perspectives*, *100*, 9-20.

Basanta, D., & Anderson, A. R. A. (2017). Homeostasis back and forth: An ecoevolutionary perspective of cancer. *Cold Spring Harbor Perspectives in Medicine*, *7*, 9.

Bastide, K., Ugolin, N., Levalois, C., Bernaudin, J. F., & Chevillard, S. (2010). Are adenosquamous lung carcinomas a simple mix of adenocarcinomas and squamous cell carcinomas, or more complex at the molecular level? *Lung Cancer*, *68*, 1, 1-9.

Banerjee H, Kane LP. (2018) Immune regulation by Tim-3. *F1000Res*, *7*, 316.

Bielenberg, D. R., & Zetter, B. R. (2015). The Contribution of Angiogenesis to the Process of Metastasis. *Cancer Journal*, *21*, 4, 267-73.

Blank, C. U., & Enk, A. (2014). Therapeutic use of anti-CTLA-4 antibodies. *International Immunology*, *27*, 1, 3–10.

Blankenstein, T., Gilboa, E., & Jaffee, E. M. (2012). The determinants of tumour immunogenicity What are the most important determinants of tumour immunogenicity, in your opinion? *Nat Rev Cancer*, *12*, 4, 307–313.

Boucard, A. A., Maxeiner, S., & Südhof, T. C. (2014). Latrophilins function as heterophilic cell-adhesion molecules by binding to teneurins: Regulation by alternative splicing. *Journal of Biological Chemistry*, *289*, 1, 387–402.

Bovaird, J. H., Ngo, T. T., & Lenhoff, H. M. (1982). Optimizing the o-phenylenediamine assay for horseradish peroxidase: Effects of phosphate and pH, substrate and enzyme concentrations, and stopping reagents. *Clinical Chemistry*, *28*, 12, 2423–2426.

Boyle, J. (2008). Molecular biology of the cell, 5th edition by B. Alberts, A. Johnson, J. Lewis, M. Raff, K. Roberts, and P. Walter. *Biochemistry and Molecular Biology Education*, *36*, 4, 317–318.

Bray, F., Ferlay, J., Soerjomataram, I., Siegel, R. L., Torre, L. A., & Jemal, A. (2018). Global cancer statistics 2018: GLOBOCAN estimates of incidence and mortality worldwide for 36 cancers in 185 countries. *CA: A Cancer Journal for Clinicians*, *68*, 6, 394-424.

Buchbinder, E. I., & Desai, A. (2016). CTLA-4 and PD-1 pathways similarities, differences, and implications of their inhibition. *American Journal of Clinical Oncology: Cancer Clinical Trials*, *39*, 1, 98–106.

Burningham, Z., Hashibe, M., Spector, L., & Schiffman, J. D. (2012). The Epidemiology of Sarcoma. *Clinical Sarcoma Research*, *2*, 1, 14.

Chabot, S., Kashio, Y., Seki, M., Shirato, Y., Nakamura, K., Nishi, N., Nakamura, T., Matsumoto, R., Hirashima, M. (2002). Regulation of galectin-9 expression and release in Jurkat T cell line cells. *Glycobiology*, *12*, 2, 111–118.

Chambers, C. A., Kuhns, M. S., Egen, J. G., & Allison, J. P. (2001). CTLA-4-mediated inhibition in regulation of T cell responses: mechanisms and manipulation in tumor immunotherapy. *Annual Review of Immunology*, *19*, 1, 565–594.

Chang, Y., Moore, P. S., & Weiss, R. A. (2017). Human oncogenic viruses: Nature and discovery. *Philosophical Transactions of the Royal Society B: Biological Sciences*, *372*, 1732, 1–9.

Chen, H., Liu, H., & Qing, G. (2018). Targeting oncogenic Myc as a strategy for cancer treatment. *Signal Transduction and Targeted Therapy*, *3*, 5, 1-7.

Choo, Y. C., & Naylor, B. (1984). Coexistent squamous cell carcinoma and adenocarcinoma of the uterine cervix. *Gynecologic Oncology*, *17*, 2, 168–174.

Clayton, K. L., Douglas-Vail, M. B., Nur-ur Rahman, A. K. M., Medcalf, K. E., Xie, I. Y., Chew, G. M., Tandon, R., Lanteri, M. C., Norris, P. J., Deeks, S. G., Ndhlovu L. C., Ostrowski, M. A. (2015). Soluble T cell immunoglobulin mucin domain 3 is shed from CD8+ T cells by the sheddase ADAM10, is increased in plasma during untreated HIV infection, and correlates with HIV disease progression. *Journal of Virology*, *89*, 7, 3723–36.

Cordon-Cardo, C., & Richont, V. M. (1994). Expression of the Retinoblastoma Protein Is Regulated in Normal Human Tissues. *American Journal of Pathology*, *144*, 3, 500-10.

Corm, S., Berthon, C., Imbenotte, M., Biggio, V., Lhermitte, M., Dupont, C., Briche, I., Quesnel, B. (2009). Indoleamine 2,3-dioxygenase activity of acute myeloid leukemia cells can be measured from patients' sera by HPLC and is inducible by IFN-γ. *Leukemia Research*, *33*, 3, 490–494.

Corthay, A. (2014). Does the immune system naturally protect against cancer? *Frontiers in Immunology*, *12*, 5, 197.

Coumans, F. A., Siesling, S., & Terstappen, L. W. (2013). Detection of cancer before distant metastasis. *BMC Cancer*, *13*, 13, 283.

Coussens, L. M., & Werb, Z. (2002). Inflammation and Cancer. *Nature, 420*, 6917, 860–867.

Criscitiello, C. (2012). Tumor-associated antigens in breast cancer. *Breast Care, 7*, 4, 262–266.

D'Arcy, V., Pore, N., Docquier, F., Abdullaev, Z. K., Chernukhin, I., Kita, G. X., Rai, S., Smart, M., Farrar, D., Pack, S., Lobanenkov, V., Klenova, E. (2008). BORIS, a paralogue of the transcription factor, CTCF, is aberrantly expressed in breast tumours. *British Journal of Cancer*, *98*, 3, 571–579.

Dajon, M., Iribarren, K., & Cremer, I. (2017). Toll-like receptor stimulation in cancer: A pro- and anti-tumor double-edged sword. *Immunobiology*, *222*, 1, 89–100.

Das, M., Zhu, C., & Kuchroo, V. K. (2017). Tim-3 and its role in regulating anti-tumor immunity. *Immunological Reviews*, *276*, 1, 97–111.

Dasgupta, Y., Koptyra, M., Hoser, G., Kantekure, K., Roy, D., Gornicka, B., Nieborowska-Skorska, M., Bolton-Gillespie, E., Cerny-Reiterer, S., Müschen, M., Valent, P., Wasik, M.A., Richardson, C., Hantschel, O., van der Kuip, H., Stoklosa, T., Skorski, T. (2016). Normal ABL1 is a tumor suppressor and therapeutic target in human and mouse leukemias expressing oncogenic ABL1 kinases. *Blood*, *27*, 17, 2131-43.

Davis, A. S., Viera, A. J., & Mead, M. D. (2014). Leukemia: an overview for primary care. *American Family Physician*, *89*, 9, 731–8.

Davis, T. E., Kis-Toth, K., Szanto, A., & Tsokos, G. C. (2013). Glucocorticoids suppress T cell function by up-regulating microRNA-98. *Arthritis and rheumatism, 65*, 7, 1882–1890.

Davydov, I. I., Fidalgo, S., Khaustova, S., Lelyanova, V. G., Grebenyuk, E., Ushkaryov,

Y. A., & Tonevitsky, A. (2009). Prediction of Epitopes in Closely Related Proteins Using a New Algorithm. *Bulletin of Experimental Biology and Medicine*, *148*, 6, 869–873.

Delacour, D., Koch, A., & Jacob, R. (2009). The role of galectins in protein trafficking. *Traffic*, *10*, 10, 1405–1413.

Devlin, E. J., Denson, L. A., & Whitford, H. S. (2017). Cancer Treatment Side Effects: A Meta-analysis of the Relationship Between Response Expectancies and Experience. *Journal of Pain and Symptom Management*, *54*, 2, 245-258.

Dicken, B. J., Bigam, D. L., Cass, C., Mackey, J. R., Joy, A. A., & Hamilton, S. M. (2005). Gastric adenocarcinoma: Review and considerations for future directions. *Annals of Surgery*, *241*, 1, 27-39

Dinarello, C. A. (2009). Immunological and Inflammatory Functions of the Interleukin-1 Family. *Annual Review of Immunology*, *27*, 1, 519–550.

Ding, X., Yang, W., Shi, X., Du, P., Su, L., Qin, Z., Chen, J., Deng, H. (2011). Tumor Necrosis Factor Receptor 1 Mediates Dendritic Cell Maturation and CD8 T Cell Response through Two Distinct Mechanisms. *J Immunol.*, *187*, 3, 1184–1191.

Dings, R. P. M., Miller, M. C., Griffin, R. J., & Mayo, K. H. (2018). Galectins as molecular targets for therapeutic intervention. *International Journal of Molecular Sciences*, *19*, 3, 1–22.

Doorakkers, E., Lagergren, J., Engstrand, L., & Brusselaers, N. (2018). Helicobacter pylori eradication treatment and the risk of gastric adenocarcinoma in a Western population. *Gut*, *67*, 12, 2092–2096.

Du, W., Yang, M., Turner, A., Xu, C., Ferris, R. L., Huang, J., Kane, L. P., Lu, B. (2017). Tim-3 as a target for cancer immunotherapy and mechanisms of action. *International Journal of Molecular Sciences*, *18*, 3, 1–12.

Dumitriu, I. E., Bianchi, M. E., Bacci, M., Manfredi, A. A., & Rovere-Querini, P. (2006). The secretion of HMGB1 is required for the migration of maturing dendritic cells. *Journal of Leukocyte Biology*, *81*, 1, 84–91.

Duronio, R. J., & Xiong, Y. (2013). Signaling pathways that control cell proliferation. *Cold Spring Harbor Perspectives in Biology*, *5*, 3, 1-12.

Nagul, E. A., McKelvie, I. D., Worsfold, P., Kolev, S. D. (2015). The molybdenum blue reaction for the determination of orthophosphate revisited: Opening the black box. *Analytica Chimica Acta*, *890*, 60-82.

Efeyan, A., & Serrano, M. (2007). p53: Guardian of the genome and policeman of the oncogenes. *Cell Cycle*, *6*, 9, 1006-10.

Estey, E., & Döhner, H. (2006). Acute myeloid leukaemia. *Lancet*, *368*, 9550, 1894–1907.

European Medicines Agency. (2019). Retrieved from https://www.ema.europa.eu/en/medicines

Falzone, L., Salomone, S., & Libra, M. (2018). Evolution of cancer pharmacological treatments at the turn of the third millennium. *Frontiers in Pharmacology*, *9*, 1300, 1-26.

Ferlay, J., Shin, H. R., Bray, F., Forman, D., Mathers, C., & Parkin, D. M. (2010). Estimates of worldwide burden of cancer in 2008: GLOBOCAN 2008. *International Journal of Cancer*, *127*, 12, 2893–2917.

Global Burden of Disease Cancer Collaboration, Fitzmaurice C, Allen C, Barber RM, Barregard L, Bhutta ZA, Brenner H, Dicker DJ, Chimed-Orchir O, Dandona R, Dandona L, Fleming T, Forouzanfar MH, Hancock J, Hay RJ, Hunter-Merrill R, Huynh C, Hosgood HD, Johnson CO, Jonas JB, Khubchandani J, Kumar GA, Kutz M, Lan Q, Larson HJ, Liang X, Lim SS, Lopez AD, MacIntyre MF, Marczak L, Marquez N, Mokdad AH, Pinho C, Pourmalek F, Salomon JA, Sanabria JR, Sandar L, Sartorius B, Schwartz SM, Shackelford KA, Shibuya K, Stanaway J, Steiner C, Sun J, Takahashi K, Vollset SE, Vos T, Wagner JA, Wang H, Westerman R, Zeeb H, Zoeckler L, Abd-Allah F, Ahmed MB, Alabed S, Alam NK, Aldhahri SF, Alem G, Alemayohu MA, Ali R, Al-Raddadi R, Amare A, Amoako Y, Artaman A, Asayesh H, Atnafu N, Awasthi A, Saleem HB, Barac A, Bedi N, Bensenor I, Berhane A, Bernabé E, Betsu B, Binagwaho A, Boneya D, Campos-Nonato I, Castañeda-Orjuela C, Catalá-López F, Chiang P, Chibueze C, Chitheer A, Choi JY, Cowie B, Damtew S, das Neves J, Dey S, Dharmaratne S, Dhillon P, Ding E, Driscoll T, Ekwueme D, Endries AY, Farvid M, Farzadfar F, Fernandes J, Fischer F, G/Hiwot TT, Gebru A, Gopalani S, Hailu A, Horino M, Horita N, Husseini A, Huybrechts I, Inoue M, Islami F, Jakovljevic M, James S, Javanbakht M, Jee SH, Kasaeian A, Kedir MS, Khader YS, Khang YH, Kim D, Leigh J, Linn S, Lunevicius R, El Razek HMA, Malekzadeh R, Malta DC, Marcenes W, Markos D, Melaku YA, Meles KG, Mendoza W, Mengiste DT, Meretoja TJ, Miller TR, Mohammad KA, Mohammadi A, Mohammed S, Moradi-Lakeh M, Nagel G, Nand D, Le Nguyen Q, Nolte S, Ogbo FA, Oladimeji KE, Oren E, Pa M, Park EK, Pereira DM, Plass D, Qorbani M, Radfar A, Rafay A, Rahman M, Rana SM, Søreide K, Satpathy M, Sawhney M, Sepanlou SG, Shaikh MA, She J, Shiue I, Shore HR, Shrime MG, So S, Soneji S, Stathopoulou V, Stroumpoulis K, Sufiyan MB, Sykes BL, Tabarés-Seisdedos R, Tadese F, Tedla BA, Tessema GA, Thakur JS, Tran BX, Ukwaja KN, Uzochukwu BSC, Vlassov VV, Weiderpass E, Wubshet Terefe M, Yebyo HG, Yimam HH, Yonemoto N, Younis MZ, Yu C, Zaidi Z, Zaki MES, Zenebe ZM, Murray CJL, Naghavi M. Global, Regional, and National Cancer Incidence, Mortality, Years of Life Lost, Years Lived With Disability, and Disability-Adjusted Life-years for 32 Cancer Groups, 1990 to 2015: A Systematic Analysis for the Global Burden of Disease Study. (2017), *JAMA Oncol*, *3*, 4, 524-548.

Folgiero, V., Cifaldi, L., Pira, G. L., Goffredo, B. M., Vinti, L., & Locatelli, F. (2015). TIM-3/Gal-9 interaction induces IFNγ-dependent IDO1 expression in acute myeloid leukemia blast cells. *Journal of Hematology and Oncology*, *8*, 1, 4–8.

Fonseca, C., & Dranoff, G. (2008). Capitalizing on the immunogenicity of dying tumor cells. *Clinical Cancer Research*, *14*, 6, 1603-1608.

Fornera, S., & Walde, P. (2010). Spectrophotometric quantification of horseradish peroxidase with o-phenylenediamine. *Analytical Biochemistry*, *407*, 2, 293–295.

Fucikova, J., Truxova, I., Hensler, M., Becht, E., Kasikova, L., Moserova, I., Vosahlikova, S., Klouckova, J., Church, S., Cremer, I., Kepp, O., Kroemer, G., Galluzzi, L., Salek, C., Spisek, R. (2016). Calreticulin exposure by malignant blasts correlates with robust anticancer immunity and improved clinical outcome in AML patients. *Blood*, *128*, 26,

3113–3124.

Fukumori, T., Oka, N., Takenaka, Y., Nangia-Makker, P., Elsamman, E., Kasai, T., Shono, M., Kanayama, H. O., Ellerhorst, J., Lotan, R., Raz, A. (2006). Galectin-3 regulates mitochondrial stability and antiapoptotic function in response to anticancer drug in prostate cancer. *Cancer Research*, *66*, 6, 3114–3119.

Gallois, A., Silva, I., Osman, I., & Bhardwaj, N. (2014). Reversal of natural killer cell exhaustion by TIM-3 blockade. *OncoImmunology*, *3*, 12, 1–3.

Gandhi L, Camidge DR, Ribeiro de Oliveira M, et al. (2011). Phase I study of Navitoclax (ABT-263), a novel Bcl-2 family inhibitor, in patients with small-cell lung cancer and other solid tumors. *J Clin Oncol, 29*, 909–16.

Garber, A. J., Pagliara, A., S., Kipnis, D. M. (1976) *J Clin Invest. 58*, 1, 7-15.

Geng, H., Zhang, G. M., Li, D., Zhang, H., Yuan, Y., Zhu, H. G., Xiao, H., Han, L. F., Feng, Z. H. (2006). Soluble Form of T Cell Ig Mucin 3 Is an Inhibitory Molecule in T Cell-Mediated Immune Response. *The Journal of Immunology*, *176*, 3, 1411–1420.

Georgiou, C. D., Grintzalis, K., Zervoudakis, G., & Papapostolou, I. (2008). Mechanism of Coomassie brilliant blue G-250 binding to proteins: a hydrophobic assay for nanogram quantities of proteins. *Anal Bioanal Chem*, *391*, 1, 391–403.

Ghadially, H., Brown, L., Lloyd, C., Lewis, L., Lewis, A., Dillon, J., Sainson, R., Jovanovic, J., Tigue, N. J., Bannister, D., Bamber, L., Valge-Archer, V., Wilkinson, R. W. (2017). MHC class i chain-related protein A and B (MICA and MICB) are predominantly expressed intracellularly in tumour and normal tissue. *British Journal of Cancer*, *116*, 9, 1208–1217.

Giacinti, C., & Giordano, A. (2006). RB and cell cycle progression. *Oncogene*, *25*, 38, 5220–5227.

Gkogkolou, P., & Böhm, M. (2012). Advanced glycation end products: Keyplayers in skin aging? *Dermato-Endocrinology*, *4*, 3, 259–270.

Gleason, M. K., Lenvik, T. R., McCullar, V., Felices, M., O'Brien, M. S., Cooley, S. A., Verneris, M. R., Cichocki, F., Holman, C. J., Panoskaltsis-Mortari, A., Niki, T., Hirashima, M., Blazar, B. R., Miller, J. S. (2012). Tim-3 is an inducible human natural killer cell receptor that enhances interferon gamma production in response to galectin-9. *Blood*, *119*, 13, 3064–3072.

Greenwood, F., C., Landon, J., Stamp, T. (1966) *J Clin Invest. 4*, 4, 429–436.

Golden-Mason, L., McMahan, R. H., Strong, M., Reisdorph, R., Mahaffey, S., Palmer, B. E., Cheng, L,, Kulesza, C., Hirashima, M., Niki, T., Rosen, H. R. (2013). Galectin-9 Functionally Impairs Natural Killer Cells in Humans and Mice. *Journal of Virology*, *87*, 9, 4835–4845.

Gonçalves Silva, I., Rüegg, L., Gibbs, B. F., Bardelli, M., Fruehwirth, A., Varani, L., Berger, S., Fasler-Kan, E., E Sumbayev, V. V. (2016). The immune receptor Tim-3 acts as a trafficker in a Tim-3/galectin-9 autocrine loop in human myeloid leukemia cells.

OncoImmunology, *5*, 7, e1195535.

Gonçalves Silva, I., Yasinska, I. M., Sakhnevych, S. S., Fiedler, W., Wellbrock, J., Bardelli, M., Varani, L., Hussain, R., Siligardi, G., Ceccone, G., Berger, S., M., Ushkaryov, Y., A., Gibbs, B., F., Fasler-Kan, E., Sumbayev, V. V. (2017). The Tim-3-galectin-9 Secretory Pathway is Involved in the Immune Escape of Human Acute Myeloid Leukemia Cells. *EBioMedicine*, *22*, 44–57.

Grotzer, M. A., Hogarty, M. D., Janss, A. J., Liu, X., Zhao, H., Eggert, A., Sutton, L. N., Rorke, L. B.,. Brodeur, G. M., Phillips, P. C. (2001). MYC messenger RNA expression predicts survival outcome in childhood primitive neuroectodermal tumor/medulloblastoma. *Clinical Cancer Research*, *7*, 8, 2425–2433.

Hanahan, D., & Weinberg, R. A. (2011). Hallmarks of cancer: the next generation. *Cell*, *144*, 5, 646–74.

Hann CL, Daniel VC, Sugar EA, et al. Therapeutic efficacy of ABT-737, a selective inhibitor of BCL-2, in small cell lung cancer. Cancer Res 2008;68:2321–8.

Harazono, Y., Nakajima, K., & Raz, A. (2014). Why anti-Bcl-2 clinical trials fail: a solution. *Cancer Metastasis Rev.*, *33*, 1, 285–294.

Hazelton, W. D., & Luebeck, E. G. (2011). Biomarker-based early cancer detection: Is it achievable? *Science Translational Medicine*, *3*, 109, 109fs9.

He, S.-J., Cheng, J., Feng, X., Yu, Y., Tian, L., & Huang, Q. (2017). The dual role and therapeutic potential of high-mobility group box 1 in cancer. *Oncotarget*, *8*, 38, 64534–64550.

Herold, M. J., McPherson, K. G., & Reichardt, H. M. (2006). Glucocorticoids in T cell apoptosis and function. *Cellular and molecular life sciences : CMLS*, *63*, 1, 60–72.

Heusschen, R., Griffioen, A. W., & Thijssen, V. L. (2013). Galectin-9 in tumor biology: A jack of multiple trades. *Biochimica et Biophysica Acta - Reviews on Cancer*, *1836*, 1, 177–185.

Hiom, S. C. (2015). Diagnosing cancer earlier: reviewing the evidence for improving cancer survival. *British Journal of Cancer*, *112*, S1, S1–S5.

Hoang, N. T., Acevedo, L. A., Mann, M. J., & Tolani, B. (2018). A review of soft-tissue sarcomas: Translation of biological advances into treatment measures. Cancer Management and Research, 10, 1089–1114.

Hofvind, S., Ursin, G., Tretli, S., & Møller, B. (2013). Breast cancer mortality in participants of the Norwegian Breast Cancer Screening Program. *Cancer*, *119*, 17, 3106–3112.

Howley, P. (2015). Infectious disease causes of cancer: Opportunities for prevention and treatment. *Transactions of the American Clinical and Climatological Association*, *126*, 117–132.

Hsu, J., Raulet, D. H., Ardolino, M., Hsu, J., Hodgins, J. J., Marathe, M., Nicolai, C., J.,

Bourgeois-Daigneault, M. C., Trevino, T., N., Azimi, C. S., Scheer, A. K., Randolph, H. E., Thompson, T. W., Zhang, L., Iannello, A., Mathur, N., Jardine, K. E., Kirn, G. A., Bell, J. C., McBurney, M. W., Raulet, D. H., Ardolino, M. (2018). Contribution of NK cells to immunotherapy mediated by PD-1 / PD-L1 blockade Graphical abstract Find the latest version : Contribution of NK cells to immunotherapy mediated by PD-1 / PD-L1 blockade. *The Journal of Clinical Investigation*, *128*, 10, 4654–4668.

Hui, J. Y. C. (2016). Epidemiology and Etiology of Sarcomas. *Surgical Clinics of North America*, *96*, 5, 901-14.

Hussain, R., Benning, K., Myatt, D., Javorfi, T., Longo, E., Rudd, T., Pulford, B.,Siligardi, G. (2015). CDApps: integrated softwarefor experimental planning and data processing at beamline B23, Diamond Light Source. *J Synchrotron Radiat.*, *22*, 862.

Hussain, R., Jávorfi, T., & Siligardi, G. (2012). Circular dichroism beamline B23 at the Diamond Light Source. *J Synchrotron Radiat.*, *19*, 132–135.

Janeway, C., Murphy, K., Travers, P., & Walport, M. (2012). *Janeway's immunobiology* (8th editio). New York: Garland Science.

Jilkine, A., & Gutenkunst, R. N. (2014). Effect of Dedifferentiation on Time to Mutation Acquisition in Stem Cell-Driven Cancers. *PLoS Computational Biology*, *10*, 3, e1003481.

John, T., Caballero, O. L., Svobodová, S. J., Kong, A., Chua, R., Browning, J., Fortunato, S., Deb, S., Hsu, M., Gedye, C. A., Davis, I. D., Altorki, N., Simpson, A. J., Chen, Y. T., Monk, M., Cebon, J. S. (2008). ECSA/DPPA2 is an embryo-cancer antigen that Is coexpressed with cancer-testis antigens in non-small cell lung cancer. *Clinical Cancer Research*, *14*, 11, 3291–3298.

Jossé, L., Xie, J., Proud, C. G., & Smales, C. M. (2016). mTORC1 signalling and eIF4E/4E-BP1 translation initiation factor stoichiometry influence recombinant protein productivity from GS-CHOK1 cells. *The Biochemical journal*, *473*, 24, 4651–4664.

Kang, C. W., Dutta, A., Chang, L. Y., Mahalingam, J., Lin, Y. C., Chiang, J. M., Hsu, C. Y., Huang, C. T., Su, W. T., Chu, Y. Y., Lin, C. Y. (2015). Apoptosis of tumor infiltrating effector TIM-3+CD8+ T cells in colon cancer. *Scientific Reports*, *5*, 1–12.

Kang MH, Kang YH, Szymanska B, et al. Activity of vincristine, L-ASP, and dexamethasone against acute lymphoblastic leukemia is enhanced by the BH3-mimetic ABT-737 in vitro and in vivo. Blood 2007;110:2057–66.

Karakosta, A., Golias, Ch., Charalabopoulos, A., Peschos, D., Batistatou, A., Charalabopoulos, K. (2005). Genetic models of human cancer as a multistep process. Paradigm models of colorectal cancer, breast cancer, and chronic myelogenous and acute lymphoblastic leukaemia. *Journal of Experimental & Clinical Cancer Research*, *24*, 4, 505-514.

Kelleher, F., Fennelly, D., & Rafferty, M. (2006). Common critical pathways in embryogenesis and cancer. *Acta Oncologica*, *45*, 4, 375–388.

Kierdorf, K., & Fritz, G. (2013). RAGE regulation and signaling in inflammation and beyond. *Journal of Leukocyte Biology*, *94*, 1, 55–68.

Kikushige, Y., & Miyamoto, T. (2013). TIM-3 as a novel therapeutic target for eradicating acute myelogenous leukemia stem cells. *International Journal of Hematology*, *98*, 6, 627–633.

Kikushige, Y., Miyamoto, T., Yuda, J., Jabbarzadeh-Tabrizi, S., Shima, T., Takayanagi, S., Niiro, H, Yurino, A., Miyawaki, K., Takenaka, K., Iwasaki, H., Akashi, K. (2015). A TIM-3 / Gal-9 Autocrine Stimulatory Loop Drives Self-Renewal of Human Myeloid Leukemia Stems and Leukemic Progression. *Stem Cell*, *17*, 3, 341–352.

Koenig, J.I., & Cho, J.Y. (2005). Provocation of kainic acid receptor mRNA changes in the rat paraventricular nucleus by insulin-induced hypoglycaemia. *Journal of neuroendocrinology*, *17*, 2, 111-8 .

Kominami, K., Nakabayashi, J., Nagai, T., Tsujimura, Y., Chiba, K., Kimura, H., Miyawaki, A., Sawasaki, T., Yokota, H., Manabe, N., Sakamaki, K. (2012). The molecular mechanism of apoptosis upon caspase-8 activation: Quantitative experimental validation of a mathematical model. *Biochimica et Biophysica Acta - Molecular Cell Research*, *1823*, 10, 1825–1840.

Konopleva M, Contractor R, Tsao T, et al. Mechanisms of apoptosis sensitivity and resistance to the BH3 mimetic ABT-737 in acute myeloid leukemia. Cancer Cell 2006;10: 375–88.

Krasnoperov, V., Bittner, M. A., Holz, R. W., Chepurny O. and Petrenko, A. G. (1999) Structural Requirements for α-Latrotoxin Binding and α-Latrotoxin-stimulated Secretion. *The Journal of Biological Chemistry*, *274*, 3590-3596.

Krock, B. L., Skuli, N., & Simon, M. C. (2011). Hypoxia-Induced Angiogenesis: Good and Evil. *Genes and Cancer*, *2*, 12, 1117–1133.

Krump, N. A., & You, J. (2018). Molecular mechanisms of viral oncogenesis in humans. *Nature Reviews Microbiology*, *16*, 11, 684–698.

Krzewski, K., & Coligan, J. E. (2012). Human NK cell lytic granules and regulation of their exocytosis. *Frontiers in Immunology*, *3*, 335, 1–16.

Kurinna, S., Konopleva, M., Palla, S. L., Chen, W., Kornblau, S., Contractor, R., Deng, X., May, W. S., Andreeff, M., Ruvolo, P. P. (2006). Bcl2 phosphorylation and active PKC α are associated with poor survival in AML. *Leukemia*, *20*, 7, 1316–1319.

Kursunel, M. A., & Esendagli, G. (2016). The untold story of IFN-γ in cancer biology. *Cytokine and Growth Factor Reviews*, *31*, 73–81.

Landy, R., Pesola, F., Castañón, A., & Sasieni, P. (2016). Impact of cervical screening on cervical cancer mortality: Estimation using stage-specific results from a nested case-control study. *British Journal of Cancer*, *115*, 9, 1140–1146.

Lara-Gonzalez, P., Westhorpe, F. G., & Taylor, S. S. (2012). The spindle assembly checkpoint. *Current Opinion in Cell Biology*, *22*, 22, 967–980.

Latest global cancer data: Cancer burden rises to 18.1 million new cases and 9.6 million cancer deaths in 2018, PRESS RELEASE N° 263. (2018). Retrieved from http://gco.iarc.fr/

Lee, E. J., & Park, J. H. (2013). Receptor for Advanced Glycation Endproducts (RAGE), Its Ligands, and Soluble RAGE: Potential Biomarkers for Diagnosis and Therapeutic Targets for Human Renal Diseases. *Genomics & Informatics*, *11*, 4, 224–229.

Lee, E. Y.-H. P., & Abbondante, S. (2014). Tissue-specific tumor suppression by BRCA1. *Proceedings of the National Academy of Sciences*, *111*, 12, 4353–4354.

Lee, Y. K., Lin, T. H., Chang, C. F., & Lo, Y. L. (2013). Galectin-3 Silencing Inhibits Epirubicin-Induced ATP Binding Cassette Transporters and Activates the Mitochondrial Apoptosis Pathway via β-Catenin/GSK-3β Modulation in Colorectal Carcinoma. *PLOS ONE*, *8*, 11, e82478.

Lelianova V. G., Davletov B. A., Sterling A., Rahman M. A., Grishin E. V., Totty N. F., Ushkaryov Y. A. (1997). *J Biol Chem*, *272*, 34, 21504-8.

Li, G., Liang, X., & Lotze, M. T. (2013). HMGB1: The central cytokine for all lymphoid cells. *Frontiers in Immunology*, *4*, 68, 1–9.

Li, J., Kokkola, R., Tabibzadeh, S., Yang, R., Ochani, M., Qiang, X., Harris, H. E., Czura, C. J., Wang, H., Ulloa, L., Wang, H., Warren, H. S., Moldawer, L. L., Fink, M. P., Andersson, U., Tracey, K. J., Yang, H. (2003). Structural basis for the proinflammatory cytokine activity of high mobility group box 1. *Molecular Medicine*, *9*, 1–2, 37–45.

Liu, Q., Zhang, H., Jiang, X., Qian, C., Liu, Z., & Luo, D. (2017). Factors involved in cancer metastasis: A better understanding to "seed and soil" hypothesis. *Molecular Cancer*, *16*, 1, 176.

Liu, S., Edgerton, S. M., Ii, D. H. M., & Thor, A. D. (2001). Measures of Cell Turnover (Proliferation and Apoptosis) and Their Association with Survival in Breast Cancer 1. *Clin Cancer Res*, *7*, 6, 1716-23.

Liu, Z., Han, H., He, X., Li, S., Wu, C., Yu, C., & Wang, S. (2016). Expression of the galectin-9-tim-3 pathway in glioma tissues is associated with the clinical manifestations of glioma. *Oncology Letters*, *11*, 3, 1829–1834.

Liu G, Kelly WK, Wilding G, Leopold L, Brill K, Somer B. An open-label, multicenter, phase I/II study of single-agent AT-101 in men with castrate-resistant prostate cancer. Clin Cancer Res 2009;15:3172–6.

Lock R, Carol H, Houghton PJ, et al. Initial testing (stage 1) of the BH3 mimetic ABT-263 by the pediatric preclinical testing program. Pediatr Blood Cancer 2008;50:1181–9

Long, E. O. (2002). Tumor cell recognition by natural killer cells. *Seminars in Cancer Biology*, *12*, 1, 57–61.

Loud, J. T., & Murphy, J. (2017). Cancer Screening and Early Detection in the 21 st Century. *Seminars in Oncology Nursing*, *33*, 3, 121–128.

Lu, F., Zhang, J., Ji, M., Li, P., Du, Y., Wang, H., Zang, S., Ma, D., Sun, X., Ji, C. (2014). miR-181b increases drug sensitivity in acute myeloid leukemia via targeting HMGB1 and Mcl-1. *International Journal of Oncology*, *45*, 1)=, 383–392.

Luzzi, K. J., MacDonald, I. C., Schmidt, E. E., Kerkvliet, N., Morris, V. L., Chambers, A. F., & Groom, A. C. (1998). Multistep nature of metastatic inefficiency: Dormancy of solitary cells after successful extravasation and limited survival of early micrometastases. *American Journal of Pathology*, *153*, 3, 865–873.

Mabuchi, R., Hara, T., Matsumoto, T., Shibata, Y., Nakamura, N., Nakamura, H., Kitagawa, J., Kanemura, N., Goto, N., Shimizu, M., Ito, H., Yamamoto, Y., Saito, K., Moriwaki, H., Tsurumi, H. (2016). High serum concentration of L-kynurenine predicts unfavorable outcomes in patients with acute myeloid leukemia. *Leukemia and Lymphoma*, *57*, 1, 92–98.

Maiga, A., Lemieux, S., Pabst, C., Lavallée, V. P., Bouvier, M., Sauvageau, G., & Hébert, J. (2016). Transcriptome analysis of G protein-coupled receptors in distinct genetic subgroups of acute myeloid leukemia: Identification of potential disease-specific targets. *Blood Cancer Journal*, *6*, 6, 1–9.

Marmot, M. G., Altman, D. G., Cameron, D. A., Dewar, J. A., Thompson, S. G., & Wilcox, M. (2013). The benefits and harms of breast cancer screening: An independent review. *British Journal of Cancer*, *108*, 11, 2205–2240.

Mazzoccoli, G., Carughi, S., De Cata, A., La Viola, M., Giuliani, A., Tarquini, R., Perfetto, F. (2003). Neuroendocrine alterations in lung cancer patients. *Neuro Endocrinol Lett*, *24*, 1-2, 77-82.

Micol, V., Sánchez-Piñera, P., Villalaín, J., De Godos, A., & Gómez-Fernández, J. C. (1999). Correlation between protein kinase C α activity and membrane phase behavior. *Biophysical Journal*, *76*, 2, 916–927.

Miller, D. M., Thomas, S. D., Islam, A., Muench, D., & Sedoris, K. (2012). c-Myc and cancer metabolism. *Clinical Cancer Research, 18*, 20, 5546-53

Möller-Hackbarth, K., Dewitz, C., Schweigert, O., Trad, A., Garbers, C., Rose-John, S., & Scheller, J. (2013). A disintegrin and metalloprotease (ADAM) 10 and ADAM17 are major sheddases of T cell immunoglobulin and mucin domain 3 (Tim-3). *Journal of Biological Chemistry*, *288*, 48, 34529–34544.

Moresco, E. M. Y., LaVine, D., & Beutler, B. (2017). Toll-like receptors. *Clinical and Basic Immunodermatology: Second Edition*, *21*, 13, R488–R493.

Morgan, A., Burgoyne, R. D., Barclay, J. W., Craig, T. J., Prescott, G. R., Ciufo, L. F., Evans, L. F., Graham, M. E. (2005). Regulation of exocytosis by protein kinase C. *Biochemical Society Transactions*, *33*, 6, 1341 LP-1344.

Miyanishi, N., Nishi, N., Abe, H., Kashio, Y., Shinonaga, R., Nakakita, S., Sumiyoshi, W., Yamauchi, A., Nakamura, T., Hirashima, M., Hirabayashi, J. (2007). Carbohydrate-recognition domains of galectin-9 are involved in intermolecular interaction with galectin-9 itself and other members of the galectin family. *Glycobiology*, *17*, 4, 423–432.

Nagae, M., Nishi, N., Murata, T., Usui, T., Nakamura, T., Wakatsuki, S., & Kato, R. (2006). Crystal structure of the galectin-9 N-terminal carbohydrate recognition domain from Mus musculus reveals the basic mechanism of carbohydrate recognition. *Journal of Biological Chemistry*, *281*, 47, 35884–35893.

Narumi, K., Miyakawa, R., Ueda, R., Hashimoto, H., Yamamoto, Y., Yoshida, T., & Aoki, K. (2015). Proinflammatory Proteins S100A8/S100A9 Activate NK Cells via Interaction with RAGE. *The Journal of Immunology*, *194*, 11, 5539–5548.

Nicholas, S. A., Bubnov, V. V, Yasinska, I. M., & Sumbayev, V. V. (2011). Involvement of xanthine oxidase and hypoxia-inducible factor 1 in Toll-like receptor 7/8-mediated activation of caspase 1 and interleukin-1β. *Cellular and Molecular Life Sciences*, *68*, 1, 151–158.

Nicholas, S. A., Coughlan, K., Yasinska, I., Lall, G. S., Gibbs, B. F., Calzolai, L., & Sumbayev, V. V. (2011). Dysfunctional mitochondria contain endogenous high-affinity human Toll-like receptor 4 (TLR4) ligands and induce TLR4-mediated inflammatory reactions. *International Journal of Biochemistry and Cell Biology*, *43*, 4, 674–681.

Nurgali, K., Jagoe, R. T., & Abalo, R. (2018). Editorial: Adverse Effects of Cancer Chemotherapy: Anything New to Improve Tolerance and Reduce Sequelae? *Frontiers in Pharmacology*, *9*, 245, 1-3.

Ocaña-Guzman, R., Torre-Bouscoulet, L., & Sada-Ovalle, I. (2016). TIM-3 regulates distinct functions in macrophages. *Frontiers in Immunology*, *7*, 229, 1–9.

Oltersdorf T, Elmore SW, Shoemaker AR, et al. An inhibitor of Bcl-2 family proteins induces regression of solid tumours. Nature 2005;435:677–81

Osińska, I., Popko, K., & Demkow, U. (2014). Perforin: An important player in immune response. *Central European Journal of Immunology*, *39*, 1, 109–115.

O'Sullivan M. L., De Wit J., Savas J. N., Comoletti D., Otto-Hitt S., Yates J. R., III, Ghosh A. (2012). FLRT proteins are endogenous latrophilin ligands and regulate excitatory synapse development. *Neuron. 73*, 903–910.

Ouakrim, D. A., Pizot, C., Boniol, M., Malvezzi, M., Boniol, M., Negri, E., Bota, M., Jenkins, M., Bleiberg, H., Autier, P. (2015). Trends in colorectal cancer mortality in Europe: Retrospective analysis of the WHO mortality database. *BMJ (Online)*, *351*, h4970, 1-10.

Ozaki, T., & Nakagawara, A. (2011). Role of p53 in cell death and human cancers. *Cancers*, *3*, 1, 994–1013.

Paci, E., Broeders, M., Hofvind, S., & Duffy, S. W. (2012). Summary of the evidence of breast cancer service screening outcomes in Europe and first estimate of the benefit and harm balance sheet. *Journal of Medical Screening*, *19 Suppl 1*, 5–13.

Panarese, I., Aquino, G., Ronchi, A., Longo, F., Montella, M., Cozzolino, I., Roccuzzo, G., Colella, G., Caraglia, M., Franco, R. (2019). Oral and Oropharyngeal squamous cell carcinoma: prognostic and predictive parameters in the etiopathogenetic route. *Expert Review of Anticancer Therapy*, *19*, 2, 105–119.

Parkin, D. M. (2001). Global cancer statistics in the year 2000. *Lancet Oncol*, *2*, 533–543.

Parkin, D. M., Bray, F., Ferlay, J., & Pisani, P. (2005). Global Cancer Statistics, 2002. *Cancer Journal for Clinicians*, *55*, 2, 74–108.

Passegué, E., Jamieson, C., Ailles, L., & Weissman, I. (2003). Normal and leukemic hematopoiesis: Are leukemias a stem cell disorder or a reacquisition of stem cell characteristics? *PNAS*, *100*, 1, 11842–11849.

Patel, A. P., Fisher, J. L., Nichols, E., Abd-Allah, F., Abdela, J., Abdelalim, A., Abraha, H. N., Agius, D., Alahdab, F., Alam, T., Allen, C. A., Anber, N. H., Awasthi, A., Badali, H., Belachew, A. B., Bijani, A., Bjørge, T., Carvalho, F., Catalá-López, F., Choi, J. Y. J., Daryani, A., Degefa, M. G., Demoz, G. T., Do, H. P., Dubey, M., Fernandes, E., Filip, I., Foreman, K. J., Gebre, A. K., Geramo, Y. C. D., Hafezi-Nejad, N., Hamidi, S., Harvey, J. D., Hassen, H. Y., Hay, S. I., Irvani, S. S. N., Jakovljevic, M., Jha, R. P.,Kasaeian, Khalil, I. A., Khan, E. A., Khang, Y. H., Kim, Y. J., Mengistu, G., Mohammad, K. A., Mokdad, A. H., Nagel, G., Naghavi, M., Naik, G., Nguyen, H. L. T., Nguyen, L. H., Nguyen, T. H., Nixon, M. R., Olagunju, A. T., Pereira, D. M., Pinilla-Monsalve, G. D., Poustchi, H., Qorbani, M., Radfar, A., Reiner, R. C., Roshandel, G., Safari, H., Safiri, S., Samy, A. M., Sarvi, S., Shaikh, M. A., Sharif, M., Sharma, R., Sheikhbahaei, S., Shirkoohi, R., Singh, J. A., Smith, M., Tabarés-Seisdedos, R., Tran, B. X., Tran, K. B., Ullah, I., Weiderpass, E., Weldegwergs, K. G., Yimer, E. M., Zadnik, V., Zaidi, Z., Ellenbogen, R. G., Vos, T., Feigin, V. L., Murray, C. J. L., Fitzmaurice, C. (2019). Global, regional, and national burden of brain and other CNS cancer, 1990–2016: a systematic analysis for the Global Burden of Disease Study 2016. *The Lancet Neurology*, *18*, 4, 376–393.

Paul, S., & Lal, G. (2017). The molecular mechanism of natural killer cells function and its importance in cancer immunotherapy. *Frontiers in Immunology*, *8*, 1124, 1–15.

Pegram, H. J., Andrews, D. M., Smyth, M. J., Darcy, P. K., & Kershaw, M. H. (2011). Activating and inhibitory receptors of natural killer cells. *Immunology and Cell Biology*, *89*, 2, 216–224.

Pelengaris, S., & Khan, M. (2013). *The Molecular Biology of Cancer* (6th ed.).

Pellettieri, J., & Alvarado, A. S. (2007). Cell Turnover and Adult Tissue Homeostasis: From Humans to Planarians. *Annual Review of Genetics*, *41*, 1, 83–105.

Peng, P. ji, Li, Y., & Sun, S. (2017). On the significance of Tim-3 expression in pancreatic cancer. *Saudi Journal of Biological Sciences*, *24*, 8, 1754–1757.

Pieper, R., Christian, R. E., Gonzales, M. I., Nishimura, M. I., Gupta, G., Settlage, R. E., Shabanowitz, J., Rosenberg, S. A., Hunt, D. J., Topalian, S. L. (1999). Biochemical Identification of a Mutated Human Melanoma Antigen Recognized by CD4 + T Cells. *The Journal of Experimental Medicine*, *189*, 5, 757–766.

Prokhorov, A., Gibbs, B. F., Bardelli, M., Rüegg, L., Fasler-Kan, E., Varani, L., & Sumbayev, V. V. (2015). The immune receptor Tim-3 mediates activation of PI3 kinase/mTOR and HIF-1 pathways in human myeloid leukaemia cells. *International Journal of Biochemistry and Cell Biology*, *59*, 11–20.

Ramsay, A. D. (1990). The Histopathological Diagnosis of Cancer. In *Cancer Biology and Management: An Introduction*. Wiley.

Rashid, G., Benchetrit, S., Fishman, D., & Bernheim, J. (2004). Effect of advanced glycation end-products on gene expression and synthesis of TNF-α and endothelial nitric

oxide synthase by endothelial cells. *Kidney International*, *66*, 3, 1099–1106.

Reuter, S., Gupta, S. C., Chaturvedi, M. M., & Aggarwal, B. B. (2010). Oxidative stress, inflammation, and cancer: How are they linked? *Free Radical Biology and Medicine*, *49*, 11, 1603-1616.

Richiardi, L., & Terracini, B. (2015). *International Agency for Research on Cancer. The first 50 years*. *International Journal of Epidemiology*, 45, 3, 967–968.

Rinehart, J., Keville, L., Clayton, S., Figueroa, J. A. (1997). Corticosteroids alter hematopoiesis in vitro by enhancing human monocyte secretion of granulocyte colony-stimulating factor. *Exp Hematol. 25*, 5, 405-12.

Riss, T. L., Moravec, R. A., Niles, A. L., Duellman, S., Benink, H. A., Worzella, T. J., & Minor, L. (2013). Cell Viability Assays. In *Assay Guidance Manual* (pp. 1–31). Retrieved from http://www.ncbi.nlm.nih.gov/pubmed/23805433

Rivlin, N., Brosh, R., Oren, M., & Rotter, V. (2011). Mutations in the p53 tumor suppressor gene: Important milestones at the various steps of tumorigenesis. *Genes and Cancer*, *2*, 4, 466-74.

Roh, J. S., & Sohn, D. H. (2018). Damage-Associated Molecular Patterns in Inflammatory Diseases. *Immune Network*, *18*, 4, e27.

Roux, P. P., Ballif, B. A., Anjum, R., Gygi, S. P., & Blenis, J. (2004). Tumor-promoting phorbol esters and activated Ras inactivate the tuberous sclerosis tumor suppressor complex via p90 ribosomal S6 kinase. *Proceedings of the National Academy of Sciences*, *101*, 37, 13489–13494.

Rue, P., & Martinez Arias, A. (2015). Cell dynamics and gene expression control in tissue homeostasis and development. *Molecular Systems Biology*, *11*, 2, 792.

Ruvolo, P. P. (2016). Galectin 3 as a guardian of the tumor microenvironment. *Biochimica et Biophysica Acta - Molecular Cell Research*, *1863*, 3, 427–437.

Salesse, S., & Verfaillie, C. M. (2002). BCR/ABL: From molecular mechanisms of leukemia induction to treatment of chronic myelogenous leukemia. *Oncogene*, *21*, 56, 8547–8559.

Salmaninejad, A., Valilou, S. F., Shabgah, A. G., Aslani, S., Alimardani, M., Pasdar, A., & Sahebkar, A. (2019). PD-1/PD-L1 pathway: Basic biology and role in cancer immunotherapy. *Journal of Cellular Physiology*, *234*, 10, 16824-16837

Sansom, D. M. (2000). CD28, CTLA-4 and their ligands: who does what and to whom? *Immunology*, *101*, 2, 169–77.

Sato, Y., Goto, Y., Narita, N., & Hoon, D. S. B. (2009). Cancer cells expressing toll-like receptors and the tumor microenvironment. In *Cancer Microenvironment, 2 Suppl 1*, 205-14.

Schaefer, M. H., & Serrano, L. (2016). Cell type-specific properties and environment shape tissue specificity of cancer genes. *Scientific Reports*, *6*, 20707, 1-14.

Schlotter, C. M., Vogt, U., Bosse, U., Mersch, B., & Waßmann, K. (2003). C-myc, not HER-2/neu, can predict recurrence and mortality of patients with node-negative breast cancer. *Breast Cancer Research*, *5*, 2, R30-R36.

Schrepf, A., Thaker, P. H., Goodheart, M. J., Bender, D., Slavich, G. M., Dahmoush, L., Penedo, F., DeGeest, K., Mendez, L., Lubaroff. D. M., Cole, S. W., Sood, A. K., Lutgendorf, S. K. (2015). Diurnal cortisol and survival in epithelial ovarian cancer. *Psychoneuroendocrinology, 53*, 256–267.

Schrepf A, Thaker PH, Goodheart MJ, Bender D, Slavich GM, Dahmoush L, Penedo F, DeGeest K, Mendez L, Lubaroff DM, Cole SW, Sood AK, Lutgendorf SK. Diurnal cortisol and survival in epithelial ovarian cancer. Psychoneuroendocrinology. 2015 Mar;53:256-67. doi: 10.1016/j.psyneuen.2015.01.010. Epub 2015 Jan 20. PMID: 25647344; PMCID: PMC4440672.

Seliger, B., Marincola, F., Ferrone, S., & Abken, H. (2008). The complex role of B7 molecules in tumor immunology. *Trends Mol Med*, *14*, 12, 550–559.

Sephton, S. E., Lush, E., Dedert, E. A., Floyd, A. R., Rebholz, W. N., Dhabhar, F. S., Spiegel, D., Salmon, P. (2013). *Brain Behav Immun. 30,* S163-S170.

Seyfried, T., & Huysentruyt, L. (2013). The Origin of Cancer Metastasis. *Crit Rev Oncog.*, *18*, 1–2, 43–73.

Shaul, Y., & Ben-Yehoyada, M. (2005). Role of c-Abl in the DNA damage stress response. *Cell Research*, *15,* 33–35.

Siligardi, G., & Hussain, R. (2015). CD Spectroscopy: An Essential Tool for Quality Control of Protein Folding. *Methods Mol Biol*, *1261*, 255–276.

Silva, I. G., Gibbs, B. F., Bardelli, M., Varani, L., & Sumbayev, V. V. (2015). Differential expression and biochemical activity of the immune receptor Tim-3 in healthy and malignant human myeloid cells. *Oncotarget*, *6*, 32, 33823-33.

Silva J. P., Ushkaryov Y. A. (2010). The latrophilins, “split personality” receptors. *Adv. Exp. Med. Biol. 706*, 59–75.

Smith J.K., Chu Q.D., Tseng J.F. (2015) Pancreatic Adenocarcinoma. In: Chu Q., Gibbs J., Zibari G. (eds) Surgical Oncology. Springer, New York, NY

Spalding, K. L., Bhardwaj, R. D., Buchholz, B. A., Druid, H., & Frisén, J. (2005). Retrospective birth dating of cells in humans. *Cell*, *122*, 1, 133–143.

Stöckli, J., Fazakerley, D. J., & James, D. E. (2011). GLUT4 exocytosis. *Journal of Cell Science*, *124*, 24, 4147–4159.

Sumbayev, V. V., Yasinska, I., Oniku, A. E., Streatfield, C. L., & Gibbs, B. F. (2012). Involvement of hypoxia-inducible factor-1 in the inflammatory responses of human LAD2 mast cells and basophils. *PLoS ONE, 7*, 3, e34259.

Sumbayev, V. V, & Nicholas, S. A. (2010). Hypoxia-inducible Factor 1 as one of the “Signaling Drivers” of Toll-like Receptor-Dependent and Allergic Inflammation.

Archivum Immunologiae et Therapiae Experimentalis, *58*, 4, 287–294.

Sumbayev, V. V, Silva, I. G., Blackburn, J., Bernhard, F., Yasinska, I. M., Garrett, M. D., Tonevitsky, A. G., Yuri, A. (2016). Expression of functional neuronal receptor latrophilin 1 in human acute myeloid leukaemia cells. *Oncotarget*, *7*, 29, 45575–45583.

Susan, E. (2007). Apoptosis: A Reveiw of Programmed Cell Death. *Toxicologic Pathology*, *35*, 4, 496–516.

Swamydas, M., & Lionakis, M. S. (2013). Isolation, Purification and Labeling of Mouse Bone Marrow Neutrophils for Functional Studies and Adoptive Transfer Experiments. *Journal of Visualized Experiments*, *7*, 29, 45575–45583.

Szczepański, T., van der Velden, V. H. J., & van Dongen, J. J. M. (2003). Classification systems for acute and chronic leukemias. *Best Practice and Research: Clinical Haematology*, *16*, 4, 561–582.

Tanaka, T., Narazaki, M., & Kishimoto, T. (2014). IL-6 in Inflammation, Immunity, and Disease, *6*, 10, a016295.

Tang, D., Kang, R., Livesey, K. M., Cheh, C. W., Farkas, A., Loughran, P., Hoppe, G., Bianchi, M. E., Tracey, K. J., Zeh, H. J., Lotze, M. T. (2010). Endogenous HMGB1 regulates autophagy. *Journal of Cell Biology*, *190*, 5, 881–892.

Tang, L., Chai, W., Ye, F., Yu, Y., Cao, L., Yang, M., Xie, M., Yang, L. (2017). HMGB1 promotes differentiation syndrome by inducing hyperinflammation via MEK/ERK signaling in acute promyelocytic leukemia cells. *Oncotarget*, *8*, 16, 27314–27327.

ten Broeke, T., Wubbolts, R., & Stoorvogel, W. (2013). MHC class II antigen presentation by dendritic cells regulated through endosomal sorting. *Cold Spring Harbor Perspectives in Biology*, *5*, 12, a016873.

Thijssen, V. L. J. L., Poirier, F., Baum, L. G., & Griffioen, A. W. (2007). Galectins in the tumor endothelium: Opportunities for combined cancer therapy. *Blood*, *110*, 8, 2819–2827.

Thomson, R. H., Allison, P. J., & Kwon, E. D. (2006). Anti-cytotoxic T lymphocytes antigen-4 (CTLA-4) immunotherapy for the treatment of prostate cancer. *Urol Oncol.*, *24*, 5, 442–447.

Tippin, B., Pham, P., & Goodman, M. F. (2004). Error-prone replication for better or worse. *Trends in Microbiology*, *12*, 6, 288-95.

Torpy, J. D., & Chrousos, P. G. (1996). The three-way interactions between the hypothalamic-pituitary-adrenal and gonadal axes and the immune system. *Bailliere's Clinical Rheumatology*, *10*, 2, 181–198.

Torre, L. A., Siegel, R. L., Ward, E. M., & Jemal, A. (2016). Global cancer incidence and mortality rates and trends - An update. *Cancer Epidemiology Biomarkers and Prevention*, *25*, 1, 16-27.

Tse C, Shoemaker AR, Adickes J, et al. ABT-263: a potent and orally bioavailable Bcl-2 family inhibitor. Cancer Res 2008;68:3421–8.

Uthoff, S. M. S., Duchrow, M., Schmidt, M. H. H., Broll, R., Bruch, H. P., Strik, M. W., & Galandiuk, S. (2002). VEGF isoforms and mutations in human colorectal cancer. *International Journal of Cancer*, *101*, 1, 32–36.

van Horssen, R., Ten Hagen, T. L. M., & Eggermont, A. M. M. (2006). TNF-alpha in Cancer Treatment: Molecular Insights, Antitumor Effects, and Clinical Utility. *The Oncologist*, *11*, 4, 397–408.

Vanessa, H., Wenshuo, W., Cornelia, D., Simon, W., Martin, T., & Wolfgang, P. (2018). Microwave-assisted one-step synthesis of white light-emitting carbon dot suspensions. *Optical Materials*, *80*, 110–119.

Vicentino, A. R. R., Carneiro, V. C., Allonso, D., Guilherme, R. de F., Benjamim, C. F., dos Santos, Xavier, F., dos Santos Pyrrho, A., de Assis Silva Gomes, J., de Castro Fonseca, M., de Oliveira, R. C., Pereira, T. A., Ladislau, L., Lambertucci, J. R., Fantappié, M. R. (2018). Emerging role of HMGB1 in the pathogenesis of schistosomiasis liver fibrosis. *Frontiers in Immunology*, *9*, 1979, 1–15.

Vigneron, N. (2015). Human Tumor Antigens and Cancer Immunotherapy. *BioMed Research International*, *2015*, 948501, 1–17.

Volynski, K. E., Meunier, F. A., Lelianova, V. G., Dudina, E. E., Volkova, T. M., Rahman, M. A., Manser, C., Grishin, E. V., Dolly, J. O., Ashley, R. H., Ushkaryov, Y. A. (2000). Latrophilin, neurexin, and their signaling-deficient mutants facilitate α-latrotoxin insertion into membranes but are not involved in pore formation. *Journal of Biological Chemistry*, *275*, 52, 41175–41183.

Wang, F., He, W., Zhou, H., Yuan, J., Wu, K., Xu, L., & Chen, Z. K. (2007). The Tim-3 ligand galectin-9 negatively regulates CD8 + alloreactive T cell and prolongs survival of skin graft. *Cellular Immunology*, *250*, 1–2, 68–74.

Wang, Q., Zeng, M., Wang, W., & Tang, J. (2007). The HMGB1 acidic tail regulates HMGB1 DNA binding specificity by a unique mechanism. *Biochemical and Biophysical Research Communications*, *360*, 1, 14–19.

Wang, W., Erbe, A. K., Hank, J. A., Morris, Z. S., & Sondel, P. M. (2015). NK cell-mediated antibody-dependent cellular cytotoxicity in cancer immunotherapy. *Frontiers in Immunology*, *6*, 368, 1–15.

Wei, M. C., Lindsten, T., Mootha, V. K., Weiler, S., Gross, A., Ashiya, M., Thompson, C. B., Korsmeyer, S. J. (2000). tBID, a membrane-targeted death ligand , oligomerizes BAK to release cytochrome c. *Genes and Development*, *14*, 16, 2060–2071. https://doi.org/10.1101/GAD.14.16.2060

Weinberg, R. A. (2007). The Nature of Cancer. In E. Zayatz & K. R. Mickey (Eds.), *The Biology of Cancer*. Garland Science, Taylor & Francis Group, LLC.

Wever, R., Krenn, B. E., & Renirie, R. (2018). Marine Vanadium-Dependent Haloperoxidases, Their Isolation, Characterization, and Application. In *Methods in Enzymology* (1st ed., Vol. 605, pp. 141–201). Elsevier Inc. https://doi.org/10.1016/bs.mie.2018.02.026

White, G. R. M., Varley, J. M., & Heighway, J. (1998). Isolation and characterization of a human homologue of the latrophilin gene from a region of 1p31.1 implicated in breast cancer. *Oncogene, 17*, 26, 3513–3519.

Wong, M. C. S., Lao, X. Q., Ho, K. F., Goggins, W. B., & Tse, S. L. A. (2017). Incidence and mortality of lung cancer: Global trends and association with socioeconomic status. *Scientific Reports, 7*, 14300, 1-9.

World Health Organization (2018). Cancer. Retrieved from https://www.who.int/en/news-room/fact-sheets/detail/cancer

Wroblewski, L. E., Peek, R. M., & Wilson, K. T. (2010). Helicobacter pylori and gastric cancer: Factors that modulate disease risk. *Clinical Microbiology Reviews*. *23*, 4, 713-39.

Wyszynski, R. W., Gibbs, B. F., Varani, L., Iannotta, D., & Sumbayev, V. V. (2016). Interleukin-1 beta induces the expression and production of stem cell factor by epithelial cells: Crucial involvement of the PI-3K/mTOR pathway and HIF-1 transcription complex. *Cellular and Molecular Immunology*, *13*, 1, 47–56.

Xie, J., Reverdatto, S., Frolov, A., Hoffmann, R., Burz, D. S., & Shekhtman, A. (2008). Structural basis for pattern recognition by the receptor for advanced glycation end products (RAGE). *Journal of Biological Chemistry, 283*, 40, 27255–27269.

Yamauchi, A., Kontani, K., Kihara, M., Nishi, N., Yokomise, H., & Hirashima, M. (2006). Galectin-9, a Novel Prognostic Factor with Antimetastatic Potential in Breast Cancer. *The Breast Journal*, *12*, s2, S196–S200.

Yang, D., Hendifar, A., Lenz, C., Togawa, K., Lenz, F., Lurje, G., Pohl, A., Winder, T., Ning, Y., Groshen, S., Lenz, H. J. (2011). Survival of metastatic gastric cancer: Significance of age, sex and race/ethnicity. *Journal of Gastrointestinal Oncology*, *2*, 2, 77-84.

Yang, H., & Tracey, J. K. (2010). Targeting HMGB1 in inflammation. *Biochim Biophys Acta, 1799*, 1-2, 149–156.

Yang, S., Xu, L., Yang, T., & Wang, F. (2014). High-mobility group box-1 and its role in angiogenesis. *Journal of Leukocyte Biology*, *95*, 4, 563–574.

Yasinska, I. M., Gibbs, B. F., Lall, G. S., & Sumbayev, V. V. (2014). The HIF-1 transcription complex is essential for translational control of myeloid hematopoietic cell function by maintaining mTOR phosphorylation. *Cellular and Molecular Life Sciences*, *71*, 4, 699–710.

Yasinska, I. M., Gonçalves Silva, I., Sakhnevych, S., Gibbs, B. F., Raap, U., Fasler-Kan, E., & Sumbayev, V. V. (2018). Biochemical mechanisms implemented by human acute myeloid leukemia cells to suppress host immune surveillance. *Cellular and Molecular Immunology*, *15*, 11, 989-991.

Yasinska, I. M., Gonçalves Silva, I., Sakhnevych, S. S., Ruegg, L., Hussain, R., Siligardi, G., Fiedler, W., Wellbrock, J., Bardelli, M., Varani, L., Raap, U., Berger, S., Gibbs, B. F., Fasler-Kan, E., Sumbayev, V. V. (2018). High mobility group box 1 (HMGB1) acts as an "alarmin" to promote acute myeloid leukaemia progression. *OncoImmunology*, *7*, 6, 1–8.

Yoshida, T., Akagi, Y., Kinugasa, T., & Shiratsuchi, I. (2011). Clinicopathological Study on Poorly Differentiated Adenocarcinoma of the Colon. *Kurume Medical Journal*, *58*, 41–46.

Yu, Y., Xie, M., Kang, R., Livesey, K. M., Cao, L., & Tang, D. (2012). HMGB1 is a therapeutic target for leukemia. *American Journal of Blood Research*, *2*, 1, 36–43.

Zappa, C., & Mousa, S. A. (2016). Non-small cell lung cancer: current treatment and future advances. *Translational Lung Cancer Research*, *5*, 3, 288–300.

Zhang, Y., Liu, Y., & Xu, X. (2017). Upregulation of miR-142-3p Improves Drug Sensitivity of Acute Myelogenous Leukemia through Reducing P-Glycoprotein and Repressing Autophagy by Targeting HMGB1. *Translational Oncology*, *10*, 3, 410–418.

Zhao B, Zhang J, Mei D, Luo R, Lu H, Xu H, H. B. (2019). Does Helicobacter pylori Eradication Reduce the Incidence of Metachronous Gastric Cancer After Curative Endoscopic Resection of Early Gastric Cancer: A Systematic Review and Meta-Analysis. *Journal of Clinical Gastroenterology*.

Zhuang, X., Zhang, X., Xia, X., Zhang, C., Liang, X., Gao, L., Zhang, X., Ma, C. (2012). Ectopic Expression of TIM-3 in Lung Cancers. *American Journal of Clinical Pathology*, *137*, 6, 978–985.

11. APPENDIX

11.1 Electrophoresis solutions

11.1.1 SDS-polyacrylamide gels

Table 9: PAGEs preparation

	4%	**7.5%**	**10%**	**12%**
H_2O	3.2 ml	5.525 ml	4.9 ml	4.4 ml
1.5 M Tris-HCl (pH 8.8)	1.25 ml	2.5 ml	2.5 ml	2.5 ml
40% Acrylamide/Bis-acrylamide	0.5 ml	1.875 ml	2.5 ml	3.0 ml
10% (w/v) SDS	50 µl	100 µl	100 µl	100 µl
10% (w/v) APS	100 µl	125 µl	125 µl	125 µl
TEMED	20 µl	25 µl	25 µl	25 µl

11.1.2 1.5 M Tris-HCL pH 8.8

Tris 181.5 g
H_2O 1 l
Adjust pH to 8.8 with HCl.

11.1.3 0.5 M Tris-HCL pH 6.8

Tris 60.5 g
H_2O 1 l
Adjust pH to 6.8 with HCl.

11.1.4 10X Running buffer (8.3)

Tris 30 g
Glycine 144 g
SDS 10 g
Add distilled water until 1 l and check the pH.

11.1.5 Sample buffer

Table 10: Sample Buffer preparation

	2X
0.5 M Tris-HCl pH 6.8	1.25 ml
10% SDS	2 ml
Glycerol	2.5 ml
Bromophenol	10 mg
H_2O	3.75

To this solution, DTT was added prior to use. For 4X sample buffer the quantity of chemical compounds was double.

11.2 Western blot buffers

11.2.1 10X Blotting Buffer (pH 8.3)

Tris 30.3 g
Glycine 144 g
H2O 1 l
Check if the pH is 8.3 but do not adjust it.

11.2.2 1X Blotting Buffer (with 20% Methanol)

10X Blotting buffer
100 ml Methanol
200 ml H2O 700 ml

11.2.3 10X TBS buffer (9% NaCl, 100 mM Tris HCl, pH 7.4)

Tris 12.11 g
NaCl 90 g
H2O 1 l
Adjust the pH to 7.4, using HCl.

11.2.4 1X TBST buffer (pH 7.4)

10X TBS buffer
100 ml Tween 20
0.5 ml H2O 900 ml

11.3 List of Publications

EBioMedicine 22 (2017) 44–57

Contents lists available at ScienceDirect

EBioMedicine

journal homepage: www.ebiomedicine.com

Research Paper

The Tim-3-galectin-9 Secretory Pathway is Involved in the Immune Escape of Human Acute Myeloid Leukemia Cells

Isabel Gonçalves Silva [a,1], Inna M. Yasinska [a,1], Svetlana S. Sakhnevych [a], Walter Fiedler [b], Jasmin Wellbrock [b], Marco Bardelli [c], Luca Varani [c], Rohanah Hussain [d], Giuliano Siligardi [d], Giacomo Ceccone [e], Steffen M. Berger [f], Yuri A. Ushkaryov [a,*], Bernhard F. Gibbs [a,g,*], Elizaveta Fasler-Kan [f,h,*], Vadim V. Sumbayev [a,*]

[a] School of Pharmacy, University of Kent, Chatham Maritime, UK
[b] Department of Oncology, Hematology and Bone Marrow Transplantation with Section Pneumology, Hubertus Wald University Cancer Center, University Medical Center Hamburg-Eppendorf, Germany
[c] Institute for Research in Biomedicine, Universita' della Svizzera italiana (USI), Bellinzona, Switzerland
[d] Beamline 23, Diamond Light Source, Didcot, UK
[e] European Commission Joint Research Centre, Ispra, Italy
[f] Department of Pediatric Surgery and Department of Clinical Research, Children's Hospital, Inselspital, University of Bern, Switzerland
[g] Department of Dermatology, University of Oldenburg, Germany
[h] Department of Biomedicine, University of Basel, Switzerland

ARTICLE INFO

Article history:
Received 16 June 2017
Received in revised form 12 July 2017
Accepted 17 July 2017
Available online 19 July 2017

Keywords:
Acute myeloid leukemia
Tim-3
Galectin-9
NK cells
Anti-leukemia immunity

ABSTRACT

Acute myeloid leukemia (AML) is a severe and often fatal systemic malignancy. Malignant cells are capable of escaping host immune surveillance by inactivating cytotoxic lymphoid cells. In this work we discovered a fundamental molecular pathway, which includes ligand-dependent activation of ectopically expressed latrophilin 1 and possibly other G-protein coupled receptors leading to increased translation and exocytosis of the immune receptor Tim-3 and its ligand galectin-9. This occurs in a protein kinase C and mTOR (mammalian target of rapamycin)-dependent manner. Tim-3 participates in galectin-9 secretion and is also released in a free soluble form. Galectin-9 impairs the anti-cancer activity of cytotoxic lymphoid cells including natural killer (NK) cells. Soluble Tim-3 prevents secretion of interleukin-2 (IL-2) required for the activation of cytotoxic lymphoid cells. These results were validated in ex vivo experiments using primary samples from AML patients. This pathway provides reliable targets for both highly specific diagnosis and immune therapy of AML.

© 2017 Published by Elsevier B.V. This is an open access article under the CC BY-NC-ND license (http://creativecommons.org/licenses/by-nc-nd/4.0/).

1. Introduction

Acute myeloid leukemia (AML) is a blood/bone marrow cancer originating from self-renewing malignant immature myeloid precursors, which rapidly becomes a systemic malignancy. It is often a fatal disease because malignant cells are capable of suppressing anti-cancer immunity by impairing the functional activity of natural killer (NK) cells and cytotoxic T cells (Golden-Mason et al., 2013; Wang et al., 2007; Khaznadar et al., 2014). Recent evidence clearly demonstrated an involvement of the T cell immunoglobulin and mucin domain 3 (Tim-3) - galectin-9 pathway in this immune escape mechanism (Golden-Mason et al., 2013; Kikushige et al., 2015; Gonçalves Silva et al., 2016). Galectin-9 is a β-galactoside-binding lectin, which has a tandem structure and contains two carbohydrate recognition domains (CRDs) fused together by a peptide (Delacour et al., 2009). Galectin-9 has a specific receptor on AML cells known as Tim-3 which also could act as its possible trafficker (galectin-9 as all other galectins lacks a signal sequence required for transport into the endoplasmic reticulum (ER) and thus requires a trafficking protein for its secretion (Hughes, 1999; Delacour et al., 2009)). However, the mechanisms underlying the activation of biosynthesis of the components of the Tim-3-galectin-9 autocrine loop, galectin-9 secretion and its effects on cytotoxic lymphocytes (NK cells and T cells) remain poorly understood.

Recently, we discovered that human AML cells – but not healthy leukocytes – express physiologically active latrophilin 1 (LPHN1; Sumbayev et al., 2016). LPHN1, an adhesion G-protein-coupled receptor, is highly expressed in neuronal axon terminals and in many secretory cells (Davletov et al., 1998; Silva and Ushkaryov, 2010). In all cells expressing this receptor, LPHN1 activation by its most potent agonist, α-latrotoxin (LTX) from black widow spider venom (Ushkaryov, 2002), triggers intracellular Ca^{2+} signaling and exocytosis of neurotransmitters and hormones (Volynski et al., 2003). Similarly, ligand-

* Corresponding authors.
E-mail addresses: Ushkaryov@kent.ac.uk (Y.A. Ushkaryov), bernhard.gibbs@uni-oldenburg.de (B.F. Gibbs), elizaveta.fasler@insel.ch (E. Fasler-Kan), V.Sumbayev@kent.ac.uk (V.V. Sumbayev).
[1] IGS and IMY contributed equally to this work.

http://dx.doi.org/10.1016/j.ebiom.2017.07.018
2352-3964/© 2017 Published by Elsevier B.V. This is an open access article under the CC BY-NC-ND license (http://creativecommons.org/licenses/by-nc-nd/4.0/).

induced activation of LPHN1 in AML cells facilitates exocytosis of cytokines and growth factors (Sumbayev et al., 2016). Production of LPHN1 in AML cells is controlled by the mammalian target of rapamycin (mTOR) (Sumbayev et al., 2016), a highly conserved serine/threonine kinase that acts as a central regulator of growth and metabolism in healthy and malignant human myeloid cells (Yasinska et al., 2014). To function in cell-cell interactions and cell signaling, LPHN1 can interact with at least two endogenous ligands, Lasso/teneurin-2 (Silva et al., 2011) and fibronectin leucine rich transmembrane protein 3 (FLRT3) (Boucard et al., 2014), although only FLRT3 seems to be expressed in peripheral tissues. In addition to triggering exocytosis by increasing cytosolic Ca^{2+}, LPHN1 can enhance the sensitivity of the release machinery by activating protein kinase C (Liu et al., 2005), which is also thought to be involved in galectin-9 secretion (Chabot et al., 2002). Based on these observations, we hypothesized that activation of LPHN1 by its ligands can induce secretion of galectin-9, thus protecting AML cells against NK and cytotoxic T cells. This hypothesis has been studied experimentally in the present study.

Here we report that the Tim-3-galectin-9 autocrine loop is activated in AML cells through protein kinase C (PKC)/mTOR pathways. These pathways trigger translation of both Tim-3 and galectin-9 and induce high levels of galectin-9 secretion as well as the release of soluble Tim-3. Importantly, this effect was also verified in the AML patients studied. Galectin-9 was found to impair AML cell killing by primary human NK cells. Soluble Tim-3 reduced the ability of T cells to secrete IL-2, a cytokine, which is required for the activation of both NK cells and cytotoxic T cells (Dhupkar and Gordon, 2017). Blood plasmas of AML patients contained significantly lower amounts of IL-2 compared to those of healthy donors. We confirmed that PKC activation occurred in AML cells in a LPHN1-dependent manner. The LPHN1 agonist LTX and natural ligand FLRT3 upregulated the Tim-3-galectin-9 autocrine loop in a PKC-dependent manner. Based on our findings, we conclude that LPHN1/PKC/mTOR/Tim-3-galectin-9 is a biosynthetic and secretory pathway which is operated by human AML cells resulting in a decrease of immune surveillance and promotion of disease progression.

2. Materials and Methods

2.1. Materials

RPMI-1640 medium, fetal bovine serum and supplements and basic laboratory chemicals were purchased from Sigma (Suffolk, UK). Maxisorp™ microtitre plates were provided either by Nunc (Roskilde, Denmark) and Oxley Hughes Ltd. (London, UK). Mouse monoclonal antibodies directed against mTOR and β-actin, as well as rabbit polyclonal antibodies against phospho-S2448 mTOR, galectin-9, HRP-labelled rabbit anti-mouse secondary antibody were purchased from Abcam (Cambridge, UK). Mouse monoclonal antibody against FLRT3 was obtained from Santa Cruz Biotechnology (Heidelberg, Germany). The polyclonal rabbit anti-peptide antibody (PAL1) against LPHN1 was described previously (Davydov et al., 2009). LTX was purified as previously described (Ashton et al., 2000). Goat anti-mouse and goat anti-rabbit fluorescence dye-labelled antibodies were obtained from LI-COR (Lincoln, Nebraska USA). ELISA-based assay kits for the detection of galectin-9, Tim-3 and IL-2 were purchased from Bio-Techne (R&D Systems, Abingdon, UK). Anti-Tim-3 mouse monoclonal antibody, its single chain variant as well as human Ig-like V-type domain of Tim-3 (amino acid residues 22–124), expressed and purified from *E. coli* (Prokhorov et al., 2015) were used in our work. Secondary antibodies for confocal laser microscopy and imaging flow cytometry (goat anti-mouse and goat anti-rabbit Alexa 488, Alexa 555 and Alexa 647) were from Invitrogen (Carlsbad, USA). All other chemicals purchased were of the highest grade of purity.

2.2. Cell Lines and Primary Human Cells

THP-1 human myeloid leukemia monocytes, K562 chronic myelogenous leukemia cells and Jurkat T cells were obtained from the European Collection of Cell Cultures (Salisbury, UK). Renal clear cell carcinoma RCC-FG1 cells were obtained from CLS Cell Lines Service (Eppelheim, Germany). Cells were cultured in RPMI 1640 media supplemented with 10% fetal bovine serum, penicillin (50 IU/ml) and streptomycin sulfate (50 μg/ml). LAD2 mast cells were kindly provided by A. Kirshenbaum and D. Metcalfe (NIH, USA). Cells were cultured in StemPro-34 serum-free media in the presence of 100 ng/ml SCF (Kirshenbaum et al., 2003).

Primary human AML mononuclear blasts (AML-PB001F, newly diagnosed/untreated) were purchased from AllCells (Alameda, CA, USA) and handled in accordance with the manufacturer's instructions. Primary human NK cells were purified from buffy coat blood (prepared from healthy donors) obtained from the National Health Blood and Transfusion Service (NHSBT, UK) following ethical approval (REC reference: 16-SS-033). Primary CD34-positive HSCs were obtained from Lonza (Basel, Switzerland).

Femur bones of six-week-old C57 BL16 mice (25 ± 2.5 g, kindly provided by Dr. Gurprit Lall, School of Pharmacy, University of Kent) were used for the experiments following approval by the Institutional Animal Welfare and Ethics Review Body. Animals were handled by authorized personnel in accordance with the Declaration of Helsinki protocols. Bone marrow was isolated from femur bone heads as described before (Swamydas and Lionakis, 2013) and whole extracts (1 mg protein/ml) were then obtained.

2.3. Primary Human Plasma Samples

Blood plasma of healthy donors was obtained from buffy coat blood (originated from healthy donors undergoing routine blood donation) which was purchased from the National Health Blood and Transfusion Service (NHSBT, UK) following ethical approval (REC reference: 16-SS-033). Primary human AML plasma samples were obtained from the sample bank of University Medical Centre Hamburg-Eppendorf (Ethik-Kommission der Ärztekammer Hamburg, reference: PV3469).

2.4. Western Blot Analysis

Tim-3, galectin-9, FLRT3, LPHN1 and Gαq were analyzed by Western blot and compared to β-actin in order to verify equal protein loading, as previously described (Yasinska et al., 2014). Briefly, cells were lysed using lysis buffer (50 mM Tris–HCl, 5 mM EDTA, 150 mM NaCl, 0.5% Nonidet-40, 1 mM PMSF, pH 8.0). After centrifugation, the protein content in the supernatants was analyzed. Finally, samples were added to the same volume of 2× sample buffer (125 mM Tris–HCl, 2% sodium dodecyl sulfate (SDS), 10% glycerine, 1 mM dithiothreitol (DTT), 0.002% bromophenol blue, pH 6.9) and boiled for 5 min. Proteins were resolved using SDS–polyacrylamide gels followed by blotting onto nitrocellulose membranes. Molecular weights were calibrated in proportion to the running distance of rainbow markers. For all primary antibodies (see Materials section) a 1:1000 dilution was used, except those against LPHN1 and FLRT3 (where a 1:500 dilution was used). β-actin staining was used to confirm equal protein loading as described previously (Yasinska et al., 2014). LI-COR goat secondary antibodies (dilution 1:2000), conjugated with fluorescent dyes, were used in accordance with manufacturer's protocol to visualize target proteins (using a LI-COR Odyssey imaging system). Western blot data were quantitatively analyzed using Odyssey software and values were subsequently normalized against those of β-actin.

2.5. Characterization of Tim-3 and Galectin-9 in Tissue Culture Medium

Secreted Tim-3 and galectin-9 were characterized in the RPMI-1640 medium used to culture THP-1 cells. The proteins were first precipitated on Maxisorp ELISA plates (see Materials section). For this purpose ELISA plates were coated overnight using single-chain antibody against Tim-3. Plates were then blocked with 2% BSA. Tissue culture medium was then applied and incubated for 4 h at room temperature, followed by extensive washing with TBST buffer. Proteins were then extracted using 0.2 M glycine-HCl buffer (pH 2.0). Extracts were neutralized using lysis buffer and subjected to Western blot analysis using mouse anti-Tim-3 and rabbit anti-galectin-9 antibodies as described before (Gonçalves Silva et al., 2016) and above.

2.6. Enzyme-linked Immunosorbent Assays (ELISAs)

Galectin-9, sTim-3 and IL-2 were measured by ELISA using R&D Systems kits according to manufacturer's protocols. In all cases the procedure involves specific detection of captured target proteins using biotinylated detection antibody. The interaction was then analyzed using streptavidin conjugated with horseradish peroxidase (HRP) according to the manufacturer's protocol. Tim-3-galectin-9 complex was also analyzed by ELISA. Single-chain antibody (described above, dilution 1:100) was used to capture the complex and biotinylated goat R&D Systems antibody against galectin-9 (detection antibody) was used to detect galectin-9 bound to Tim-3. HRP-labelled streptavidin was then used to perform quantitative analysis according to the R&D Systems protocol for the galectin-9 assay kit. Phosphorylation of mTOR was analyzed by ELISA as previously described (Yasinska et al., 2014).

2.7. In Cell Assays and in Cell Westerns

We employed a standard LI-COR in-cell Western (ICW) assay (methanol was used as permiabilization agent) to analyze total Tim-3 and galectin-9 expressions in the studied cells. The in-cell (ICA, also called on-cell) assay was employed to characterize Tim-3 and galectin-9 surface presence in the studied cells. We also used this assay to visualize binding of LAD2 cells to NK cells. IgE-sensitized LAD2 cells were exposed for 5 min to 1 μg/ml, carefully washed with sterile PBS and exposed to LI-COR goat anti-mouse labelled secondary antibody. Following washing with PBS, cells were scanned using a LI-COR Odyssey imaging system (Gonçalves Silva et al., 2016).

2.8. Confocal Microscopy and Imaging Flow Cytometry

THP-1 cells were grown on 12 mm cover glasses in 24-well plates. Cells were treated (o/n) with PMA and then fixed/permeabilized for 20 min with ice-cold MeOH or MeOH/acetone. Alternatively cells were fixed in a freshly prepared 2% paraformaldehyde, washed 3 times with PBS and then permeabilized with 0.1%TX-100. Cover glasses were blocked for 1 h at RT with 10% goat serum in PBS. 1 μg/ml anti-Tim-3 antibody and anti-galectin-9 antibody were used as primary antibodies and incubated o/n at 4 °C. Goat-anti-mouse Alexa Fluor 488 and goat-anti-rabbit Alexa Fluor 555 were used as secondary antibodies. Cells were incubated with secondary antibodies for 45 min at RT. The preparations were examined on Olympus laser scanning confocal microscope as described (Prokhorov et al., 2015; Fasler-Kan et al., 2010). Images were collected and analyzed using proprietary image acquisition software. Imaging flow cytometry was performed in accordance with a previously described protocol (Fasler-Kan et al., 2016). Briefly, permiabilized cells were stained with mouse anti-Tim-3 and rabbit anti-galectin-9 antibodies for 1 h at room temperature. Goat anti-mouse Alexa Fluor 647 and goat-anti-rabbit Alexa Fluor 488 were used as secondary antibodies. Images were collected and analyzed using IDEAS analytical software on ImageStream X mark II (Amnis-EMD-Millipore, USA).

2.9. Synchrotron Radiation Circular Dichroism Spectroscopy

Human recombinant Tim-3, human recombinant galectin-9 and Tim-3-galectin-9 complex were analyzed using SRCD spectroscopy at beam line 23, Diamond Light Source (Didcot, UK). SRCD measurements were performed using 0.2 μg/ml of samples in 10 cm path length cell, 3 mm aperture diameter and 800 μl capacity using Module B with 1 nm increment, 1 s integration time, 1.2 nm bandwidth at 23 °C (Hussain et al., 2012a, 2012b; Siligardi and Hussain, 2015). The results obtained were processed using CDApps (Hussain et al., 2015) and OriginLab™.

2.10. PKCα Activity Assay

The catalytic activity of PKCα was measured as described before based on its ability to phosphorylate specific substrate in a reaction buffer containing 20 mM Tris-HCl (pH 7.5), 20 μM ATP, 5 mM $MgCl_2$ and 200 μM $CaCl_2$ (Micol et al., 1999). Phosphate groups attached to the substrate were detected using colorimetric assay (Abooali et al., 2014).

2.11. Cell Viability Assay

Cell viability was analyzed using the Promega UK Ltd. (Southampton, UK) assay kit. We used an MTS colorimetric assay for assessing cell metabolic activity. NAD(P)H-dependent cellular oxidoreductase enzymes playing crucial role in human myeloid cell survival (Sumbayev and Nicholas, 2010), reflect the number of viable cells present. Cells were incubated with 3-(4,5-dimethylthiazol-2-yl)-5-(3-carboxymethoxyphenyl)-2-(4-sulfophenyl)-2H-tetrazolium (MTS) and then absorbance was measured at 490 nm in accordance with the manufacturer's protocol.

2.12. Leukemia Cell Protection Assay

K562 and NK cells were cultured separately or as a 1:2 co-culture (K562:NK) for 16 h, at 37 °C, in the absence or presence of 0.5–5 ng/ml of galectin-9. The unfixed cell cultures were then imaged under an inverted microscope (TE200, Nikon), using phase-contrast lighting, a digital camera and the WinFluor image acquisition software (J. Dempster, University of Strathclyde). Raw images were analyzed using the ImageJ software (Schindelin et al., 2015), including illumination correction, background subtraction, overlapping cells separation, edge artefacts elimination, and particle size optimization (based on the size difference between K562 and NK cells). The selected areas were then applied to the raw images for automatic cell counting.

2.13. Statistical Analysis

Each experiment was performed at least three times and statistical analysis when comparing two events at a time was conducted using a two-tailed Student's *t*-test. Multiple comparisons were performed using ANOVA test. Post-hoc Bonferroni correction was applied. Statistical probabilities (p) were expressed as * where $p < 0.05$; **, $p < 0.01$ and *** when $p < 0.001$.

3. Results

3.1. Differential Proteolytic Enzymes are Involved in the Secretion of the Tim-3 and Galectin-9 Complex in Human AML Cells

We investigated differential proteolytic shedding of free and galectin-9-bound Tim-3 from the surface of human AML cells as a possible mechanism for the secretion of these proteins. Firstly, we examined the medium used to culture THP-1 human AML cells with or without 16 h exposure to 100 nM phorbol 12-myristate 13-acetate (PMA) known to activate proteolytic shedding of Tim-3 (Moller-

Hackbarth et al., 2013). We then immunoprecipitated Tim-3 from the medium and extracted the precipitate as outlined in the Materials and Methods. Extracts were subjected to Western blot analysis followed by specific detection of galectin-9 and Tim-3. Specific galectin-9 bands appeared at around 32 kDa (molecular weight of galectin-9) as well as 52 kDa (Fig. 1A). Interestingly, the 52 kDa band was also detectable by anti-Tim-3 antibody (Fig. 1A), suggesting that this band corresponds to the unbroken Tim-3-galectin-9 complex. Furthermore, specific Tim-3 bands appeared at around 33 kDa (molecular weight of soluble Tim-3 – sTim-3) and around 20 kDa. This 20 kDa band is likely to be a fragment of Tim-3 shed together with galectin-9 being released from the complex during the Western blot procedure (Fig. 1A). This suggests that the Tim-3 protein fragment complexed with galectin-9 might be shed at different cleavage site(s). Interestingly, the amount of all the proteins detected was clearly higher in PMA-treated samples.

It has recently been found that Tim-3 can be shed from the cell surface by a disintegrin and metalloproteinase domain-containing proteins (ADAM) 10/17 (Moller-Hackbarth et al., 2013). We therefore investigated whether these proteases are associated with release of free Tim-3 and/or of the galectin-9-Tim-3 complex. We exposed THP-1 cells for 16 h to 100 nM PMA, after which the PMA-containing medium was removed and replaced with the same medium containing 100 μM GI254023X (ADAM 10 and 17 inhibitor) or 100 μM BB-94, a matrix metalloproteinase inhibitor. The cells were incubated for 4 h and levels of Tim-3 and galectin-9 were then measured in the culture medium by ELISA. We also measured soluble Tim-3-galectin-9 complex by capturing Tim-3 using a single-chain antibody and then detecting galectin-9 using a biotinylated anti-galectin-9 antibody. We found that PMA treatment significantly upregulated sTim-3 release as well as the release of galectin-9 (a similar increase was observed in the Tim-3-galectin-9 complex, Fig. 1B). GI254023X and BB-94 decreased PMA-induced sTim-3 release but did not affect the release of either galectin-9 or the Tim-3-galectin-9 complex (Fig. 1B), suggesting that this complex is differentially shed from the cell surface.

3.2. Protein Kinase C is Involved in the Activation of Tim-3 and Galectin-9 co-secretion by AML Cells

We considered the levels of Tim-3 and galectin-9 remaining in THP-1 cells following 16 h of exposure to specific PKC activator PMA. It was found that, despite the levels of released sTim-3, galectin-9 and Tim-3-galectin-9 complex were increased in PMA-treated cells, the levels of respective cell-associated proteins decreased (Fig. 2). Interestingly, a specific band in the range of 70 kDa detectable by both anti-Tim-3 and anti-galectin-9 antibodies was present in all the assays (Fig. 2). This molecular weight corresponds to a sum of those of uncleaved Tim-3 and galectin-9. This indicates that a complex between full Tim-3 and galectin-9 is first formed before undergoing shedding, which results in a release of its soluble form corresponding to the 52 kDa species, as described above. Our observations were confirmed by co-localization assays using confocal microscopy (Fig. 3). Following 24 h exposure to 100 nM PMA, paraformaldehyde-fixed non-permeabilized and methanol-permeabilized THP-1 human AML cells were investigated. We found that both galectin-9 and Tim-3 were present on the cell surface. In permeabilized cells there was clear evidence of co-localization

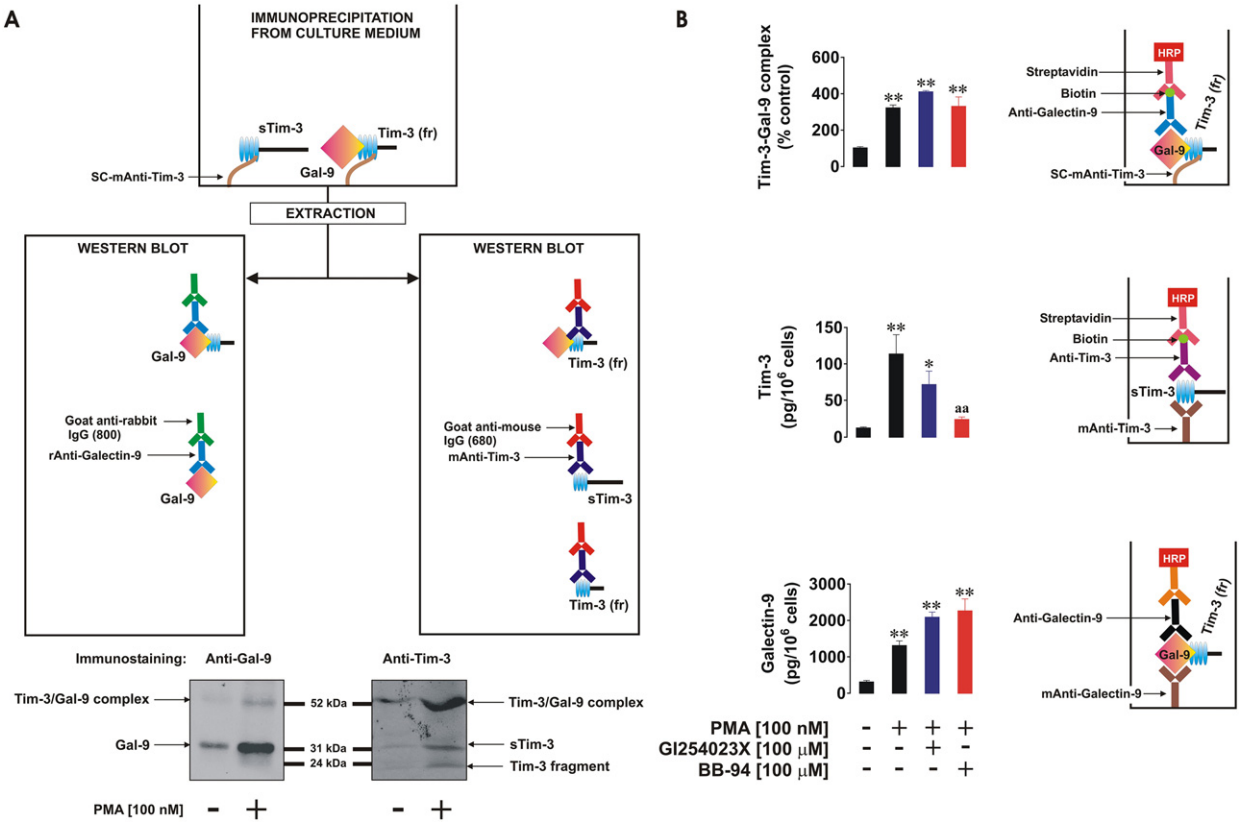


Fig. 1. Free and galectin-9-bound Tim-3 is shed differentially from the cell surface. THP-1 cells were exposed for 16 h to 100 nM PMA; medium was then exchanged for fresh PMA-free medium and cells exposed to the indicated concentrations of GI254023X (ADAM10/17 inhibitor) and BB-94 (matrix metalloproteinase inhibitor). Non treated THP-1 cells were incubated for 16 h after which medium was changed and cells incubated for further 4 h and used as a control. Western blot characterization of galectin-9 and Tim-3 variants (20 kDa fragment (Tim-3 (fr)) and 33 kDa (sTim-3)) was performed in medium collected after final 4 h of incubation of resting and PMA-pre-treated THP-1 cells as outlined in the Materials and Methods (A). All the samples were subjected to ELISA-based detection of galectin-9, soluble Tim-3 and Tim-3-galectin-9 complex (B). Images are from one experiment representative of six which gave similar results. Quantitative data represent mean values ± SEM of six independent experiments; $^{*}p < 0.05$; $^{**}p < 0.01$ vs. control.

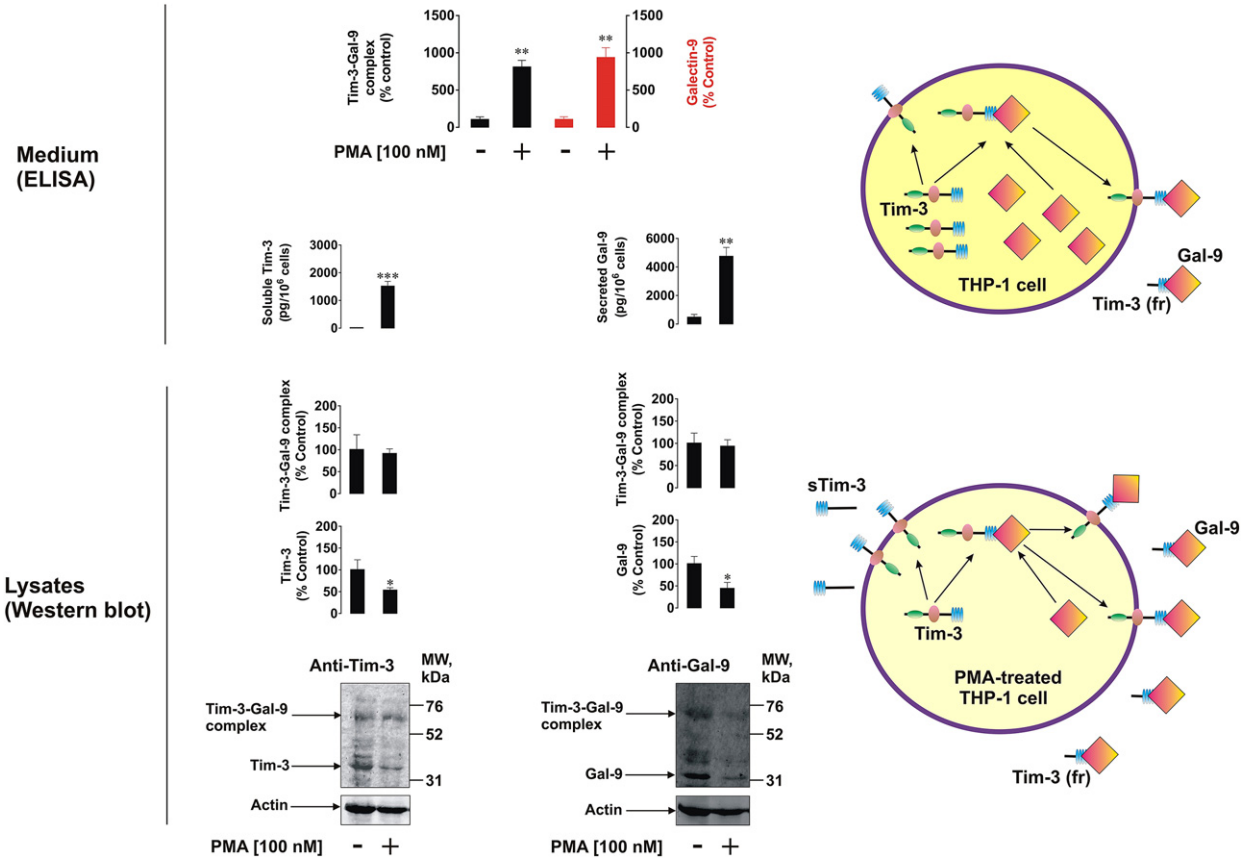


Fig. 2. PMA activates Tim-3 and galectin-9 production and release as well as generation of Tim-3-galectin-9 complex. THP-1 cells were treated with 100 nM PMA for 16 h. Non-treated THP-1 cells were used as a control. Cells were then harvested and galectin-9 as well as Tim-3 were analyzed in whole cell extracts by Western blot. Both proteins and Tim-3-galectin-9 complexes were analyzed by ELISA in the medium used to treat the cells. The bar diagram on the top shows the comparative analysis (expressed in % control) of galectin-9 and Tim-3-galectin-9 complex levels released by non-treated and PMA-treated THP-1 cells. Images are from one experiment representative of three which gave similar results. Quantitative data are the mean values ± SEM of three independent experiments; $^{*}p < 0.05$; $^{**}p < 0.01$; $^{***}p < 0.001$ vs. control.

of both proteins. These findings were confirmed using imaging flow cytometry (Supplementary Fig. 1). In non-permeabilized cells we saw sectors full of either Tim-3 or galectin-9, without substantial co-localization. Given that galectin-9 is soluble, it can remain on the cell surface only if it is bound to its receptor, Tim-3 (Fig. 3). Taken together our findings suggest that Tim-3 is either externalized on its own or acts as a trafficker for galectin-9 (which lacks the signal domain required for secretion and thus requires a trafficker). Given that PMA, a specific PKC activator, significantly increases Tim-3 and galectin-9 secretion, it is likely that PKC is involved in the Tim-3 and galectin-9 co-secretion process.

3.3. Levels of Soluble Tim-3 and Galectin-9 are Highly Increased in the Blood Plasma of AML Patients: Characterization of the Tim-3-galectin-9 Complex in Human Blood Plasma

We then sought to confirm our findings in primary samples collected from AML patients. We analyzed plasma samples from 98 AML patients versus healthy donors and found that galectin-9 and Tim-3 levels were strikingly increased in blood plasma of AML patients (Fig. 4A, B, E and F). Five randomly selected plasma samples from the group of studied AML patients and five from healthy donors were then subjected to detection

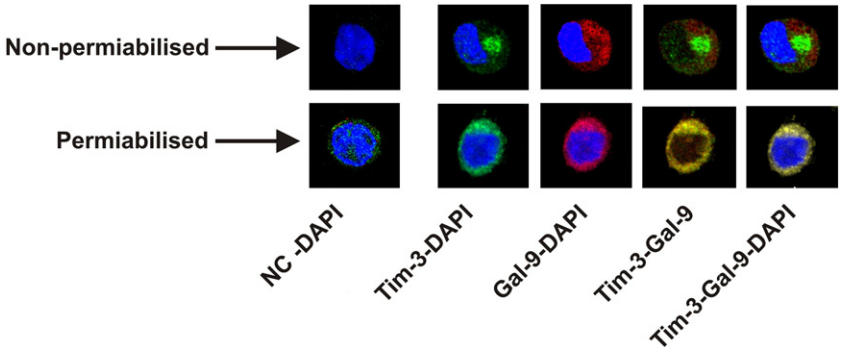


Fig. 3. Co-localization of Tim-3 and galectin-9 in PMA-activated THP-1 cells. Co-localization of Tim-3 and galectin-9 was analyzed in non-permeabilized and permeabilized THP-1 cells following 24 h of exposure to 100 nM PMA using confocal microscopy (see Materials and Methods for details). Images are from one experiment representative of six which gave similar results.

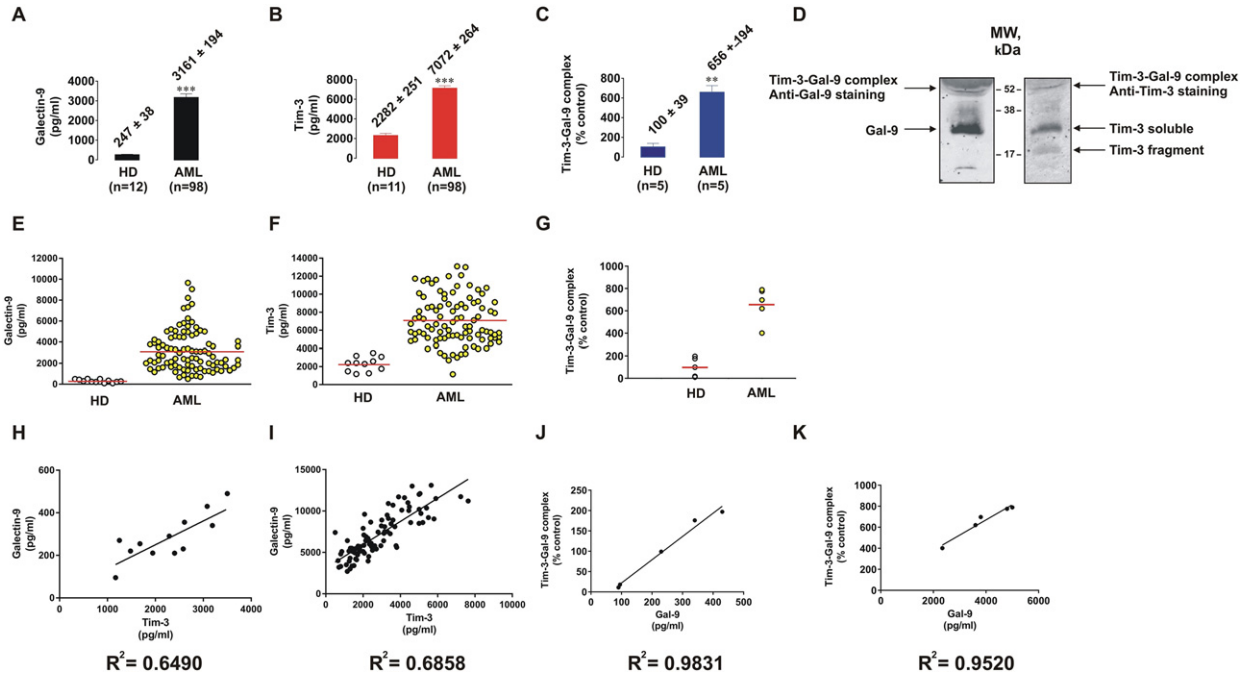


Fig. 4. Levels of galectin-9 and soluble Tim-3 are highly increased in blood plasma of AML patients. Galectin-9 and Tim-3 were measured by ELISA in blood plasma obtained from healthy donors and AML patients (A, B, E and F). The levels of Tim-3-galectin-9 complex were measured by ELISA in blood plasma of five randomly picked healthy donors and AML patients (C and G). Tim-3 and galectin-9 were characterized by Western blot in blood plasma from five randomly chosen AML patients (D). Correlations between Tim-3 and galectin-9 as well as between galectin-9 and Tim-3-galectin-9 complex was then determined (H, I, J and K). Images are from one experiment representative of five which gave similar results. Quantitative data represent mean values ± SEM of three independent experiments; $^{*}p < 0.05$; $^{**}p < 0.01$; $^{***}p < 0.001$ vs. control.

of Tim-3-galectin-9 complex by ELISA as described above. The level of increase in Tim-3-galectin-9 complex in AML samples was similar to that of galectin-9 (Fig. 4C and G). We then randomly chose five plasma samples from the group of studied AML patients and analyzed Tim-3 and galectin-9 levels by Western blot (Fig. 4D). Prior to loading onto the SDS-PAGE, samples were sonicated and boiled for 5 min at 95 °C. We found that sTim-3 and galectin-9 were clearly detectable. We could also see a clear band (probably representing the soluble form of the Tim-3-galectin-9 complex) at around 52 kDa (detectable by both anti-Tim-3 and anti-galectin-9 antibodies). This suggests that the complex released by THP-1 cells (Fig. 1) and the one found in blood plasma is unlikely to be formed after secretion. If this had been the case, its molecular weight would have been around 65 kDa (33 kDa for sTim-3 and 32 kDa for galectin-9) rather than 52 kDa. A specific band was also detectable at around 20 kDa (Fig. 4D). These results are in line with those obtained for soluble forms of Tim-3, galectin-9 and Tim-3-galectin-9 complex released by THP-1 cells confirming that sTim-3 and Tim-3 complexed with galectin-9 are likely to be differentially shed from plasma membranes of AML cells. Interestingly, there is a clear evidence of a correlation between Tim-3 and galectin-9 levels in the plasma of both healthy donors and AML patients and these correlation levels were very similar to each other (Fig. 4H and I) suggesting a co-release of both proteins in both cohorts.

3.4. Tim-3 Binding Alters the Conformation of Galectin-9

In order to assess the biophysical properties of Tim-3, galectin-9 and the Tim-3-galectin-9 complex we investigated them using synchrotron radiation circular dichroism (SRCD) spectroscopy at Diamond Light Source (Beam Line 23, Supplementary Fig. 2). Structural organization of Tim-3 and galectin-9 as well as their interaction are schematically presented in the Fig. 5A. Galectin-9 interacts with non-glycosylated Tim-3 with nanomolar affinity ($Kd = 2.8 \times 10^{-8}$ M); the binding can be further strengthened by interaction of galectin-9 with glycosylated Tim-3 (Prokhorov et al., 2015). Indeed, the complex is detectable by Western blot, which means that interaction between a lectin and sugar is taking place. SRCD spectroscopy was also performed on galectin-9 and Tim-3 mixed to a stoichiometry of 1:1 molar ratio (Fig. 5B). Galectin-9 when mixed with Tim-3 showed a CD spectrum significantly different from the simulated spectrum indicating that the interaction of galectin-9 with Tim-3 causes significant conformational change of the proteins with a clear increase in β-strand component. Based on the above, one might speculate that Tim-3 binding could alter the conformation of galectin-9, resulting in increased ability to interact with receptors in target cells. Since galectin-9 is a tandem protein with two sugar binding domains, one domain could bind Tim-3 (or other proteins) and leave the other domain open for interaction with a receptor molecule associated with the plasma membrane of a target cell (for example membrane associated Tim-3).

3.5. Latrophilin 1, Protein Kinase C and mTOR-Dependent Translation Play a Crucial Role in Tim-3 and Galectin-9 Production and Secretion

LPHN1 mRNA was found in primary human CD34-positive stem cells (Maiga et al., 2016). We were able to detect LPHN1 protein in them (at a slightly higher molecular weight than in THP-1 cells (around 140 kDa)), while in THP-1 it is detectable at 130 kDa (Supplementary Fig. 3) as well as in primary AML cells (Sumbayev et al., 2016). No Tim-3 or galectin-9 protein expression was detectable in primary human CD34-positive stem cells (Supplementary Fig. 3).

For this experimental set-up we used THP-1 cells and exposed them to 100 nM PMA or 250 pM α-latrotoxin (LTX, a highly specific and potent ligand of LPHN1 (Sumbayev et al., 2016)). We found that both PMA and LTX downregulated intracellular Tim-3 and galectin-9 levels (though not significantly) and significantly increased activating phosphorylation of the mammalian target of rapamycin (mTOR) at S2448 (Fig. 6A and B). One hour pre-treatment of THP-1 cells with 70 nM Gö6983 (PKCα inhibitor) before exposure to PMA or LTX led to attenuation of stimulus-induced mTOR activation and downregulation of intracellular Tim-3 and galectin-9 levels. Interestingly, in the cells exposed just to Gö6983, phospho-S2448 mTOR and intracellular Tim-3/galectin-9 levels were not different

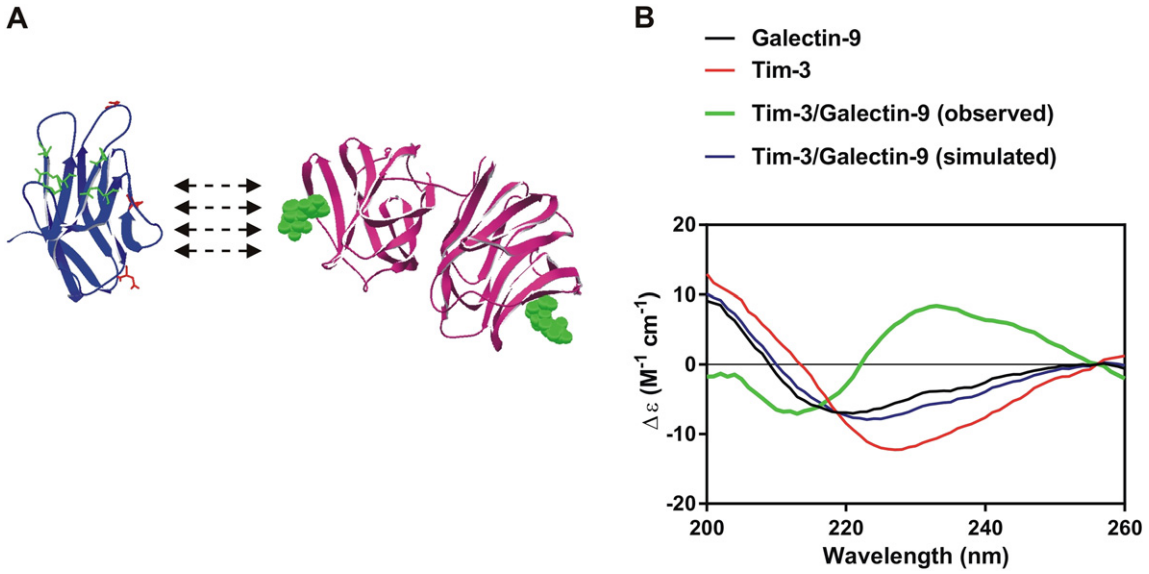


Fig. 5. Interaction of Tim-3 with galectin-9 leads to major conformational changes increasing solubility of the protein complex. (A) The schematic structural models of Tim-3 extracellular domain (left) and galectin-9 (right). In the Tim-3 structure, amino acid residues involved in galectin-9-independent binding are highlighted in green. Residues, which are potential targets for glycosylation, are highlighted in red. In galectin-9, sugar molecules, which could potentially bind the protein, located close to the carbohydrate binding sites are shown in green. (B) The SRCD spectroscopy of Tim-3, galectin-9 and Tim-3-galectin-9 interaction (both simulated and real curves are presented).

from the control. Both PMA and LTX highly upregulated release of both sTim-3 and galectin-9 from THP-1 cells. Gö6983 completely attenuated this increase in both cases, but did not change basic levels of Tim-3 and galectin-9 secretion, which suggests that basic (background) release of galectin-9 and Tim-3 does not depend on PKCα (Fig. 6D).

In summary, both PMA and LTX induce production of both Tim-3 and galectin-9 in THP-1 cells. We confirmed that THP-1 cells express Gαq (Supplementary Fig. 4A) and PMA as well as LTX induce highly significant upregulation of PKCα kinase activity (Supplementary Fig. 4B). Pre-treatment of THP-1 cells with 10 μM AZD2014 (a highly specific mTOR inhibitor) before exposure to PMA or LTX reduced intracellular Tim-3 and galectin-9 levels as well as release of both proteins (Fig. 6C and D). This indicates that PMA or LTX-induced translation of both proteins depends on the mTOR pathway. Importantly, the solvents used to dissolve pharmacological inhibitors had no effect on any of the studied protein levels or their secretion (data not shown).

These results were validated using primary human AML cells. For this purpose we exposed primary human AML mononuclear blasts AML-PB001F for 24 h to LTX followed by detection of secreted galectin-9 and Tim-3. We found that AML-PB0011F expressed LPHN1 and the secreted levels of both proteins were significantly increased in LTX-treated AML cells (Supplementary Fig. 5) confirming the findings obtained in THP-1 cells.

To confirm the physiological role of LPHN1 in galectin-9 release we exposed THP-1 cells to FLRT3, which is one of physiological ligands of LPHN1 (Boucard et al., 2014). We found that 10 nM FLRT3 induced significant upregulation of galectin-9 and sTim-3 release (Fig. 7A, a scheme of the experiment is presented in Supplementary Fig. 6A); it also upregulated PKCα activity in THP-1 cells (Supplementary Fig. 4B). To confirm

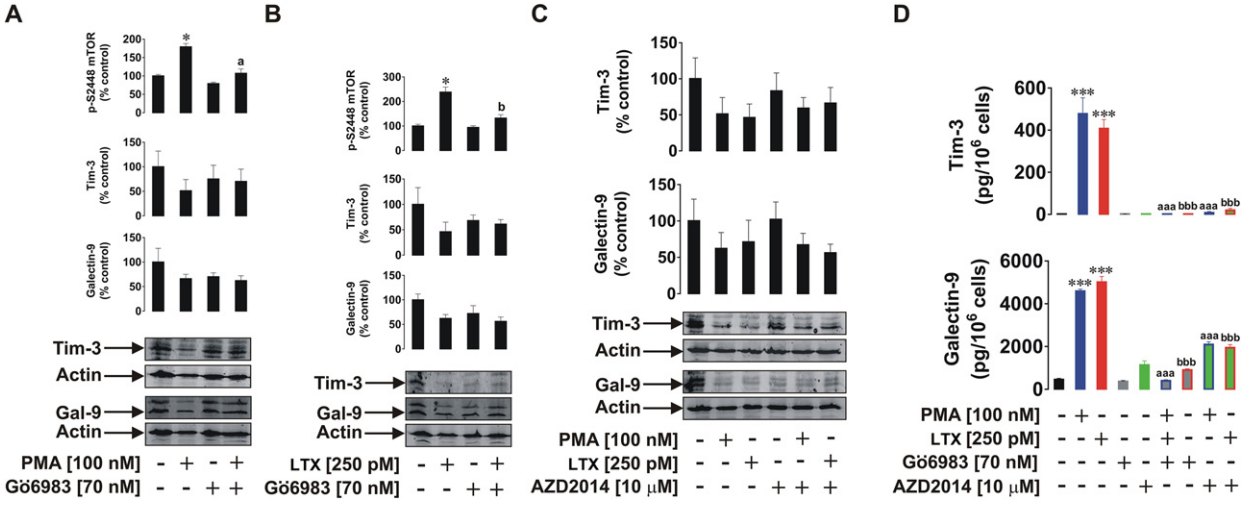


Fig. 6. LPHN1, PKCα and mTOR pathways are involved in Tim-3 and galectin-9 production and secretion in AML cells. THP-1 cells were exposed to the indicated concentrations of PMA or LTX for 16 h with or without 1 h pre-treatment with the PKCα inhibitor Gö6983 (A, B, D) or the mTOR inhibitor AZD2014 (C, D). Cellular levels of Tim-3 and galectin-9 were analyzed by Western blot. Released Tim-3 and galectin-9 were detected by ELISA. Images are from one experiment representative of three which gave similar results. Quantitative data are the mean values ± SEM of three independent experiments; $^{*}p < 0.05$; $^{**}p < 0.01$; $^{***}p < 0.001$ vs. control. Symbols "a" or "b" are used instead of "*" to indicate differences vs. PMA and LTX-treated cells, respectively.

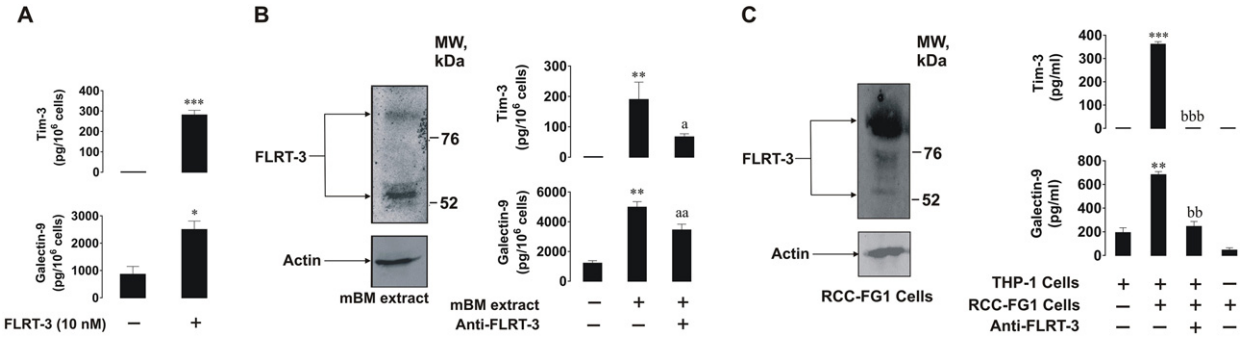


Fig. 7. FLRT3, a physiological ligand of LPHN1, induces galectin-9 and Tim-3 secretion. (A) THP-1 cells were exposed for 16 h to 10 nM extracellular domain of human recombinant FLRT3 followed by measurement of released Tim-3 and galectin-9 by ELISA. (B) THP-1 cells were exposed to mouse bone marrow (mBM) extracts for 16 h with or without 1 h pre-treatment with 5 μg/ml anti-FLRT3 antibody. The presence of FLRT3 in mBM extracts was confirmed by Western blot analysis. Secreted Tim-3 and galectin-9 were measured by ELISA. (C, left) RCC-FG1 cells express FLRT3 as confirmed by Western blotting. (C, right) RCC-FG1 cells were co-cultured with THP-1 cells at a ratio of 1 THP-1:2 RCC-FG1 with or without 1 h pre-treatment with 5 μg/ml FLRT3 neutralizing antibody. Secreted galectin-9 and Tim-3 were measured by ELISA. Images are from one experiment representative of three which gave similar results. Quantitative data depict mean values ± SEM of three independent experiments; $^{*}p < 0.05$; $^{**}p < 0.01$; $^{***}p < 0.001$ vs. control. Symbols "a" or "b" are used instead of "*" to indicate differences vs. cells treated with mBM extracts or co-cultured with RCC-FG1 cells, respectively.

that this effect was physiologically relevant, we exposed THP-1 cells for 16 h to mouse bone marrow (mBM) extracts (10 μg protein/ml, which contain FLRT3, Fig. 7B, a scheme of the experiment is presented in Supplementary Fig. 6B) obtained as outlined in the Materials and Methods. Treatments were conducted with or without 1 h pre-treatment with 5 μg/ml FLRT3 neutralizing mouse antibody. We found that mBM extracts significantly upregulated galectin-9 and sTim-3 secretion in THP-1 cells. FLRT3 neutralizing mouse antibody reduced the effects of mBM extracts but did not block them (Fig. 7B). This means that BM contains several activators of galectin-9 secretion in AML cells. Finally, we co-cultured THP-1 cells with RCC-FG1 renal carcinoma cells (which are highly adherent) in the ratio 1 THP-1:2 RCC-FG1. RCC-FG1 cells express high levels of FLRT3 and release almost undetectable amounts of galectin-9 (Fig. 7C, a scheme of the experiment is presented in Supplementary Fig. 6C). Cells were kept together for 16 h in the absence or presence of 5 μg/ml FLRT3 neutralizing antibody and then galectin-9 and sTim-3 secretion levels were analyzed. We found that the presence of RCC-FG1 cells significantly increased galectin-9 and sTim-3 release and FLRT3 neutralization attenuated these effects. The presence of RCC-FG1 cells significantly upregulated PKCα activity, an effect that was also attenuated by neutralization of the FLRT3 (Supplementary Fig. 4C). These results suggest that FLRT3 stimulates the release of galectin-9 from AML cells.

3.6. Galectin-9 and sTim-3 Attenuate AML Cell Killing Activity of NK Cells

Recent evidence suggested that galectin-9 (either soluble or cell surface associated) can interact with Tim-3 or possibly other receptors on

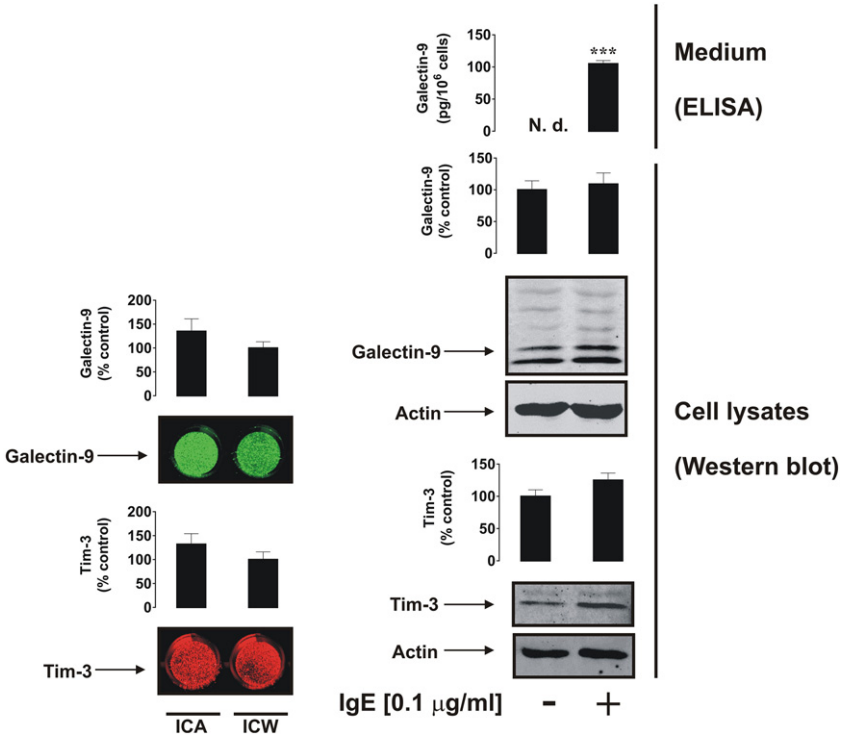


Fig. 8. LAD2 cells express and externalize Tim-3 and galectin-9. Left panel: surface-based and total Tim-3 and galectin-9 were measured in LAD2 human mast cell sarcoma cells using LI-COR in cell assay (ICA, non-permeabilized cells) and in cell Western (ICW, permeabilized cells). Right panel: protein levels of Tim-3 and galectin-9 were measured in resting and IgE-sensitized LAD2 cells by Western blot. Galectin-9 release was characterized using ELISA. Images are from one experiment representative of three which gave similar results. Quantitative data show mean values ± SEM of three independent experiments; $^{***}p < 0.001$ vs. control.

cytotoxic lymphoid cells including NK cells and cytotoxic T cells (Gleason et al., 2012). It may be proposed that Tim-3-galectin-9 interaction is involved in the creation of immunological synapses between target cells and cytotoxic lymphoid cells. To investigate this we used LAD2 human mast cell sarcoma cells kindly provided by Prof. Metcalfe and Dr. Kirshenbaum (NAID, NIH, USA; Kirshenbaum et al., 2003). These cells express both Tim-3 and galectin-9 with both proteins located mostly on the cell surface (Fig. 8) and not rapidly shed. This can thus be used to visualize the formation of immunological synapses between the two cell types. They also express high affinity IgE receptors (FcεRI) which are not expressed by NK cells and thus can be used to distinguish between the two cell types.

Resting LAD2 cells do not release detectable amounts of galectin-9 and sensitization with IgE (which was used in order to label the cells for visualization) does not augment galectin-9 secretion considerably (Fig. 8). We therefore immobilized primary human NK cells isolated from buffy coats of human blood on ELISA plates as outlined in Materials and Methods. NK cells express Tim-3 (several glycosylation variants, Supplementary Fig. 7) but do not produce detectable amounts of galectin-9 protein. We applied IgE-sensitized LAD2 cells (Sumbayev et al., 2012) to the NK cells at a ratio of 1:1 with or without 15 min pre-incubation with galectin-9 neutralizing antibody. Isotype control antibody was also used instead of galectin-9 antibody to rule out the IgG effect. LAD2 cells were then flagged using mouse IgM anti-IgE followed by visualization using anti-mouse LI-COR secondary antibody (which recognizes IgM, see Materials and Methods for further details). We found that LAD2 cells were binding to NK cells and the presence of galectin-9 neutralizing antibody (but not isotype control antibody) abrogated this effect (Fig. 9, a scheme of the experiment is presented in Supplementary Fig. 8). These results confirm that galectin-9 produced by LAD2 cells participates in their interactions with NK cells. Furthermore, abrogation of the effect by anti-galectin-9 antibodies may indicate that the Tim-3-galectin-9 interaction is the only pathway through which these cells could interact. This is most likely a result of IgE sensitization of LAD2 cells which highly increases the presence of galectin-9 on their surface.

We then used K562 chronic myeloid leukemia cells which do not release detectable amounts of galectin-9 (as confirmed by ELISA). K562 cells were exposed to PMA for 24 h in 96 well Maxisorp plates. Medium was replaced with PMA-free RPMI-1640 medium containing isolated primary human NK cells at a ratio of 1 K562:2 NK in the absence or presence of 5 ng/ml human recombinant galectin-9. Cells were co-incubated for 16 h and their viability was then assessed using an MTS test. We found that the presence of NK cells significantly reduced the viability of K562 cells however, the presence of galectin-9 attenuated K562 killing effect (Fig. 10A). Viability of NK cells was not affected in any of the cases (Fig. 10A). Interestingly, the cytotoxic attack by NK cells also led to a dramatic change in the behavior of K562 cells, causing their massive aggregation. Using phase contrast microscopy, we determined the effect of galectin-9 on cell aggregation in individual or combined K562 and NK cell cultures. In the absence of galectin-9, there was clear evidence of K562 cells aggregating in the presence of NK cells (Fig. 10B). Galectin-9, in a dose-dependent manner, decreased the aggregation of K562 cells by NK cells, such that no K562 cell aggregation was detectable in the presence of 5 ng/ml galectin-9 (Fig. 10C). Galectin-9 itself had no visible effect on either of the two cell types alone. Thus, galectin-9 clearly protects myeloid leukemia cells from being killed by NK cells.

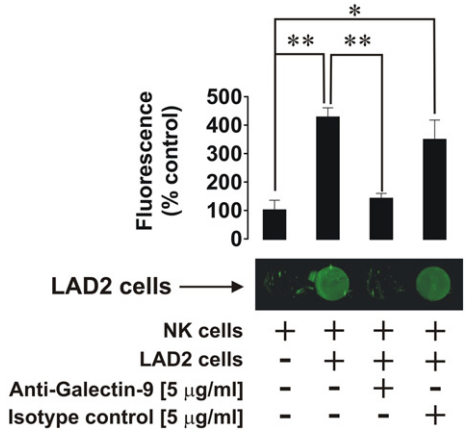


Fig. 9. Galectin-9 participates in the formation of an "immunological synapse" between NK cells and LAD2 cells. Primary human NK cells were immobilized on the surface of Maxisorp plates. Cells were then co-incubated for 30 min with LAD2 cells with or without 30 min pre-treatment of LAD2 cells with 5 μg/ml galectin-9 neutralizing antibody (or the same amount of isotype control antibody). LAD2 cells were then visualized using LI-COR assay as outlined in Materials and Methods. Images are from one experiment representative of five which gave similar results. Quantitative data represent mean values ± SEM of five independent experiments; $^{*}p < 0.05$; $^{**}p < 0.01$.

We then investigated the interactions between AML THP-1 cells and primary human NK cells. THP-1 cells were exposed to 100 nM PMA for 16 h. The medium was then replaced with PMA-free medium containing NK cells at a ratio of 2 NK cells:1 THP-1 cells and left for 6 h in the absence or presence of 5 μg/ml galectin-9-neutralizing antibody. Tim-3 and galectin-9 were then measured in the NK cells by Western blot analysis, and viability of THP-1 cells, activities of granzyme B, caspase-3 and galectin-9 release were monitored. We found that THP-1 cell viability was reduced when galectin-9 was neutralized (Fig. 11). This was in line with increased caspase-3 activity and granzyme B activities. Galectin-9 release was not affected (Fig. 11, galectin-9 bound to neutralizing antibody is detectable in our system). We confirmed that resting NK cells did not produce detectable amounts of galectin-9. However, this protein on its own, and in the form of unbroken Tim-3-galectin-9 complex, was detectable in NK cells co-cultured with THP-1 cells and was reduced in the presence of galectin-9 neutralizing antibody. This suggests that THP-1 cells were the source of galectin-9, which was most likely bound to Tim-3 on the surface of NK cells, preventing the delivery of NK cell-derived granzyme B into THP-1 cells and inhibiting the caspase-3-dependent apoptotic pathway.

Recently, a possible reciprocal link between levels of sTim-3 and IL-2, a cytokine, which activates cytotoxic activity of NK cells and T cells, was reported (Geng et al., 2006). We also found that in the plasma of healthy donors the levels of sTim-3 were significantly lower compared to AML patients (Fig. 4) whereas the levels of IL-2 were significantly higher (Fig. 12A and B). To investigate a possible direct influence of sTim-3, we exposed Jurkat T cells (resting Jurkat T cells produce detectable amounts of IL-2) to increasing concentrations of Tim-3 for 24 h. We found a striking sTim-3 concentration-dependent and significant reduction of IL-2 release from Jurkat T cells. This indicates that sTim-3 is capable of binding a target protein (or a group of target proteins) and reducing IL-2 production thus preventing induction of NK cell and T lymphocyte anti-cancer activities.

Taken together, our results demonstrate a pathobiochemical pathway in AML cells. It is associated with activation of PKCα by LPHN1 (or any other receptors with similar activity) leading to the expression and exocytosis of sTim-3 and galectin-9, which prevent the activation of cytotoxic lymphocytes and impair their malignant cell killing activity.

4. Discussion

AML is a malignancy affecting bone marrow and blood and is a severe, and often fatal, systemic disease. AML cells escape host immune attack involving NK and cytotoxic T cells by impairing their activity (Golden-Mason et al., 2013; Kikushige et al., 2015; Gonçalves Silva et al., 2016). However, the biochemical mechanisms underlying the immune escape of malignant white blood cells remain unclear. Recently, it was shown that AML cells express high levels of the immune receptor Tim-3 and release galectin-9 which impairs the activity of NK cells and cytotoxic T cells (Gonçalves Silva et al., 2016). We have also suggested that Tim-3, as a membrane associated glycoprotein, might act as a trafficker for galectin-9 (Gonçalves Silva et al., 2016). As for all galectins,

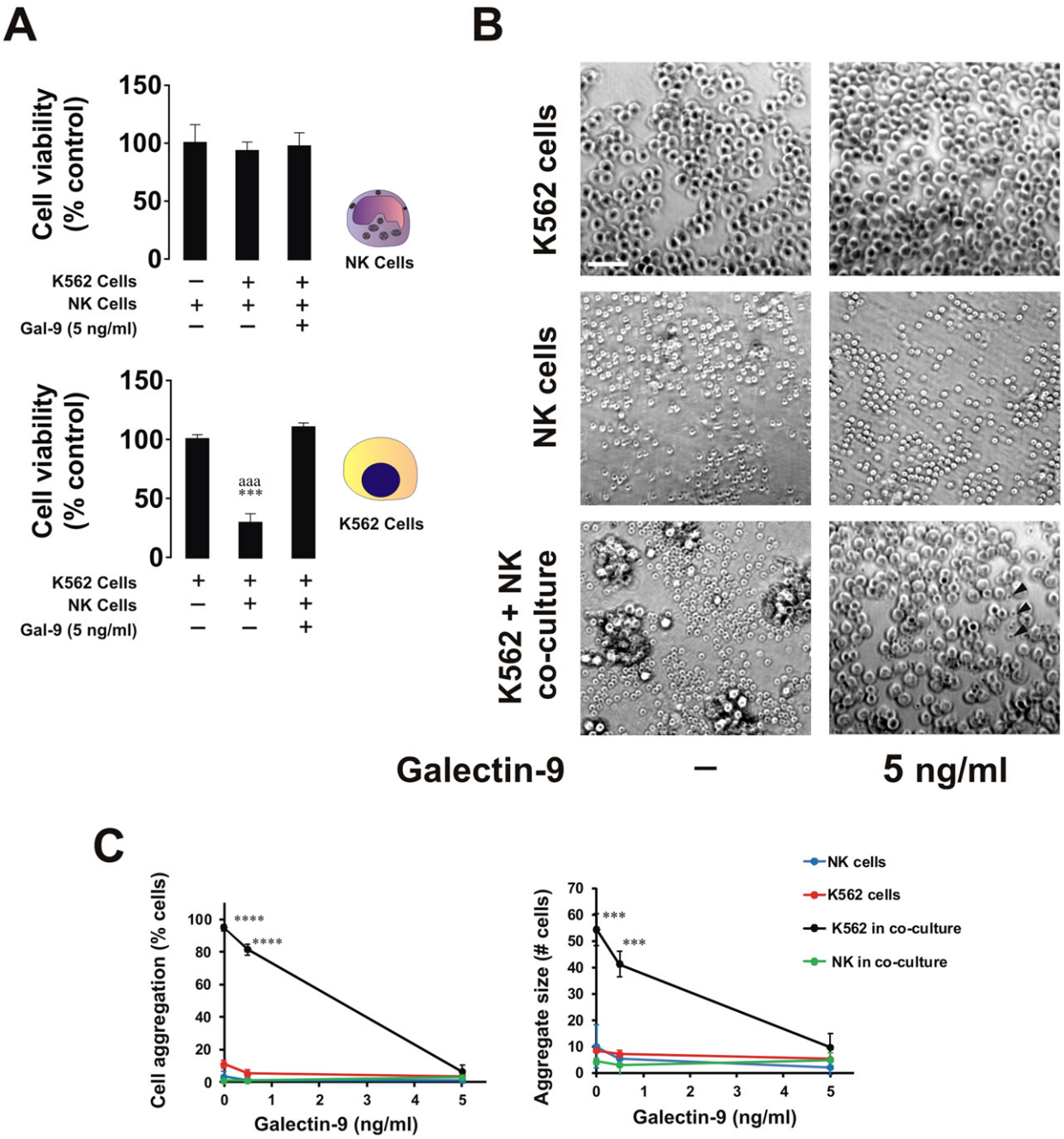


Fig. 10. Galectin-9 protects myeloid leukemia K562 cells from being killed by primary human NK cells. (A) K562 cells were co-cultured for 16 h with primary human NK cells (at a ratio of 1 K562:2 NK) in the absence or presence of 5 ng/ml galectin-9. Viability of K562 and NK cells was then measured using an MTS test. Images are from one experiment representative of three which gave similar results. Quantitative data represent mean values ± SEM of three independent experiments; ***$p < 0.001$ vs. control. (B) K562 cells were co-cultured for 16 h with primary human NK cells (at a K562:NK ratio of 1:2) in the presence of different concentrations of galectin-9 (0–5 ng/ml). Cells were imaged using phase-contrast microscopy. The images are from one representative experiment of six ($n = 6$), which gave similar results. Scale bar (the same for all images), 50 μm. (C) The NK cell-induced aggregation of K562 cells was quantified as a function of galectin-9 concentration. Left panel: percent of cells found in aggregates in individual cultures and in co-culture. Right panel: the size of cell aggregates in individual cultures and in co-culture. The data represent the mean values ± SD of six independent experiments; *, $p < 0.05$; **, $p < 0.01$; ****, $p < 0.0001$.

galectin-9 is synthesized on free ribosomes and since it lacks the signal domain required for secretion it thus needs a trafficker in order to be released (Delacour et al., 2009). When on the cell surface, Tim-3 is known to be shed by ADAM 10/17 proteolytic enzymes thus producing sTim-3, the function of which remains unknown (Moller-Hackbarth et al., 2013). We found, that Tim-3 could be shed in its free form as well as in complex with galectin-9; however, differential shedding is taking place. The Tim-3 fragment in the complex is about 20 kDa molecular weight, while sTim-3 is around 33 kDa. SRCD analysis of the complex suggests that the interaction between Tim-3 and galectin-9 proteins leads to major conformational change, possibly increasing the ability of galectin-9 to interact with the target proteins. Since galectin-9 is a tandem protein containing two domains (Delacour et al., 2009), one of them might be interacting with Tim-3, while the other one could bind to a target receptor molecule, for example another molecule of Tim-3 associated with the plasma membrane of the target cell (Nagae et al., 2006). This may explain the high efficiency of galectin-9 in triggering Tim-3 on NK cells, which do not express galectin-9 and thus contain unoccupied Tim-3 on their surface.

Since we can observe the Tim-3-galectin-9 complex on Western blots following denaturing SDS-gel electrophoresis (Figs. 1, 2 and 4; ~52 kDa soluble form and ~70 kDa cell-derived form), it is likely that

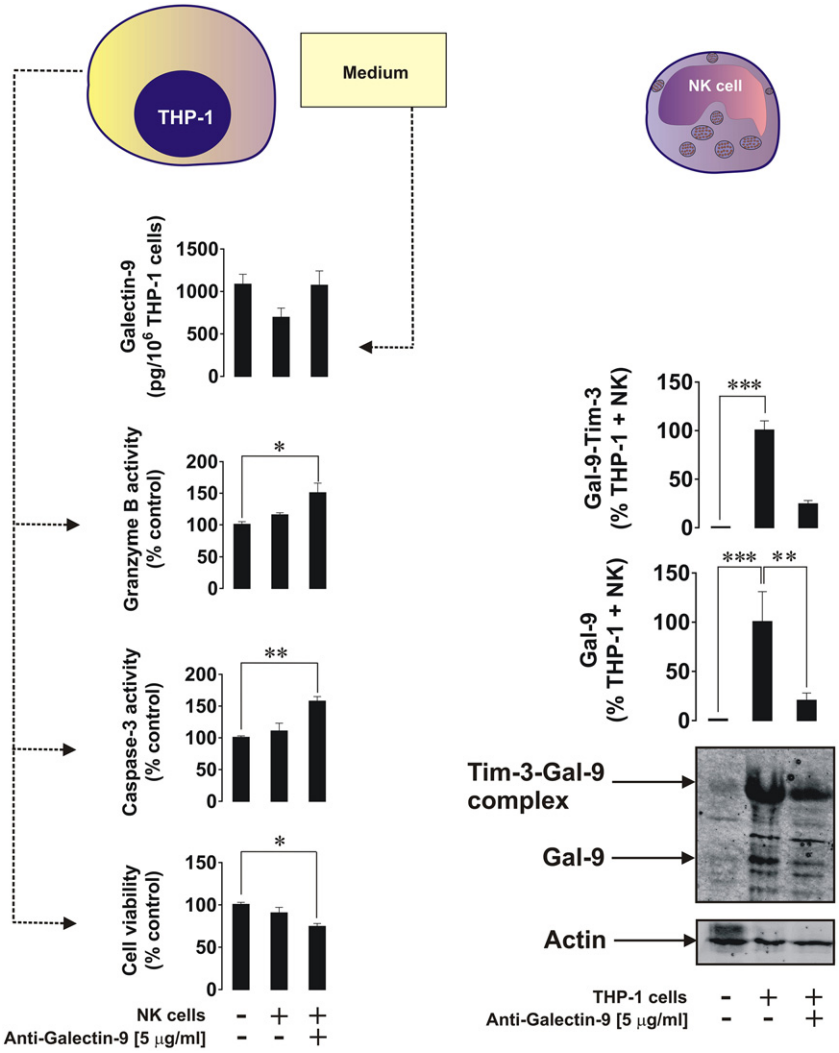


Fig. 11. Cell-derived galectin-9 attenuates AML cell killing activity of primary human NK cells. THP-1 cells were co-incubated with primary human NK cells (ratio – 1 THP-1:2 NK) for 6 h followed by detection of THP-1 cell viability by the MTS test, measurement of activities of granzyme B and caspase 3 in THP-1 cell lysates and released galectin-9 (left panel). Galectin-9 levels from NK cells were determined by Western blot (right panel). Images are from one experiment representative of three which gave similar results. Quantitative data show mean values ± SEM of three independent experiments; $^{*}p < 0.05$; $^{**}p < 0.01$; $^{***}p < 0.001$ vs control.

the binding between proteins is further strengthened by the interaction of galectin-9 with Tim-3-associated glycosides. Interestingly, the complex is detectable by Western blot with both anti-Tim-3 and anti-galectin-9 antibodies. However, when these antibodies are sequentially applied to the same blot, the second antibody fails to detect the respective protein in the same band (unless the first antibody is stripped off), due to steric hindrance. This effect explains why Tim-3 located on the cell surface and covered by galectin-9 cannot be co-stained by the antibody in confocal microscopy co-localization analysis (Fig. 3). Another point supporting this conclusion is that there was also clear evidence of co-localization of Tim-3 and galectin-9 in permiabilized THP-1 cells upon exposure to PMA (Fig. 3, Supplementary Fig. 1).

Previously it was reported that the release of both Tim-3 and galectin-9 depends on PKCα and proteolysis (Chabot et al., 2002). Our

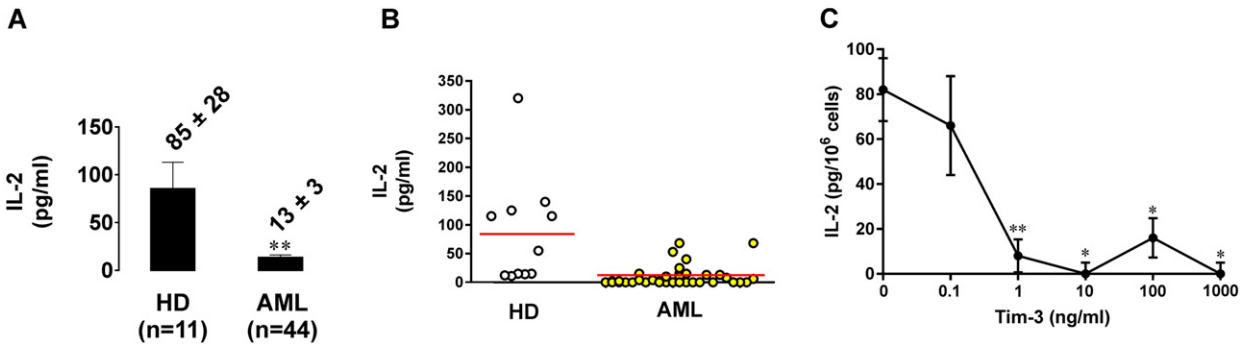


Fig. 12. Soluble Tim-3 attenuates IL-2 release. (A and B) IL-2 levels were measured by ELISA in blood serum of healthy donors and AML patients. (C) Jurkat T cells were exposed to the increasing concentrations of Tim-3 for 24 h followed by detection of secreted IL-2 by ELISA. Data show mean values ± SEM of three independent experiments; $^{*}p < 0.05$; $^{**}p < 0.01$.

results confirmed these findings. PMA treatments induced PKCα activation, which activated exocytosis of Tim-3 and galectin-9 as well as their mTOR-dependent production in THP-1 AML cells (Fig. 6).

Interestingly, natural and exogenous ligands of LPHN1, a G-protein coupled neuronal receptor expressed also in CD34-positive human stem cells (Supplementary Fig. 3) and AML cells but not healthy white blood cells, activated the PKCα pathway. They also induced both mTOR-dependent translation of Tim-3 and galectin-9 as well as their exocytosis. The effect was observed in THP-1 and primary human AML blasts. PKCα is known to provoke agglomeration of SNARE complex responsible for exocytosis (Stockli et al., 2011; Morgan et al., 2005). Since FLRT3, one of natural ligands of LPHN1, is present in bone marrow (Fig. 7) it might explain how LPHN1 causes PKCα activation. Interestingly, constitutively active PKCα in malignant primary AML cells correlates with a very poor prognosis and high mortality rate of patients (Kurinna et al., 2006). This suggests that AML cells constantly release high levels of Tim-3 and galectin-9. Bone marrow also expresses other PKCα-activating proteins. When we exposed THP-1 cells to mouse bone marrow extracts, galectin-9 release was significantly higher compared to resting THP-1 cells. FLRT3 neutralizing antibody significantly reduced but did not abolish FLRT3 induced PKCα-dependent galectin-9 release. This suggests that galectin-9 and Tim-3 are synthesized and exocytozed by AML cells in a PKCα and mTOR-dependent manner, using available plasma membrane-associated PKCα activating receptors (for example LPHN1) to induce the whole pathway.

Galectin-9 prevents the delivery of granzyme B into AML cells (this is a perforin and mannose-6-phosphate receptor-dependent process (Supplementary Fig. 9)). Inside AML cells granzyme B performs cleavage of the protein Bid into tBid, thus inducing mitochondrial dysfunction and cytochrome C release followed by caspase 3 activation. Proteolytic activation of caspase 3, in addition to the classic pathway, might also be directly catalyzed by granzyme B (Lee et al., 2014). Our results with galectin-9 confirmed this concept (Fig. 11). Recently it was reported that galectin-9 induces interferon-gamma (IFN-γ) release from NK cells (Gleason et al., 2012). IFN-γ interacts with AML cells inducing the activity of indoleamine 2,3-dioxygenase (IDO1), an enzyme which converts L-tryptophan into formyl-L-kynurenine, which is then converted into L-kynurenine and released (Corm et al., 2009; Folgiero

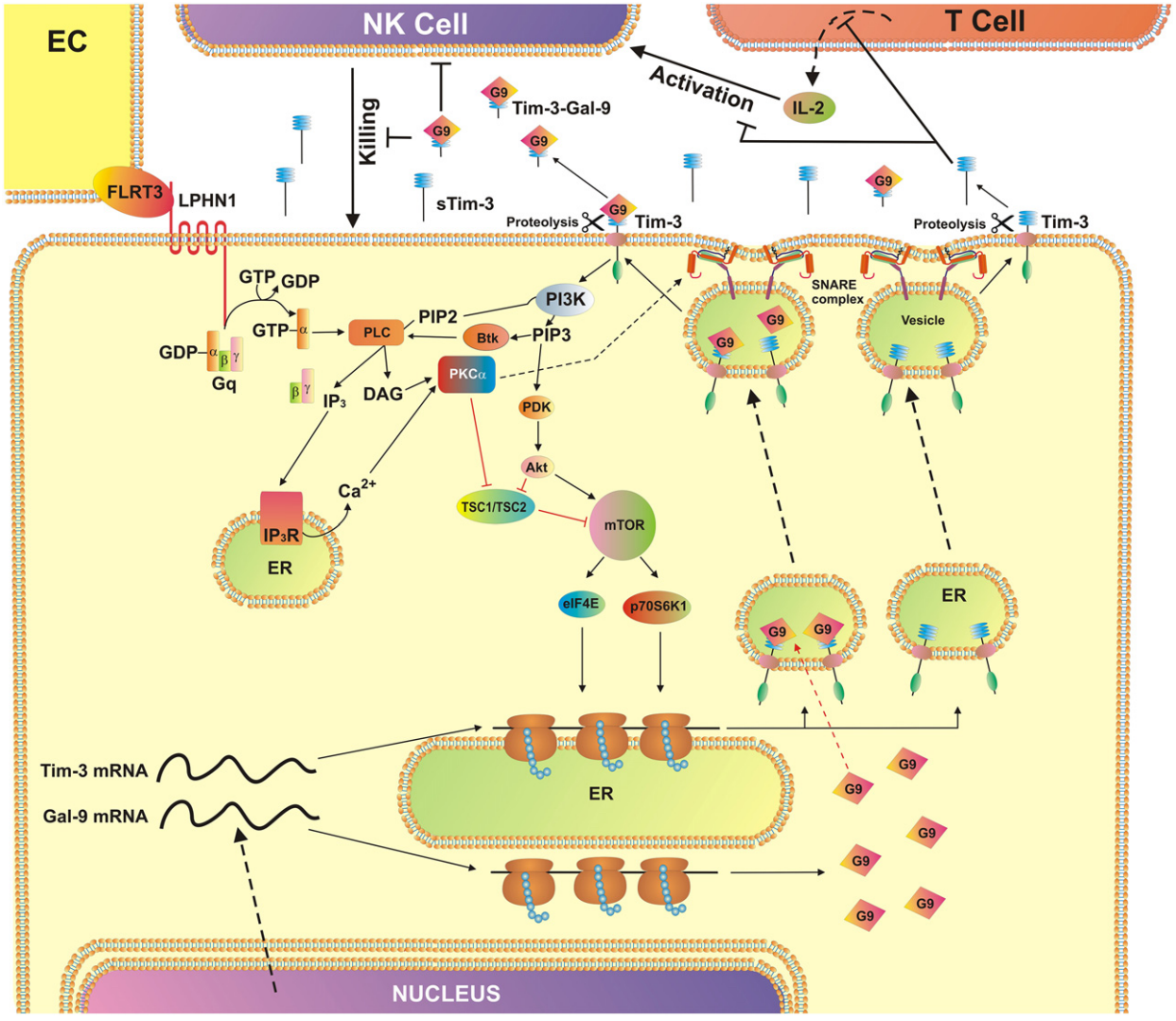


Fig. 13. AML cell-based pathobiochemical pathway showing LPHN1-induced classic activation of PKCα, which triggers translation of Tim-3 and galectin-9 as well as their secretion which is required for immune escape. The interaction of FLRT3 located on the surface of endothelial cells (EC) with LPHN1 leads to the activation of PKCα through the classic Gq/PLC/Ca^{2+} pathway. Ligand-bound LPHN1 activates Gq, which in then stimulates PLC. This leads to phosphatidyl-inositol-bisphosphate (PIP2) degradation and production of inositol-trisphospate (IP_3) and diacylglycerol (DAG). IP_3 interacts with ER-associated IP_3 receptor (IP3R) leading to Ca^{2+} mobilization. PKCα is activated by DAG and Ca^{2+} activates mTOR translational pathway through downregulation of TSC1/TSC2. mTOR controls translation of Tim-3 and galectin-9. PKCα also phosphorylates Munc18 exocytosis regulator protein which provokes formation of SNARE complexes that tether vesicles to the plasma membrane. This pre-activates the release machinery, and elevated cytosolic Ca^{2+} lead to exocytosis of free and galectin-9-complexed Tim-3. Both types of Tim-3 are differentially shed from the cell surface by proteolytic enzymes. Soluble Tim-3 prevents IL-2 secretion required for activation of NK cells and cytotoxic T cells. Galectin-9 impairs AML cell killing activity of NK cells (and other cytotoxic lymphocytes).

et al., 2015; Mabuchi et al., 2016). L-kynurenine affects the ability of NK cells to kill AML cells, an effect which was seen in our experiments and presented in Supplementary Fig. 9. Soluble Tim-3 was shown to significantly downregulate production of IL-2, a cytokine required for activation of NK cells and cytotoxic T lymphocytes.

Taken together, our results show that human AML cells possess a secretory pathway which leads to the production and release of sTim-3 and galectin-9. Both proteins prevent the activation of NK cells and impair their AML cell-killing activity. This pathway, which involves the LPHN1-dependent activation of Tim-3 and galectin-9 production is summarized in Fig. 13. The described pathway presents both biomarkers for AML diagnostics and potential targets (both sTim-3 and galectin-9) for AML immune therapy and thus can be considered as a fundamental discovery.

Grant Support

This work was supported by a Daphne Jackson Trust postdoctoral fellowship (to IMY), University of Kent Faculty of Sciences Research Fund (to VVS and YAU), Batzebär grant (to EFK and SB) and Oncosuisse grant KFS-3728-08-2015 (to LV and MB). Funders had no role in study design, data collection, data analysis, interpretation or writing of the report.

Acknowledgements

We thank Prof. Michelle D. Garrett (School of Biosciences, University of Kent, UK) for generously providing us with AZD2014. We are grateful to Dr. Gurprit S. Lall (School of Pharmacy, University of Kent, UK) for kindly providing us with biological materials for bone marrow extraction. Antibody against Gαq was generously provided by Dr. Emma Veale, School of Pharmacy, University of Kent, UK. We are most grateful to Dr. Natasha S. Barteneva, School of Science and Technology, Nazarbayev University, Astana, Kazakhstan for her generous help with imaging flow cytometry. We thank Diamond Light Source for access to B23 beamline (SM12578).

Conflict of Interest

The authors declare no potential conflicts of interest.

Author Contributions

IGS and IMY conducted most of the experiments, analyzed the data and contributed to manuscript writing, data interpretation and figure assembly. SSS conducted the experiments reported in Figs. 2 and 7 as well as Supplementary Figs. 4 and 6, analyzed the data, contributed to manuscript writing and figure assembly. WF and JW were collecting plasma/providing blood plasma samples obtained from AML patients. MB and LV generated antibodies against Tim-3 and human recombinant Tim-3 protein fragment used in the study. RH, GS and GC conducted the experiments associated with SRCD and analyzed the data. SB contributed to the study design and concept development. YAU and BFG designed the experiments associated with cell-cell interactions, analyzed and interpreted the data, contributed to the concept development and manuscript writing. EFK designed and interpreted co-localization experiments, strongly contributed to design of experiments associated with Tim-3 and galectin-9 secretion, concept development and manuscript writing. VVS – designed the whole study, strongly participated in all the data collection, data analysis and interpretation, developed the concept and wrote the manuscript.

Appendix A. Supplementary data

Supplementary data to this article can be found online at http://dx.doi.org/10.1016/j.ebiom.2017.07.018.

References

Abooali, M., Lall, G.S., Coughlan, K., Lall, H.S., Gibbs, B.F., Sumbayev, V.V., 2014. Crucial involvement of xanthine oxidase in the intracellular signalling networks associated with human myeloid cell function. Sci. Rep. 4, 6307.

Ashton, A.C., Rahman, M.A., Volynski, K.E., Manser, C., Orlova, E.V., Matsushita, H., Davletov, B.A., van Heel, M., Grishin, E.V., Ushkaryov, Y.A., 2000. Tetramerisation of α-latrotoxin by divalent cations is responsible for toxin-induced non-vesicular release and contributes to the Ca^{2+}-dependent vesicular exocytosis from synaptosomes. Biochimie 82, 453–468.

Boucard, A.A., Maxeiner, S., Sudhof, T.C., 2014. Latrophilins function as heterophilic cell-adhesion molecules by binding to teneurins: regulation by alternative splicing. J. Biol. Chem. 289, 387–402.

Chabot, S., Kashio, Y., Seki, M., Shirato, Y., Nakamura, K., Nishi, N., Nakamura, T., Matsumoto, R., Hirashima, M., 2002. Regulation of galectin-9 expression and release in Jurkat T cell line cells. Glycobiology 12, 111–118.

Corm, S., Berthon, C., Imbenotte, M., Biggio, V., Lhermitte, M., Dupont, C., Briche, I., Quesnel, B., 2009. Indoleamine 2,3-dioxygenase activity of acute myeloid leukemia cells can be measured from patients' sera by HPLC and is inducible by IFN-gamma. Leuk. Res. 33, 490–494.

Davletov, B.A., Meunier, F.A., Ashton, A.C., Matsushita, H., Hirst, W.D., Lelianova, V.G., Wilkin, G.P., Dolly, J.O., Ushkaryov, Y.A., 1998. Vesicle exocytosis stimulated by α-latrotoxin is mediated by latrophilin and requires both external and stored Ca^{2+}. EMBO J. 17, 3909–3920.

Davydov, I.I., Fidalgo, S., Khaustova, S.A., Lelyanova, V.G., Grebenyuk, E.S., Ushkaryov, Y.A., Tonevitsky, A.G., 2009. Prediction of epitopes in closely related proteins using a new algorithm. Bull. Exp. Biol. Med. 148, 869–873.

Delacour, D., Koch, A., Jacob, R., 2009. The role of galectins in protein trafficking. Traffic 10, 1405–1413.

Dhupkar, P., Gordon, N., 2017. Interleukin-2: old and new approaches to enhance immune-therapeutic efficacy. Adv. Exp. Med. Biol. 995, 33–51.

Fasler-Kan, E., Barteneva, N., Ketterer, S., Wunderlich, K., Huwyler, J., Gygax, D., Flammer, J., Meyer, P., 2010. Activation of the JAK-STAT intracellular pathway in human retinal pigment epithelial cell line ARPE-19. Int. J. Interf. Cytokine Mediat. Res. 2, 127–136.

Fasler-Kan, E., Baiken, Y., Vorobjev, I.A., Barteneva, N.S., 2016. Analysis of nucleocytoplasmic protein shuttling by imaging flow cytometry. Methods Mol. Biol. 1389, 127–137.

Folgiero, V., Cifaldi, L., Li Pira, G., Goffredo, B.M., Vinti, L., Locatelli, F., 2015. TIM-3/Gal-9 interaction induces IFNgamma-dependent IDO1 expression in acute myeloid leukemia blast cells. J. Hematol. Oncol. 8, 36.

Geng, H., Zhang, G.M., Li, D., Zhang, H., Yuan, Y., Zhu, H.G., Xiao, H., Han, L.F., Feng, Z.H., 2006. Soluble form of T cell Ig mucin 3 is an inhibitory molecule in T cell-mediated immune response. J. Immunol. 176, 1411–1420.

Gleason, M.K., Lenvik, T.R., McCullar, V., Felices, M., O'Brien, M.S., Cooley, S.A., Verneris, M.R., Cichocki, F., Holman, C.J., Panoskaltsis-Mortari, A., et al., 2012. Tim-3 is an inducible human natural killer cell receptor that enhances interferon gamma production in response to galectin-9. Blood 119, 3064–3072.

Golden-Mason, L., McMahan, R.H., Strong, M., Reisdorph, R., Mahaffey, S., Palmer, B.E., Cheng, L., Kulesza, C., Hirashima, M., Niki, T., et al., 2013. Galectin-9 functionally impairs natural killer cells in humans and mice. J. Virol. 87, 4835–4845.

Gonçalves Silva, I., Ruegg, L., Gibbs, B.F., Bardelli, M., Fruehwirth, A., Varani, L., Berger, S.M., Fasler-Kan, E., Sumbayev, V.V., 2016. The immune receptor Tim-3 acts as a trafficker in a Tim-3/galectin-9 autocrine loop in human myeloid leukemia cells. Oncoimmunology 5, e1195535.

Hughes, R.C., 1999. Secretion of the galectin family of mammalian carbohydrate-binding proteins. Biochim. Biophys. Acta 1473, 172–185.

Hussain, R., Javorfi, T., Siligardi, G., 2012a. Circular dichroism beamline B23 at the Diamond Light Source. J. Synchrotron Radiat. 19, 132–135.

Hussain, R., Jávorfi, T., Siligardi, G., 2012b. Spectroscopic analysis: synchrotron radiation circular dichroism. Compr. Chiral. 8, 438–448.

Hussain, R., Benning, K., Myatt, D., Javorfi, T., Longo, E., Rudd, T.R., Pulford, B., Siligardi, G., 2015. CDApps: integrated software for experimental planning and data processing at beamline B23, Diamond Light Source. J. Synchrotron Radiat. 22, 862.

Khaznadar, Z., Henry, G., Setterblad, N., Agaugue, S., Raffoux, E., Boissel, N., Dombret, H., Toubert, A., Dulphy, N., 2014. Acute myeloid leukemia impairs natural killer cells through the formation of a deficient cytotoxic immunological synapse. Eur. J. Immunol. 44, 3068–3080.

Kikushige, Y., Miyamoto, T., Yuda, J., Jabbarzadeh-Tabrizi, S., Shima, T., Takayanagi, S., Niiro, H., Yurino, A., Miyawaki, K., Takenaka, K., et al., 2015. A TIM-3/Gal-9 autocrine stimulatory loop drives self-renewal of human myeloid leukemia stem cells and leukemic progression. Cell Stem Cell 17, 341–352.

Kirshenbaum, A.S., Akin, C., Wu, Y., Rottem, M., Goff, J.P., Beaven, M.A., Rao, V.K., Metcalfe, D.D., 2003. Characterization of novel stem cell factor responsive human mast cell lines LAD 1 and 2 established from a patient with mast cell sarcoma/leukemia; activation following aggregation of FcepsilonRI or FcgammaRI. Leuk. Res. 27, 677–682.

Kurinna, S., Konopleva, M., Palla, S.L., Chen, W., Kornblau, S., Contractor, R., Deng, X., May, W.S., Andreeff, M., Ruvolo, P.P., 2006. Bcl2 phosphorylation and active PKC alpha are associated with poor survival in AML. Leukemia 20, 1316–1319.

Lee, J., Lee, S.J., Lim, K.T., 2014. ZPDC glycoprotein (24 kDa) induces apoptosis and enhances activity of NK cells in N-nitrosodiethylamine-injected Balb/c. Cell. Immunol. 289, 1–6.

Liu, J., Wan, Q., Lin, X., Zhu, H., Volynski, K., Ushkaryov, Y., Xu, T., 2005. α-Latrotoxin modulates the secretory machinery via receptor-mediated activation of protein kinase C. Traffic 6, 756–765.

Mabuchi, R., Hara, T., Matsumoto, T., Shibata, Y., Nakamura, N., Nakamura, H., Kitagawa, J., Kanemura, N., Goto, N., Shimizu, M., et al., 2016. High serum concentration of L-kynurenine predicts unfavorable outcomes in patients with acute myeloid leukemia. Leuk. Lymphoma 57, 92–98.

Maiga, A., Lemieux, S., Pabst, C., Lavallee, V.P., Bouvier, M., Sauvageau, G., Hebert, J., 2016. Transcriptome analysis of G protein-coupled receptors in distinct genetic subgroups of acute myeloid leukemia: identification of potential disease-specific targets. Blood Cancer J. 6, e431.

Micol, V., Sanchez-Pinera, P., Villalain, J., de Godos, A., Gomez-Fernandez, J.C., 1999. Correlation between protein kinase C alpha activity and membrane phase behavior. Biophys. J. 76, 916–927.

Moller-Hackbarth, K., Dewitz, C., Schweigert, O., Trad, A., Garbers, C., Rose-John, S., Scheller, J., 2013. A disintegrin and metalloprotease (ADAM) 10 and ADAM17 are major sheddases of T cell immunoglobulin and mucin domain 3 (Tim-3). J. Biol. Chem. 288, 34529–34544.

Morgan, A., Burgoyne, R.D., Barclay, J.W., Craig, T.J., Prescott, G.R., Ciufo, L.F., Evans, G.J., Graham, M.E., 2005. Regulation of exocytosis by protein kinase C. Biochem. Soc. Trans. 33, 1341–1344.

Nagae, M., Nishi, N., Murata, T., Usui, T., Nakamura, T., Wakarsuki, S., Kato, R., 2006. Crystal structure of the galectin-9 N-terminal carbohydrate recognition domain from Mus musculus reveals the basic mechanism of carbohydrate recognition. J. Biol. Chem. 281, 35884–35893.

Prokhorov, A., Gibbs, B.F., Bardelli, M., Ruegg, L., Fasler-Kan, E., Varani, L., Sumbayev, V.V., 2015. The immune receptor Tim-3 mediates activation of PI3 kinase/mTOR and HIF-1 pathways in human myeloid leukemia cells. Int. J. Biochem. Cell Biol. 59, 11–20.

Schindelin, J., Rueden, C.T., Hiner, M.C., et al., 2015. The ImageJ ecosystem: an open platform for biomedical image analysis. Mol. Reprod. Dev. 82, 518–529.

Siligardi, G., Hussain, R., 2015. CD Spectroscopy: An Essential Tool for Quality Control of Protein Folding. RJ Owen, ed. Methods Mol. Biol 1261. Springer, NY, pp. 255–276.

Silva, J.P., Ushkaryov, Y.A., 2010. The latrophilins, "split-personality" receptors. Adv. Exp. Med. Biol. 706, 59–75.

Silva, J.P., Lelianova, V.G., Ermolyuk, Y.S., Vysokov, N., Hitchen, P.G., Berninghausen, O., Rahman, M.A., Zangrandi, A., Fidalgo, S., Tonevitsky, A.G., Dell, A., Volynski, K.E., Ushkaryov, Y.A., 2011. Latrophilin 1 and its endogenous ligand Lasso/teneurin-2 form a high-affinity transsynaptic receptor pair with signaling capabilities. Proc. Natl. Acad. Sci. U. S. A. 108, 12113–12118.

Stockli, J., Fazakerley, D.J., James, D.E., 2011. GLUT4 exocytosis. J. Cell Sci. 124, 4147–4159.

Sumbayev, V.V., Nicholas, S.A., 2010. Hypoxia-inducible factor 1 as one of the "signaling drivers" of toll-like receptor-dependent and allergic inflammation. Arch. Immunol. Ther. Exp. 58, 287–294.

Sumbayev, V.V., Yasinska, I., Oniku, A.E., Streatfield, C.L., Gibbs, B.F., 2012. Involvement of hypoxia-inducible factor-1 in the inflammatory responses of human LAD2 mast cells and basophils. PLoS One 7, e34259.

Sumbayev, V.V., Gonçalves Silva, I., Blackburn, J., Gibbs, B.F., Yasinska, I.M., Garrett, M.D., Tonevitsky, A.G., Ushkaryov, Y.A., 2016. Expression of functional neuronal receptor latrophilin 1 in human acute myeloid leukemia cells. Oncotarget 7, 45575–45583.

Swamydas, M., Lionakis, M.S., 2013. Isolation, purification and labeling of mouse bone marrow neutrophils for functional studies and adoptive transfer experiments. JoVE e50586.

Ushkaryov, Y., 2002. α-Latrotoxin: from structure to some functions. Toxicon 40, 1–5.

Volynski, K.E., Capogna, M., Ashton, A.C., Thomson, D., Orlova, E.V., Manser, C.F., Ribchester, R.R., Ushkaryov, Y.A., 2003. Mutant α-latrotoxin (LTX^{N4C}) does not form pores and causes secretion by receptor stimulation: this action does not require neurexins. J. Biol. Chem. 278, 31058–31066.

Wang, F., He, W., Zhou, H., Yuan, J., Wu, K., Xu, L., Chen, Z.K., 2007. The Tim-3 ligand galectin-9 negatively regulates CD8 + alloreactive T cell and prolongs survival of skin graft. Cell. Immunol. 250, 68–74.

Yasinska, I.M., Gibbs, B.F., Lall, G.S., Sumbayev, V.V., 2014. The HIF-1 transcription complex is essential for translational control of myeloid hematopoietic cell function by maintaining mTOR phosphorylation. Cell. Mol. Life Sci. 71, 699–710.

ONCOIMMUNOLOGY
2018, VOL. 7, NO. 6, e1438109 (8 pages)
https://doi.org/10.1080/2162402X.2018.1438109

Taylor & Francis
Taylor & Francis Group

ORIGINAL RESEARCH

OPEN ACCESS Check for updates

High mobility group box 1 (HMGB1) acts as an "alarmin" to promote acute myeloid leukaemia progression

Inna M. Yasinska[a,*], Isabel Gonçalves Silva[a,*], Svetlana S. Sakhnevych[a], Laura Ruegg[a], Rohanah Hussain[b], Giuliano Siligardi[b], Walter Fiedler[c], Jasmin Wellbrock[c], Marco Bardelli[d], Luca Varani[d], Ulrike Raap[e], Steffen Berger[f], Bernhard F. Gibbs[e,a], Elizaveta Fasler-Kan[f,g], and Vadim V. Sumbayev[a]

[a]Medway School of Pharmacy, Universities of Kent and Greenwich, Chatham Maritime, United Kingdom; [b]Beamline 23, Diamond Light Source, Didcot, UK; [c]Department of Oncology, Hematology and Bone Marrow Transplantation with Section Pneumology, Hubertus Wald University Cancer Center, University Medical Center Hamburg-Eppendorf, Germany; [d]Institute for Research in Biomedicine, Universita' della Svizzera italiana (USI), Bellinzona, Switzerland; [e]Department of Medicine (Dermatology and Allergology), University of Oldenburg, Germany; [f]Department of Pediatric Surgery and Department of Biomedical Research, Children's Hospital, Inselspital, University of Bern, Switzerland; [g]Department of Biomedicine, University Hospital Basel and University of Basel, Basel, Switzerland

ABSTRACT

High mobility group box 1 (HMGB1) is a non-histone protein localised in the cell nucleus, where it interacts with DNA and promotes nuclear transcription events. HMGB1 levels are elevated during acute myeloid leukaemia (AML) progression followed by participation of this protein in triggering signalling events in target cells as a pro-inflammatory stimulus. This mechanism was hypothesised to be employed as a survival pathway by malignant blood cells and our aims were therefore to test this hypothesis experimentally. Here we report that HMGB1 triggers the release of tumour necrosis factor alpha (TNF-α) by primary human AML cells. TNF-α induces interleukin 1 beta (IL-1β) production by healthy leukocytes, leading to IL-1β-induced secretion of stem cell factor (SCF) by competent cells (for example endothelial cells). These results were verified in mouse bone marrow and primary human AML blood plasma samples. In addition, HMGB1 was found to induce secretion of angiogenic vascular endothelial growth factor (VEGF) and this process was dependent on the immune receptor Tim-3. We therefore conclude that HMGB1 is critical for AML progression as a ligand of Tim-3 and other immune receptors thus supporting survival/proliferation of AML cells and possibly the process of angiogenesis.

ARTICLE HISTORY
Received 7 December 2017
Revised 30 January 2018
Accepted 2 February 2018

KEYWORDS
Acute myeloid leukaemia; high mobility group box 1; Tim-3; stem cell factor; inflammation

High mobility group box 1 (HMGB1) is a non-histone protein localised in the nucleus, where it binds DNA in order to promote nuclear transcription processes.[1] In addition, HMGB1 was recently found to function as a damage-associated molecular pattern (DAMP) when released passively from either dead, dying/injured cells or secreted by immune/cancer cells in response to endogenous and/or exogenous stimuli, such as hypoxia, endotoxin etc..[2-4] This process is followed by participation of HMGB1 in triggering signalling events in target cells.[1-4] Therefore, it is often called "alarmin" in order to reflect its function as a factor secreted by cells affected by a stressor.[1] It has recently been found that HMGB1 levels are significantly elevated during acute myeloid leukaemia (AML, blood/bone marrow cancer).[5,6] Moreover, AML cells were shown to express high levels of HMGB1.[5,6] Elevated levels of secreted HMGB1 associated with AML progression are likely to be caused by a combination of increased expression of this protein in AML cells and conditions supporting its secretion such as hypoxia and death of the cells in the tumour microenvironment.[5-7]

Upon release, HMGB1 can interact with several immune receptors, including Toll-like receptors 2 and 4 (TLRs 2 and 4) as well as receptor of advanced glycation end products (RAGE).[8] Recent evidence has suggested a possible interaction of HMGB1 with the immune receptor Tim-3 (T cell immunoglobulin and mucin domain 3) which is highly expressed in human acute myeloid leukaemia (AML) cells.[1,2] However, the role of HMGB1 in leukaemia progression remains unstudied. Interestingly, signalling pathways triggered by TLRs 2/4, RAGE and Tim-3 include activation of the phosphatidylinositol-3 kinase (PI-3 K)/mammalian target of rapamycin (mTOR) pathway, which directly controls initiation of translation of proteins crucial for cell survival as well as cytokines including tumour necrosis factor α (TNF-α), a pleiotropic inflammatory cytokine participating in a variety of physiological processes associated with control of host immune defence and respectively haematopoiesis.[9-14] This pathway also triggers accumulation of hypoxia-inducible factor-1 α (HIF-1α), an inducible subunit of HIF-1 transcription complex, which induces glycolysis and angiogenesis on

CONTACT Vadim V. Sumbayev V.Sumbayev@kent.ac.uk; Elizaveta Fasler-Kan elizaveta.fasler@insel.ch; Bernhard F. Gibbs bernhard.gibbs@uni-oldenburg.de

Supplemental data for this article can be accessed on the publisher's website.

*IMY and IGS have contributed equally to this work.

© 2018 Inna M. Yasinska, Isabel Gonçalves Silva, Svetlana S. Sakhnevych, Laura Ruegg, Rohanah Hussain, Giuliano Siligardi, Walter Fiedler, Jasmin Wellbrock, Marco Bardelli, Luca Varani, Ulrike Raap, Steffen Berger, Bernhard F. Gibbs, Elizaveta Fasler-Kan and Vadim V. Sumbayev. Published with license by Taylor & Francis Group, LLC
This is an Open Access article distributed under the terms of the Creative Commons Attribution-NonCommercial-NoDerivatives License (http://creativecommons.org/licenses/by-nc-nd/4.0/), which permits non-commercial re-use, distribution, and reproduction in any medium, provided the original work is properly cited, and is not altered, transformed, or built upon in any way.

genomic level.[9,12] However, the effects of HMGB1 on signalling events described above remain hypothetic and are not comprehensively or conceptually studied yet.

Here we report for the first time that HMGB1 triggers the release of TNF-α by primary human AML cells independently of Tim-3. TNF-α induces interleukin 1 beta (IL-1β) production by healthy leukocytes and subsequent IL-1β-induced secretion of stem cell factor (SCF) by competent cells (for example endothelial cells). Treatment of mouse bone marrow cells with HMGB1 led to significant increase in TNF-α, IL-1β and SCF production. The levels of TNF-α, IL-1β and SCF in blood plasma of AML patients were also significantly upregulated in comparison to healthy individuals. SCF, a ligand of the Kit growth factor receptor is required for survival and proliferation of AML cells. We also show that HMGB1 induces the secretion of angiogenic protein vascular endothelial growth factor (VEGF) and this process is controlled by Tim-3. Synchrotron radiation circular dichroism (SRCD) spectroscopy confirmed that HMGB1 can specifically bind Tim-3. We conclude that HMGB1 as an alarmin participates in AML progression by interacting with Tim-3 and other immune receptors thus supporting the survival/proliferation of AML cells and possibly the process of angiogenesis.

Materials and methods

Materials

RPMI-1640 medium, foetal bovine serum, supplements as well as basic laboratory chemicals were purchased from Sigma (Suffolk, UK). Maxisorp^{TM} microtitre plates were obtained from Nunc (Roskilde, Denmark) and Oxley Hughes Ltd (London, UK). Mouse monoclonal antibodies directed against HIF-1α, mTOR and β-actin, as well as rabbit polyclonal antibodies against phospho-S2448 mTOR, RAGE and HRP-labelled rabbit anti-mouse secondary antibody were purchased from Abcam (Cambridge, UK). Antibodies against phospho-S65 and non-phosphorylated (total) eukaryotic initiation factor 4E binding protein 1 (eIF4E-BP1) were obtained from Cell Signaling Technology (Danvers, MA USA). Goat anti-mouse and goat anti-rabbit fluorescence dye-labelled antibodies were obtained from LI-COR (Lincoln, Nebraska USA). ELISA-based assay kits for the detection of TNFα, IL-1β, SCF and VEGF were purchased from Bio-Techne (R&D Systems, Abingdon, UK). Anti-Tim-3 mouse monoclonal antibody, its single chain variant as well as human Ig-like V-type domain of Tim-3 (amino acid residues 22–124) and human HMGB1 expressed and purified from *E. coli* (see below for more details) were used in our experiments.[11,15] All other chemicals purchased were of the highest grade of purity commercially available.

Cell lines and primary cells

THP-1 human myeloid leukemia monocytes and MCF-7 epithelial breast cancer cells were obtained from the European Collection of Cell Cultures (Salisbury, UK). Cells were cultured in RPMI 1640 medium (R8758 – Sigma (Suffolk, UK) with L-glutamine and sodium bicarbonate, liquid, sterile-filtered, suitable for cell culture) supplemented with 10% foetal bovine serum, penicillin (50 IU/ml) and streptomycin sulphate (50 μg/ml).

Primary human AML mononuclear blasts (AML-PB001 F, newly diagnosed/untreated) were purchased from AllCells (Alameda, CA, USA) and handled in accordance with the manufacturer's instructions following ethical approval (REC reference: 16-SS-033).

Bone marrow was isolated from femur bones of six-week-old C57 BL16 mice (25 $\pm$ 2.5 g, kindly provided by Dr. Gurprit Lall, School of Pharmacy, University of Kent) which were used for the experiments following approval by the Institutional Animal Welfare and Ethics Review Body. Animals were handled by authorised personnel in accordance with the Declaration of Helsinki protocols. Bone marrow was isolated from femur bone heads as described before.[15,16] Cells were kept in RPMI 1640 medium supplemented with 10% foetal bovine serum, penicillin (50 IU/ml) and streptomycin sulphate (50 μg/ml).

Primary human blood plasma samples

Blood plasma from healthy donors was obtained from buffy coat blood (which originated from donors undergoing routine blood donation) provided by the National Health Blood and Transfusion Service (NHSBT, UK) following ethical approval (REC reference: 16-SS-033). Primary human AML plasma samples were obtained from the sample bank of University Medical Centre Hamburg-Eppendorf (Ethik-Kommission der Ärztekammer Hamburg, reference: PV3469).

HMGB1 purification

HMGB1 was produced and purified from *E. Coli* Rosetta DE2 competent. Cells were grown at 37°C in LB medium and harvested 3 hours after induction with isopropyl β-D-1-thiogalactopyranoside (IPTG) at OD_{600} 0.7. The pellet was collected by centrifugation, re-suspended and sonicated on ice with 5 $\times$ 30 seconds of pulsing and 30 seconds rest (buffer contained 20 mM TrisHCl pH 8; 150 mM NaCl; 10 mM imidazole; 2 Beta-SH and 0.2% Triton X100). Following high-speed centrifugation, HMGB1 containing supernatant was subjected to Ni-affinity and size exclusion chromatography. The protein was then eluted at a volume consistent with monomeric HMGB1.

After size exclusion HMGB1 was passed through an anion exchange (Q) column to ensure LPS removal, eluted in sodium phosphate buffer with 1.5M NaCl and finally dialysed extensively (at least 36 hours) against PBS buffer. Absence of LPS contamination was confirmed using mammalian cell lines.

HMGB1 protein was prepared for structural studies and hence highly pure. It was routinely tested for size and degradation by size exclusion (during purification) and dynamic light scattering (final product). Sample concentration was determined by UV spectroscopy. Proper folding was controlled by NMR and CD spectroscopy (all samples required a CD spectrum equivalent to that of the samples characterised with bidimensional 15 N NMR spectroscopy). This protein displayed activity similar to the human recombinant protein expressed in HEK293 cells obtained from Sigma (Suffolk, UK, SRP6265, as verified using THP-1 and primary human AML cells). The

ability of HMGB1 to interact with TLRs seen in our experiments confirmed similarities in the redox state of preparations used in our work in comparison to the pro-inflammatory form of HMGB1 released by dead/dying or stressed cancer/immune and other cells.

Western blot analysis

Tim-3, HIF-1α, phospho-S65 and total eIF4E-BP1 as well as RAGE were analysed using Western blot.[13,14] β-actin staining was used to confirm equal protein loading as described previously. LI-COR goat secondary antibodies (dilution 1:2000), conjugated with fluorescent dyes, were used in accordance with manufacturer's protocol to visualise target proteins (using a LI-COR Odyssey imaging system). Western blot data were quantitatively analysed using Odyssey software and values were subsequently normalised against those of β-actin. In order to quantitate levels of mTOR-dependent phosphorylation of eukaryotic initiation factor 4 E binding protein 1 (eIF4E-BP), we measured phospho-S65-eIF4E-BP and total quantity of eIF4E-BP on a different membrane to avoid the influence of possible incomplete membrane stripping following quantitative analysis. Values were normalised against those of β-actin for corresponding membranes. The ratio between normalised phospho-S65-eIF4E-BP and total eIF4E-BP was calculated in order to characterise eIF4E-BP phosphorylation levels. The following equation was implemented:

$$\mathrm{pS65-eIF4E-BP\ level} = \frac{[\mathrm{pS65-eIF4E-BP}]}{[\mathrm{Actin}]} \div \frac{[\mathrm{eIF4E-BP\ total}]}{[\mathrm{Actin}]}$$

This ratio in control samples was considered as 100%.

Enzyme-linked immunosorbent assays (ELISAs)

Human or mouse TNF-α, IL-1β, SCF as well as human VEGF, either in cell culture media or human blood plasma were measured by ELISA using R&D Systems kits according to manufacturer's protocols. Phosphorylation of mTOR was analysed by ELISA as previously described.[13]

In cell assays and in cell Westerns

We employed a standard LI-COR in-cell Western (ICW) assay (methanol was used as permeabilization agent) to characterise Tim-3 total levels in studied cells. The in-cell (ICA, also called on-cell) assay was employed to detect Tim-3 surface presence in the cells. Following washing with PBS, cells were scanned using a LI-COR Odyssey imaging system.[17]

Detection of PI-3K activity

PI-3K activity was measured in cell lysates as described previously.[18] Briefly, cell lysates were incubated with 30 μl 0.1 mg/ml substrate (PI-4,5-diphosphate emulsion) in kinase assay buffer. The latter was prepared from 20 mM Tris (pH 7.5), 100 mM NaCl, 0.5 mM EDTA, 8 mM $MgCl_2$ and 40 μM ATP in a total volume of 100 μl at 37°C with constant agitation. Reactions were terminated by adding 1 ml of hexane/isopropanol (13:7, v:v) mixture and 0.2 ml of a mixture of 2 M KCl/HCl_{conc} (8:0.25, v:v). After vortexing the organic phases were washed with HCl (0.5 ml; 0.1 M). This was followed by detection of phosphate groups using a colorimetric assay. The values obtained in the control samples of each experiment per 1 mg protein were counted as 100% of the PI-3 K activity. Other values were normalised and expressed as % control.

Synchrotron radiation circular dichroism (SRCD) spectroscopy

Human recombinant Tim-3 and HMGB-1, either alone or in combination, were analysed using SRCD spectroscopy at beamline B23, Diamond Light Source (Didcot, UK). B23, equipped with a highly collimated microbeam, allows for the use of a small aperture long path length microcuvette which is unattainable with benchtop instruments due to divergent beams since samples available are of very low volume and concentrations. SRCD measurements were performed using 0.2 μM of samples in a 1 cm path length cell of 3 mm aperture diameter and 60 μl capacity using a Module B instrument with a 1 nm increment, 1 s integration time, 1.2 nm bandwidth at 23 °C.[19-24] Temperature denaturation measurements were collected over the temperatures 20°C – 95°C (in 5°C increments) for HMGB1, Tim-3 and the 1:1 mixture. The results obtained were processed using CDApps[25] and OriginPro®. For thermal denaturation measurements, change in CD (mdeg) at a specific wavelength was plotted against the corresponding temperature for fitting using the Gibbs-Helmholtz equation derived from Boltzmann distribution,[26,27] sigmoidal two-state denaturation curve to a Boltzmann distribution and the expression modified to include parameters for fitting of thermal denaturation data for the calculation of the melting temperature (T_m). Titration experiments were conducted as described for standard far-UV measurements, with the modification of measurements collected after the addition of incremental volumes of Tim-3 stock as described previously.[28] The change of CD (mdeg) at single wavelength was plotted against respective ligand concentration (μM) using OriginPro® and fitted with the Hill binding[29] function to determine the K_d for binding.

Statistical analysis

Each ELISA and cell experiment was performed at least three times and statistical analysis when comparing two events at a time was conducted using a two-tailed Student's *t*-test. Multiple comparisons were performed using an ANOVA test. Post-hoc Bonferroni correction was applied. Statistical probabilities (p) were expressed as * where $p < 0.05$; **, $p < 0.01$ and *** when $p < 0.001$.

Results

HMGB1 induces moderate activation of PI3-K/mTOR pathway, TNF-α and VEGF secretion in human AML cells

We used monocytic THP-1 human acute myeloid leukaemia cells which express Tim-3, but keep most of it inside the cell (Fig. 1 left panel), and primary human AML cells (AML-PB001F) where most Tim-3 is expressed on the cell surface (Fig. 1 right panel). Cells were exposed for 4 h to 1 μg/ml HMGB1 with or without 1 h pre-treatment with single-chain antibody against Tim-3, which does not display Tim-3 agonistic properties and also prevents the interaction of other ligands with it. We found that HMGB1 induced activation of PI-3K in both THP-1 and primary human AML cells. In both cell types this effect was non-significantly downregulated by the presence of anti-Tim-3 antibody (Fig. 1). This was consistent with a moderate activation of mTOR (phosphorylation at S2448) and increased phosphorylation of mTOR substrate eukaryotic initiation factor 4 E binding protein 1 (eIF4E-BP1). Increased TNF-α secretion took place in both cases. Neither process observed was influenced by the presence of anti-Tim-3 antibody, suggesting that the effects observed are Tim-3-independent.

Pre-treatment of THP-1 cells for 1 h with 2 μg/ml neutralising antibodies directed against TLR2, TLR4 and RAGE

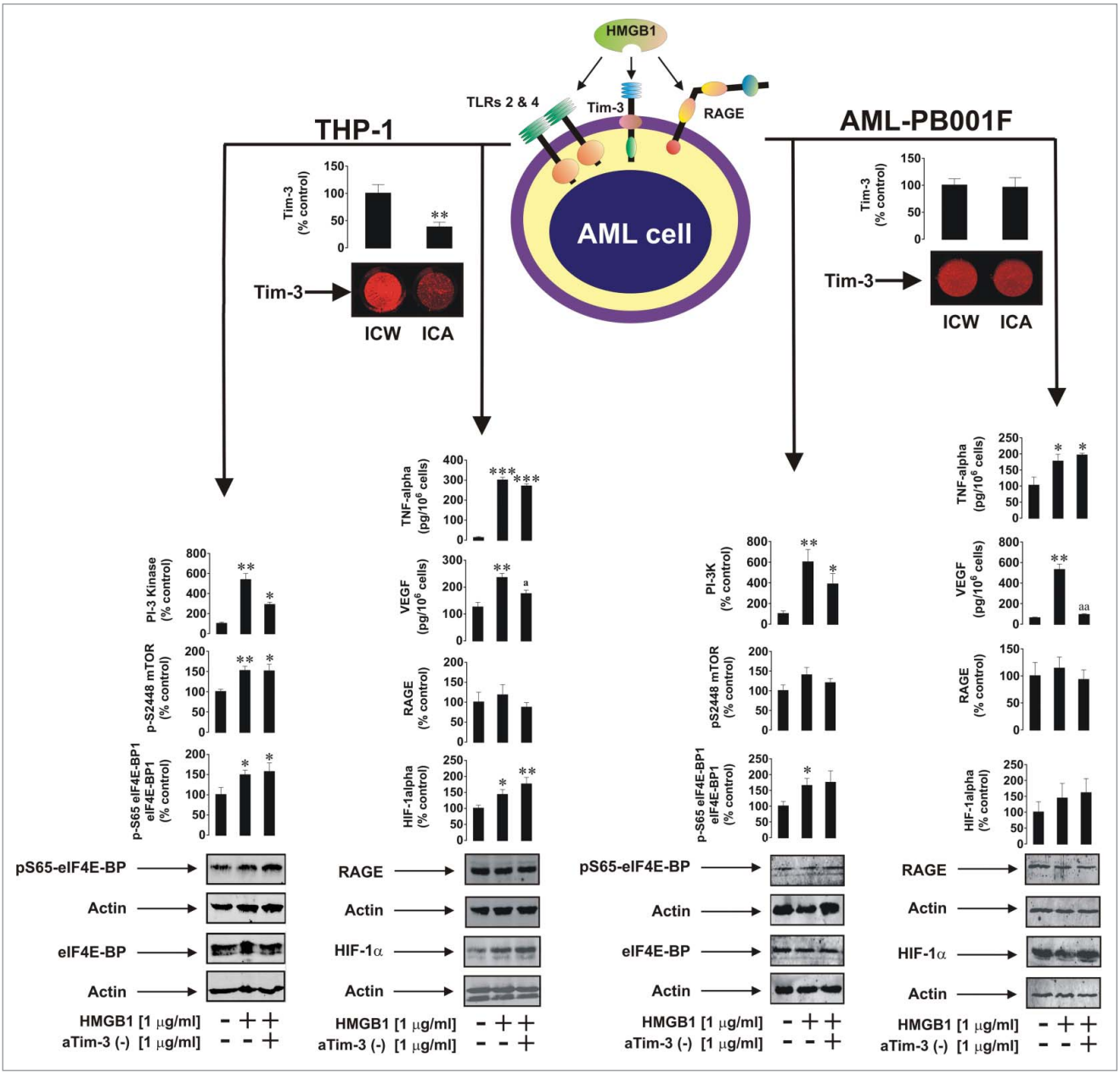


Figure 1. Differential receptors are involved in HMGB1-induced biological responses of human AML cells. Total levels of the immune receptor Tim-3 and its surface presence were characterised in THP-1 and primary human AML-PB001F cells by in-cell Western (ICW) and in-cell (on-cell) assay (ICA) respectively (see Materials and Methods for details). Both cell types were exposed to 1 μg/ml HMGB1 for 4 h with or without 1 h pre-treatment with single chain anti-Tim-3 antibody (aTim-3 (-)) followed by Western blot analysis of phospho-S65 *vs* total eIF4E-BP1, HIF-1α and RAGE expression as well as by detection of phospho-S2448 mTOR, release of TNF-α and VEGF using ELISA. PI-3 K activity was monitored by colorimetric assay. Images are from one experiment representative of five which gave similar results. Data is shown as mean values ± SEM of five independent experiments. * $p < 0.05$; **, $p < 0.01$ and *** when $p < 0.001$ *vs* control; ^{a} $p < 0.05$; ^{aa}, $p < 0.01$ *vs* HMGB1.

followed by 4 h of exposure to 1 μg/ml HMGB1 showed that TLRs 2 and 4, but not RAGE, are involved in HMGB1-induced TNF-α secretion (Supplementary Fig. 1). However, it does not rule out the fact that during long-term exposure RAGE might contribute to HMGB1-induced intracellular TNF-α expression which can be upregulated by RAGE ligands[30]

Consequently, we detected the activation of HIF-1α accumulation in THP-1 cells but not in AML cells which had high background levels of HIF-1α and thus probably did not respond to HMGB1 treatment (Fig. 1). In both cell types, however, we observed a significant increase in VEGF secretion (Fig. 1) which was significantly reduced (but not HIF-1α accumulation as seen from either Western blot data or intracellular VEGF levels (this was verified by ELISA performed on the cell lysates – data not shown)) by the presence of anti-Tim-3 antibody. The level of downregulation was proportional to the amount of Tim-3 present on the surface of each cell type. THP-1 and primary AML cells express TLRs 2 and 4. They also express high levels of RAGE, as verified by Western blot analysis (Fig. 1), which suggests that HMGB1 induces activation of the PI-3K/mTOR pathway and HIF-1α accumulation as well as TNF-α secretion through classic immune receptors like TLRs2/4, and RAGE, while secretion of VEGF is a Tim-3-dependent process.

Characterisation of HMGB1-Tim-3 interactions in vitro

We then sought to obtain confirmation of direct interactions between HMGB1 and Tim-3 using the recombinant, purified Ig-like V-type domain of human Tim-3 (residues 22–124) and human HMGB1. We employed SRCD spectroscopy for both qualitative and quantitative binding assays. Titration of 200 nM HMGB1 with increasing amounts of Tim-3 (Fig. 2A) indicated a high nanomolar binding affinity ($K_d = 10^{-7}$ M). The SRCD spectrum of a 1:1 HMGB1-Tim-3 complex appeared different from the sum of the SRCD spectra of the individual components (Fig. 2B), suggesting the presence of conformational rearrangements upon formation of the complex. Far UV thermal denaturation studies were also performed on the complex, further supporting the above data (Supplementary Figs. 2 and 3).

HMGB1 induces TNF-α secretion by human AML leading to upregulation of SCF production

Since it was obvious that both the AML cell line (THP-1) and primary AML cells secreted TNF-α in response to stimulation with HMGB1, we studied the effects of released TNF-α on the production of IL-1β by primary healthy human leukocytes (PHL). Cell culture medium obtained after stimulation of THP-1 cells with 1 μg/ml HMGB1 was used to treat primary healthy leukocytes for 4 h with or without 1 h pre-treatment with 2 μg/ml TNF-α-neutralising antibody. We found that in the absence of TNF-α-neutralising antibody, PHL released IL-1β, while in the presence of TNF-α-neutralising antibody PHL did not release detectable amounts of IL-1β. Medium containing IL-1β was used to culture MCF-7 breast cancer epithelial cells (these cells express IL-1 receptor type 1 and are capable of releasing stem cell factor (SCF)) for 24 h in the absence or presence of 2 μg/ml of IL-1β-neutralising antibody. We found that, in the presence of IL-1β-neutralising antibody, MCF-7 did not release detectable amounts of SCF, while in the absence of it SCF release was clearly detectable. These results (all shown in Fig. 3A) suggest that HMGB1 induces the release of TNF-α by AML cells. TNF-α induces IL-1β secretion by PHL. Released IL-1β stimulates the production of SCF by endothelial/epithelial cells. SCF is required for proliferation of AML cells and thus supports leukaemia progression.

We sought to obtain confirmation of this biological test using mouse bone marrow cells *ex vivo*. Mouse bone marrow cells were exposed to 1 μg/ml HMGB1 for 24 h. We observed that the levels of secreted TNF-α, IL-1β and SCF were significantly increased compared to non-treated bone marrow cells (Fig. 3B) and that the ratio between these cytokines was similar to that observed in the biological test shown in Fig. 3A.

We then measured the levels of TNF-α, IL-1β and SCF in the blood plasma of 10 healthy human donors and 45 AML patients. We found that the levels of all three factors were significantly increased (Fig. 3C – I). There was a clear evidence of correlation between IL-1β *vs* TNF-α, SCF vs IL-1β and SCF vs

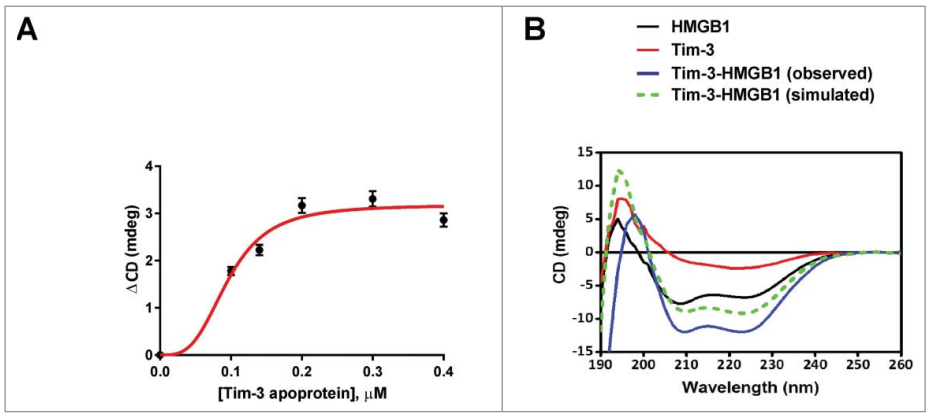


Figure 2. Interaction of HMGB1 and the immune receptor Tim-3. Interaction of HMGB1 protein with Tim-3 was analysed using SRCD spectroscopy-based titration which was conducted in the far UV region using 0.2 μM HMGB1 and increasing stoichiometric concentrations of Tim-3 (A). Changes in CD signal monitored at 222 nm were plotted against Tim 3 concentration using Hill function. Qualitative binding was verified by analysis of interactions of equimolar concentrations of Tim-3 and HMGB1 using SRCD spectroscopy (B).

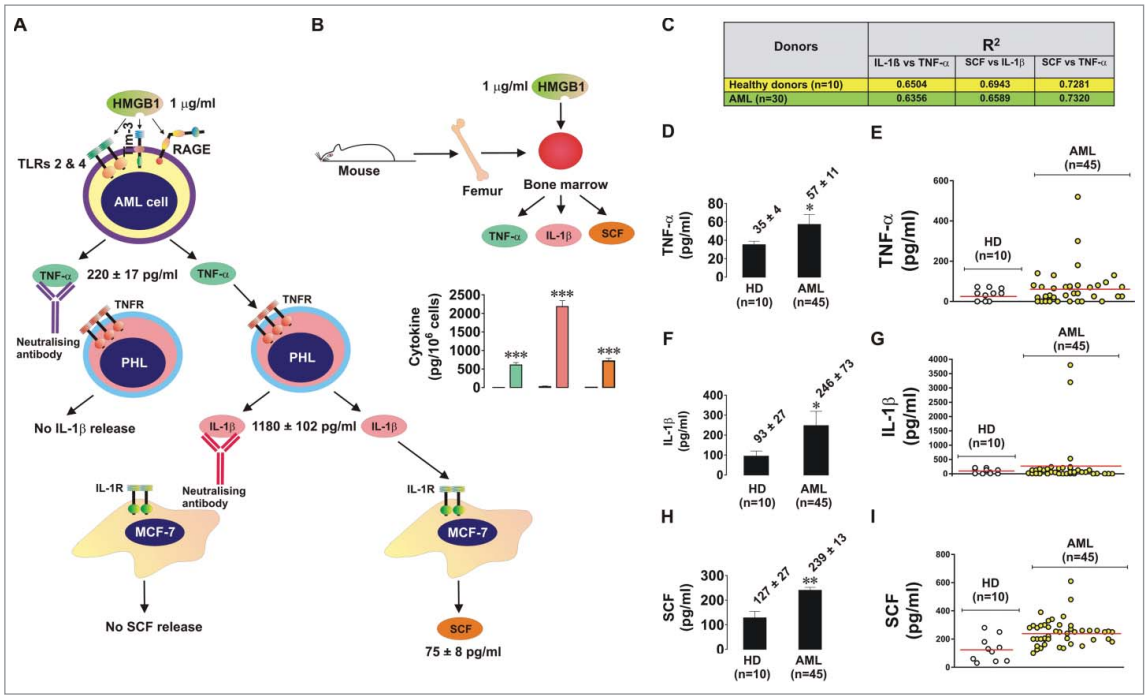


Figure 3. HMGB1 induces an intercellular signalling cascade leading to SCF secretion. (A) Primary human AML cells (AML-PB-001F) were exposed for 4 h to HMGB1 followed by collection of the culture medium (detection of TNF-α was performed in this medium using ELISA), which was used to culture primary human healthy leukocytes for 4 h in the absence or presence of TNF-α-neutralising antibody. Medium was collected (levels of IL-1β were measured by ELISA) and used to culture MCF-7 breast cancer epithelial cells for 4 h in the absence or presence of IL-1β-neutralising antibody. Following this exposure, medium was collected and SCF was measured in it by ELISA. (B) Primary mouse bone marrow cells (10^6 cells per 3 ml medium) were exposed for 24 h to 1 μg/ml HMGB1 followed by detection of TNF-α, IL-1β and SCF by ELISA. (C – I). Levels of TNF-α, IL-1β and SCF were measured in the blood plasma of healthy donors and AML patients by ELISA. Mean values ± SEM are presented as well as levels of each protein in blood plasma of each analysed donor/patient. $^{*}p < 0.05$; $^{**}p < 0.01$ *vs* control.

TNF-α (Fig. 3C and Supplementary Fig. 4) in the blood plasma of both healthy donors and AML patients which contained detectable amounts of all the studied cytokines/SCF suggesting that there is a link between these three factors regardless of the presence of HMGB1. But the increase in all three factors suggests that HMGB1 activates this intercellular cascade in order to increase the levels of secreted SCF thus supporting leukaemia progression.

Discussion

HMGB1 is an "alarmin" which can be secreted by stressed and dying cells as well as cancer and immune cells, and thus was suggested to play a role in leukaemia progression.[1-7] Recent evidence demonstrated that HMGB1 can also act as a ligand of the immune receptor Tim-3 which is highly expressed on the surface of human AML cells.[1,2] However, the signalling activity of HMGB1 in AML cells has not been elucidated and was thus the main aim of our work.

In both, a human AML cell line (THP-1 cells) and primary AML cells (AML-PB001F) we demonstrated that HMGB1 upregulates the activity of the PI-3 K/mTOR pathway, thus leading to increased TNF-α secretion and accumulation of HIF-1α as well as VEGF release (Fig. 1). However, except VEGF secretion (not HIF-1α-dependent expression), these effects were not Tim-3-mediated since Tim-3 neutralising single-chain antibody did not affect any of the processes described above (except for VEGF release). Importantly, non-differentiated THP-1 cells express moderate levels of Tim-3 on their surface – this process has to be induced by activation of PKCα (for example PMA or latrophilin 1 ligands).[15] Primary AML cells which use Tim-3/galectin-9 pathway in order to escape immune attack express much higher levels of Tim-3 protein on their surface. This difference was proportional to that in HMGB1-induced VEGF release in THP-1 and primary AML cells. Furthermore, neutralisation of Tim-3 led to attenuation of HMGB1-induced VEGF secretion in both cases suggesting that this is a Tim-3-mediated process.

Highly sensitive SRCD spectroscopic analysis of HMGB1-Tim-3 interactions confirmed that these two proteins interact with each other specifically, but the apparent affinity was moderately high ($K_d = 10^{-7}$ M). This affinity, however, can be increased by glycosides which normally bind to Tim-3 (the protein used in the studies was sugar-free). All these results suggest that this interaction is probably rather more secretory than a signal transduction event *per se*. Interestingly, the formation of the protein complex was accompanied by an increase in α-helical content at the expense of the β-strand presumably arising mainly from the Tim-3 protein. Biological tests demonstrated that TNF-α released from primary human AML cells in an HMGB1-dependent manner is capable of inducing IL-1β secretion by primary human healthy leukocytes. This is in line with recent observations suggesting upregulation of both TNF-α and IL-1β secretion in response to stimulation with HMGB1.[5,6] This reaction is a very important step in AML progression since IL-1β interacts with IL-1 receptor type I and induces production and secretion of SCF required for proliferation of AML cells. Human AML cells express high levels of Kit receptor, which recognises SCF, and

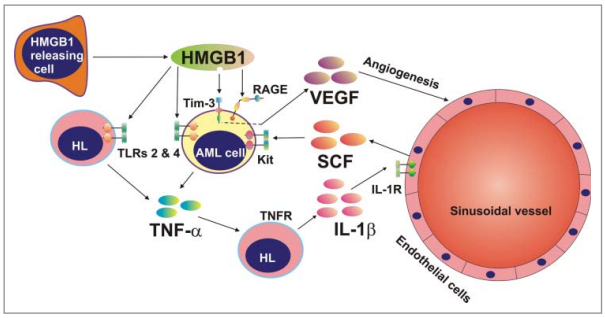


Figure 4. HMGB1 induces SCF and VEGF production *via* interaction with differential signalling receptors. The scheme shows that secreted HMGB1 is capable of inducing TNF-α secretion by living AML cells (and possibly healthy leukocytes, based on results obtained in the experiments with mouse bone marrow samples). Secreted TNF-α induces IL-1β production by healthy leukocytes which then induces SCF release in endothelial cells. These processes are Tim-3-independent. HMGB1 also induces VEGF secretion by AML cells in Tim-3-dependent manner.

this haematopoietic factor thus becomes highly oncogenic since AML cells are capable of inducing SCF production by healthy cells. The same effect was seen in primary mouse bone marrow cells. When exposed to HMGB1, levels of TNF-α, IL-1β and SCF increased suggesting that HMGB1 can, in principle, induce this effect in bone marrow too. However, production of HMGB1 is not observed in healthy bone marrow[1,2] since there are not enough stressed/dying or injured cells in order to produce it (in our samples over 95% of cells were viable as determined by trypan blue exclusion, data not shown). However, in leukaemic bone marrow this process is likely to take place due to lack of oxygen and increased HMGB1 expression in transformed cells.

Finally, we found that in blood plasma of AML patients, the levels of TNF-α, IL-1β and SCF were significantly higher compared to blood plasma from healthy donors.

We therefore concluded that in human bone marrow affected by AML, and respectively, by hypoxic conditions, cells release HMGB1 which induces TNF-α production and subsequent secretion of IL-1β which stimulates SCF production/secretion by endothelial cells. This SCF is used to further stimulate the survival/proliferation of AML cells. While these processes are Tim-3-independent, HMGB-1 interacts with Tim-3 and induces VEGF secretion, which is required to induce angiogenesis in bone marrow so that hypoxic conditions caused by increasing AML cell numbers can be relieved. This mechanism is summarised in the Fig. 4 (a more detailed scheme illustrating the possible interactions in the bone marrow is shown in Supplementary Fig. 5).

HMGB1 has already been considered as a possible therapeutic target for leukaemia treatment.[7] Furthermore, targeting HMGB1 has recently been shown to increase drug sensitivity in AML.[30] Our findings demonstrate additional insights that HMGB1 could be considered as a possible therapeutic target in AML and further confirm the efficiency of targeting Tim-3 (here to specifically block AML-induced angiogenesis) in anti-AML therapy.

Disclosure of potential conflicts of interest

No potential conflicts of interest were disclosed.

Acknowledgments

This work was supported by a Daphne Jackson Trust postdoctoral fellowship (to IMY), University of Kent Faculty of Sciences Research Fund (to VVS), Batzebär grant (to EFK and SB), SNF grant 310030 166445 and Oncosuisse grant KFS-3728-08-2015 (both to LV). We thank Diamond Light Source for access to B23 beamline (SM12578). We are grateful to Dr. Gurprit S. Lall (School of Pharmacy, University of Kent, UK) for kindly providing us with biological materials for bone marrow extraction.

References

1. He SJ, Cheng J, Feng X, Yu Y, Tian L, Huang Q. The dual role and therapeutic potential of high-mobility group box 1 in cancer. Oncotarget. 2017;8:64534–64550. doi:10.18632/oncotarget.17885. PMID:28969092.
2. Chiba S, Baghdadi M, Akiba H, Yoshiyama H, Kinoshita I, Dosaka-Akita H, Fujioka Y, Ohba Y, Gorman JV, Colgan JD, et al. Tumor-infiltrating DCs suppress nucleic acid-mediated innate immune responses through interactions between the receptor TIM-3 and the alarmin HMGB1. Nat Immunol. 2012;13:832–842. doi:10.1038/ni.2376. PMID:22842346.
3. Kang R, Zhang Q, Zeh HJ 3rd, Lotze MT, and Tang D. HMGB1 in cancer: good, bad, or both? Clin Cancer Res. 2013;19:4046–4057. doi:10.1158/1078-0432.CCR-13-0495. PMID:23723299.
4. Krysko O, Love Aaes T, Bachert C, Vandenabeele P, Krysko DV. Many faces of DAMPs in cancer therapy. Cell Death Dis. 2013;4:e631. doi:10.1038/cddis.2013.156. PMID:23681226.
5. Zhang Y, Liu Y, Xu X. Upregulation of miR-142-3p Improves Drug Sensitivity of Acute Myelogenous Leukemia through Reducing P-Glycoprotein and Repressing Autophagy by Targeting HMGB1. Transl Oncol. 2017;10:410–418. doi:10.1016/j.tranon.2017.03.003. PMID:28445844.
6. Tang L, Chai W, Ye F, Yu Y, Cao L, Yang M, Xie M, Yang L. HMGB1 promotes differentiation syndrome by inducing hyperinflammation via MEK/ERK signaling in acute promyelocytic leukemia cells. Oncotarget. 2017;8:27314–27327. doi:10.18632/oncotarget.15432 PMID:28404891.
7. Yu Y, Xie M, Kang R, Livesey KM, Cao L, Tang D. HMGB1 is a therapeutic target for leukemia. Am J Blood Res. 2012;2:36–43. PMID:22432086.
8. Zhang F, Su X, Huang G, Xin XF, Cao EH, Shi Y, Song Y. sRAGE alleviates neutrophilic asthma by blocking HMGB1/RAGE signalling in airway dendritic cells. Sci Rep. 2017;7:14268. doi:10.1038/s41598-017-14667-4. PMID:29079726.
9. Sumbayev VV, Nicholas SA. Hypoxia-inducible factor 1 as one of the "signaling drivers" of Toll-like receptor-dependent and allergic inflammation. Arch Immunol Ther Exp (Warsz). 2010;58:287–294. doi:10.1007/s00005-010-0083-0. PMID:20502970.
10. Sumbayev VV, Yasinska IM. Mechanisms of hypoxic signal transduction regulated by reactive nitrogen species. Scand J Immunol. 2007;65:399–406. doi:10.1111/j.1365-3083.2007.01919.x. PMID:17444949.
11. Prokhorov A, Gibbs BF, Bardelli M, Ruegg L, Fasler-Kan E, Varani L, Sumbayev VV. The immune receptor Tim-3 mediates activation of PI3 kinase/mTOR and HIF-1 pathways in human myeloid leukaemia cells. Int J Biochem Cell Biol. 2015;59:11–20. doi:10.1016/j.biocel.2014.11.017. PMID:25483439.
12. Goncalves Silva I, Gibbs BF, Bardelli M, Varani L, Sumbayev VV. Differential expression and biochemical activity of the immune receptor Tim-3 in healthy and malignant human myeloid cells. Oncotarget. 2015;6:33823–33833. doi:10.18632/oncotarget.5257. PMID:26413815.
13. Yasinska IM, Gibbs BF, Lall GS, Sumbayev VV. The HIF-1 transcription complex is essential for translational control of myeloid hematopoietic cell function by maintaining mTOR phosphorylation. Cell Mol Life Sci. 2014;71:699–710. doi:10.1007/s00018-013-1421-2. PMID:23872956.
14. Nicholas SA, Bubnov VV, Yasinska IM, Sumbayev VV. Involvement of xanthine oxidase and hypoxia-inducible factor 1 in Toll-like receptor 7/8-mediated activation of caspase 1 and interleukin-1beta. Cell Mol Life Sci. 2011;68:151–158. doi:10.1007/s00018-010-0450-3. PMID:20632067.
15. Goncalves Silva I, Yasinska IM, Sakhnevych SS, Fiedler W, Wellbrock J, Bardelli M, Varani L, Hussain R, Siligardi G, Ceccone G, et al. The

Tim-3-galectin-9 secretory pathway is involved in the immune escape of human acute myeloid leukemia cells. EBioMedicine. 2017;22:44–57. doi:10.1016/j.ebiom.2017.07.018. PMID:28750861.
16. Swamydas M, Lionakis MS. Isolation, purification and labeling of mouse bone marrow neutrophils for functional studies and adoptive transfer experiments. J Vis Exp. 2013;10:e50586. doi:10.3791/50586. PMID:23892876..
17. Goncalves Silva I, Ruegg L, Gibbs BF, Bardelli M, Fruehwirth A, Varani L, Berger SM, Fasler-Kan E, Sumbayev VV. The immune receptor Tim-3 acts as a trafficker in a Tim-3/galectin-9 autocrine loop in human myeloid leukemia cells. OncoImmunology. 2016;5:e1195535. doi:10.1080/2162402X.2016.1195535. PMID:27622049.
18. Abooali M, Lall GS, Coughlan K, Lall HS, Gibbs BF, Sumbayev VV. Crucial involvement of xanthine oxidase in the intracellular signalling networks associated with human myeloid cell function. Sci Rep. 2014;4:6307. doi:10.1038/srep06307. PMID:25200751.
19. Hussain R, Siligardi G. Characterisation of conformational and ligand binding properties of membrane proteins using synchrotron radiation circular dichroism (SRCD). Adv Exp Med Biol. 2016;922:43–59. doi:10.1007/978-3-319-35072-1_4. PMID:27553234.
20. Javorfi T, Hussain R, Myatt D, and Siligardi G. Measuring circular dichroism in a capillary cell using the b23 synchrotron radiation CD beamline at diamond light source. Chirality. 2010;22Suppl 1:E149–153. doi:10.1002/chir.20924. PMID:21038386.
21. Hussain R, Javorfi T, Siligardi G. Circular dichroism beamline B23 at the Diamond Light Source. J Synchrotron Radiat. 2012;19:132–135. doi:10.1107/S0909049511038982. PMID:22186655.
22. Hussain R, Jávorfi T, Siligardi G. Spectroscopic Analysis: Synchrotron Radiation Circular Dichroism. Comprehensive Chiral. 2012;8:438–448. doi:10.1016/B978-0-08-095167-6.00841-7.
23. Siligardi G, Hussain R. Biomolecules interactions and competitions by non-immobilised ligand interaction assay by circular dichroism. Enantiomer. 1998;3:77–87. PMID:9783430.
24. Siligardi G, Hussain R. CD spectroscopy: an essential tool for quality control of protein folding. Methods Mol Biol. 2015;1261:255–276. doi:10.1007/978-1-4939-2230-7_14. PMID:25502204.
25. Hussain R, Benning K, Myatt D, Javorfi T, Longo E, Rudd TR, Pulford B, Siligardi G. CDApps: integrated software for experimental planning and data processing at beamline B23, Diamond Light Source. J Synchrotron Radiat. 2015;22:862. doi:10.1107/S1600577515007602. PMID:25931108.
26. Singleton DG, Hussain R, Siligardi G, Kumar P, Hrdlicka P J, Berova N, Stulz E. Increased duplex stabilization in porphyrin-LNA zipper arrays with structure dependent exciton coupling, Org. Biomol. Chem. 2016;14:149–157. doi:10.1039/c5ob01681a. PMID:26416024.
27. Greenfield NJ. Using circular dichroism collected as a function of temperature to determine the thermodynamics of protein unfolding and binding interactions. Nat Protoc. 2006;1:2527–2535. doi:10.1038/nprot.2006.204. PMID:17406506.
28. Siligardi G, Panaretou B, Meyer P, Singh S, Woolfson DN, Piper PW, Pearl LH, Prodromou C. Regulation of Hsp90 ATPase activity by the co-chaperone Cdc37p/p50cdc37. J Biol Chem. 2002;277:20151–20159. doi:10.1074/jbc.M201287200. PMID:11916974.
29. Hill V. The possible effects of the aggregation of the molecules of hæmoglobin on its dissociation curves. J Physiol. 1910;40:iv–vii. doi:10.1371/journal.pone.0041098. PMID:22844429.
30. Rashid G, Benchetrit S, Fishman D, Bernheim J. Effect of advanced glycation end-products on gene expression and synthesis of TNF-alpha and endothelial nitric oxide synthase by endothelial cells. Kidney international. 2004;66:1099–1106. doi:10.1111/j.1523-1755.2004.00860.x. PMID:15327404.
31. Lu F, Zhang J, Ji M, Li P, Du Y, Wang H, Zang S, Ma D, Sun X, Ji C. miR-181b increases drug sensitivity in acute myeloid leukemia via targeting HMGB1 and Mcl-1. Int J Oncol. 2014;45:383–392. doi:10.3892/ijo.2014.2390. PMID:24756163.

CORRESPONDENCE

Cortisol facilitates the immune escape of human acute myeloid leukemia cells by inducing latrophilin 1 expression

Svetlana S. Sakhnevych[1], Inna M. Yasinska[1], Alison M. Bratt[1], Ouafa Benlaouer[1], Isabel Gonçalves Silva[1], Rohanah Hussain[2], Giuliano Siligardi[2], Walter Fiedler[3], Jasmin Wellbrock[3], Bernhard F. Gibbs[1,4], Yuri A. Ushkaryov[1] and Vadim V. Sumbayev[1]

Cellular & Molecular Immunology _####################_; https://doi.org/10.1038/s41423-018-0053-8

Dear Editor,

The progression of acute myeloid leukemia (AML)—the most severe blood/bone marrow cancer—is determined by the ability of malignant cells to escape host immune surveillance. However, the systemic regulatory mechanisms underlying this phenomenon remain largely unknown. In this study, we discovered a fundamental systemic biochemical strategy that allows AML cells to employ physiological systems within the body to survive and escape immune attack. We found that AML cells use a crucial human adrenal cortex hormone (cortisol) to induce the expression of neuronal receptor latrophilin 1 (LPHN1), which facilitates exocytosis. This receptor interacts with the blood plasma protein fibronectin leucine rich transmembrane protein 3 (FLRT3) to cause secretion of the immune suppressor galectin-9, which impairs the anticancer activities of cytotoxic lymphoid cells.

AML is a cancer of the blood and bone marrow that originates from self-renewing malignant immature myeloid cells and rapidly progresses into a systemic, and very often fatal, malignancy.[1] AML cells employ physiological systems in the body to produce factors required for proliferation/disease progression.[2,3] This includes the hijacking of stem cell factor (SCF), a major hematopoietic growth factor that controls AML progression and thus can become highly oncogenic.[2,3] The expression and release of SCF can be triggered by AML cells via cytokines (e.g., interleukin-1β).[2] Recent evidence clearly demonstrated that AML cells are also capable of impairing the activities of cytotoxic lymphoid cells (e.g., natural killer (NK) cells and cytotoxic T cells).[4] One of the biochemical mechanisms underlying this phenomenon lies in the ability of AML cells to secrete the protein galectin-9. This tandem-type galectin binds the immune receptor Tim-3 and induces a variety of intracellular and cell-to-cell signaling events leading to the inactivation of NK cells, as well as the death of cytotoxic T cells.[4,5] We recently reported that the process of galectin-9 secretion in AML cells is stimulated by the unique G protein-coupled receptor LPHN1, which normally functions in neurons to facilitate exocytosis.[4,6] LPHN1 is also found in hematopoietic stem cells (HSCs), but its expression disappears at the early stages of their maturation.[4,7] However, upon malignant transformation, AML cells preserve their abilities to express LPHN1 and to produce high levels of galectin-9 and Tim-3, in which the latter is involved in trafficking galectin-9 during the secretion process (HSCs express neither galectin-9 nor Tim-3[4]).

It is currently unknown which molecular mechanisms trigger elevated levels of LPHN1 expression in primary human AML cells, and in general, the mechanisms of upregulation of LPHN1 expression at the genomic level remain unclear. It is also unknown whether FLRT3, a natural LPHN1 ligand,[4,8] is present in human blood plasma and in other tissues associated with AML. Unraveling these mechanisms is crucial to understanding the pathways that control the ability of AML cells to protect themselves against cytotoxic lymphoid cells and, thus, was the aim of the present study.

RESULTS AND DISCUSSION

To investigate the effects of cortisol on LPHN1 transcription, we exposed primary and THP-1 human AML cells, primary human HSCs and primary healthy human leukocytes to 1 μM cortisol for 24 h and subjected to cells to quantitative real-time PCR to analyze LPHN1 mRNA levels. We found that all the tested cell types, except primary healthy leukocytes, transcribed detectable amounts of LPHN1 mRNA, and, in all these cases, the levels were significantly upregulated by treatment with cortisol (Fig. 1a). In both THP-1 and primary human AML cells, LPHN1 protein levels were also clearly upregulated (Fig. 1b, c). In contrast, primary human healthy leukocytes did not express detectable amounts of LPHN1 protein, and this was not altered by the effects of cortisol (Fig. 1d). Comparative analysis of LPHN1 protein expression in primary human AML cells, THP-1 cells, and primary human healthy leukocytes is shown in Supplementary figure 1.

Cortisol treatments did not upregulate galectin-9 secretion in any of these cell types (Fig. 1b–d), suggesting that LPHN1 needs to be activated by a ligand to induce galectin-9 release.

Analysis of blood plasma levels of cortisol in AML patients vs. those in healthy donors (samples were collected at the same time of the day to avoid the influence of circadian dynamics) demonstrated that the cortisol levels were significantly higher in the blood plasma of AML patients than in healthy donors (Fig. 1e). Galectin-9 levels were also substantially higher in AML patients (Fig. 1f), which is in line with our previous observations.[4] Furthermore, there was no correlation between cortisol and galectin-9 levels in the blood plasma of healthy donors, while in AML patients, there was a clear correlation (Fig. 1g), suggesting that galectin-9 secretion might be linked to LPHN1 expression in this circumstance.

If LPHN1 is expressed on the surface of blood cells, it can also be shed by proteolysis and therefore be present in the plasma.

[1]Medway School of Pharmacy, Universities of Kent and Greenwich, Chatham Maritime, UK; [2]Beamline B23, Diamond Light Source, Didcot, UK; [3]Department of Oncology, Hematology and Bone Marrow Transplantation with Section Pneumology, Hubertus Wald University Cancer Center, University Medical Center Hamburg-Eppendorf, Hamburg, Germany and [4]Department of Medicine, Dermatology and Allergology, University of Oldenburg, Oldenburg, Germany
Correspondence: Vadim V. Sumbayev (V.Sumbayev@kent.ac.uk)

Received: 18 May 2018 Accepted: 22 May 2018
Published online: 15 June 2018

© CSI and USTC 2018

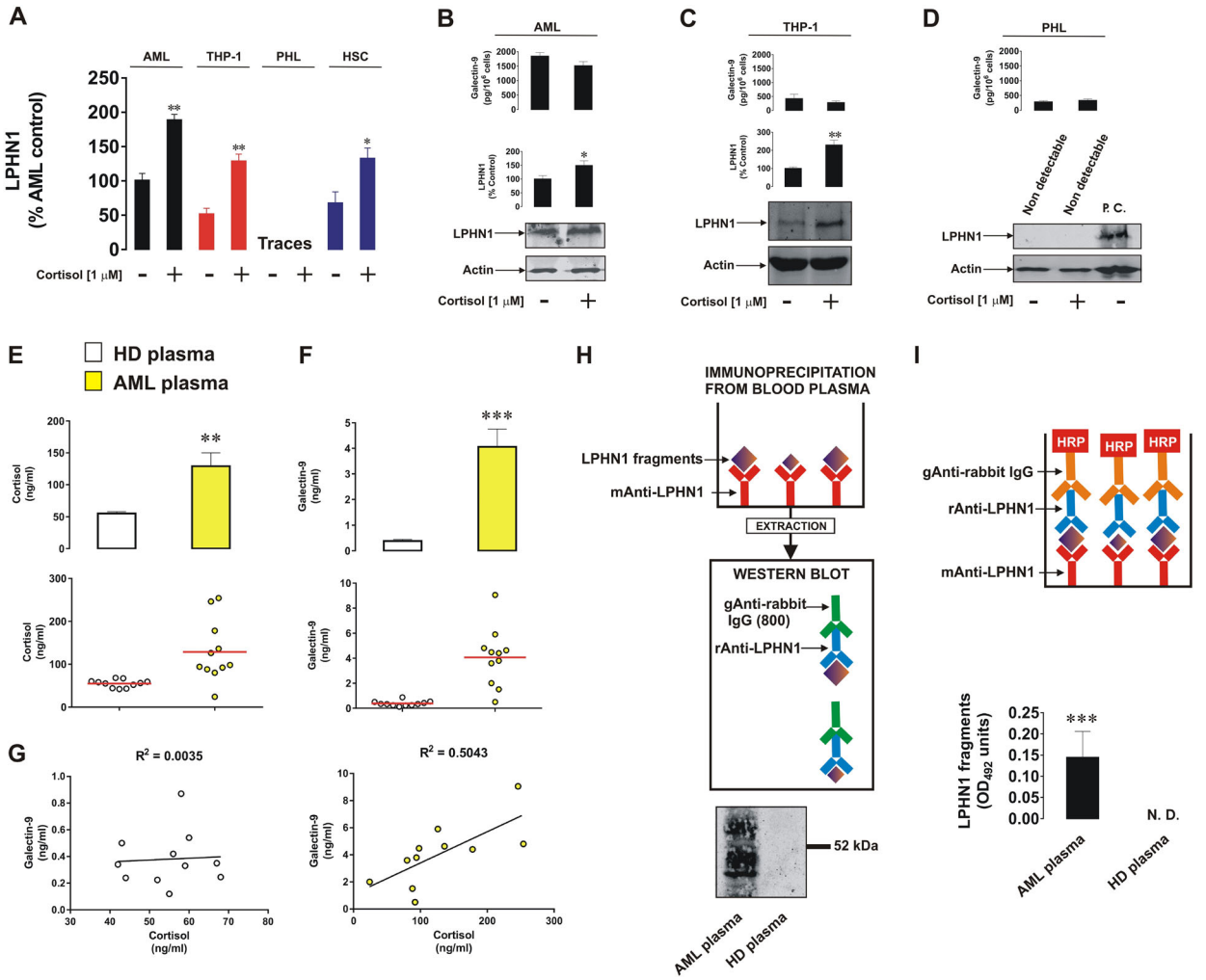


Fig. 1 Cortisol induces LPHN1 expression in human AML cells and in hematopoietic stem cells but not in primary healthy human leukocytes. Primary human AML cells, THP-1 cells, and hematopoietic stem cells, as well as primary healthy leukocytes were exposed to 1 μM cortisol for 24 h followed by analysis of LPHN1 gene transcription via quantitative real-time PCR (**a**) and Western blot analysis (**b** primary AML cells, (**c**) THP-1 cells, (**d**) PHL). For PHL, lysates from LPHN1-overexpressing NB2A cells were used as a positive control. ELISA was used to measure secreted galectin-9 levels. Blood plasma from 10 healthy donors and 10 AML patients was collected at the same time of the day to ensure comparability of the cortisol levels. Cortisol (**e**) and galectin-9 (**f**) levels were measured by ELISA, and the correlation between the levels of these two proteins was analyzed (**g**). Soluble LPHN1 fragments were immunoprecipitated and detected by Western blot (**h**) and ELISA (**i**), as outlined in the Materials and Methods section. Images are from one experiment but are representative of 4–6 replicates, all of which showed similar results. Data represent the mean values ± SEM of 6–10 independent experiments.; $*p < 0.05$; $**p < 0.01$; $***p < 0.01$ vs. control

LPHN1 in blood plasma samples from AML patients was immunoprecipitated, extracted, and subjected to Western blot analysis using several LPHN1 antibodies. A clear fragment was detectable at ~67–68 kDa, and smaller fragments were detectable as well, but only in plasma from AML patients, while in the blood plasma from healthy donors, there was no evidence of the presence of LPHN1 fragments (Fig. 1h). These fragments were also detectable by ELISA (Fig. 1i, see Materials and Methods for description of the ELISA format).

As reported before,[4] we observed that exposure of THP-1 AML cells to 10 nM FLRT3 for 16 h resulted in a significant increase in galectin-9 secretion (Fig. 2a). This effect was not detectable in primary healthy human leukocytes (Fig. 2a). Importantly, 1 h pre-exposure of THP-1 cells to rabbit polyclonal antibody recognizing LPHN1 (clone name RL1[9]) prior to the 16-h treatment with 10 nM FLRT3 attenuated FLRT3-induced galectin-9 release, confirming the involvement of LPHN1 in this process (Fig. 2a). The antibody employed specifically recognized target molecules on the surface of THP-1 cells (Supplementary figure 2). We used the mouse neuroblastoma cell line NB2A, which does not express LPHN1,[10] as a negative control and measured the interaction of the antibody with the cell surface using a Li-Cor on-cell assay as described in the Materials and Methods (please see supplementary information). Exposure of THP-1 cells to 1 μg/ml RL1 for 16 h did not affect galectin-9 secretion levels (data not shown), suggesting that this antibody does not exert an LPHN1 agonistic effect.

Interestingly, we found that blood plasma from both healthy donors and AML patients contains approximately equal amounts of secreted FLRT3 (most likely by proteolytic shedding) with a molecular weight of approximately 55 kDa (which corresponds to the molecular weight of FLRT3 shed from the cell surface by proteinases[11]). Another specific band was observed at ~27–28 kDa, which most likely corresponds to a smaller cleavage fragment of the FLRT3 extracellular domain (Fig. 2b). The amounts of this smaller fragment were also equal in blood plasma from healthy donors and AML patients (Fig. 2b). To explore which blood plasma-based ligands can induce galectin-9 secretion in AML cells, we cultured THP-1 cells in RPMI 1640 medium containing antibiotics (as outlined in Materials and Methods—see supplementary information) and replacing the 10% fetal bovine serum

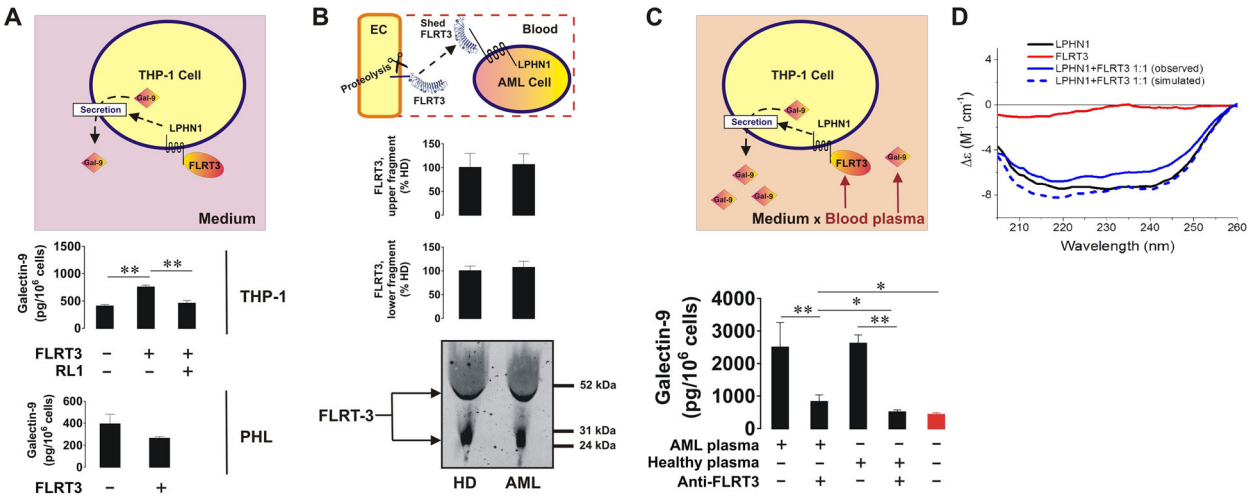


Fig. 2 FLRT3 induces galectin-9 secretion in AML cells in a LPHN1-dependent manner. THP-1 cells and PHL were exposed to 10 nM human recombinant FLRT3 for 16 h, followed by detection of secreted galectin-9 by ELISA. In THP-1 cells, the treatment was performed with or without 1 h pre-exposure to 1 µg/ml RL1 anti-LPHN1 polyclonal antibody (**a**). The levels of released FLRT3 fragments were analyzed in the blood plasma from healthy donors and AML patients using Western blot (**b**). THP-1 cells were exposed for 16 h to 10% blood plasma either from healthy donors or AML patients, with or without pretreatment with FLRT3-neutralizing antibody. The levels of secreted galectin-9 were analyzed using ELISA. (**c**) Secondary structure and conformational changes of LPHN1, FLRT3, and the complex of the two proteins were characterized using SRCD spectroscopy as outlined in the Materials and Methods (**d**). Images are shown from one representative experiment of four replicates, all of which showed similar results. Data are shown as the mean values ± SEM from four independent experiments; *$p < 0.05$; **$p < 0.01$ vs. control

(FBS) with blood plasma from either healthy donors or AML patients. Cells were incubated for 16 h with or without a 30-min preincubation with anti-FLRT3 antibody to neutralize FLRT3 activity. Galectin-9 secretion levels were significantly higher in the presence of either sources of human blood plasma than in the presence of FBS (negative control). Anti-FLRT3 antibody attenuated galectin-9 secretion (Fig. 2c). The binding of LPHN1 and FLRT3 was further confirmed using SRCD spectroscopy. We found that the two proteins interact with each other with high affinity such that a conformational change is induced in both proteins, as seen from far UV synchrotron radiation circular dichroism (SRCD) spectra (Fig. 2d). This is further confirmation of the high-affinity interaction of LPHN1 and FLRT3 observed in previous studies[8] using different techniques.

Taken together, our results demonstrate, for the first time, that cortisol upregulates LPHN1 expression at the transcriptional level, thus stimulating its translation in human AML cells. AML leads to decreased blood plasma glucose levels,[5] which normally leads to upregulation of the secretion of corticotropin-releasing hormone (CTRH) from the hypothalamus.[12] CTRH induces the secretion of adrenocorticotropic hormone (ACTH) from the pituitary gland.[12] ACTH upregulates cortisol production in the adrenal cortex.[12] Cortisol is then employed by AML cells. In healthy human leukocytes, cortisol is not capable of inducing LPHN1 transcription/translation, possibly because of gene repression. Interaction of AML cell-derived LPHN1 with released FLRT3 available in blood plasma facilitates the secretion of galectin-9. The latter protects AML cells against immune attack, which could otherwise be performed by NK cells or cytotoxic T cells (Supplementary figure 3). Importantly, LPHN1 fragments are present in the blood plasma from AML patients but not from healthy donors. These fragments were detectable by both Western blot analysis and ELISA, which indicates the possibility of detecting these fragments for a rapid AML diagnosis, although differential verification tests have yet to be performed. Our results suggest a fundamentally novel mechanism used by AML cells to progress the disease. They use a common endogenous human hormone (cortisol) to induce LPHN1 expression by employing a widely available ligand (FLRT3, which is always present in blood plasma) to escape host immune surveillance. Thus, AML cells engage crucial functional systems of the human body to support their survival and attenuate the anticancer activities of cytotoxic lymphoid cells. Our work indicates that galectin-9 and secreted FLRT3 are the most promising targets for anti-AML immune therapy.

ACKNOWLEDGEMENTS

This work was supported by a Daphne Jackson Trust postdoctoral fellowship (to I. M. Y.) and the University of Kent Faculty of Sciences Research Fund (to V. S.). We thank Diamond Light Source for access to B23 beamline (SM12578).

ADDITIONAL INFORMATION

The online version of this article (https://doi.org/10.1038/s41423-018-0053-8) contains supplementary material.

Competing interests: The authors declare no competing interests.

Publisher's note: Springer Nature remains neutral with regard to jurisdictional claims in published maps and institutional affiliations.

REFERENCES

1. Estey, E. & Döhner, H. Acute myeloid leukaemia. *Lancet* **368**, 1894–1907 (2006).
2. Wyszynski, R. W., Gibbs, B. F., Varani, L., Iannotta, D. & Sumbayev, V. V. Interleukin-1 beta induces the expression and production of stem cell factor by epithelial cells: crucial involvement of the PI-3K/mTOR pathway and HIF-1 transcription complex. *Cell. Mol. Immunol.* **13**, 47–56 (2016).
3. Yasinska, I. M. et al. High mobility group box 1 (HMGB1) acts as an "alarmin" to promote acute myeloid leukaemia progression. *OncoImmunology* **7**, e1438109 (2018).
4. Goncalves Silva, I. et al. The tim-3-galectin-9 secretory pathway is involved in the immune escape of human acute myeloid leukemia cells. *EBioMedicine* **22**, 44–57 (2017).
5. Goncalves Silva, I. et al. The immune receptor Tim-3 acts as a trafficker in a Tim-3/galectin-9 autocrine loop in human myeloid leukemia cells. *OncoImmunology* **5**, e1195535 (2016).
6. Sumbayev, V. V. et al. Expression of functional neuronal receptor latrophilin 1 in human acute myeloid leukaemia cells. *Oncotarget* **7**, 45575–45583 (2016).

7. Maiga, A. et al. Transcriptome analysis of G protein-coupled receptors in distinct genetic subgroups of acute myeloid leukemia: identification of potential disease-specific targets. *Blood Cancer J.* **6**, e431 (2016).
8. Boucard, A. A., Maxeiner, S. & Sudhof, T. C. Latrophilins function as heterophilic cell-adhesion molecules by binding to teneurins: regulation by alternative splicing. *J. Biol. Chem.* **289**, 387–402 (2014).
9. Volynski, K. E. et al. Latrophilin, neurexin, and their signaling-deficient mutants facilitate α-latrotoxin insertion into membranes but are not involved in pore formation. *J. Biol. Chem.* **275**, 41175–41183 (2000).
10. Silva, J. P. et al. Latrophilin 1 and its endogenous ligand Lasso/teneurin-2 form a high-affinity transsynaptic receptor pair with signaling capabilities. *Proc. Natl Acad. Sci. USA* **108**, 12113–12118 (2011).
11. Yamaguchi, S. et al. FLRT2 and FLRT3 act as repulsive guidance cues for Unc5-positive neurons. *EMBO J.* **30**, 2920–2933 (2011).
12. Tabata, I., Ogita, F., Miyachi, M. & Shibayama, H. Effect of low blood glucose on plasma CRF, ACTH, and cortisol during prolonged physical exercise. *J. Appl. Physiol.* **71**, 1807–1812 (1991).

frontiers in Pharmacology

RESEARCH SNAPSHOT
published: 05 April 2019
doi: 10.3389/fphar.2019.00342

Mitochondrial Defunctionalization Supresses Tim-3-Galectin-9 Secretory Pathway in Human Colorectal Cancer Cells and Thus Can Possibly Affect Tumor Immune Escape

Svetlana S. Sakhnevych[1], *Inna M. Yasinska*[1], *Elizaveta Fasler-Kan*[2,3]* and *Vadim V. Sumbayev*[1]*

[1] Medway School of Pharmacy, Universities of Kent and Greenwich, Chatham, United Kingdom, [2] Department of Pediatric Surgery and Department of Biomedical Research, Children's Hospital, Inselspital, University of Bern, Bern, Switzerland, [3] Department of Biomedicine, University Hospital Basel and University of Basel, Basel, Switzerland

OPEN ACCESS

Edited by:
Chiranjib Chakraborty, Galgotias University, India

Reviewed by:
Raghvendra Mohan Srivastava, Memorial Sloan Kettering Cancer Center, United States
Emerson Soares Bernardes, Instituto de Pesquisas Energéticas e Nucleares (CNEN), Brazil

***Correspondence:**
Elizaveta Fasler-Kan
elizaveta.fasler@insel.ch
Vadim V. Sumbayev
V.Sumbayev@kent.ac.uk

Specialty section:
This article was submitted to Experimental Pharmacology and Drug Discovery, a section of the journal Frontiers in Pharmacology

Received: 15 December 2018
Accepted: 19 March 2019
Published: 05 April 2019

Citation:
Sakhnevych SS, Yasinska IM, Fasler-Kan E and Sumbayev VV (2019) Mitochondrial Defunctionalization Supresses Tim-3-Galectin-9 Secretory Pathway in Human Colorectal Cancer Cells and Thus Can Possibly Affect Tumor Immune Escape. Front. Pharmacol. 10:342. doi: 10.3389/fphar.2019.00342

The Tim-3-galectin-9 secretory pathway is known to protect various types of cancer cells against host immune surveillance. We found that pharmacologically induced mitochondrial dysfunction leads to a reduced galectin-9 expression/exocytosis in human colorectal cancer cells and re-distribution of this protein (the effect described for various cellular proteins) into mitochondria.

Keywords: galectin-9, Tim-3, immune surveillance, mitochondria, colorectal cancer

RESULTS

It has recently been discovered that the immune receptor Tim-3 (T cell immunoglobulin and mucin domain-containing protein 3) and it's ligand galectin-9 determines the capability of various types of malignant cells [e.g., acute myeloid leukemia (AML), colorectal cancer] to escape host immune surveillance (Kang et al., 2015; Gonçalves Silva et al., 2017; Sakhnevych et al., 2018; Yasinska et al., 2018b). Also, some of the galectin family members (for example galectin-3) were found to be able to protect AML and colorectal cancer cells against apoptosis through mitochondrial stabilization in a B cell lymphoma protein (Bcl) 2-dependent manner (Lee et al., 2013; Ruvolo, 2016). We asked whether galectin-9 has the same intracellular anti-apoptotic activity in addition to its extracellular immunosuppressive role. We used a pharmacological inhibitor 5-[(4-bromophenyl)methylene]-a-(1-methylethyl)-4-oxo-2-thioxo-3-thiazolidineacetic acid (BH3I-1, **Figure 1A**), a synthetic cell permeable Bcl-X_L antagonist, which induces apoptosis via inhibition of interactions between the BH3 domain and Bcl-X_L thus defunctionalyzing mitochondria. We found that BH3I-1 was capable of inducing apoptosis in Colo 205 colorectal adenocarcinoma cells of epithelial origin (based on increased caspase-3 activity and decreased viability of the cells, **Figure 1A**). Silencing either galectin-9 or its receptor and possible trafficker Tim-3 did not affect the pro-apoptotic activity of BH3I-1 suggesting that galectin-9 is unlikely to display anti-apoptotic activity in this case. Interestingly, the action of BH3I-1 did not affect the activity of mammalian target of rapamycin (mTOR) translational pathway as seen from its capability to phosphorylate eukaryotic initiation

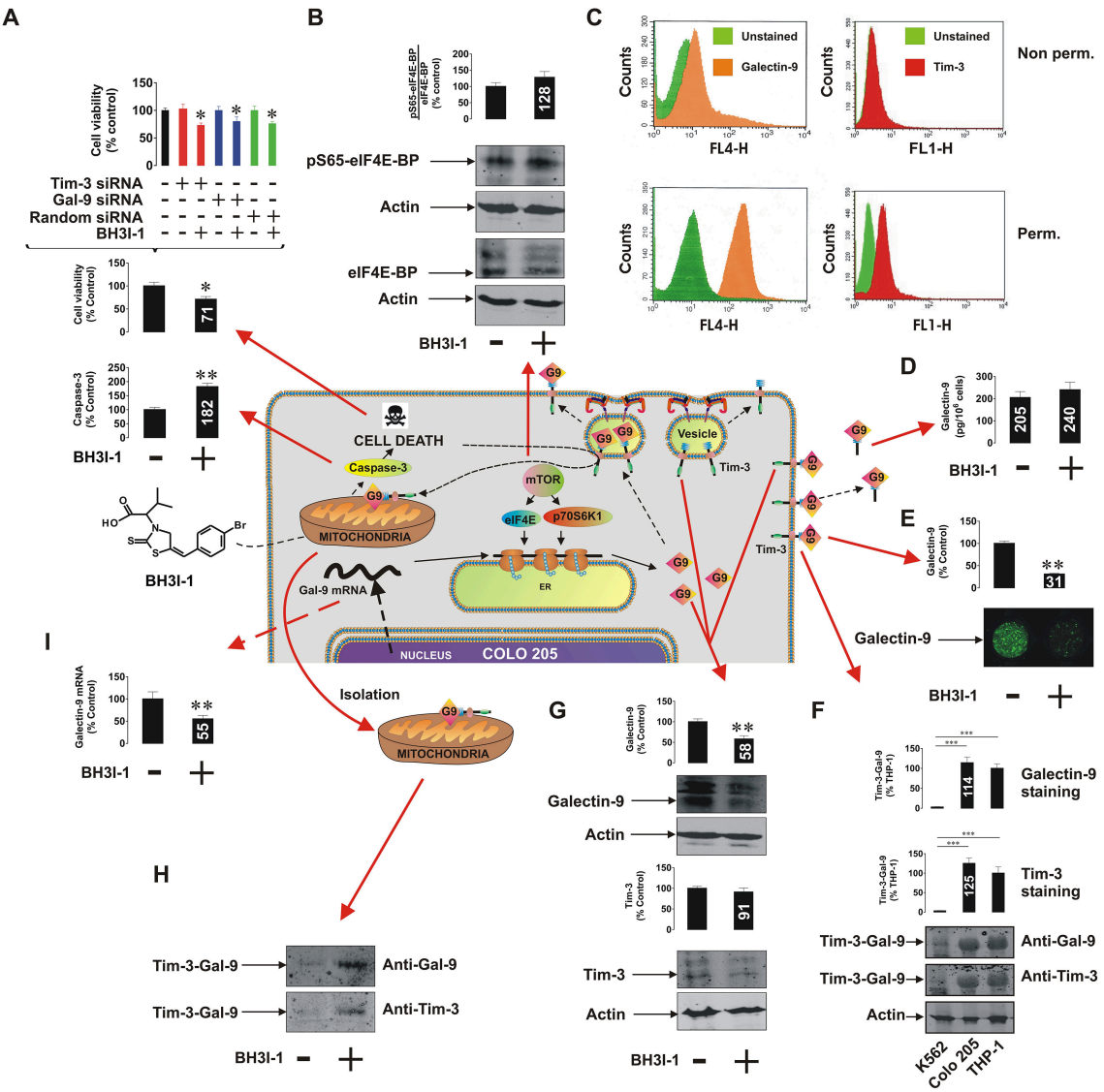


FIGURE 1 | Pro-apoptotic defunctionalization of mitochondria reduces galectin-9 expression and leads to its redistribution in human Colo 205 colorectal adenocarcinoma cells. Colo 205 cells were exposed to 100 μM BH3I-1 for 24 h followed by **(A)** detection of cell viability using an MTS test and colorimetric assay of caspase-3 activity. Cell viability was also tested for normal and Tim-3 or galectin-9 knockdown Colo 205 cells. **(B)** Following 24 h of exposure to BH3I-1 S65-phosphorylation levels of eIF4E-BP were analyzed by Western blot. **(C)** Surface presence and total cellular levels of Tim-3 and galectin-9 were analyzed in Colo 205 cells using FACS. **(D)** Secreted levels of galectin-9 were analyzed in Colo 205 cells following 24 h of exposure to BH3I-1 by ELISA. **(E)** Surface levels of galectin-9 in non-treated and BH3I-1-stimulated Colo 205 cells were compared using an on-cell assay. **(F)** The presence of Tim-3-galectin-9 complex in Colo 205 cells was confirmed using Western blot analysis (bands were appearing at around 70 KDa, better detectable when temperature denaturation is not applied). THP-1 cells were used as a positive and K562 as a negative control. **(G)** Levels of Tim-3 and galectin-9 were analyzed in Colo 205 lysates following 24 h of exposure to BH3I-1 by Western blot. **(H)** Mitochondrial extracts were obtained from non-treated and BH3I-1-stimulated Colo 205 cells and subjected to Western blot analysis to detect Tim-3 and galectin-9. Total protein levels were measured using a Bradford assay and equal protein amounts were loaded onto the gels. **(I)** Galectin-9 mRNA levels were analyzed in non-treated Colo 205 cells and those exposed to BH3I-1 using qRT-PCR. In the scheme galectin-9 is abbreviated as G9. Quantitative results are shown as mean values (crucial mean values are written inside respective bars) ± SEM of 3–6 independent experiments. $^{*}p < 0.05$; $^{**}p < 0.01$; $^{***}p < 0.001$ vs. control. The scheme in the centre of the figure is based on our work on Tim-3-galectin-9 secretory pathway (Gonçalves Silva et al., 2017).

factor-4E-binding protein (eIF4E-BP, **Figure 1B**). Obviously, one could suggest that Colo 205 cells accumulate galectin-9 on their surface and inside the cells based on FACS analysis (**Figure 1C**). Reduced levels of surface-based Tim-3 might indicate its masking by galectin-9 (Yasinska et al., 2018a). BH3I-1 does not affect the ability of Colo 205 cells to secrete galectin-9 (**Figure 1D**) but significantly reduces its surface presence (**Figure 1E**) as measured by on-cell assay. Colo 205 cells accumulate the Tim-3-galectin-9 complex (**Figure 1F**) at a level comparable to THP-1 AML cells (K562 chronic ML cells expressing traces

of galectin-9 were used as a negative control). Both proteins are also clearly detectable in Colo 205 cells by Western blot (**Figure 1G**) and treatment with BH3I-1 reduces intracellular levels of galectin-9. Importantly, Western blot analysis of Colo 205 mitochondrial extracts showed that the Tim-3-galectin-9 complex is accumulated in mitochondria upon stimulation with BH3I-1 (**Figure 1H**). The intracellular levels of galectin-9 mRNA were significantly reduced upon stimulation with BH3I-1, as detected by quantitative real-time PCR (qRT-PCR, **Figure 1I**).

Interestingly, the ability of Colo 205 cells to secrete galectin-9 is lower compared to THP-1 AML cells and the levels of secretion in both cell types are proportional to cellular Tim-3 levels (**Supplementary Figure 1**). This further supports conclusion regarding the involvement of Tim-3 in galectin-9 secretion (Gonçalves Silva et al., 2017).

We have also investigated two other types of epithelial cells—non-malignant human kidney RC-124 and malignant human HepG2 hepatoma cells. Both cell types have abundant mitochondria, however they are often [especially non-malignant, like RC-124—confirmed by a direct chemical measurement as described of the drug-associated bromine (Sollo et al., 1971) uptake in these cells, data not shown] less permeable for inhibitors of this type compared to colorectal cancer and AML cells. Therefore, 6 h of exposure to 1 mM H_2O_2 was used in order to defunctionalize mitochondria (Nicholas et al., 2011). We found that galectin-9 levels were significantly reduced in both cell types but the Tim-3-galectin-9 complex was only accumulated in the mitochondria of HepG2 and not RC-124 cells (**Supplementary Figure 2**).

MATERIALS AND METHODS

Commercially available Colo 205, RC-124, HepG2, THP-1, and K562, accompanied by authentication certificates, were used in this study. Mitochondria isolation, Western blot, on-cell assays, qRT-PCR, ELISA, and FACS analysis were performed as described before (Nicholas et al., 2011; Gonçalves Silva et al., 2016, 2017; Yasinska et al., 2018a). Detailed description of materials and methods used is provided in **Supplementary Information**.

DISCUSSION

Our results indicate that colorectal cancer cells operate the Tim-3-galectin-9 secretory pathway, where Tim-3 acts as a galectin-9 binding partner and possible trafficker. Pro-apoptotic mitochondrial dysfunction leads to a decreased transcription of galectin-9 mRNA leading to its reduced translation. However, exocytosis of galectin-9 is affected by mitochondrial defunctionalization leading to a re-distribution of the Tim-3-galectin-9 complex into mitochondria where galectin-9 could possibly interact with mitochondrial glycoproteins. The physiological relevance of this process is unclear but may well be a part of the regulated cell suicide programme which might involve transfer of galectin-9 into mitochondria so that it can't be involved in protection of a dying cell thus allowing its smooth elimination. Our further studies indicate that this phenomenon might be applicable mainly to malignant epithelial cells (**Figure 1**, **Supplementary Figure 2**). Importantly, targeted defunctionalization of mitochondria in malignant cells may be a novel strategy for anti-cancer immunotherapy since it reduces cell surface presence of galectin-9 capable of suppressing anti-cancer activity of cytotoxic lymphoid cells.

AUTHOR CONTRIBUTIONS

SS performed majority of the experiments reported in the **Figure 1** and significant number of experiments reported in **Supplementary Figures 1**, **2**, analyzed the data and contributed to manuscript writing. IY performed analysis of Tim-3-galectin-9 interactions and significant amount of experiments reported in **Supplementary Figure 2**, contributed to data analysis and manuscript writing. EF-K contributed to study design, performed FACS analysis, contributed to data analysis, and manuscript writing. VS designed the study, supervised the whole project, put the data together, wrote the manuscript.

SUPPLEMENTARY MATERIAL

The Supplementary Material for this article can be found online at: https://www.frontiersin.org/articles/10.3389/fphar.2019.00342/full#supplementary-material

REFERENCES

Gonçalves Silva, I., Ruegg, L., Gibbs, B. F., Bardelli, M., Fruewirth, A., Varani, L., et al. (2016). The immune receptor Tim-3 acts as a trafficker in a Tim-3/galectin-9 autocrine loop in human myeloid leukaemia cells. *Oncoimmunology* 5:e1195535. doi: 10.1080/2162402X.2016.1195535

Gonçalves Silva, I., Yasinska, I. M., Sakhnevych, S. S., Fiedler, W., Wellbrock, J., Bardelli, M., et al. (2017). The Tim-3-galectin-9 secretory pathway is involved in the immune escape of human acute myeloid leukemia cells. *EBio Med.* 22, 44–57. doi: 10.1016/j.ebiom.2017.07.018

Kang, C. W., Dutta, A., Chang, L. Y., Mahalingam, J., Lin, Y. C., Chiang, J. M., et al. (2015). Apoptosis of tumor infiltrating effector TIM-3+CD8+ T cells in colon cancer. *Sci. Rep.* 5:15659. doi: 10.1038/srep15659

Lee, Y. K., Lin, T. H., Chang, C. F., and Lo, Y. L. (2013). Galectin-3 silencing inhibits epirubicin-induced ATP binding cassette transporters and activates the mitochondrial apoptosis pathway via beta-catenin/GSK-3beta modulation in colorectal carcinoma. *PLoS ONE* 8:e82478. doi: 10.1371/journal.pone.0082478

Nicholas, S. A., Coughlan, K., Yasinska, I., Lall, G. S., Gibbs, B. F., Calzolai, L., et al. (2011). Dysfunctional mitochondria contain endogenous high-affinity human Toll-like receptor 4 (TLR4) ligands and induce TLR4-mediated inflammatory reactions. *Int. J. Biochem. Cell Biol.* 43, 674–681. doi: 10.1016/j.biocel.2011.01.012

Ruvolo, P. P. (2016). Galectin 3 as a guardian of the tumor microenvironment. *Biochim. Biophys. Acta* 1863, 427–437. doi: 10.1016/j.bbamcr.2015.08.008

Sakhnevych, S. S., Yasinska, I. M., Bratt, A. M., Benlaouer, O., Gonçalves Silva, I., Hussain, R., et al. (2018). Cortisol facilitates the immune escape of human

acute myeloid leukemia cells by inducing latrophilin 1 expression. *Cell. Mol. Immunol.* 15, 994–997. doi: 10.1038/s41423-018-0053-8

Sollo, F. W., Larson, T. E., and McGurk, F. F. (1971). Coloimetric methods for bromine. *Environ. Sci. Technol.* 5, 240–246. doi: 10.1021/es60050a009

Yasinska, I. M., Ceccone, G., Ojea-Jimenez, I., Ponti, J., Hussain, R., and Siligardi, G. (2018a). Highly specific targeting of human acute myeloid leukaemia cells using pharmacologically active nanoconjugates. *Nanoscale* 10, 5827–5833. doi: 10.1039/C7NR09436A

Yasinska, I. M., Gonzalves Silva, I., Sakhnevych, S. S., Ruegg, L., Hussain, R., Siligardi, G., et al. (2018b). High mobility group box 1 (HMGB1) acts as an "alarmin" to promote acute myeloid leukaemia progression. *Oncoimmunology* 7:e1438109. doi: 10.1080/2162402X.2018.1438109

Conflict of Interest Statement: The authors declare that the research was conducted in the absence of any commercial or financial relationships that could be construed as a potential conflict of interest.

Copyright © 2019 Sakhnevych, Yasinska, Fasler-Kan and Sumbayev. This is an open-access article distributed under the terms of the Creative Commons Attribution License (CC BY). The use, distribution or reproduction in other forums is permitted, provided the original author(s) and the copyright owner(s) are credited and that the original publication in this journal is cited, in accordance with accepted academic practice. No use, distribution or reproduction is permitted which does not comply with these terms.

frontiers in Immunology

ORIGINAL RESEARCH
published: 11 July 2019
doi: 10.3389/fimmu.2019.01594

Check for updates

The Tim-3-Galectin-9 Pathway and Its Regulatory Mechanisms in Human Breast Cancer

Inna M. Yasinska[1†], Svetlana S. Sakhnevych[1†], Ludmila Pavlova[2†], Anette Teo Hansen Selnø[1], Ana Maria Teuscher Abeleira[3,4], Ouafa Benlaouer[1], Isabel Gonçalves Silva[1], Marianne Mosimann[3,4], Luca Varani[5], Marco Bardelli[5], Rohanah Hussain[6], Giuliano Siligardi[6], Dietmar Cholewa[3], Steffen M. Berger[3], Bernhard F. Gibbs[1,7], Yuri A. Ushkaryov[1], Elizaveta Fasler-Kan[3,8*], Elena Klenova[2*] and Vadim V. Sumbayev[1*]*

[1] Medway School of Pharmacy, Universities of Kent and Greenwich, Chatham Maritime, United Kingdom, [2] School of Biological Sciences, University of Essex, Colchester, United Kingdom, [3] Department of Pediatric Surgery, Department of Biomedical Research, Children's Hospital, Inselspital, University of Bern, Bern, Switzerland, [4] Zentrum Für Medizinische Bildung, Biomedizinische Analytik HF, Bern, Switzerland, [5] Institute for Research in Biomedicine, Universita' della Svizzera italiana, Bellinzona, Switzerland, [6] Beamline B23, Diamond Light Source, Didcot, United Kingdom, [7] Division of Experimental Allergology and Immunodermatology, University of Oldenburg, Oldenburg, Germany, [8] Department of Biomedicine, University Hospital Basel and University of Basel, Basel, Switzerland

Human cancer cells operate a variety of effective molecular and signaling mechanisms which allow them to escape host immune surveillance and thus progress the disease. We have recently reported that the immune receptor Tim-3 and its natural ligand galectin-9 are involved in the immune escape of human acute myeloid leukemia (AML) cells. These cells use the neuronal receptor latrophilin 1 (LPHN1) and its ligand fibronectin leucine rich transmembrane protein 3 (FLRT3, and possibly other ligands) to trigger the pathway. We hypothesized that the Tim-3-galectin-9 pathway may be involved in the immune escape of cancer cells of different origins. We found that studied breast tumors expressed significantly higher levels of both galectin-9 and Tim-3 compared to healthy breast tissues of the same patients and that these proteins were co-localized. Increased levels of LPHN2 and expressions of LPHN3 as well as FLRT3 were also detected in breast tumor cells. Activation of this pathway facilitated the translocation of galectin-9 onto the tumor cell surface, however no secretion of galectin-9 by tumor cells was observed. Surface-based galectin-9 was able to protect breast carcinoma cells against cytotoxic T cell-induced death. Furthermore, we found that cell lines from brain, colorectal, kidney, blood/mast cell, liver, prostate, lung, and skin cancers expressed detectable amounts of both Tim-3 and galectin-9 proteins. The majority of cell lines expressed one of the LPHN isoforms and FLRT3. We conclude that the Tim-3-galectin-9 pathway is operated by a wide range of human cancer cells and is possibly involved in prevention of anti-tumor immunity.

Keywords: galectin-9, TIM-3, breast cancer, immune evasion, immune surveillance

OPEN ACCESS

Edited by:
Alexandr Bazhin, Hospital of the University of Munich, Germany

Reviewed by:
Mazdak Ganjalikhani Hakemi, Isfahan University of Medical Sciences, Iran
Stephen John Ralph, Griffith Health, Griffith University, Australia

***Correspondence:**
Inna M. Yasinska
I.Yasinska-24@kent.ac.uk
Elizaveta Fasler-Kan
elizaveta.fasler@insel.ch
Elena Klenova
klenovae@essex.ac.uk
Vadim V. Sumbayev
V.Sumbayev@kent.ac.uk

[†] These authors have contributed equally to this work

Specialty section:
This article was submitted to Cancer Immunity and Immunotherapy, a section of the journal Frontiers in Immunology

Received: *02 May 2019*
Accepted: *26 June 2019*
Published: *11 July 2019*

Citation:
Yasinska IM, Sakhnevych SS, Pavlova L, Teo Hansen Selnø A, Teuscher Abeleira AM, Benlaouer O, Gonçalves Silva I, Mosimann M, Varani L, Bardelli M, Hussain R, Siligardi G, Cholewa D, Berger SM, Gibbs BF, Ushkaryov YA, Fasler-Kan E, Klenova E and Sumbayev VV (2019) The Tim-3-Galectin-9 Pathway and Its Regulatory Mechanisms in Human Breast Cancer. Front. Immunol. 10:1594. doi: 10.3389/fimmu.2019.01594

INTRODUCTION

Human malignant tumors have developed a variety of biochemical mechanisms which allow them to escape host immune surveillance, thus leading to disease progression (1, 2). This applies to both liquid and solid tumors (1). It has recently become evident that acute myeloid leukemia (AML) cells, originating from self-renewing myeloid haematopoietic precursors, operate an immunosuppressive pathway which includes facilitation of exocytosis of the T cell immunoglobulin and mucin domain containing protein 3 (Tim-3) and its natural ligand, galectin-9 (2–4). Galectin-9 is a tandem protein which contains two ligand-binding domains fused together by a peptide linker (several isoforms have been identified) (5). As with other galectins, galectin-9 lacks a secretory domain and thus requires trafficking in order to be translocated onto the cell surface where it could be secreted by proteolytic shedding (5). Tim-3 acts both as a receptor and a possible trafficker for galectin-9 (2, 4, 6). When associated with the plasma membrane, the Tim-3-galectin-9 complex triggers downstream signaling contributing to cell renewal, thus forming an autocrine loop (6). On the other hand, proteolytic shedding results in release of both a soluble form of Tim-3 and galectin-9 (2). Both Tim-3 and galectin-9 act to suppress anti-cancer immune surveillance (2). Secreted galectin-9 contributes to anti-cancer immune suppression by killing cytotoxic T lymphocytes and impairing the activity of natural killer (NK) cells, thus allowing for disease progression (2, 4). Soluble Tim-3 also downregulates the production of interleukin-2 (IL-2), a cytokine required for the activation of both NK cells and cytotoxic T lymphocytes (2).

AML cells express the G-protein coupled neuronal receptor latrophilin 1 (LPHN1) which is produced by haematopoietic stem cells (HSCs) but disappears upon their maturation (7, 8). In case that HSCs undergo malignant transformation, thus becoming AML cells, they preserve the ability to express LPHN1 (7, 8). Interacting with its natural ligand, fibronectin leucine rich transmembrane protein 3 (FLRT3) and possibly other ligands (2, 3), LPHN1 facilitates translocation of Tim-3 and galectin-9 onto the cell surface via GαQ [G protein transducing the signal from LPHN (7)]—phospholipase C (PLC)—protein kinase C alpha (PKCα) biochemical pathway, which is followed by proteolytic shedding of the complex or ligand-free Tim-3 (2), creating an immune suppressive "double edged sword." Translation of Tim-3 and galectin-9 in these cells is controlled by the mammalian target of rapamycin (mTOR) pathway (2), one of the master regulators of protein biosynthesis.

Interestingly, other LPHN isoforms, in particular LPHN2, were found to be ubiquitously expressed especially in breast tumors (9). Human breast tumor cells were also found to express galectin-9, where it was shown to be involved in cell aggregation, thus preventing metastasis (10). On the other hand, the Tim-3-galectin-9 pathway plays a role in suppressing cytotoxic T cells in solid tumors, for example in colon cancer (11). However, the biochemical events underlying these processes have not been studied yet and it is therefore important to investigate whether the activity of the Tim-3-galectin-9 secretory pathway is specific solely to AML cells or whether it is also common for breast and other solid tumors. This will help us to understand the fundamental pathophysiological role of the pathway and its underlying biochemistry.

Therefore, the aim of our work was to investigate the biochemical activity of the Tim-3-galectin-9 pathway in human breast cancer and its possible role in suppressing cytotoxic T cell activity. In addition, we assessed the differential expression of the components of the Tim-3-galectin-9 pathway in human solid tumor cells.

Here we report that primary breast tumors express significantly higher levels of Tim-3, and especially galectin-9, compared to healthy tissues of the same patients. Importantly, Tim-3 and galectin-9 were co-localized. Breast tumors also expressed LPHN2 and LPHN3 as well as FLRT3. The PLC/PKC secretory biochemical pathway was significantly upregulated in breast tumors compared to healthy tissues. Breast cancer cell lines expressed all these components and biochemical studies were conducted using MCF-7 cells. Breast cancer cells were unable to secrete galectin-9, but were capable of maintaining its cell surface expression. The process of externalization was upregulated by exogenous FLRT3 most likely in a PLC/PKC-dependent manner. Surface-based galectin-9 was able to protect MCF-7 cells against T cell-induced death. Furthermore, we found that human cell lines originating from a wide range of different cancers express detectable amounts of both Tim-3 and galectin-9 proteins. The majority of these cell lines expressed at least one of the LPHN isoforms as well as FLRT3, suggesting that various types of solid and liquid tumors can in principle operate the FLRT3/LPHN/Tim-3/galecting-9 pathway.

MATERIALS AND METHODS

Materials

RPMI-1640 medium, fetal bovine serum and supplements as well as basic laboratory chemicals were purchased from Sigma (Suffolk, UK). Maxisorp™ microtitre plates were provided either by Oxley Hughes Ltd (London, UK) or Nunc (Roskilde, Denmark). Mouse monoclonal antibodies directed against mTOR and β-actin, as well as rabbit polyclonal antibodies against phospho-S2448 mTOR, galectin-9, HRP-labeled rabbit anti-mouse secondary antibody were purchased from Abcam (Cambridge, UK). Mouse monoclonal antibody against FLRT3 was obtained from Santa Cruz Biotechnology (Heidelberg, Germany). Antibodies against phospho-S65 and total eIF4E-BP were obtained from Cell Signaling Technology (Danvers, MA USA). The polyclonal rabbit anti-peptide antibodies (PAL1, PAL2, and PAL3) against LPHN1, LPHN2, and LPHN3, respectively, were previously described (12). Rabbit polyclonal antibody against poly-(ADP-ribose)-polymerase (PAR) was purchased from Enzo Life Sciences LTD (Exeter, UK). Goat anti-mouse and goat anti-rabbit fluorescence dye-labeled antibodies were obtained from LI-COR (Lincoln, Nebraska USA). ELISA kits for the quantitation of galectin-9, Tim-3, and IL-2 were purchased from Bio-Techne (R&D Systems, Abingdon, UK). Anti-Tim-3 mouse monoclonal antibody was employed as previously described (13). Secondary antibodies for confocal laser

microscopy (TRITC labeled antibody (goat anti-mouse IgG) and t FITC labeled antibody (goat anti-rabbit IgG) were from Abcam (Cambridge, UK). All other chemicals purchased were of the highest grade of purity.

Cell Lines and Primary Human Cells

Cell lines, listed in **Supplementary Table 1**, were obtained from either European Collection of Cell Cultures, American Tissue Culture Collection (ATTC) or CLS Cell Lines Service GmbH. Cell lines were accompanied by identification test certificates and were grown according to corresponding tissue culture collection protocols. LAD2 mast cells were kindly provided by Prof Metcalfe and Dr. Kirshenbaum (NAID, NHI, USA) and cultured according to the protocol described before (14).

MCF-7 breast cancer cells were purchased from the European Collection of Cell Cultures (the cell lines provided were accompanied by identification test certificates). Cells were cultured in RPMI 1640 media supplemented with 10% fetal bovine serum, penicillin (50 IU/ml), and streptomycin sulfate (50 μg/ml).

TALL-104 cytotoxic ***T*** lymphocytes derived from human ***a***cute ***l***ymphoblastic ***l***eukemia (TALL) were purchased from the American Tissue Culture Collection. Cells were cultured according to the ATCC instructions. Briefly, ATCC-formulated Iscove's Modified Dulbecco's Medium was used. To make the complete growth medium we added 100 units/ml recombinant human IL-2; 2.5 μg/ml human albumin; 0.5 μg/ml D-mannitol and fetal bovine serum to a final concentration of 20%. Primary human leukocytes (PHL) were isolated from buffy coat blood (originated from healthy donors though routine blood donation). The buffy coat blood was obtained from the National Health Blood and Transfusion Service (NHSBT, UK) following ethical approval (REC reference: 16-SS-033).

Human Tissue Samples

Primary human tumor tissue samples paired together with peripheral tissues (also called "normal" or "healthy" of the same patients) were collected surgically from breast cancer patients treated at the Colchester General Hospital, following informed, and written consent taken before surgery. Paired normal (healthy) peripheral tissues were removed during macroscopic examination of a tumor by pathologists. Blood samples were collected before breast surgery from patients with primary breast cancer (PBC) and before treatment from patients with metastatic breast cancer (MBC). Samples were also collected from healthy donors (individuals with no diagnosed pathology), which were used as control samples. Blood separation was performed using buoyancy density method employing Histopaque 1119-1 (Sigma, St. Louis, MO) according to the manufacturer's protocol. Ethical approval documentation for these studies was obtained from the NRES Essex Research Ethics Committee and the Research & Innovation Department of the Colchester Hospitals University, NHS Foundation Trust [MH 363 (AM03) and 09/H0301/37].

Western Blot Analysis

The components of the Tim-3, galectin-9, FLRT3, LPHNs 2/3, and mTOR pathways as well as GαQ, PARP, and CD3 were detected in cell and tissue lysates by Western blot and normalized to β-actin levels in order to confirm equal protein loading as reported earlier (2). Cells were lysed in 50 mM Tris–HCl, 5 mM EDTA, 150 mM NaCl, 0.5% Nonidet-40, 1 mM PMSF, pH 8.0.

Tissue lysates for Western blot analysis were prepared as described previously (15). Briefly, 100 mg of frozen tissues were grounded into a powder in dry ice, followed by the addition of 100 μl of the tissue lysis buffer (20 mM Tris/HEPES pH 8.0, 2 mM EDTA, 0.5 M NaCl, 0.5% sodium deoxycholate, 0.5% Triton X-100, 0.25 M Sucrose, supplemented with 50 mM 2-mercaptoethanol, 50 μM PMSF, 1 μM pepstatin supplied just before use). Tissues were homogenized using a Polytron Homogenizer (Capitol Scientific, USA) and a syringe was used in order to acquire a homogenous cell suspension. These tissue suspensions were then filtered through medical gauzes and centrifuged at +4°C at 10,000 g for 15 min. Proteins present in supernatants were precipitated by incubation of the samples on ice for 30 min with equal volumes of ice-cold acetone. Protein pellets were obtained by centrifugation at +4°C, 10,000 g for 15 min followed by air drying at room temperature and then lysed using the SDS-lysis buffer described above.

Li-Cor goat secondary antibodies (dilution 1:2,000), conjugated with infrared fluorescent dyes, were used as described in the manufacturer's protocol to visualize target proteins (Li-Cor Odyssey imaging system was applied). Western blot data were quantitatively analyzed using Odyssey software and values were subsequently normalized against those of β-actin or total protein loaded.

Enzyme-Linked Immunosorbent Assays (ELISAs)

Galectin-9, soluble Tim3 (sTim-3) and IL-2 were measured by ELISA using R&D Systems kits according to manufacturer's protocols. Phosphorylation of mTOR was analyzed by ELISA as previously described (16).

ELISA was also used to detect Tim-3-galectin-9 complex as described before (4) in the tissue homogenates. Homogenates were prepared in the ratio 1 g of tissue and 4 ml of lysis (extraction) buffer containing 50 mM Tris pH 7.5, 150 mM NaCl, 5 mM EDTA, and 0.5% NP-40. Mouse anti-Tim-3 (mAnti-Tim-3) was used as a capture antibody and biotinylated goat anti-galectin-9 (gAnti-Galectin-9, R&D Systems) for detection. The reaction was visualized using HRP-labeled streptavidin (R&D Systems; **Figure 2A**—see the scheme). In all cases plates were washed with TBST and bound secondary antibodies visualized using peroxidase reaction (ortho-phenylenediamine/H_2O_2).

Quantitative Real-Time PCR (qRT-PCR)

To detect galectin-9 mRNA levels, we used qRT-PCR (4). We isolated total RNA using a GenElute™ mammalian total RNA preparation kit (Sigma-Aldrich), followed by reverse transcriptase–polymerase chain reaction (RT-PCR) of a target protein mRNA (performed according to the manufacturer's protocol). This was followed by qRT-PCR. The following primers were used: Galectin-9, 5′-CTTTCATCACCACCATTCTG-3′ and 5′-ATGTGGAACCTCTGAGCACTG-3′ actin, 5′-TGACGGGG TCACCCACACT-GTGCCCATCTA-3′, 5′-CTAGAAGCATTT

GCGGTCG-ACGATGGAGGG-3′. Reactions were performed using a LightCycler® 480 qRT-PCR machine and SYBR Green I Master kit (obtained from Roche, Burgess Hill, UK). The work was performed according to the manufacturer's protocol. Values representing galectin-9 mRNA levels were normalized against those of β-actin.

On Cell Assays

On cell assays were employed to detect surface presence of galectin-9 and CD8. We used Li-Cor secondary antibody to recognize anti CD8 primary antibody and then visualized as described before (4, 17).

Confocal Microscopy

Tissue Sectioning

Tissue sections were produced using a freezing microtome with the cutting thickness of 5–6 μm. Each tissue section was sliced onto a poly-D-lysine-coated microscope slide (BDH).

Immunofluorescence Staining for Bioimaging Analysis

Endogenous peroxidase activity was blocked by incubating slides in 3% in H_2O_2 for 15 min. The slides were then permeabilised using PBS containing 0.26% Triton for 20 min at room temperature and blocked with serum obtained from the same species as the secondary antibody in the following buffer: PBS, 0.05% Tween, 2% serum, 1% BSA for at least 30 min. Tim-3 and galectin-9 expressions were detected by incubating slides with antibodies described above diluted in PBS (pH 7.4 containing 0.05% Tween, 1% BSA (1:200 dilution) for 2 h at room temperature and washed three times with PBS. Slides were then incubated in the dark for 1 h with anti-IgG-FITC-labeled secondary antibody (1:400 dilution) and then washed three times with PBS followed by Fluoro-Gel mounting media containing DAPI nuclei-staining reagent. Negative controls were prepared by incubating the slides with secondary antibody alone. Images were taken using Confocal Laser Scanning Microscopy (BioRad Hercules).

Fluorescence Co-localization Imaging

For image acquisition, a Nikon A1si laser scanning confocal microscope was used with a Plan Fluor DIC 40x magnifying, 1.3-numerical aperture (N.A.) oil-immersion objective. NIS Elements software (version 3.21.03, Nikon, Tokyo, Japan) was employed for data analysis. Cell images were acquired in three channels for DAPI (excitation at 399 nm with laser power 10 arbitrary units [AU], emission collection at 450 nm; nuclei labeling), Alexa Fluor 488 (excitation wavelength 488 nm with laser power 10 AU and, emission wavelength at 525 nm (corresponds to a green channel, galectin-9), Alexa Fluor 555 (excitation 561 nm with laser power 10 AU, emission collection at 595 nm, red channel, Tim-3), with a photomultiplier tube gain of 100 AU. No offset was used, and pinhole size was set between 1.2 and 2 times the Airy disk size of the used objective, depending on signal strength.

PLC and PKCα Activity Assays

The activity of PLC was measured based on the ability of this enzyme to cleave the ester bond between glycerol and phosphoric acid of the substrate phosphatidylinositol-4,5-bis-phosphate (PIP_2). PIP_2 (150 μM), was re-suspended in the assay buffer containing 20 mM Tris-HCl buffer (pH 7.2) containing 0.1% sodium deoxycholate, 300 μM $CaCl_2$, 100 μM EDTA, and 100 mM NaCl by sonication. Reaction was started by adding the substrate followed by incubation for 60 min at 37°C. Uncleaved substrate and IP_3 (the reaction product) were then measured using electrophoretic (33% polyacrylamide gel) separation, followed by toluidine blue staining and colorimetric assay (13, 18). The catalytic activity of PKCα was measured as described before based on its ability to phosphorylate specific substrate in a reaction buffer containing 20 mM Tris-HCl (pH7.5), 20 μM ATP, 5 mM $MgCl_2$, and 200 μM $CaCl_2$ (19). Phosphate groups attached to the substrate were detected spectrophotometrically (20).

Cell Viability Assay

Cell viability was analyzed using a commercial assay kit (Promega UK Ltd., Southampton, UK). We used an MTS colorimetric assay for assessing cell metabolic activity. NAD(P)H-dependent cellular oxidoreductase enzymes playing a crucial role in human myeloid cell survival reflect the number of viable cells present. Cells were incubated with 3-(4,5-dimethylthiazol-2-yl)-5-(3-carboxymethoxyphenyl)-2-(4-sulfophenyl)-2H-tetrazolium (MTS) and then absorbance was measured at 490 nm in accordance with the manufacturer's protocol.

Synchrotron Radiation Circular Dichroism (SRCD) Spectroscopy

Human recombinant LPHN2 (olfactomedin-like domain, MyBioSource, San Diego, CA, USA) and FLRT3, either alone or in combination (equimolar ratio), were analyzed using SRCD spectroscopy at beamline B23, Diamond Light Source (Didcot, UK) (3, 21, 22). SRCD measurements were performed using 0.7 μM of samples in a 1 cm path length cell of 3 mm aperture diameter and 60 μl capacity using a Module B instrument at 23°C. Integration time was 1 s, the increment−1 nm and bandwidth−1.2 nm. The results obtained were processed using CDApps and OriginPro®.

Statistical Analysis

Each experiment was performed at least three times and statistical analysis when comparing two events at a time was conducted using a two-tailed Student's *t*-test. Multiple comparisons were performed using ANOVA. *Post-hoc* Bonferroni correction was applied. Statistical probabilities (p) were expressed as * for $p < 0.05$; ** for $p < 0.01$, and *** for $p < 0.001$.

RESULTS

Expression and Activity of the FLRT3/LPHN/Tim3/galectin-9 Pathway in Breast Tumors

We found that primary breast tumors expressed galectin-9, Tim-3, LPHN2, and FLRT3 (**Figures 1A,B**); as well as detectable amounts of LPHN3 (**Supplementary Figure 1**). Interestingly, in addition to a specific FLRT3 bands, a clear band appears at around 55 kDa (highlighted by a question mark). This may

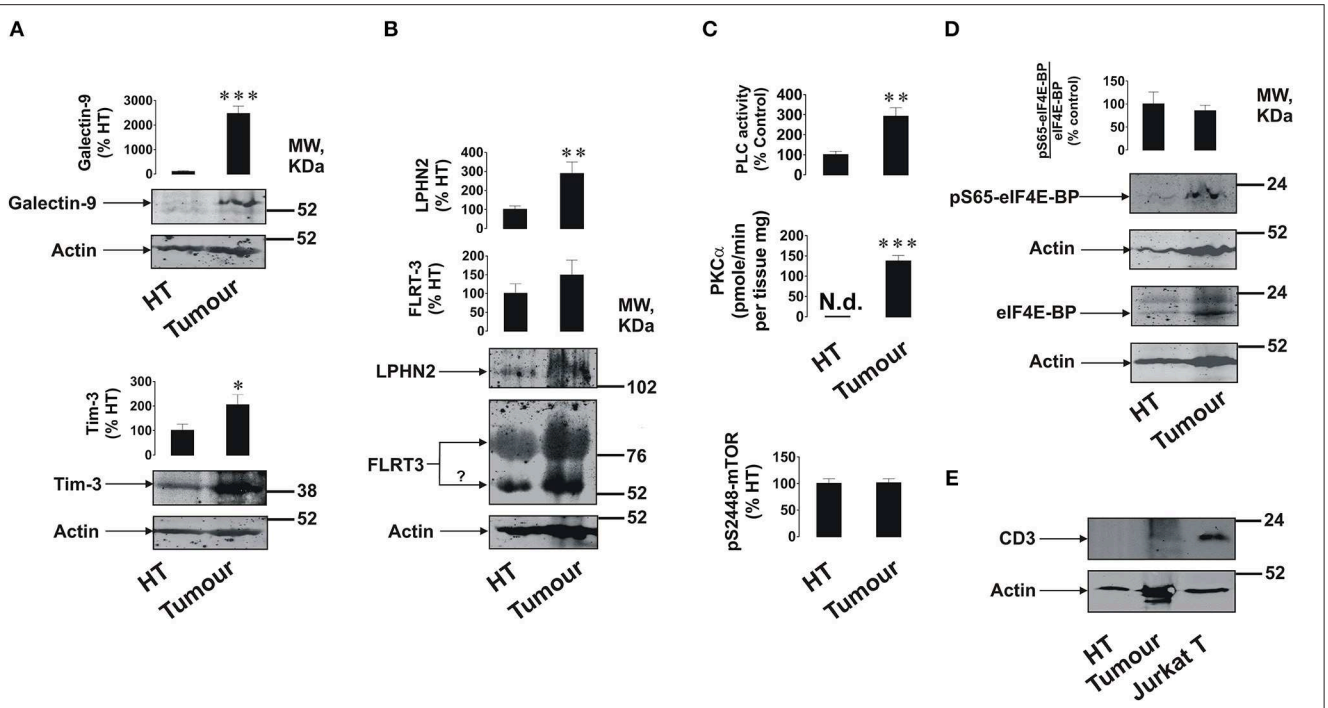


FIGURE 1 | Expression of FLRT3/LPHN/Tim-3/galectin-9 pathway components and activities of PLC/PKCα and mTOR pathways in primary human breast tumors. Expression levels of Tim-3, galectin-9 **(A)**, FLRT3, and LPHN2 **(B)** were analyzed in primary breast malignant tumors and healthy breast tissues (HT) of five patients ($n = 5$) by Western blot. Activities of PLC, PKCα, and the levels of phospho-S2448 mTOR were detected as outlined in the Materials and Methods **(C)**. The amounts of phospho-S65 and total eIF4E-BP (mTOR substrate) were analyzed using Western blot **(D)**. The levels of CD3 (biomarker of T cells) were also measured using lysate of Jurkat T cells as a positive control **(E)**. Molecular weight markers (MW) are expressed in kDa. Images are from one experiment representative of five which gave similar results. Other results are shown as mean values ± SEM. *$p < 0.05$; **$p < 0.01$, and ***when $p < 0.001$ vs. control.

represent FLRT3 which underwent proteolytic processing (3). Importantly, expression levels of Tim-3, galectin-9 and LPHN2 were significantly higher (about 15–20 fold for galectin-9, $p < 0.001$, 2 fold for Tim-3, $p < 0.05$ and 2.5–3 fold for LPHN2, $p < 0.01$) in tumors compared to healthy tissues isolated from the same patients. A band specific for galectin-9 appeared at around 55 kDa when 12% PAGE was used (this is the gel concentration normally used for galectin-9 detection) in each case and was not detectable by the anti-Tim-3 antibody. This indicates that this band is not the Tim-3-galectin-9 complex but probably a galectin-9 isoform bound to carbohydrates (as a lectin) which is unlikely to be secreted. This was confirmed when the same sample was ran using 10% PAGE and the specific band appeared above 31 kDa molecular weight marker (**Supplementary Figure 2**) confirming that, in a 12 % gel, protein running was "delayed" possibly due to the presence of glycosides or other post-translational modifications affecting the protein properties/shape but not the molecular weight. Activities of PLC and PKCα were significantly higher ($p < 0.01$ for PLC and $p < 0.001$ for PKCα) in tumor tissue homogenates compared to those of healthy tissues (**Figure 1C**). However, unlike in AML cells (2), the S2448 phosphorylation level of mTOR was similar in both healthy and tumor tissues (**Figure 1C**). The ratio between phospho-S65 eIF4E-BP and its total amount was also similar in both tissue types, although the amount of both phospho-S65 and total eIF4E-BP was higher in tumor tissues (**Figure 1D**).

Importantly, analysis of CD3 (a marker of T cells) demonstrated that this protein is undetectable in healthy and barely detectable in tumor tissue lysates suggesting that the analyzed proteins are mainly expressed by breast tumor cells and not tumor-infiltrated lymphocytes (**Figure 1E**).

In order to assess if Tim-3 is complexed to galectin-9 as in leukemia cells, we performed detection of the Tim-3-galectin-9 complex in tissue homogenates as outlined in the Materials and Methods. We found that the complex was barely detectable in normal tissue homogenates but was clearly detectable in tumor tissue extracts (**Figure 2A**). Next, measurement of Tim-3 and galectin-9 in tissues was performed using confocal microscopy. In line with the data shown in **Figures 1**, **2A**, we observed that both proteins are abundant in tumor tissue slices and are also co-localized (**Figure 2B**). Analysis of blood plasma samples obtained from patients with both primary and metastatic breast tumors showed that levels of galectin-9 and soluble Tim-3 were lower compared to healthy donors (**Figure 3**). Respectively, both patient groups demonstrated non-significantly higher levels of IL-2 (**Figure 3**).

MCF-7, BC-8701, and MDA-MB-231 breast cancer cells (**Supplementary Table 1** and **Supplementary Figure 1**) all expressed Tim-3, galectin-9, FLRT3, and at least one LPHN isoform. The highest level of LPHN2 was expressed by MDA-MB-231 cells, which is in line with previously reported observations (9). To further investigate the mechanism we selected MCF-7

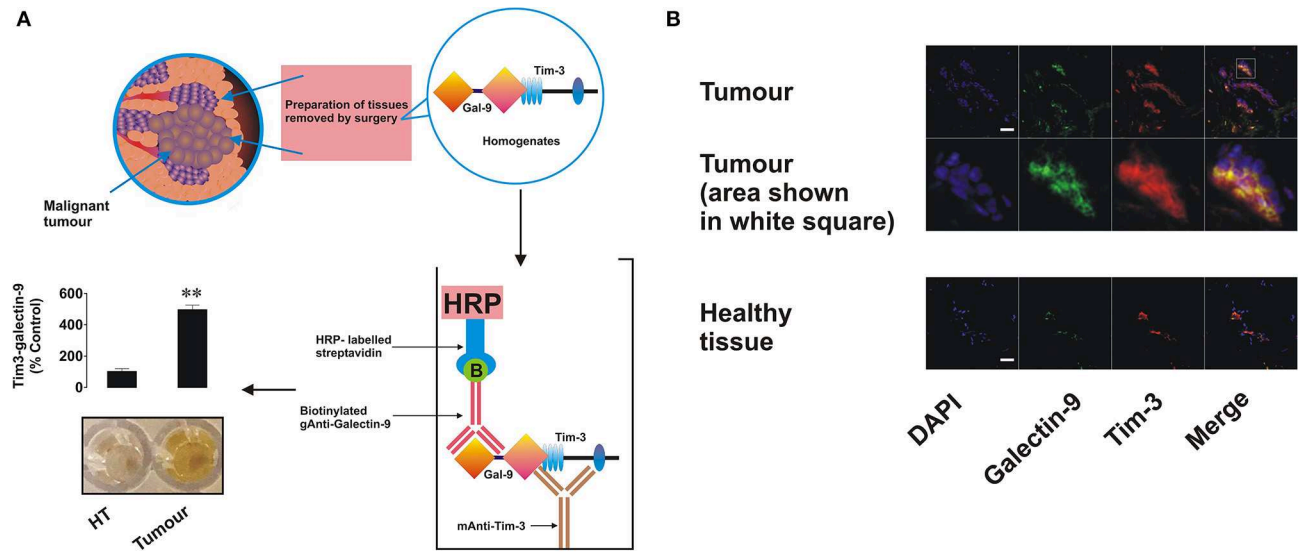


FIGURE 2 | Expression, interaction, and co-localization of Tim-3 and galectin-9 in primary human breast tumors. **(A)** Presence of the Tim-3-galectin-9 complex in primary normal and tumor tissue extracts was analyzed using ELISA as outlined in the Materials and Methods. **(B)** Expression and co-localization of galectin-9 and Tim-3 were analyzed in primary human breast tumors and healthy tissues of the same patients using confocal microscopy (see Materials and Methods for further details). Images are from one experiment representative of five which gave similar results. Scale bars correspond to 20 μm.

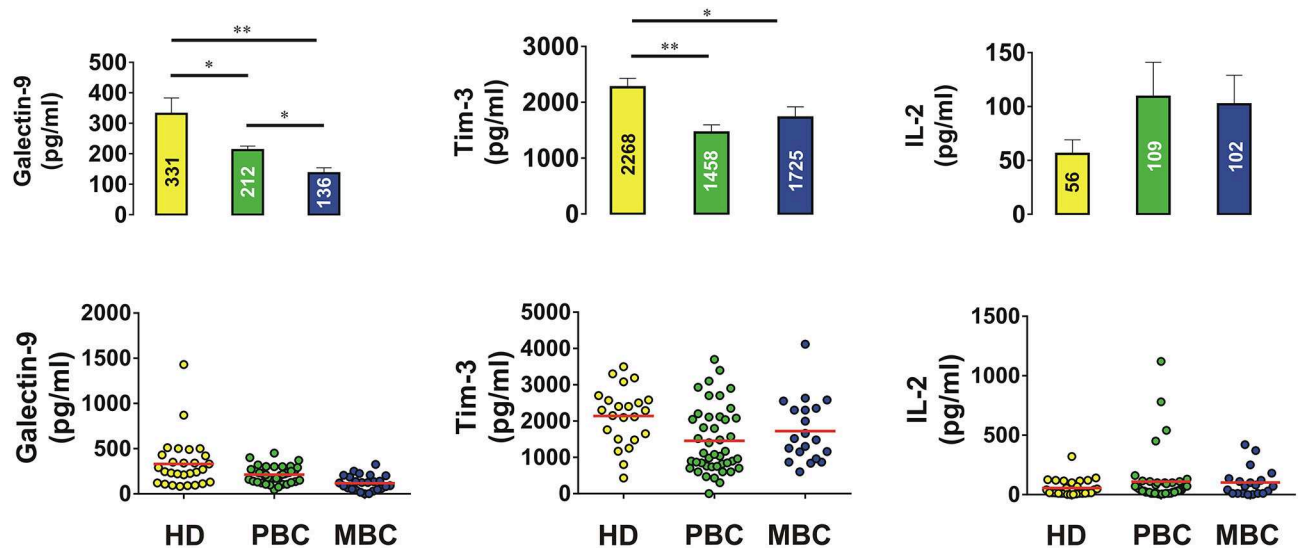


FIGURE 3 | Levels of galectin-9, Tim-3, and IL-2 in blood plasma of human healthy donors and patients suffering from primary and metastatic breast tumors. Concentrations of galectin-9, soluble Tim-3, and IL-2 were analyzed in blood plasma of healthy donors and breast cancer patients by ELISA. Data are shown as mean values ± SEM of 20 for healthy donors (HD), 42 for primary breast cancer (PBC) patients, and 20 for metastatic breast cancer (MBC) patients. $*p < 0.05$; $**p < 0.01$ and vs. HD.

breast cancer cells since they are the only cell line analyzed which expressed detectable amounts of both LPHNs 2 and 3 (as in primary breast tumors, **Supplementary Figures 1A,C**). They also expressed Tim-3 and galectin-9 (Tim-3-galectin-9 complex was also detectable, **Figure 4A**). Galectin-9 mRNA levels in MCF-7 cells were also significantly higher compared to normal human breast tissue (**Supplementary Figure 1B**). The level of galectin-9 mRNA in primary human breast tumor tissues was much higher compared to the normal tissue (**Supplementary Figure 1B**) and, importantly, the ratio of galectin-9 mRNA in tumor and normal tissues was similar to the respective levels of protein detected (**Figure 1A**). Also these results suggest that MCF-7 cells as well as primary healthy and malignant cells express identical galectin-9, thus re-confirming

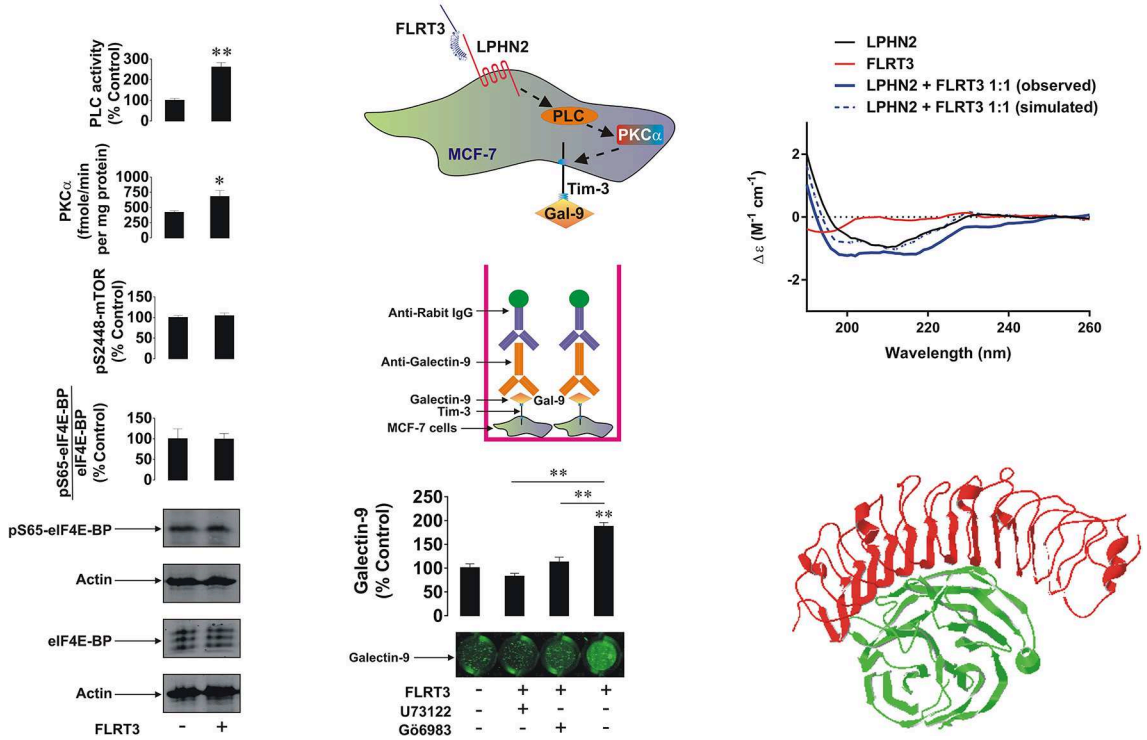


FIGURE 4 | FLRT3 induces translocation of galectin-9 onto the surface of MCF-7 breast cancer cells. **(A)** MCF-7 cells were exposed for 4 h to 10 nM FLRT3 and activities of PLC, PKCα, the levels of phospho-S2448 mTOR and the amounts of phospho-S65 and total eIF4E-BP (an mTOR substrate) were analyzed as described in the Materials and Methods. **(B)** MCF-7 cells were exposed for 4 h to 10 nM FLRT3 with or without 1 h pre-treatment with 30 μM U73122 (PLC inhibitor) or 70 nM Gö6983 (PKCα inhibitor). Surface presence of galectin-9 was measured by on-cell assay. **(C)** Secondary structure and conformational changes of LPHN2 olfacomedin-like domain (FLRT3-inding region), FLRT3, and the complex of the two proteins mixed at the equimolar ratio were characterized using SRCD spectroscopy as outlined in the Materials and Methods. An interaction between olfactomedin-like domain of LPHN3 and FLRT3 generated by Swiss PDB viewer [5 cmn.pdb file downloaded through PubMed database was used (13)] is presented to illustrate the structural basis of this interaction. Images are from one experiment representative of four which gave similar results. Other results are shown as mean values ± SEM of at least three independent experiments. *$p < 0.05$; **$p < 0.01$ vs. control.

that the same protein was detected by Western blot (**Figure 1** and **Supplementary Figure 1A**).

LPHN2 expression in MCF-7 cells was lower than in MDA-MB-231 but comparable with primary tumors. Furthermore, primary breast tumors and MCF-7 cells expressed comparable amounts of LPHN3 (**Supplementary Figure 1C**). It is important to mention that there are possible minor variations in LPHN2 gene in breast cancer cells lines (23) and possibly in primary breast tumors, however the translated protein has no variations in amino acid sequence. Both primary breast tumor and MCF-7 cells expressed GαQ (**Supplementary Figure 1D**), which indicates the presence of an adaptor protein required for transduction of signals *via* G-protein-coupled receptors (LPHN isoforms). Cells were also exposed for 4 h to 10 nM human recombinant FLRT3 followed by detection of phospho-S65/total eIF4E-BP, phospho-S2448 mTOR, activities of PLC and PKCα as well as cell surface presence of galectin-9. As shown in **Figure 4A**, exposure to FLRT3 did not affect mTOR activity but significantly upregulated the activities of PLC and PKCα. Galectin-9 surface presence was also significantly upregulated as measured by on-cell assay (**Figure 4B**). Importantly, pre-treatment of the cells for 1 h with 30 μM U73122 (PLC inhibitor) and 70 nM Gö6983 (PKCα inhibitor) before 4 h exposure to 10 nM FLRT3 attenuated FLRT3-induced galectin-9 translocation onto the cell surface (**Figure 4B**). This confirms that FLRT3-induced translocation of galectin-9 onto the surface of MCF-7 cells is controlled by the PLC/PKCα pathway.

To further verify the interaction of FLRT3 with the olfactomedin-like domain of LPHN2 [for LPHNs 1 and 3 this has already been confirmed (3, 24–26)] we performed SRCD spectroscopy analyzing spectra (thus characterizing secondary structure and conformational changes) of the olfactomedin-like domain of LPHN2 and FLRT3 alone and their equimolar combination. We found that binding of FLRT3 took place in a similar fashion as previously reported for LPHN1 (**Figure 4C**). This suggests that all three LPHN isoforms interact with FLRT3 in a similar way (a 3D interaction of LPHN3 oflactomedin-like domain and FLRT3 is presented in **Figure 4C**).

Galectin-9 Protects Breast Cancer Cells Against Cytotoxic Immune Attack

To assess the effect of galectin-9 in protecting breast cancer cells against cytotoxic cell-dependent killing we co-cultured MCF-7 cells (adherent) with cytotoxic ALL-derived TALL-104 CD8-positive T lymphocytes (we used these rather than NK cells since mainly T cells infiltrate solid tumors; as NK cells, TALL-104 cells express Tim-3, and not galectin-9) for 16 h at a ratio of 4 MCF-7 cells: 1 TALL-104 cells (**Figure 5A**—this ratio was selected experimentally to achieve moderate effects in order to be able to trace biochemical mechanisms). The co-culture was performed in either the absence or presence of 5 μg/ml galectin-9 neutralizing antibody to evaluate the contribution of surface-based galectin-9. Following the treatment TALL-104 cells were collected, lysed, and subjected to Western blot analysis of full-length and cleaved PARP (marker of apoptosis). We found that in TALL-104 cells co-cultured with MCF-7 cells the level of PARP cleavage was significantly (about 3 fold, $p < 0.05$) increased and the presence of anti-galectin-9 antibody attenuated the effect (**Figure 5B**). Increased level of PARP cleavage indicates a higher number of apoptotic cells. An on-cell assay was used to assess the level of infiltration of TALL-104 cells into the MCF-7 cell monolayer. We observed that CD8 was absent in the MCF-7 cells when cultured on their own, but it was detected when MCF-7 cells were co-cultured with TALL-104. It was further significantly increased when the cells were co-cultured in the presence of galectin-9 neutralizing antibody, suggesting that the ability of TALL-104 cells to attack MCF-7 cells is increased when galectin-9 activity is disabled (**Figure 5B**). Isotype control antibody (used at the same concentration of 5 μg/ml) did not affect interactions between TALL-104 and MCF-7 cells, confirming the role of galectin-9 in this process (**Figure 5C**). Importantly, cell surface presence of galectin-9 was significantly upregulated in the presence of TALL-104 cells as measured by the on-cell assay (**Figure 5D**). Similar effect was observed before in other solid tumors (27). Viability of MCF-7 cells was also decreased in the presence of TALL-104 cells and galectin-9 neutralizing antibody (but not isotype control) as measured by an MTS test (**Figure 5E**). This is a strong indication that galectin-9 is capable of protecting breast tumor cells against cytotoxic cell-dependent killing.

The Majority of Solid and Liquid Tumors Express Key Components of the FLRT3/LPHN/Tim-3/galectin-9 Pathway

To investigate the expression of FLRT3/LPHN/Tim-3/galectin-9 pathway components in cancer cells of different origins, we screened various human cancer cell lines (derived from brain, colorectal, kidney, blood/mast cell, liver, breast, prostate, lung, and skin tumors) and various non-malignant cell lines and primary cells, using Western blot analysis. Comparative analysis was performed by measuring infrared fluorescence of the bands divided by the total quantity of the loaded protein. This approach was taken because the cells analyzed originated from different tissues and thus the levels of each housekeeping protein (such as beta-actin, for example) vary depending on the origin of the cells. Results of quantitative analysis are summarized in **Figure 6** and Western blot images are presented in **Supplementary Table 1**. Tim-3 and galectin-9 were present in all the studied cancer cells, except for the chronic myeloid leukemia (CML) cell line, K562, which expressed Tim-3 but only traces of galectin-9, in agreement with previously reported observations (2). Of note, this could be one of the reasons why CML cells entering the circulation are rapidly eliminated by cytotoxic lymphoid cells. As indicated above, we also measured the levels of secreted galectin-9 in different cells lines and observed variations dependent on their origin (**Supplementary Table 1**). The highest levels of galectin-9 were detected in hematological (except for K562 cells) and colorectal cancer cells. Other cell types expressed moderate levels and prostate cancer cells expressed lower but detectable levels of at least one variant of galectin-9 (**Figure 6**, **Supplementary Table 1**). Non-malignant cells, expressed lower amounts of galectin-9 and also Tim-3 compared to cancerous cells of similar origins. Furthermore, the majority of the cells expressed at least one LPHN isoform, as well as FLRT3. Some of the cells did not express FLRT3 but expressed LPHN isoforms (**Figure 6**, **Supplementary Table 1**). This most likely means that LPHN expressing cells use blood-based soluble FLRT3 to trigger the pathway since blood does not contain the other LPHN ligand teneurin-2 (7).

DISCUSSION

The molecular mechanisms underlying the ability of cancer cells to escape host immune surveillance remain poorly understood. Recent evidence clearly demonstrated that some tumor cells (AML in particular) operate the Tim-3-galectin-9 secretory pathway which is capable of disabling cytotoxic lymphoid cells (2, 3). However, a growing body of evidence suggests that some solid tumors [for example colorectal tumors (11)] also express Tim-3 and galectin-9 and use these proteins to escape host immune attack. We studied the activity of this pathway in breast and other solid and liquid tumors. We also investigated the pathway in both breast tumors and healthy breast tissues obtained from the same patients as well as in breast tumor cell lines.

Using Western blot analysis and confocal microscopy we found very low levels of galectin-9 in human breast tissue cells peripheral to tumor (**Figures 1**, **2**), which were significantly increased in tumor cells. Importantly, as in AML cells, Tim-3, and galectin-9 are co-localized in breast tumor cells and are capable to form complex (**Figure 2A** and **Supplementary Figure 1A**). However, this tumor-associated galectin-9 is unlikely to be secreted since blood plasma levels of galectin-9 are lower than in healthy donors. Interestingly, high levels of Tim-3 are known to be expressed by solid tumor-infiltrating lymphocytes (27, 28), which could be used by tumor-derived galectin-9 to kill them. Our results have confirmed that Tim-3 and galectin-9 are expressed mainly by tumor cells, since CD3 (a T cell biomarker) was barely detectable in tumor and undetectable in healthy

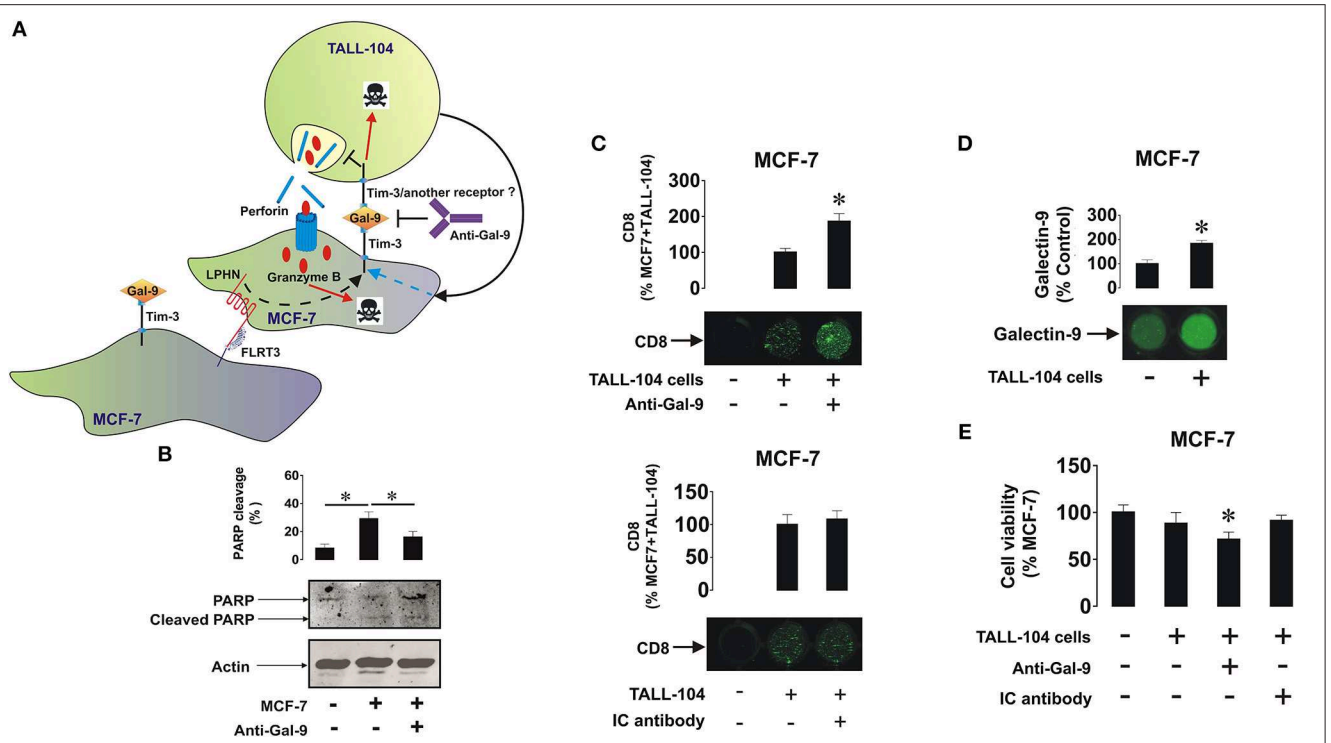


FIGURE 5 | Galectin-9 protects MCF-7 cells against T cell-dependent cytotoxic immune attack. **(A)** MCF-7 cells were co-cultured with TALL-104 cytotoxic T lymphocytes at a ratio of 4 : 1 for 16 h (the ratio was determined by the aggressive behavior of TALL-104 cells) in the absence or presence of 5 μg/ml galectin-9 neutralizing antibody or 5 μg/ml isotype control antibody. **(B)** After the experiment TALL-104 cells were lysed and PARP cleavage, as an indicator of the rate of apoptotic cells, was measured using Western blot analysis. **(C)** CD8 expressions (reflecting the infiltration of TALL-104 into the MCF-7 layer) were measured by on-cell assay. **(D)** Galectin-9 surface presence was measured using on-cell assay in resting MCF-7 cells and those co-cultured with TALL-104 cells **(E)** Viability of MCF-7 cells was measured by MTS test. Images are from one experiment representative of five which gave similar results. Other results are presented as mean values ± SEM of five independent experiments. *$p < 0.05$ vs. control.

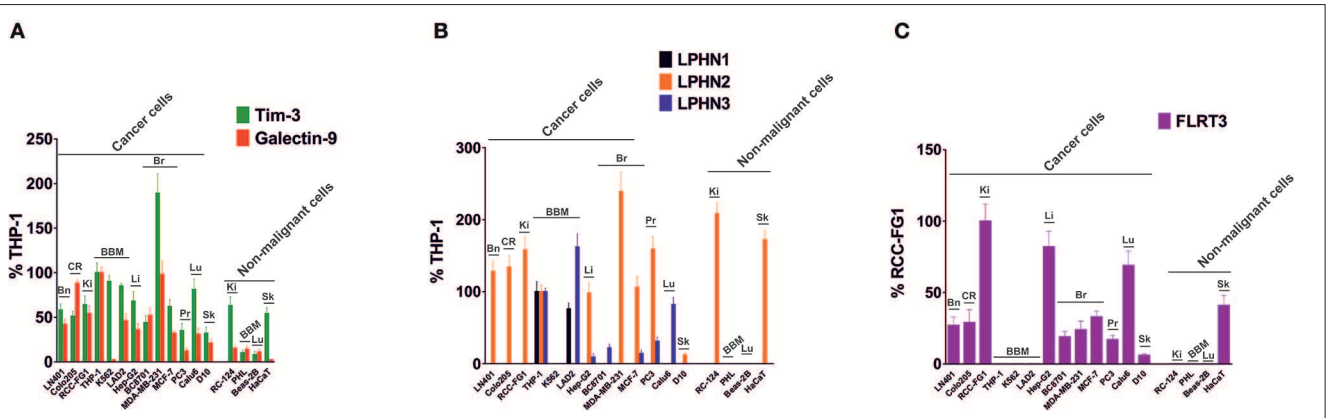


FIGURE 6 | Expression of Tim-3, galectin-9, LPHNs 1, 2, and 3 as well as FLRT3 proteins in various human cancer cell lines. Lysates of indicated cells were subjected to Western blot analysis as outlined in Materials and Methods (images are presented in **Supplementary Table 1**). Detected infrared fluorescence of the bands divided by the total protein amounts loaded (measured using Bradford assay) was used as a measure of protein quantity. Levels of Tim-3 & total galectin-9 **(A)** and LPHNs 1, 2, & 3 **(B)** were expressed as a % of those levels present in THP-1 cells (expressed as 100%). Since THP-1 cells lack FLRT3 expression, the levels of this protein were expressed as % RCC-FG1 **(C)**, respectively considering FLRT3 level in these cells as 100%. Bn, brain; CR, colorectal; Ki, kidney; BBM, blood, bone marrow and mast cells; Li, liver; Br, breast; Pr, prostate; Lu, lung; Sk, skin. Data are presented as mean values ± SEM of three independent experiments.

tissue lysates (**Figure 1E**). Furthermore, both proteins are co-localized suggesting that they are expressed by the same cells (**Figure 2B**). Levels of soluble Tim-3 were also downregulated in blood plasma of breast cancer patients which is in line with galectin-9 values. Importantly, as indicated above, our results indicate that galectin-9 is unlikely to be secreted by breast tumors,

since its levels do not increase in patient blood plasma and the studied human breast cancer cell lines were incapable of secreting galectin-9. Furthermore, the molecular weight of tissue-based galectin-9 suggests that it is most likely associated with plasma membrane-based glycosides, as previously described in somatic cells (29–31). This binding would of course keep it attached to the cell surface and prevent its release.

Taken together, these results suggest that the FLRT3/LPHN/Tim-3/galectin-9 pathway possibly functions mainly to transfer galectin-9 onto the cell surface rather than to secrete it as in the case with AML cells. This would explain the lower level of mTOR pathway activation in breast tumor cells compared to AML cells (2), where secretion takes place and subsequently requires replacement of the proteins through biosynthesis. Interestingly, the findings reported here on the protein level are in line with gene expression data for human breast cancer presented in The Cancer Genome Atlas.

Remarkably, the level of IL-2 was non-significantly increased in blood plasma of breast cancer patients, but not in AML patients, including those with primary and metastatic breast tumors. This suggests that induction of the cytotoxic activity of NK cells and cytotoxic T cells can still take place. This observation is supported by the fact that plasma levels of soluble Tim-3 are also lower, since Tim-3 was shown to downregulate IL-2 secretion by specialized T cells (2).

Tumor tissue cells expressed LPHN2 (significantly higher levels compared to healthy tissues), LPHN3, and FLRT3 (LPHN ligand). In line with this, the activities of PLC and PKCα were significantly higher in tumors compared to healthy tissues. The activity of mTOR was not upregulated, although basal levels

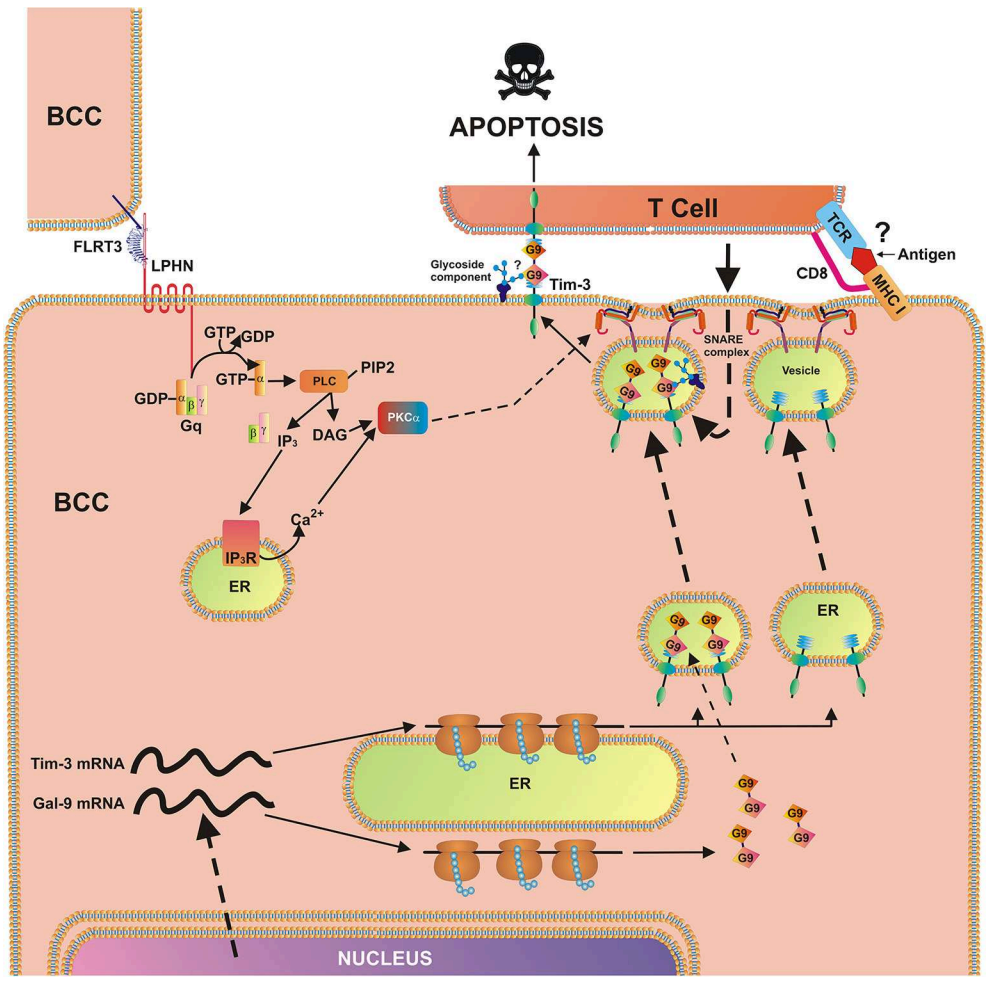


FIGURE 7 | Breast cancer cell-based pathobiochemical pathways showing LPHN-induced activation of PKCα, which triggers the translocation of Tim-3 and galectin-9 onto the cell surface which is required for immune escape. The interaction of FLRT3 with LPHN isoform leads to the activation of PKCα, most likely through the classic Gq/PLC/Ca^{2+} pathway. Ligand-bound LPHN activates Gq, which in turn stimulates PLC. This leads to phosphatidyl-inositol-bisphosphate (PIP_2) degradation and production of inositol-trisphospate (IP_3) and diacylglycerol (DAG). PKCα is then activated by DAG and cytosolic Ca^{2+}. PKCα provokes the formation of SNARE complexes that tether vesicles to the plasma membrane. Galectin-9 impairs the cancer cell killing activity of cytotoxic T cells (and other cytotoxic lymphocytes). Possible (not directly confirmed) interactions of galectin-9 with glycoside component and T cell receptor (TCR)/CD8, with MHC I, and antigen are highlighted with question mark "?" to indicate the fact that it is a hypothetic interaction, since TALL-104 cells used in the study kill tumor cells in MHC-independent manner (32).

of the mTOR substrate (eIF4E-BP) were significantly higher in tumor cells.

We found that exposure of MCF-7 breast cancer cells to 10 nM FLRT3 induces activation of PLC and PKCα. Recently it has been found that FLRT3 activates the PKCα pathway *via* LPHN isoforms (2). The activity of mTOR was not increased after 4 h of exposure to FLRT3. FLRT3-induced externalization of galectin-9 onto the cell surface was observed. This is in line with previous observations made in AML cells where galectin-9 secretion was shown to be triggered by LPHN in a PKCα-dependent manner (2). Importantly, in both leukemia (2) and MCF-7 cells FLRT-3-induced effects are moderate. The effects observed with latrotoxin (a LPHN1 ligand) in AML cells are much stronger compared to those of FLRT3 (2). These moderate effects indicate that they are most likely continuous and thus keep the pathway operating in order to protect malignant cells against cytotoxic lymphoid cells on an ongoing basis but in a manner that does not allow exhaustion of the cell. On the other hand, there are clearly other pathways operated by breast cancer cells to suppress the activity of cytotoxic immune cells. For example presence of TALL-104 cells significantly upregulates galectin-9 surface presence in MCF-7 breast cancer cells. Biochemical pathways underlying this phenomenon remain to be identified. Based on these observations, it can be concluded that the FLRT3-LPHN-Tim-3-galectin-9 pathway is functional in other cancer cells and in particular in breast cancer cell lines and primary tumors. In this case, however, we do not observe a FLRT3-LPHN-dependent activation of mTOR but rather a moderate, yet significant, activation of PLC/PKCα. In contrast, FLRT3-LPHN1 interactions in AML cells are capable of activating the mTOR pathway. The biological effect of LPHN2-FLRT3 results in the translocation of the Tim-3-galectin-9 complex onto the cell surface but since there is no proteolytic shedding/secretion, constant protein renewal is not required as it is in AML cells. A scheme representing the involvement of FLRT3-LPHN and other possible interactions in the activation of Tim-3-galectin-9 immunosuppressive pathway is shown in **Figure 7**. Intriguingly, in line with our observations that galectin-9 levels in PC3 prostate cancer cells are low compared to other cancer cells, these cells were recently reported to be rapidly killed by TALL-104 cells used in our work (32).

Interestingly, it has been previously reported that galectin-9 demonstrates anti-metastatic potential in breast cancer (10, 33). Possible reasons underlying such an activity were suggested to be galectin-9-induced cell aggregation and reduced adhesion of breast cancer cells to the extracellular matrix (10). These studies support our hypothesis regarding the possible interaction of galectin-9 with membrane-associated glycosides, since this process is known to participate in determining the membrane potential (30, 31, 34), which is a crucial factor affecting cell aggregation. Importantly, as a result of alternative splicing, galectin-9 may be present in three main isoforms characterized by the length of the linker peptide: long (49 amino acids), medium (27 amino acids) and short (15 amino acids) (5, 29–31, 33, 34). As one can see from the data reported in **Supplementary Table 1**, some of the cell types can express only one isoform, others two, or all three but the biochemical reasons underlying this phenomenon remain to be understood.

Additionally, NK cells interacting with galectin-9 on the breast cancer cell surface may release interferon gamma (IFN-γ) in response (2, 35) which could activate cytotoxic lymphoid cells located in the area of the tumor microenvironment. These cells can attack and kill malignant cells breaking off from the tumor thus preventing their circulation and metastasis. Overall, it appears that galectin-9 could protect the tumor which produces it in order to evade host immune attack, but this may not promote metastasis.

CONCLUSION

Our findings demonstrate the activity of the Tim-3-galectin-9 biochemical pathway in breast and various other types of human cancer cells and its possible implication in suppression of host anti-cancer immune surveillance. This pathway can be recommended for targeting in order to design novel anti-cancer immunotherapeutic approaches based on inhibiting the Tim3-galectin-9 pathobiochemical pathway thus enabling the immune system to attack and eradicate malignant tumors.

DATA AVAILABILITY

The datasets used and/or analyzed during the current study are available from the corresponding author on reasonable request.

ETHICS STATEMENT

Ethical approval documentation for these studies was obtained from the NRES Essex Research Ethics Committee and the Research & Innovation Department of the Colchester Hospitals University, NHS Foundation Trust [MH 363 (AM03) and 09/H0301/37]. Buffy coat blood was purchased from the National Health Blood and Transfusion Service (NHSBT, UK) following ethical approval (REC reference: 16-SS-033).

AUTHOR CONTRIBUTIONS

IY, SS, and LP generated most of the data presented in the **Figures 1–6**. AT, MM, AMT, IG, SS, and IY generated the data presented in the **Figure 6** and **Supplementary Table 1**. OB generated some of the data reported in the **Figure 4**. LV and MB generated the anti-Tim-3 antibody. DC and SB provided critical advise and contributed to manuscript writing and data interpretation. BG helped with experiments using primary human samples and contributed to manuscript writing. RH and GS together with SS, OB, IY, and VS performed SRCD spectroscopy and performed data analysis. YU developed anti-LPHN antibodies. EF-K designed the experiments using cell lines, wrote the manuscript. EK designed experiments using primary human samples, obtained primary human samples, and wrote the manuscript. VS designed the study, supervised the process of data

analysis and interpretation, organizations of figures and tables, experimental design, and wrote the manuscript.

FUNDING

This work was supported by a Daphne Jackson Trust postdoctoral fellowship (to IY), University of Kent Faculty of Sciences Research Fund (to VS) and Batzebär grant (to EF-K and SB). We thank Diamond Light Source for access to B23 beamline (SM20755).

SUPPLEMENTARY MATERIAL

The Supplementary Material for this article can be found online at: https://www.frontiersin.org/articles/10.3389/fimmu.2019.01594/full#supplementary-material

REFERENCES

1. Rotman J, Koster BD, Jordanova ES, Heeren AM, de Gruijl TD. Unlocking the therapeutic potential of primary tumor-draining lymph nodes. *Cancer Immunol Immunother*. (2019). doi: 10.1007/s00262-019-02330-y. [Epub ahead of print].
2. Gonçalves Silva I, Yasinska IM, Sakhnevych SS, Fiedler W, Wellbrock J, Bardelli M, et al. The Tim-3-galectin-9 secretory pathway is involved in the immune escape of human acute myeloid leukemia cells. *EBioMed*. (2017) 22:44–57. doi: 10.1016/j.ebiom.2017.07.018
3. Sakhnevych SS, Yasinska IM, Bratt AM, Benlaouer O, Gonçalves Silva I, Hussain R, et al. Cortisol facilitates the immune escape of human acute myeloid leukemia cells by inducing latrophilin 1 expression. *Cell Mol Immunol*. (2018) 15:994–7. doi: 10.1038/s41423-018-0053-8
4. Gonçalves Silva I, Ruegg L, Gibbs BF, Bardelli M, Fruewirth A, Varani L, et al. The immune receptor Tim-3 acts as a trafficker in a Tim-3/galectin-9 autocrine loop in human myeloid leukaemia cells. *OncoImmunology*. (2016) 5:e1195535. doi: 10.1080/2162402X.2016.1195535
5. Delacour D, Koch A, Jacob R. The role of galectins in protein trafficking. *Traffic*. (2009) 10:1405–13. doi: 10.1111/j.1600-0854.2009.00960.x
6. Kikushige Y, Miyamoto T, Yuda J, Jabbarzadeh-Tabrizi S, Shima T, Takayanagi S, et al. A TIM-3/Gal-9 autocrine stimulatory loop drives self-renewal of human myeloid leukemia stem cells and leukemic progression. *Cell Stem Cell*. (2015) 17:341–52. doi: 10.1016/j.stem.2015.07.011
7. Sumbayev VV, Goncalves Silva I, Blackburn J, Gibbs BF, Yasinska IM, Garrett MD, et al. Expression of functional neuronal receptor latrophilin 1 in human acute myeloid leukemia cells. *Oncotarget*. (2016) 7:45575–83. doi: 10.18632/oncotarget.10039
8. Maiga A, Lemieux S, Pabst C, Lavallee VP, Bouvier M, Sauvageau G, et al. Transcriptome analysis of G protein-coupled receptors in distinct genetic subgroups of acute myeloid leukemia: identification of potential disease-specific targets. *Blood Cancer J*. (2016) 6:e431. doi: 10.1038/bcj.2016.36
9. White GR, Varley JM, Heighway J. Isolation and characterization of a human homologue of the latrophilin gene from a region of 1p31.1 implicated in breast cancer. *Oncogene*. (1998) 17:3513–9. doi: 10.1038/sj.onc.1202487
10. Irie A, Yamauchi A, Kontani K, Kihara M, Liu D, Shirato Y, et al. Galectin-9 as a prognostic factor with antimetastatic potential in breast cancer. *Clin Cancer Res*. (2005) 11:2962–8. doi: 10.1016/S0960-9776(05)80073-6
11. Kang CW, Dutta A, Chang LY, Mahalingam J, Lin YC, Chiang JM, et al. Apoptosis of tumor infiltrating effector TIM-3+CD8+ T cells in colon cancer. *Sci Rep*. (2015) 5:15659. doi: 10.1038/srep15659
12. Davydov II, Fidalgo S, Khaustova SA, Lelyanova VG, Grebenyuk ES, Ushkaryov YA, et al. Prediction of epitopes in closely related proteins using a new algorithm. *Bull Exp Biol Med*. (2009) 148:869–73. doi: 10.1007/s10517-010-0838-y
13. Prokhorov A, Gibbs BF, Bardelli M, Ruegg L, Fasler-Kan E, Varani L, et al. The immune receptor Tim-3 mediates activation of PI3 kinase/mTOR and HIF-1 pathways in human myeloid leukemia cells. *Int J Biochem Cell Biol*. (2015) 59:11–20. doi: 10.1016/j.biocel.2014.11.017
14. Kirshenbaum AS, Akin C, Wu Y, Rottem M, Goff JP, Beaven MA, et al. Characterization of novel stem cell factor responsive human mast cell lines LAD 1 and 2 established from a patient with mast cell sarcoma/leukemia; activation following aggregation of FcepsilonRI or FcgammaRI. *Leuk Res*. (2003) 27:677–82. doi: 10.1016/S0091-6749(03)80727-3
15. D'Arcy V, Pore N, Docquier F, Abdullaev ZK, Chernukhin I, Kita GX, et al. BORIS, a paralogue of the transcription factor, CTCF, is aberrantly expressed in breast tumours. *Br J Cancer*. (2008) 98:571–9. doi: 10.1038/sj.bjc.6604181
16. Yasinska IM, Gibbs BF, Lall GS, Sumbayev VV. The HIF-1 transcription complex is essential for translational control of myeloid hematopoietic cell function by maintaining mTOR phosphorylation. *Cell Mol Life Sci*. (2014) 71:699–710. doi: 10.1007/s00018-013-1421-2
17. Sakhnevych SS, Yasinska IM, Fasler-Kan E, Sumbayev VV. Mitochondrial Defunctionalisation supresses tim-3-galectin-9 secretory pathway in human colorectal cancer cells and thus can possibly affect tumour immune escape. *Front. Pharmacol*. (2019) 10:342. doi: 10.3389/fphar.2019.00342
18. Li C, Lev S, Desmarini D, Kaufman-Francis K, Saiardi A, Silva APG, et al. IP3–4 kinase Arg1 regulates cell wall homeostasis and surface architecture to promote clearance of Cryptococcus neoformans infection in a mouse model. *Virulence*. (2017) 8:1833–48. doi: 10.1080/21505594.2017.1385692
19. Micol V, Sanchez-Pinera P, Villalain J, de Godos A, Gomez-Fernandez JC. Correlation between protein kinase C alpha activity and membrane phase behavior. *Biophys J*. (1999) 76:916–27. doi: 10.1016/S0006-3495(99)77255-3
20. Abooali M, Lall GS, Coughlan K, Lall HS, Gibbs BF, Sumbayev VV. Crucial involvement of xanthine oxidase in the intracellular signalling networks associated with human myeloid cell function. *Sci Rep*. (2014) 4:6307. doi: 10.1038/srep06307
21. Yasinska IM, Ceccone G, Ojea-Jimenez I, Ponti J, Hussain R, Siligardi G, et al. Highly specific targeting of human acute myeloid leukaemia cells using pharmacologically active nanoconjugates. *Nanoscale*. (2018) 10:5827–33. doi: 10.1039/C7NR09436A
22. Yasinska IM, Calzolai L, Raap U, Hussain R, Siligardi G, Sumbayev VV, et al. Specific targeting of basophil and mast cell pro-allergic reactivity using functionalised gold nanoparticles. *Front Pharmacol*. (2019) 10:333. doi: 10.3389/fphar.2019.00333
23. Fan M, Krutilina R, Sun J, Sethuraman A, Yang CH, Wu ZH, Yue J, et al. Comprehensive analysis of microRNA (miRNA) targets in breast cancer cells. *J Biol Chem*. (2013) 288:27480–93. doi: 10.1074/jbc.M113.491803
24. Lu YC, Nazarko OV, Sando R III, Salzman GS, Li NS, Sudhof TC, et al. Structural basis of latrophilin-FLRT-UNC5 interaction in cell adhesion. *Structure*. (2015) 23:1678–91. doi: 10.1016/j.str.2015.06.024
25. Boucard AA, Maxeiner S, Sudhof TC. Latrophilins function as heterophilic cell-adhesion molecules by binding to teneurins: regulation by alternative splicing. *J Biol Chem*. (2014) 289:387–402. doi: 10.1074/jbc.M113.504779
26. O'Sullivan ML, de Wit J, Savas JN, Comoletti D, Otto-Hitt S, Yates JR III, et al. FLRT proteins are endogenous latrophilin ligands and regulate excitatory synapse development. *Neuron*. (2012) 73:903–10. doi: 10.1016/j.neuron.2012.01.018
27. Li H, Wu K, Tao K, Chen L, Zheng Q, Lu X, et al. Tim-3/galectin-9 signaling pathway mediates T-cell dysfunction and predicts poor prognosis in patients with hepatitis B virus-associated hepatocellular carcinoma. *Hepatology*. (2012) 56:1342–51. doi: 10.1002/hep.25777
28. Wang Y, Zhao E, Zhang Z, Zhao G, Cao H. Association between Tim3 and Gal9 expression and gastric cancer prognosis. *Oncol Rep*. (2018) 40:2115–26. doi: 10.3892/or.2018.6627
29. Wada J, Kanwar YS. Identification and characterization of galectin-9, a novel beta-galactoside-binding mammalian lectin. *J Biol Chem*. (1997) 272:6078–86. doi: 10.1074/jbc.272.9.6078
30. Wiersma VR, de Bruyn M, Wei Y, van Ginkel RJ, Hirashima M, Niki T, et al. The epithelial polarity regulator LGALS9/galectin-9 induces fatal

frustrated autophagy in KRAS mutant colon carcinoma that depends on elevated basal autophagic flux. *Autophagy*. (2018) 11:1373–88. doi: 10.1080/15548627.2015.1063767

31. Mishra R, Grzybek M, Niki T, Hirashima M, Simons K. Galectin-9 trafficking regulates apical-basal polarity in Madin-Darby canine kidney epithelial cells. *Proc Natl Acad Sci USA*. (2010) 107:17633–8. doi: 10.1073/pnas.1012424107
32. Cerignoli F, Abassi YA, Lamarche BJ, Guenther G, Santa Ana D, Guimet D, et al. *In vitro* immunotherapy potency assays using real-time cell analysis. *PLoS ONE*. (2018) 13:e0193498. doi: 10.1371/journal.pone.0193498
33. Yamauchi A, Kontani K, Kihara M, Nishi N, Yokomise H, Hirashima M. Galectin-9, a novel prognostic factor with antimetastatic potential in breast cancer. *Breast J.* (2006) 12(5 Suppl 2):S196–200. doi: 10.1111/j.1075-122X.2006.00334.x
34. Nagae M, Nishi N, Nakamura-Tsuruta S, Hirabayashi J, Wakatsuki S, et al. Structural analysis of the human galectin-9 N-terminal carbohydrate recognition domain reveals unexpected properties that differ from the mouse orthologue. *J Mol Biol.* (2008) 375:119–35. doi: 10.1016/j.jmb.2007.09.060
35. Gleason MK, Lenvik TR, McCullar V, Felices M, O'Brien MS, Cooley SA, et al. Tim-3 is an inducible human natural killer cell receptor that enhances interferon gamma production in response to galectin-9. *Blood*. (2012) 119:3064–72. doi: 10.1182/blood-2011-06-360321

Conflict of Interest Statement: The authors declare that the research was conducted in the absence of any commercial or financial relationships that could be construed as a potential conflict of interest.

Copyright © 2019 Yasinska, Sakhnevych, Pavlova, Teo Hansen Selnø, Teuscher Abeleira, Benlaouer, Gonçalves Silva, Mosimann, Varani, Bardelli, Hussain, Siligardi, Cholewa, Berger, Gibbs, Ushkaryov, Fasler-Kan, Klenova and Sumbayev. This is an open-access article distributed under the terms of the Creative Commons Attribution License (CC BY). The use, distribution or reproduction in other forums is permitted, provided the original author(s) and the copyright owner(s) are credited and that the original publication in this journal is cited, in accordance with accepted academic practice. No use, distribution or reproduction is permitted which does not comply with these terms.